Targeting chromosomal instability: Screening and characterization of CIN killers

Submitted in total fulfilment of the requirements of the degree of Doctor of Philosophy

By

Zeeshan Shaukat

THE UNIVERSITY of ADELAIDE

Discipline of Genetics
School of Molecular and Biomedical Science

May 2014

Table of Contents

Thesis Summary

Chromosomal INstability (CIN), a hallmark of cancer cells, refers to a state in which cells have an increased rate of gain or loss of whole chromosomes or large chromosomal fractions. CIN is linked to the progression of tumours with poor clinical outcomes such as drug resistance and metastasis. Chromosomal instability is mainly caused by defective chromosomal segregation during mitosis and normally prevented by cellular checkpoints. As CIN is not found in normal cells, it offers a cancer-specific target for therapy, which may be particularly valuable because CIN is common in advanced tumours that are resistant to conventional therapy.

In this study, to identify targets which can specifically induce apoptosis in CIN cells, a CIN model was generated by knocking down the spindle assembly checkpoint in *Drosophila.* Defects in the checkpoint lead to high rate of chromosomal segregation defects (lagging chromosomes and chromosome bridges). An RNAi screening approach was used and the set of kinases and phosphatases was screened to identify those candidates that induce apoptosis only in CIN cells. Genes identified include those involved in JNK signaling pathways, mitotic cytoskeletal regulation and metabolic pathways. This screen demonstrates that it is feasible to selectively kill cells with CIN induced by spindle checkpoint defects. It has identified candidates that are currently being pursued as cancer therapy targets (e.g. Nek2: NIMA related kinase 2), confirming that the screen is able to identify promising drug targets of clinical significance.

Further screening and characterization of the JNK pathway demonstrated that signaling through JNK is required to tolerate CIN which is consistent with the fact that many tumours show high levels of JNK expression. JNK signaling is involved in the DNA damage repair process by maintaining an efficient damage repair and anti-oxidant levels which resolves DNA damage before entry into mitosis. Knockdown of the JNK pathway results in unrepaired DNA damage which leads apoptosis only in CIN cells via the caspase dependent pathway, partly independent of p53. Similarly, it was observed that the G2 length, which is required for DNA damage repair is crucial for the survival of CIN cells. These results suggest that JNK is necessary for the proper regulation of the DNA damage induced delay prior to mitotic entry and crucial for the survival of CIN cells, which are already coping with elevated levels of stress.

In addition, CIN can enable tumours to acquire genetic diversity which can provide an advantage in terms of growth and proliferation under stress and also provide resistance against cancer therapies, but this comes at the cost of significant stress to tumour cells. CIN cells evolve their metabolic pathways to increase the ability to tolerate and survive under oxidative and proteotoxic stress, but are still sensitive to these pathways. This study demonstrates the possibility to target both CIN and metabolism for the treatment of highly diverse drug resistant tumours. Further metabolic genes were screened and we demonstrated that CIN cells are particularly sensitive to certain metabolic alterations that do not affect normal cells. These metabolic disruptions lead to high levels of oxidative stress in CIN cells, which are already managing elevated reactive oxygen species (ROS) levels. These potential therapeutic targets are clinically highly desirable because of their potential effects on unstable and highly resistant CIN tumours.

In conclusion, a new *Drosophila* model for CIN was used to demonstrate the principle that it is possible to selectively kill CIN cells. Our RNAi screen identified candidates whose depletion has the potential to kill proliferating CIN cells without affecting their normal counterpart. An efficient DNA damage repair mechanism is required to tolerate CIN and can be used as a target to kill these unstable cells which are already dealing with high levels of DNA damage from ROS. Furthermore, CIN cells are sensitive to metabolic alterations, especially those which are needed to tolerate high levels of proteotoxic and oxidative stress. This study is a significant advance in understanding the target pathways which are involved in CIN tolerance. Further characterization of these pathways may help to identify mechanisms by which cancer cells can tolerate the adverse effects of CIN and aneuploidy which in turn may lead to the identification of novel targets that can specifically kill advanced and drug resistant-CIN tumour cells without harming normal cells.

Declaration

I certify that this work contains no material which has been accepted for the award of any other degree or diploma in my name, in any university or other tertiary institution and, to the best of my knowledge and belief, contains no material previously published or written by another person, except where due reference has been made in the text. In addition, I certify that no part of this work will, in the future, be used in a submission in my name, for any other degree or diploma in any university or other tertiary institution without the prior approval of the University of Adelaide and where applicable, any partner institution responsible for the joint-award of this degree.

I give consent to this copy of my thesis when deposited in the University Library, being made available for loan and photocopying, subject to the provisions of the Copyright Act 1968.

The author acknowledges that copyright of published works contained within this thesis resides with the copyright holder(s) of those works. I also give permission for the digital version of my thesis to be made available on the web, via the University's digital research repository, the Library Search and also through web search engines, unless permission has been granted by the University to restrict access for a period of time.

---------- ----------

Zeeshan Shaukat Dated

Acknowledgments

First and foremost I would like to thank Almighty Allah for His immense blessings and for making my dream come true.

I would like to express my sincerest gratitude to my supervisor and the best mentor, Dr Stephen Gregory, for his persistent encouragement, patience, guidance and support throughout my study. It was a great privilege and honour to work and study under his guidance. I am extremely grateful for what he has offered me, without his support this thesis would not have been completed. I would also like to thank my co-supervisors, Prof Robert Richards and Prof Robert Saint for their valuable comments, ideas and encouragements, which helped me to improve my research.

It would not have been possible to write this doctoral thesis without the help and support of the kind people around me. I am very grateful to my lab members and research colleagues: Dawei liu, Shannon Nicolson, Heidi Wong, Rashid Hussain, Amanda Choo, Cheng Shoo, Seyyed Hani Moussavi Nik, Dr. Clare van Eyk, Dr. Saumya Samarawera and Dr. Louise O'Keefe.

I would like to acknowledge the financial, academic and technical support of the University of Adelaide, particularly Graduate centre for ASI Research scholarship, IBP-R for research training, RED for language support, library, IT services, and School of Molecular and Biomedical Sciences for providing the research facilities and environment. I would also like to thank NHMRC for providing all the research funds.

My very special thanks to the people to whom I owe everything I am today, my father (Shaukat Ali) and mother (Shamim Akhtar), who have given me their unequivocal support, care, prayers and affection. I would like to thank my loving sister (Monazzah Yousuf) and brother (Farhan Shaukat). Last but not least, my heartfelt thank goes to my beloved daughter (Aleeza) and wife (Dr. Sara Altaf). Sara always encouraged me to do this study and gave her patience during the entire period of carrying out this study.

Finally, I would like to thank my close friends Maaz Akhtar, Syed Mohammad Yousuf, Mohammad Tabeer Malik, Saqib Masood Chaudhary, Mudassar Altaf and Fahad Saleem, for always being there when I needed you the most.

List of Publications

- Zeeshan Shaukat, Heidi Wong, Shannon Nicolson, Robert B. Saint, & Stephen L. Gregory*. (2012) A screen for selective killing of cells with chromosomal instability induced by a spindle checkpoint defect. PloS one, 7 (10), e47447.

- Heidi Wong, Zeeshan Shaukat, Jianbin Wang, Robert Saint, & Stephen L. Gregory*. (2014) JNK signaling is needed to tolerate chromosomal instability. *Cell Cycle*, 13 (4), 0-9.

- Zeeshan Shaukat, Dawei Liu, Amanda Choo, Rashid Hussain, Louise O'Keefe, Robert Richards, Robert Saint and Stephen L. Gregory*. (under review for Oncogene) Chromosomal Instability Causes Sensitivity to Metabolic Stress.

Abbreviations

17-AAG	17-N-allylamino-17-demethoxygeldanamycin
AICAR	5-amino-1-β-D-ribofuranosyl-imidazole-4-carboxamide
AP1	Activator protein 1
APC	Adenomatous polyposis coli
APC/C	Anaphase promoting complex/cyclosome
Asp	Abnormal spindle protein
ATM	Ataxia telangiectasia mutated
Aur	Aurora kinases
AURKA	Aurora kinase A / Aurora A
AURKB	Aurora kinase B / Aurora B
BFB	Breakage-Fusion-bridge
BRCA1	Breast cancer 1
BUB	Budding uninhibited by benzimidazoles
BubR1	Bub1-related protein kinase
CD95	Cluster of differentiation 95 (FAS receptor)
Cdc20	Cell division cycle 20 homologue
CDK1	Cyclin B dependent kinase 1
CDKs	Cyclin dependent kinases
CENP-E	Centromere linked motor protein E
Chk2	Checkpoint kinase 2
CIN	Chromosomal instability
DDR	DNA damage response
DNA	Deoxyribonucleic acid
DSB	Double strand break
FOXO	Forkhead box protein O
Fzr1	Fizzy-related protein homolog 1
G6PD	Glucose-6-phosphate dehydrogenase
HEC1	Highly expressed in cancer protein 1
HIF	Hypoxia-inducible factor
Hippo	Hippo (hpo gene), Salvador/Warts/Hippo (SWH) signaling pathway,
HSP90	Heat shock protein 90
IDH	Isocitrate dehydrogenase
JNK	c-Jun N-terminal kinases
k-MT	kinetochore–microtubule
KRAS	Kirsten rat sarcoma viral oncogene homolog

KSP/Eg5	Kinesin spindle protein
Mad2	Mitotic arrest deficient 2
MAPKKK	Mitogen-activated protein kinase kinase kinase
Mps1	Monopolar Spindle 1
MSI	Microsatellite instability
MT	Microtubules
mTORC1	Mammalian target of rapamycin complex 1
MVA	Mosaic Variegated Aneuploidy
NADPH	Nicotinamide adenine dinucleotide phosphate-oxidase
Nek2	NIMA-related kinase 2
NHEJ	Non homologous end joining
NIMA	Never In Mitosis Gene A
Notch	Notch proteins: a family of transmembrane proteins
p53	Tumour protein (SDS-PAGE: 53 kDa) p53
PAS	Per Arnt Sim
PASK	PAS domain containing serine/threonine kinase
PI3K	Phosphoinositide 3-kinases
PLK1	Polo-like kinase 1
Plk4	Polo-like kinase 4
PP1	Protein phosphatase 1
PTEN	Phosphatase and tensin homolog
Rad21	RAD21 homolog (S. pombe), kleisin subunits of Cohesin Rad21
Rad54	DNA repair and recombination protein RAD54
Rae1	RNA export 1
Ras	Rat sarcoma
Rb	Retinoblastoma
RNAi	RNA interference
Rod	Rough deal
SAC	Spindle assembly checkpoint
SAK	Snk akin kinase
Scc1	kleisin subunits of Cohesin Scc1
Smc1	Structural Maintenance of Chromosome 1
Smc3	Structural maintenance of chromosomes 3,
SOD1	Superoxide dismutase 1
STAG3	Stromal antigen 3
TCA	Tricarboxylic acid cycle
Trp53	Transformation-related protein 53
Wnt	From: Wingless gene (*Drosophila*), a homolog of int-1
zw10	Zeste white 10, kinetochore associated protein homolog

Thesis outline

Chromosomal instability (CIN) is the hallmark of cancer cells. Chromosomal instability is also linked to tumourigenesis and poor clinical outcomes. CIN cancers are resistant to conventional therapies and require new therapies. CIN is highly tolerated in cancers and provides an opportunity to be specifically targeted. **Chapter 1** of this thesis is a literature review, which describes chromosomal instability, its types and mechanism and its use as a therapeutic target for cancer. **Chapter 2** is based on a published article (Shaukat et al, 2012) from this study which explains the generation of a *Drosophila* CIN model. Chapter 2 also explains the screening of candidates whose knockdown can induce apoptosis in CIN cells without affecting the normal cells. Along with other centrosomal candidates, some JNK pathway candidates were identified which were then further analysed for their role in CIN specific cell death. This characterization is published (Wong et al, 2014) and is a part of this thesis as **chapter 3**.

The initial screening also identified metabolic candidates which are interesting because CIN cells cause metabolic alterations in cancer cells for the adaptation against cellular and external stresses. This CIN specific alteration offers the possibility to target CIN. Further screening of metabolic candidates in our CIN model demonstrated that the CIN cells are sensitive to certain metabolic alterations, especially those which are involved in maintaining the redox potential of the cell as well as oxidative stress response pathway genes. The outcome of this screening and characterization is presented in **chapter 4** of this thesis as a submitted manuscript for publication (under review for Oncogene). All the publication based chapters contain their own introduction, methods, results and discussions. **Chapter 5** includes the combined discussion of the results, their significance, current model and future directions.

Chapter 1

INTRODUCTION

1.1- Cancer

Cancer is a generic term for a large group of diseases caused by the failures in cell cycle control, that leads to aberrant cell growth and division, which then results in uncontrolled invasion and metastasis. Cancer is one of the leading causes of premature death. Every year, approximately 14 million people are diagnosed with cancer worldwide [http://www.who.int]. In 2012, 8.2 million deaths are reported worldwide and the WHO estimates approximately 21.3 million new cases and 13.1 million cancer-related deaths will occur in 2030 [http://www.who.int, http://globocan.iarc.fr]. In Australia, nearly 43,700 people died from cancer in 2011. 124,910 new cases of cancer were diagnosed in 2012 which will increase up to 150,000 by 2020 [http://www.cancer.org.au].

1.2- Cancer therapy

Surgery, radiation and chemotherapy are the important treatment strategies for cancer. Surgery is an effective way to cure early-stage solid cancers, but the treatment of advanced and metastatic cancers requires additional hormonal and chemical therapies (Caley & Jones, 2012). The most successful chemotherapies currently used for the treatment of cancer interfere with the normal functioning and progression of the cell cycle (Schmidt & Bastians, 2007).

One class of classical therapeutic agents target Microtubules (MT) of the mitotic spindle assembly and modulate the dynamics of MT. For example, vinca alkaloids and colchicine are tubulin binding agents that act by inhibiting the polymerization of tubulin. Taxanes and epothilones act as MT stabilization agents (Ivachtchenko et al, 2007; Sudakin & Yen, 2007). These drugs disrupt the function of the mitotic spindle, which result in the activation of the Spindle Assembly Checkpoint (SAC). The SAC arrests cells in metaphase in response to the structural alignment defects and allow the cellular machinery to either repair these defects or induces apoptosis (Zhou & Giannakakou, 2005; Schmidt & Bastians, 2007). The SAC is further reviewed in section 1.7.5. However, microtubules are also very important in normal non-dividing and differentiating cells for their involvement in vital cell functions e.g. intracellular transport, cell shape, integrity and localization. Therefore, the treatment with these mitotic poisons results in significant haematological and neurological side effects (Goa

& Faulds, 1994; Lobert, 1997; Rowinsky, 1997). Other potential limitations for these drugs include the emergence of drug resistance which results in treatment failure in almost 90% patients with advanced cancer (Longley & Johnston, 2005). Currently, new microtubule inhibitors are in clinical trials and showing less drug resistance, but they are still not ideal because of their side effects on the normal host cells (Harrison et al, 2009).

DNA damaging drugs are also used to treat cancer, and these are mainly dependent on the DNA damage checkpoint and spindle assembly checkpoint for the induction of apoptosis or mitotic catastrophe (Parker et al, 1990; Minotti et al, 2004; Kelland, 2007). However, the *p53* gene is mutated or its loss of function is common in most cancers, which enables them to tolerate high levels of DNA damage (Vazquez et al, 2008). p53 mutations are commonly acquired in patients who were previously treated with DNA-damaging chemical drugs (Sturm et al, 2003). DNA damage is usually recognized by the DNA damage response (DDR) pathway, which initiates repair in normal cells so this damage should kill DDR compromised cancer cells. However, in some cancer cells with a defective DDR, DNA damage leads to genome instability, drug resistance and cancer development (Bouwman & Jonkers, 2012). In SAC compromised tumours, aneuploidy and drug resistance also reduce the efficacy of these drugs (Masuda et al, 2003).

Currently, a diverse group of proteins (Kinases, phosphatases, kinesins and cyclins), which are involved in the regulation of the cell cycle are the focus of studies to identify their role as potential therapeutic targets (Malumbres & Barbacid, 2007). These include cyclin dependent kinases (CDKs) and regulators of DNA-damage checkpoint, SAC and cytokinesis. Some of these often express/operate abnormally in cancerous cells and could serve as a potential target for cancer therapy (Bettencourt-Dias et al, 2004). Currently, the front runners in cancer therapy are the inhibitors of mitotic targets including Polo-like kinase 1, Aurora kinases, Mps1, Cenp-E, survivin and KSP/Eg5. Their development and clinical evaluation is reviewed in (Schmidt & Bastians, 2007; Salmela & Kallio, 2013).

Most of the current therapies for cancer are not ideal because of their side effects on the normal dividing cells in the body (Caley & Jones, 2012). Specially, pediatric cancers are difficult to treat due to the abundance of dividing cells in the organs, because their body is still growing (Kufe et al, 2003). Moreover, drug resistance and relapses are

common features of advanced tumours and the use of combination therapies is also unable to treat these tumours (Caley & Jones, 2012). These tumours often show high levels of chromosomal instability which is linked to drug resistance and poor clinical outcomes (Carter et al, 2006; Choi et al, 2009).

Chromosomal INstability (CIN) is a common feature of nearly all solid tumours (Mertens et al, 1994; Lengauer & Vogelstein, 1998). The presence of chromosomal instability makes these tumours more adaptive to cellular and environmental stresses as well as resistant to multiple drugs, making them difficult to target with regular therapies (Gao et al, 2007; Heilig et al, 2009; Sotillo et al, 2010). However, tolerating a high level of CIN is a characteristic feature of cancer cells, which is not common in normal cells, so CIN can potentially be used as a tumour specific target for cancer therapy.

In this thesis, we explored the possibility of targeting CIN which can be used for the treatment of advanced cancer. An induced-CIN model in *Drosophila melanogaster* was generated to identify and characterize genes that could potentially target CIN cells specifically. CIN/aneuploidy related stress and damage is also explored as a target by altering stress sensing and repair pathways. Targeting CIN could help in limiting the ability of cancer cells to evolve drug resistance and other poor clinical outcomes, which may increase the efficacy of current therapies.

1.3- Chromosomal instability

Genomic instability or genetic aberrations are commonly observed in solid tumours and some haematological malignancies. It broadly covers alterations from the single nucleotide level to the chromosomal level (McGranahan et al, 2012). Some of these alterations result in a stable form of aneuploidy and others lead to a continuous reshuffling of genomic material; both can lead to tumourigenesis. Genomic instability can be further characterised into at least two major sub-types, one is microsatellite instability (MSI) and the other is chromosomal instability (Oda et al, 2005).

Microsatellites are the simple repeated nucleotide sequences which remain stable during the whole life span. Mutation in the DNA mismatch repair system leads to continuous alterations in these microsatellites, termed microsatellite instability. These unstable microsatellites lead to a hyper-mutator phenotype which is linked to tumour formation

and progression: about 15% of colorectal cancers show MSI (Ionov et al, 1993; Arzimanoglou et al, 1998). MSI in cancer is often associated with good prognosis regardless of tumour stage (Buecher et al, 2013). MSI tumours are less prone to metastasis and associated with increased patient survival (Thibodeau et al, 1993). The role of MSI in cancer is recently reviewed by (Yim, 2012; Buecher et al, 2013; Heinimann, 2013).

Chromosomal instability is defined as a failure of cells to maintain a stable chromosome number and integrity. It refers to a state in which cells have an ongoing increased rate of gain or loss of whole chromosomes or large chromosomal fractions (Gao et al, 2007; Geigl et al, 2008; Heilig et al, 2009; Thompson et al, 2010). Chromosomal instability has been observed in tumours for more than a century and now it is considered as one of the hallmarks of advanced tumours (Mertens et al, 1994). CIN is the major cause of chromosomal alterations or aneuploidy. Almost 90% of solid tumours and 50% of haematopoietic tumours exhibit aneuploidy (Mitelman et al, 2012). CIN is linked with tumour progression and poor clinical outcomes such as metastasis and adaptability to environmental and chemical stresses (Carter et al, 2006; Choi et al, 2009). Drug resistance and relapse is also common in cancers with CIN as they evolve rapidly, making them difficult to target with regular therapies (Swanton et al, 2009; Sotillo et al, 2010).

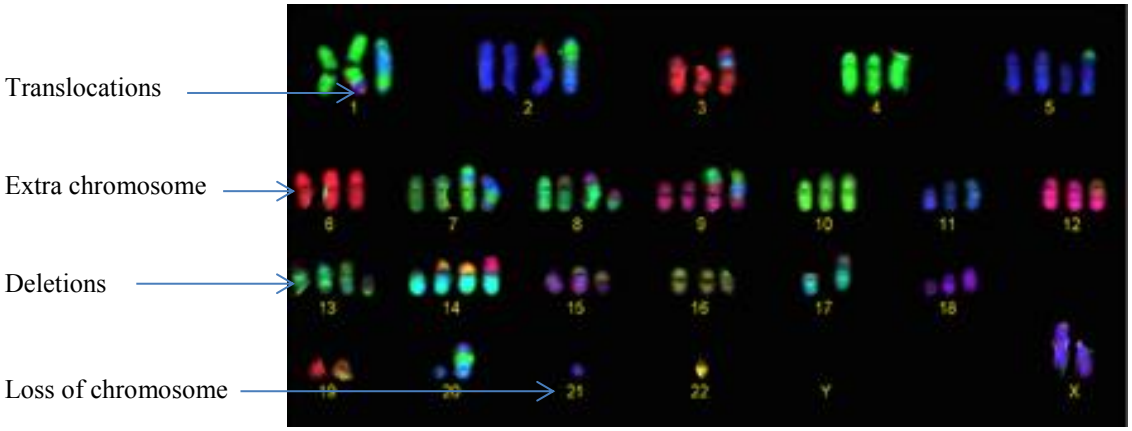

Figure 1.1: *Karyotype of a typical CIN cancer cell (osteosarcoma cell line), showing structural and numerical CIN.* [Taken from (Jansson & Medema, 2013)]

1.4- Types of Chromosomal instability

Normally the cell cycle is tightly controlled by different checkpoints which ensure the fidelity of this sensitive process and protect the dividing cells from different internal and external stresses (Harrison et al, 2009). Any misregulation in these safeguard systems can result in daughter cells whose genomes deviate from the normal karyotype [(Kops et al, 2005); Figure 1.1]. CIN is primarily characterized in two types, numerical CIN and structural CIN. Both types of CIN are often present in a cancer and are linked to heterogeneity and continuous evolution of genome (Mitelman et al, 1997).

1.4.1- Structural chromosomal instability

Structural chromosomal instability refers to high rate of sub-chromosomal alterations which leads to gain or loss of small regions of chromosome via translocations, insertion, deletions and amplification of DNA. In many cancers, translocation is the most effective way of producing structural CIN (Mitelman et al, 1997). This can lead to the formation or over expression of oncogenes by the fusion or duplication of genes or to knockout of tumour suppressor genes (Hansemann, 1891; Nowell, 1962; Thompson & Compton, 2011). Mutations in the double-strand DNA damage repair machinery can lead to translocations and structural CIN (Duker, 2002; Natarajan & Palitti, 2008). Non homologous end joining (NHEJ) is an error prone DNA damage repair pathway, which contributes to structural CIN by joining two non-specific broken ends of DNA (Natarajan & Palitti, 2008). Double strand breaks (DSB) can thus generate non-specific chromosomal fusions especially at dysfunctional telomeres (Hastie & Allshire, 1989). Fusion at telomeres leads to the formation of di-centric chromosomes or ring chromosomes, which leads to the formation of chromatin bridges at anaphase because of improper attachment of microtubules to these di-centric chromosomes (Figure 1.3). These unresolved chromosomal bridges result in breakage at cytokinesis and fusion again in the subsequent cell cycle [Figure 1.5; (McClintock, 1938; McClintock, 1941; Gisselsson et al, 2001)]. This Breakage-Fusion-bridge (BFB) cycle is often found in tumours with dysfunctional telomeres, aberrant DNA repair pathway and replication stress (Hastie & Allshire, 1989; Gisselsson et al, 2001; Bristow & Hill, 2008; Burrell et al, 2013), resulting in instability and intra tumour heterogeneity (Gisselsson et al, 2000). A high frequency of structural chromosomal aberrations directly correlates with higher grade tumours (Mitelman et al, 1997; Nishizaki et al, 1997; Nishizaki et al, 1997).

1.4.2- Numerical chromosomal instability

Numerical CIN is a prominent type of CIN in which the gain or loss of whole chromosome occurs with higher rates as compared to normal cells. Abnormal chromosome number or aneuploidy can exist in a stable state and can easily be targeted but unstable aneuploidy is more common and exhibits more adaptability to internal and external stresses (Lengauer et al, 1997; Nowak et al, 2002; Rajagopalan et al, 2003). Continuous shuffling of genetic material helps these cells to acquire drug resistance and it is also related to tumour advancement, metastasis and poor prognosis (Kuukasjarvi et al, 1997; Carter et al, 2006; Choi et al, 2009; Sheffer et al, 2009). A widely accepted theory about how CIN or aneuploidy are linked to tumourigenesis is that the gain or loss of whole chromosomes results in the gain of oncogenes or the loss of tumour suppressor genes (Baker et al, 2009; Kolodner et al, 2011).

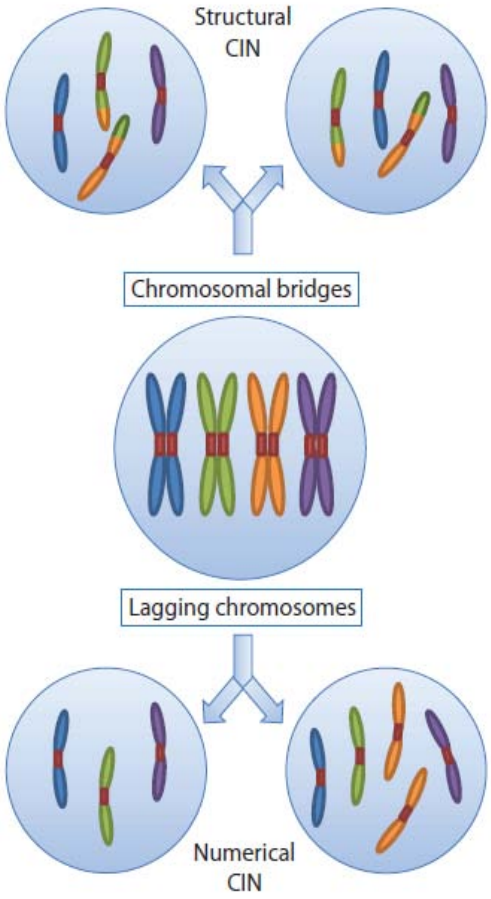

Figure 1.2: *Segregation defects and types of chromosomal instability*

In normal cells chromosome missegregation is a rare event, however in CIN cancers the chromosome segregation error rate is high (once in every fifth division) (Lengauer et al, 1997; Thompson & Compton, 2008). Numerical CIN is mainly causedby lagging chromosomes (Figure 1.2) which can be caused by several mechanisms: cohesion defects, merotely, aberrant kinetochore-microtubule attachment, centrosome amplification or a weakened spindle assembly checkpoint, which are further discussed in Section 1.7.

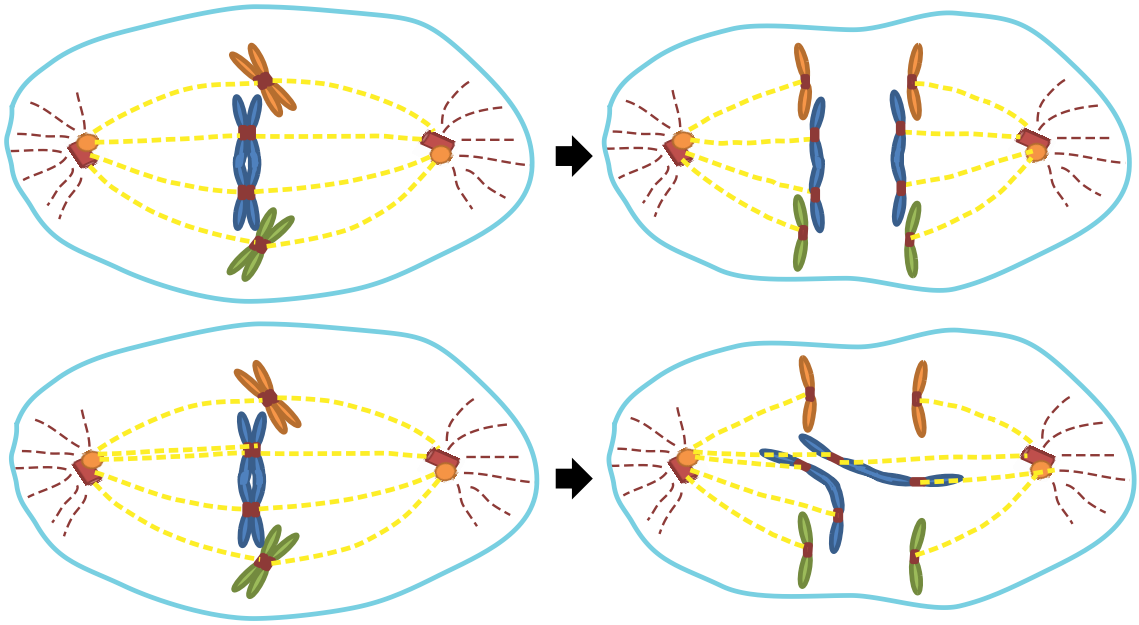

Figure 1.3: *Normal and defective segregation in di-centric chromosome*

1.5- Chromosomal instability and aneuploidy

Chromosomal instability and aneuploidy, are both hallmarks of cancer (Hanahan & Weinberg, 2000; Hanahan & Weinberg, 2011). CIN is the principal cause of aneuploidy but aneuploidy does not necessarily lead to CIN. In past studies, CIN and aneuploidy were often considered the same because of similar diagnostic markers, but now CIN and aneuploidy are considered as two distinct but interlinked processes (Thompson & Compton, 2008). Chromosomal instability is defined as a continuous high rate of genomic reshuffling (both numerical and structural) (Lengauer et al, 1997) and aneuploidy is defined as a stable state of abnormal karyotype. In some aneuploid tumours, all cells show the same karyotypic defect and can easily be targeted (Kaneko & Knudson, 2000; Paulsson & Johansson, 2009). In contrast, chromosomal instability,

because of its dynamic nature, results in tumour heterogeneity and makes cancer a moving target. Both CIN and aneuploidy are commonly found in human tumours and are linked to tumourigenesis and poor clinical outcomes (Carter et al, 2006; Pfau & Amon, 2012). Thus, understanding the cause and consequences of CIN and aneuploidy could provide an attractive opportunity to intervene in the process of tumourigenesis, adaptability and aggressiveness in order to develop effective therapies for cancer.

1.6- Mechanisms of Chromosomal instability

Chromosomal instability is mainly caused by defective segregation which is linked to defects in the spindle assembly checkpoint, kinetochore-microtubule attachment, DNA damage response or centrosomal function (Gollin, 2005; Thompson et al, 2010). In addition, DNA replication stress and the state of cellular metabolism are also reported to be related to CIN (Bristow & Hill, 2008; Burrell et al, 2013). The most common chromosomal segregation errors observed in CIN-cancer cells are lagging chromosomes and chromosomal bridges (Thompson et al, 2010).

Lagging chromosomes mainly result in numerical CIN (Figure 1.2). A chromosome that does not attach properly to microtubules requires more time to resolve this misattachment; if not resolved it is unable to segregate at anaphase and is left behind at the metaphase plate (Thompson & Compton, 2008). Normally this happens when a kinetochore of one of the chromatids is attached to both spindle poles [(Gregan et al, 2011); see Figure 1.4]. This type of defective attachment is termed ‘merotelic’ attachment, which is normally resolved by kinesins during metaphase. Kinesins reduce the stability of microtubules at the kinetochore, allowing the release of merotelic attachments and establishing the correct orientation and tension between the kinetochores. The spindle assembly checkpoint is the major control mechanism that prevents the progression of mitosis from metaphase to anaphase until all the chromosomes are properly aligned and attached to the spindle (Musacchio, 2007; Varetti & Musacchio, 2008; Nezi & Musacchio, 2009). However, unlike other mal-orientations, merotely does not trigger the spindle checkpoint. The reason is that the merotelic attachments do not produce unattached kinetochores and can also generate tension across sister kinetochores.(Gregan et al, 2011). SAC deficiency could also lead to merotely or lagging chromosome because of shorter mitosis which allows less time for the cellular machinery to resolve any misattachment (Buffin et al, 2007). The list of

mutations that affects the SAC is long, and includes over- and under-expression of SAC proteins. Clinically, loss of Rb (in retinoblastoma) or Adenomatous Polyposis Coli (APCin colorectal cancer) are known to effect SAC function (Dikovskaya et al, 2007; Zhang et al, 2009; Thompson et al, 2010). Certain chemical treatments which stabilize microtubule-kinetochore attachments or those which disrupt the dynamics of microtubule-kinetochore attachments can also result in lagging chromosomes (DeLuca et al, 2006). Moreover, multipolar spindles can also lead to merotely and CIN (Figure 1.6).

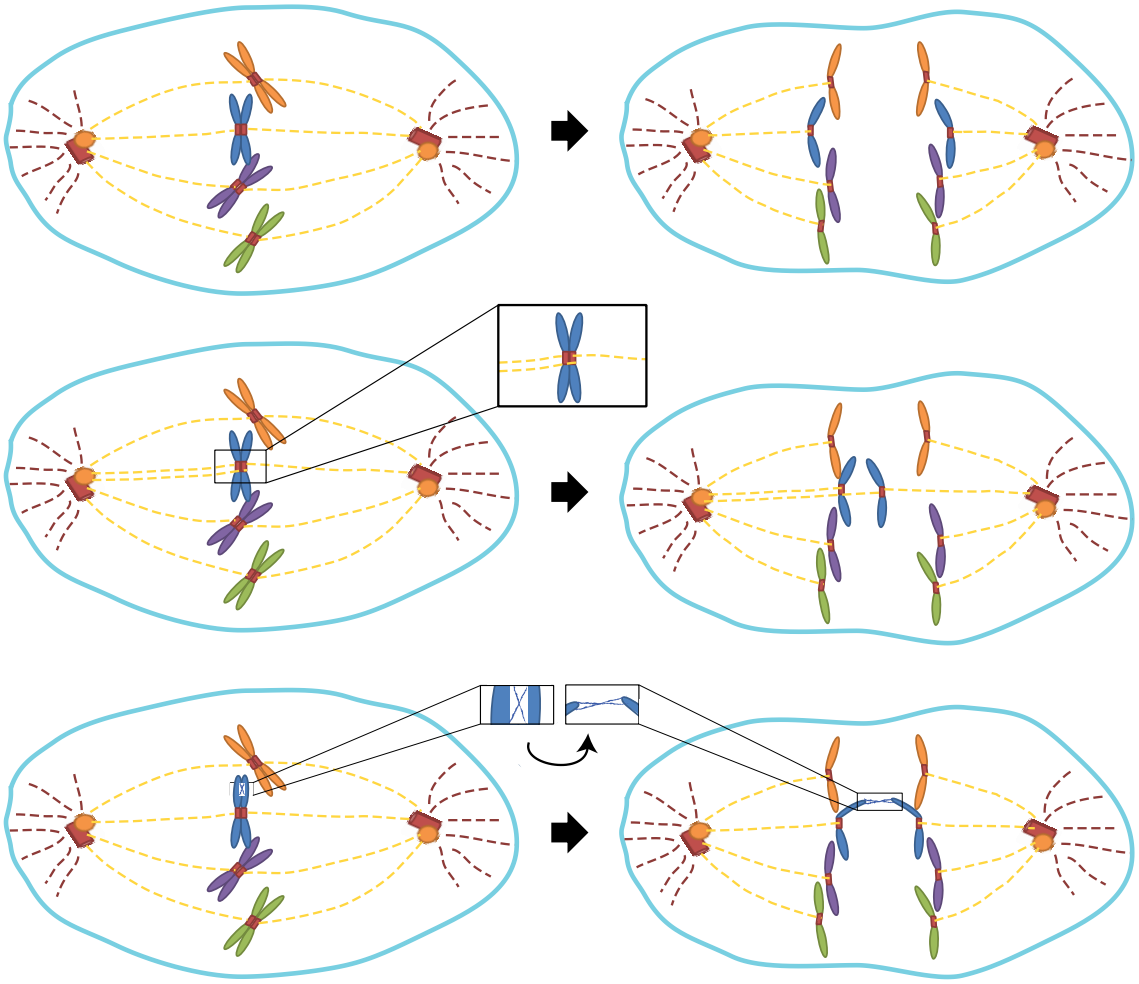

Figure 1.4: *Aberrant spindle-chromosome attachments and chromosomal bridges lead to chromosomal instability.*

The other most common mechanism of CIN is the formation of chromosome bridges at anaphase. This is caused when a particular chromosome is di-centric and attached to both poles, in this case the centromeres are pulled apart but the chromatids remain linked, which leads to physical breakage via the cleavage furrow at cytokinesis

(Cleaver, 2011; Fenech et al, 2011; Janssen et al, 2011). Aberrant DNA damage, cohesion defects and replication stress are also linked to unresolved attachments between chromatids which results in ultra-fine bridges of DNA between the daughter nuclei (Figure 1.4) again leading to double strand breaks. Furthermore, the lack of an error-free DNA repair mechanism for double strand breaks in G1, again leads to nonspecific fusion and breakage in the subsequent mitosis, resulting in structural CIN (Masuda & Takahashi, 2002).

Cancer cells can tolerate a high level of CIN, which indicates that the cell cycle checkpoints are unable to arrest and resolve this ongoing loss of genomic integrity (Campbell et al, 2010; Gregan et al, 2011) which helps them to acquire resistance against the internal and external stresses.

1.7- Causes of Chromosomal instability in Cancer (Numerical)

Cancer is a complex disease and CIN makes it more complex and difficult to target. CIN can be caused by several mechanisms, which are linked to different types and grades of tumour. Different causes that have been postulated to be responsible for these genomic aberrations are outlined below i.e. defects in sister chromatid cohesion (Barber et al, 2008; Zhang et al, 2008; Meyer et al, 2009), merotelic attachments (Cimini et al, 2001; Cimini, 2008), improper attachment of kinetochore to the mitotic spindle (DeLuca et al, 2006), centrosome amplification (Carmena et al, 2009; Gregan et al, 2011), supernumerary centrosomes (Ganem et al, 2009) and an aberrant spindle assembly checkpoint (Wang et al, 2002; Grabsch et al, 2003; Hanks et al, 2004; Holland & Cleveland, 2009), which is the best-characterized cause of chromosomal instability.

1.7.1- Cohesion Defects

Cohesion holds the sister chromatids together during mitosis until the SAC is satisfied (Nasmyth, 2011). Cohesion is essential for the faithful segregation of replicated chromosomes during mitosis. Aberrant cohesion leads to loosely attached or unattached sister chromatids floating around in the cell and generates difficulties in the equal distribution of chromatids between the two daughter cells. Similarly, alteration in cohesion release from chromosomes causes the failure of sister chromatid separation

and results in numerical CIN (Figure 1.5; Jallepalli et al, 2001; Barber et al, 2008; Thompson et al, 2010).

Premature separation or partial failure of segregation leads to chromosomal instability or aneuploidy and the complete failure of chromatid separation leads to tetraploidy (Thompson et al., 2010). Genes (i.e. *Smc1, Smc3, Scc1 (Rad21), STAG1, STAG2, STAG3* and *separase*) involved in the cohesion of sister chromatids and are often mutated in CIN cancers (Jallepalli et al, 2001; Yu et al, 2003; Wirth et al, 2006; Barber et al, 2008; Zhang et al, 2008; Iwaizumi et al, 2009; Mannini & Musio, 2011; Xu et al, 2011). Furthermore, members of the core cohesion complex (i.e. Scc1 and Smc3) and cohesion regulators (i.e. separase) are overexpressed in some CIN cancers (Mannini & Musio, 2011).

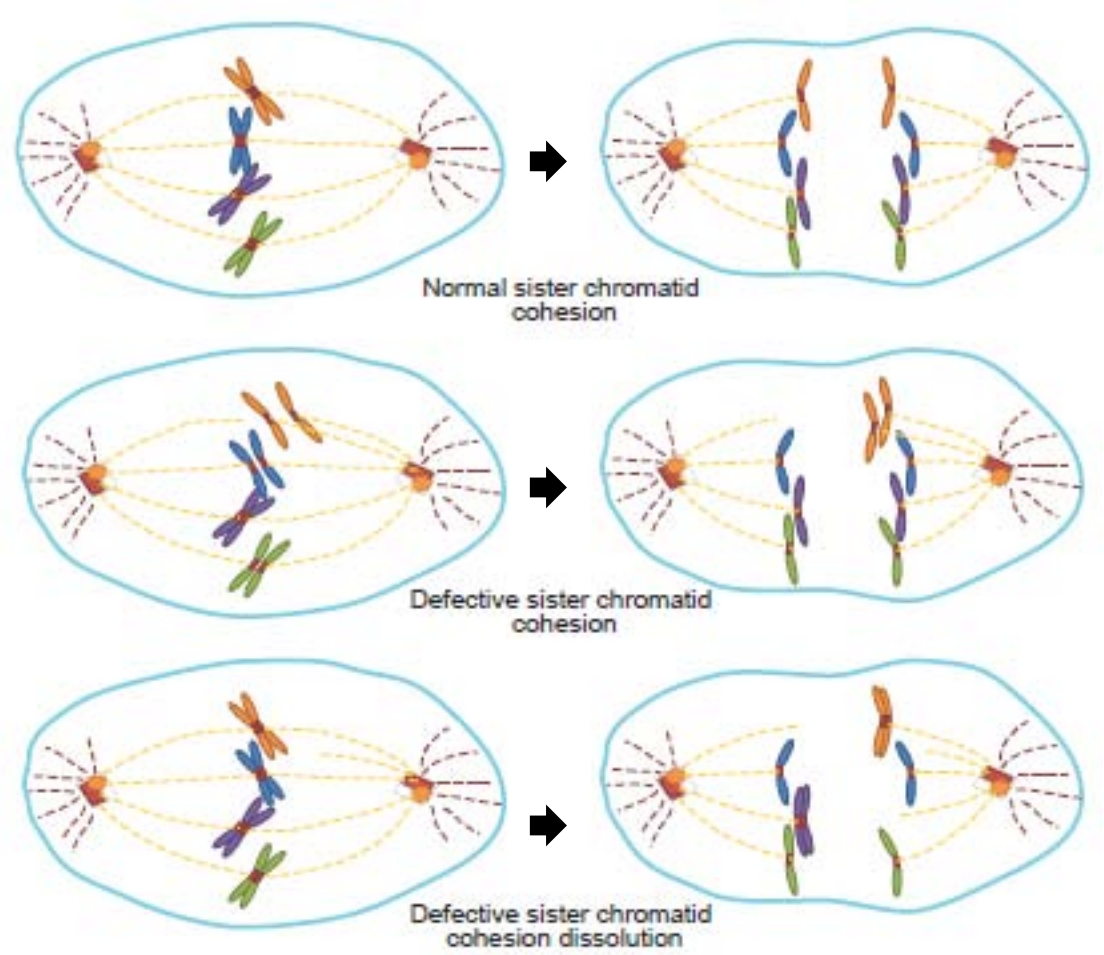

Figure 1.5: *Cohesion defects lead to chromosomal instability*

In conclusion, there is a strong association between aberrant sister chromatid cohesion machinery, chromosomal instability and cancers (Solomon et al, 2011). Apart from its

role in sister chromatid segregation, the cohesion complex has also been implicated in the control of gene expression and the regulation of the DNA damage checkpoint (Strom & Sjogren, 2005; Dorsett, 2011), which could also facilitate chromosomal instability.

1.7.2- Merotelic attachments.

As discussed earlier, lagging chromosomes are mainly formed due to merotelic attachments between kinetochores and microtubules. This happens when a kinetochore is simultaneously attached to microtubules originating from opposite spindle poles (see figure 1.4) (Cimini et al, 2001). Each human kinetochore can possibly accommodate ~20–25 microtubules. Merotely is undetectable to the SAC because both kinetochores have some connections to the correct pole, which generates adequate tension across the sister kinetochores (Gregan et al, 2011; Holland & Cleveland, 2012). Lagging chromosomes, which are formed due to merotely, often end up in the correct daughter cell after detachment from the microtubule of the wrong spindle pole. However if microtubules from the right spindle pole detached, the lagging chromosome ends up at wrong spindle pole leaving both the daughter cells aneuploid. If a similar number of microtubules from different poles are attached to a single kinetochore then the lagging chromosome may stay longer at the metaphase plate and fail to reach to the main nuclear assembly near the spindle pole, resulting in the formation of a micronucleus. Normal cells also make brief merotelic attachments which are corrected by the timely detachment of microtubules from the wrong kinetochore. This depends on the stability of microtubule attachments, which is controlled by kinesins and kinases (Lampson et al, 2004; Pinsky et al, 2006). Two leading causes of these merotelic attachments are hyperstability of kinetochore–microtubule (k-MT) interactions and centrosome amplification.

1.7.3- Kinetochore-microtubule attachments

A high rate of mal-orientation of kinetochore-microtubule attachments and hyper-stability is common in CIN cancers (Thompson & Compton, 2008; Bakhoum et al, 2009b; Compton, 2011). Merotely occurs at higher rates in hyper-stabilised k-MT attachments, requiring more time to resolve these errors. Over expression of the SAC protein Mad2 (Mitotic Arrest deficient 2), provides hyper-stability to kinetochore–

microtubule attachments which leads to CIN and tumours (Tanaka et al, 2001; Sotillo et al, 2007; Kato et al, 2011; Kabeche & Compton, 2012). Anything which shortens the duration of mitosis can reduce the ability of the cell to correct these errors before the onset of anaphase. A deficiency for Mad2 leads to merotelic attachments, which leads to lagging chromosomes and aneuploidy, because of less time in mitosis (Michel et al, 2001). BubR1 (Bub1-related protein kinase), Aurora kinase B (aurora B) and protein phosphatase 1 (PP1) are involved in the regulation of kinetochore-microtubules dynamics (Cimini et al, 2006; Emanuele et al, 2008; Liu et al, 2009). Inhibitors of aurora B increase the stability of k-MT and can be used as a therapy for cancer as they induce senescence and apoptosis (Cimini et al, 2006; Liu et al, 2009; Gurtler et al, 2010). Kinetochore-microtubule attachment and stability is discussed in detail by (Cimini, 2007; Bakhoum & Compton, 2012).

1.7.4- Supernumerary Centrosomes

The centrosome is a regulatory and functional hub which controls the process of cell division. They maintain microtubule organization and bipolar symmetry which helps in faithful chromosome segregation. Centrosome duplication is strictly controlled during the cell cycle and the amplification of centrosomes leads to segregation defects and CIN cancers. Supernumerary centrosomes were first implicated in tumourigenesis by Thedor Boveri in 1914 and have been often reported in aneuploid tumours (Boveri, 1914; Pihan et al, 1998; Lingle et al, 2002; Anderhub et al, 2012). Extra centrosomes delay mitosis through the SAC in order to increase the chance of proper K-MT attachments before the onset of anaphase (Yang et al, 2008). Interestingly, at anaphase these multiple centrosomes typically cluster in such a way that leads to bipolar spindle formation (Brinkley, 2001; Quintyne et al, 2005; Basto et al, 2008).

Supernumerary centrosomes increase the chance of merotelic attachments and lead to high rates of chromosomal segregation defects or CIN (Ganem et al, 2009; Silkworth et al, 2012). Centrosome duplication is controlled by numerous genes which are extensively reviewed recently by German A. Pihan (Pihan, 2013).

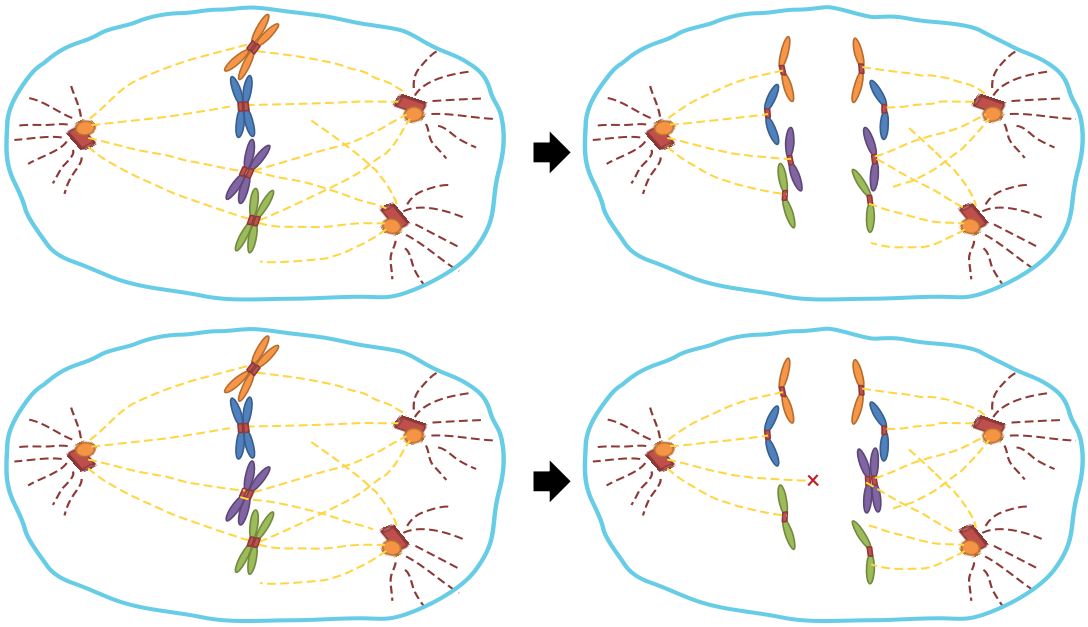

Figure 1.5: *Multi-polar spindle and merotelic attachments lead to chromosomal instability.*

1.7.5- Spindle assembly checkpoint:

The spindle assembly checkpoint is the only mechanism in mitosis that ensures correct DNA separation and cell cleavage. It prevents the onset of anaphase until all the chromosomes are properly aligned and attached to the spindle (Musacchio, 2007; Varetti & Musacchio, 2008; Nezi & Musacchio, 2009). First characterized in yeast (Li & Murray,1991; Hoyt et al, 1991; Hartwell & Smith, 1985), it consists of regulator proteins i.e. Mitotic arrest deficient (MAD; including MAD1, MAD2 and MAD3), Budding Uninhibited by Benzimidazole (BUB; including BUB 1, BUB 2 and BUB 3) and Cell Division Cycle CDC20. These SAC components, after being recruited at unattached kinetochores, delay the initiation of anaphase by inhibiting the anaphase promoting complex/cyclosome (APC/C). APC/C is required for the degradation of Cyclin B and securin (an anaphase inhibitor). Securin degradation frees separase, which is then simultaneously activated by the dephosphorylating activity of cyclin B dependent CDK1 kinase. Activated separase cleaves the cohesion molecules and promotes separation of sister chromatids. The SAC must detect aberrant kinetochore attachments at metaphase and prevent entry into anaphase until the problem in kinetochore attachment is resolved (Rieder & Maiato, 2004; Musacchio, 2007).

The SAC senses unattached kinetochores via the tension at kinetochores as the spindle pulls on either side. Lack of tension at any kinetochore normally leads to metaphase arrest or ultimately exposes the cell to apoptosis, if the cellular machinery is unable to resolve the error. An impaired SAC can lead to early anaphase onset and increase the probability of segregation defects, linked to leukaemia, colon cancer and breast cancer (Decordier et al, 2008). The list of mutations known to have effects on chromosomal segregation is long, and includes over- and under-expression of spindle checkpoint proteins and clinically relevant cancer mutations (Li et al, 2003; Holland & Cleveland, 2009 - Table 1). Clinically, mutations of Rb in retinoblastoma or Adenomatous Polyposis Coli (APC) in colorectal cancer are related to SAC defects (Cahill et al, 1998; Percy et al, 2000; Kim et al, 2005; Thompson et al, 2010). Inhibition of the SAC proteins Mad2 or BubR1 have been shown to shorten metaphase, causing CIN, aneuploidy and tumour susceptibility in humans and mouse models (Michel et al, 1994; Michel et al, 2001; Hanks et al, 2004; Lee et al, 2008; Schvartzman et al, 2010). Complete inhibition of the SAC is lethal (Kops et al, 2004; Baritaud et al, 2010) but p53 deficient cancer cells can accommodate this insult leading to CIN without apoptosis.

In contrast, as described earlier, the SAC cannot sense merotely and is unable to protect the cell from the missegreggation effects of merotely (Cimini et al, 2001), which is consistent with the clinical settings where aneuploid cancers have an intact SAC that is capable of detecting gross spindle abnormalities (Wood et al, 2007; Gascoigne & Taylor, 2008). It appears that most CIN cancers have a partially compromised spindle checkpoint, which is unable to detect the kind of chromosome segregation errors that are causing the instability. Consistent with this view, partial inhibition of SAC activity leads to high incidence of aneuploidy and tumourigenesis in mice (Li & Benezra, 1996; Michel et al, 2001; Dai et al, 2004).Clinically, the weakened SAC activity due to mutation of BubR1 results in Mosaic Variegated Aneuploidy (MVA) (Goshima & Vale, 2003), consistent with Boveri's hypothesis that aneuploidy can induce tumourigenesis (Boveri, 1914). MVA is an extremely rare disease that causes growth retardation, microcephaly and childhood cancer, with a higher rate of premature segregation of chromatids (Hanks et al, 2004; Matsuura et al, 2006). Reduced expression of Mad1, Mad2, Bub1 and CENP-E leads to spontaneous tumours. Also, more than 80% of colorectal cancer patients carry mutations in APC which can result in sequestering of

SAC proteins (Mad2 and BubR1) leading to a weak spindle checkpoint and ultimately aneuploidy (Draviam et al, 2006; Dikovskaya et al, 2007; Zhang et al, 2009).

In *Drosophila*, *mad2* mutations lead to a shorter metaphase, giving less time for the cellular machinery to correct any misorientation of chromosomes before the onset of anaphase (Buffin et al, 2007). Lagging chromosomes and chromosomal bridges are common in SAC protein mutants such as *mad2, bubR1*, *rough deal (rod)*, *zw10*, and *bub3* (Chapter 2; Basu et al, 1999; Prencipe et al, 2009). Similar to the spindle assembly checkpoint, mutations in other cell cycle regulators and checkpoint proteins (e.g. P53, ATM, BRCA1, Rb, cyclins, cyclin dependent kinases etc.) can also lead to CIN and aneuploidy (Thompson et al, 2010). The SAC is a well characterized mechanism for controlling missegregation which is why we have selected SAC inhibition to induce chromosomal instability in *Drosophila*.

1.8- Outcomes of chromosomal instability and aneuploidy

Chromosomal instability is a common feature of nearly all solid tumours and is also found in some haematological malignancies (Mertens et al, 1994). The main outcomes of CIN are aneuploidy and cancer, specially in those cells which are able to evade apoptosis (Wassmann & Benezra, 2001; Weaver et al, 2007; Thompson & Compton, 2008; Baker et al, 2009; Sotillo et al, 2010).

The link between chromosomal instability and tumourigenesis has been in discussion since 1914 when Theodore Boveri first observed the high number of aneuploid cells in cancer (Boveri, 1914) and now CIN is one of the hallmarks of cancer, also considered as a marker for advanced tumours (Mertens et al, 1994; Florl & Schulz, 2008; Walther et al, 2008). CIN is involved in tumour initiation and growth (Schvartzman et al, 2010): induction of CIN in mice leads to the formation of spontaneous lymphomas, liver and lung tumours (Cahill et al, 1998; Weaver et al, 2007). In addition, overexpression of the SAC in mice led to CIN and the development of mammary adenocarcinomas (Schvartzman et al, 2010). In most of these studies, another alteration was induced to get a viable CIN model so it is not clear whether CIN alone can initiate tumourigenesis (Fujiwara et al, 2005; Florl & Schulz, 2008; Schvartzman et al, 2010). Similarly, some cancers types are more prone to the development of CIN (Swanton et al, 2009). Imbalanced metabolism due to aneuploidy can result in DNA damage by generating

oxidative stress, leading to tumourigenesis (Williams et al, 2008). P53 normally limits tumourigenesis in aneuploid cells by inducing apoptosis in response to DNA damage but loss of p53 function is common in cancer (Vazquez et al, 2008).

It is not clear whether CIN may be sufficient to induce tumourigenesis. Loss or gain of chromosomes or parts of chromosomes due to CIN results in a wide range of phenotypes that will depend upon which gene or set of genes are lost or duplicated. One model is that low levels of CIN can be tolerated by cells initially and then the CIN enables these cells to acquire mutations in tumour suppressor genes that lead to more CIN tolerance and tumourigenesis. After the initiation of a tumour by mutation in oncogenes, CIN could act as a driver for the progression of the tumour in the latter stages which is consistent with established correlation of CIN with the aggressiveness and grades of tumour (Walther et al, 2008; M'kacher et al, 2010; Sotillo et al, 2010). Genomic instability can also drive tumourigenesis in non-cancerous stem cells (Miura et al, 2006; Shiras et al, 2007). In addition, chromosome missegreggation can directly lead to tumourigenesis by inducing DNA damage and translocation (Janssen & Medema, 2011) which facilitates the cell to acquire more mutations and heterogeneity.

On the other hand aneuploidy can act as an inhibitor of tumour growth and progression (Weaver & Cleveland, 2007; Pfau & Amon, 2012). In yeast, aneuploidy results in growth retardation, which is linked to an energy burden, proteotoxic and metabolic stress (Torres et al, 2007; Pfau & Amon, 2012). In humans, all the autosomal monosomies and most of the trisomies are lethal, except the small chromosomes (chromosome 13, 18 & 21) which encode fewer genes. Similarly aneuploid cell lines show a low growth rate as compared to diploid cell lines derived from cancer (Thompson & Compton, 2008). Furthermore, induction of CIN showed anti-tumourigenicity in the liver (Weaver et al, 2007) because liver cells are already highly aneuploid and it is shown that the increase in CIN beyond a certain level can be cytotoxic (Janssen & Medema, 2011). Induction of missegregation (via CENP-E) in tumours with pre-existing chromosomal instability or aneuploidy results in tumour suppression, due to a viability threshold effect (Kops et al, 2004). However, a reduced level of CENP-E leads to CIN and tumours in mice (Weaver & Cleveland, 2007). Excessive levels of aneuploidy also result in increased sensitivity to DNA damaging drugs (Weaver & Cleveland, 2007). In summary, CIN and aneuploidy cause sensitivity

to any further increase in stress, so stress can be used as a potential target for the treatment of tumours with chromosomal instability.

Nonetheless, the continuous effects of chromosomal instability in aneuploid cells allow them to evolve under selective conditions and overcome the suppression of growth (Pavelka et al, 2010). The intra-tumour heterogeneity leads to the gain of cellular fitness and adaptability against cellular and environmental stresses (Komarova, 2006). CIN also provides adaptability against metabolic stress by reprogramming metabolic pathways, which is common in cancer (Warburg, 1956; Yuneva et al, 2007; Puzio-Kuter, 2011). There is a strong relationship between CIN levels and poor prognosis (Walther et al, 2008; Choi et al, 2009), CIN can also leads to multi-drug resistance, metastasis, low survival rate and relapse (Duesberg et al, 2000; Nakamura et al, 2003; Jonkers et al, 2005; Li et al, 2005; Swanton et al, 2009; Sotillo et al, 2010; Lee et al, 2011)

In conclusion, the consequences of CIN and aneuploidy are linked to poor clinical outcomes i.e. low survival rate, drug resistance, metastasis and relapse. However, CIN can also act as an inhibitor of tumour. These effects are based on the optimal level of CIN or aneuploidy for each type of tissue. A low level of CIN and aneuploidy leads to a slow accumulation of mutations which results in tumourigenesis and low-moderate CIN levels can give rise to selective adaption to internal and external stresses and also linked to poor prognosis. On the other hand, excessive levels of CIN and aneuploidy in cells that are not adapted to them, results in deleterious effects which can lead to tumour suppression and cell death (Pfau & Amon, 2012). On the basis of these variable outcomes and the difference in CIN tolerance levels between normal and cancer cells, CIN has been considered as a target to overcome the negative clinical effects (tumourigenesis, metastasis, drug resistance) of CIN and/or to enhance apoptosis in tumours with chromosomal instability. The following section explains why CIN is a good target for cancer therapy and the details of previously used and current CIN targets.

1.9- Chromosomal instability as cancer target

As discussed previously, CIN in cancer leads to poor clinical outcomes, especially drug resistance which makes these tumours difficult to target with regular therapies (Swanton

et al, 2009; Sotillo et al, 2010). CIN levels are higher in malignant tumours than in benign ones (Yunis, 1983; Mitelman et al, 1997) and cancer cells can tolerate high levels of CIN compared to normal cells (Mitelman et al, 1997; Campbell et al, 2010; Janssen & Medema, 2011), so this difference offers an attractive target for a cancer-specific therapy.

Many approaches for targeting chromosomal instability for the treatment of cancer are currently in preclinical stages (Cimini et al, 2006; DeLuca et al, 2006; Bakhoum et al, 2009; Thompson et al, 2010). These include the manipulation of CIN levels in order to get better prognosis, generate sensitivity to current therapies or to decrease the cellular fitness. Alternatively, CIN cells can be targeted by altering the mechanisms which cancers use to tolerate high levels of CIN or CIN related stresses.

Kinetochores as a regulator of microtubule attachments to chromosome have been considered as a potential therapeutic target to modify levels of missegreggation in cancer (Cimini et al, 2006; Bakhoum et al, 2009; Bakhoum et al, 2009b). Alterations in the stability of microtubules also affect the process of segregation. Hyperstability of microtubules results in the increase of chromosomal missegreggation rate and the inhibitors of microtubule destabilizing proteins ((Liu et al, 2009); Aurora B) are in use as therapeutic targets (Payton et al, 2010; Tsuboi et al, 2011), because high levels of CIN are linked to decreased tumour fitness (Torres et al, 2007; Weaver & Cleveland, 2007; Birkbak et al, 2011; Pfau & Amon, 2012). In contrast, destabilization of attached microtubules up to a certain extent leads to a decrease in chromosomal instability which results in better prognosis (Bakhoum et al, 2009; Bakhoum et al, 2009b).

There are a few other studies that suggest the potential of manipulating CIN levels for anti-cancer therapy. For example, enhancement of chromosomal instability by telomerase inhibition can also increase the efficiency of conventional therapies and also decreases cellular fitness which can lead to cell death in tumours (Dome et al, 2005; Stewenius et al, 2007). Similarly, while reduction of CENP-E in mice results in a high rate of spleen and lung tumour formation, a further increase in CIN leads to high drug sensitivity and a decrease in tumourigenesis (Weaver et al, 2007). Bub1 deficiency in mice is linked to CIN and tumourigenesis, but further induction of CIN by depleting PTEN results in the reduction of tumour formation (Baker et al, 2009). Alteration in SAC activity is also linked to segregation defects: partial inhibition increases the

sensitivity to Paclitaxel only in cancer cells (Janssen et al, 2009). Inhibition of the SAC in tumour cells leads to growth inhibition (Colombo et al, 2010), especially in CIN tumours where cells with larger number of chromosomes need more time to properly align themselves for segregation (Janssen & Medema, 2011). Supernumerary centrosomes increase the chances of missegreggation and CIN, and mutations that alter the centrosome duplication cycle or affect the bipolar clustering of extra centrosomes, lead to chromosome missegreggation and can be used to target cells with pre-existing centrosome-related CIN (Rebacz et al, 2007; Kwon et al, 2008; Mazzorana et al, 2011; Kawamura et al, 2013; Korzeniewski et al, 2013).

There are many other mechanisms which are involved in controlling the faithful segregation of chromosomes to the daughter cells and alteration in these mechanisms could potentially be used to manipulate the level of CIN for therapeutic use. However, the manipulation CIN levels as a therapy is limited by the common adverse effects (i.e. haematological and neurological side effects) which are linked to mitotic drugs (Goa & Faulds, 1994; Lobert, 1997; Rowinsky, 1997). Furthermore, as discussed earlier, an increase in the rate of missegreggation in normal cells could potentially lead to tumourigenesis, drug resistance, metastasis and relapse (Gao et al, 2007; Heilig et al, 2009; Sotillo et al, 2010). However, targeting CIN optimally according to the levels of pre-existing CIN could potentially be used to make cells sensitive to other effective treatments.

An alternative approach to target CIN cells is to manipulate the mechanisms which are involved in tolerating high levels of CIN or the adaptations which cancer cells acquire to tolerate CIN related stresses. CIN and aneuploidy lead to energy and proteotoxic stress. Many cancers show overexpression of genes which are involved in protein translation and protein folding. Inhibition of proteins comprising these pathways can lead to growth suppression and cell death (Torres et al, 2007). For example, inhibition of autophagy (AICAR) and HSP90 (17-AAG) leads to growth suppression in colon cancer cell lines with pre-existing CIN (Tang et al, 2011; Pfau & Amon, 2012). Aneuploidy is also linked to metabolic alteration and oxidative stress; cancer cells modify themselves to tolerate these stresses. Targeting these metabolic adaptations could lead to cancer specific cell death (DeBerardinis et al, 2008). For example, higher antioxidant capacity and overexpression of oxidative stress response genes is common

in cancers, and knockdown of these genes leads to an increase in oxidative stress and hence cell death. G6PD, a key enzyme which regulates antioxidant and nucleotide levels via the pentose phosphate pathway, is higher in some cancers (Wang et al, 2012) and its inhibition makes the cell sensitive to radiotherapy and chemical oxidants (Zhang et al, 2014). Similarly, malic enzyme is also overexpressed in tumours and is involved in maintaining the redox potential of the cell, its knockdown inhibits the progression of these tumours (Ren et al, 2010). Other enzymes such as Catalase, Peroxiredoxins, and Thioredoxin Peroxidase protect the cell from oxidative damage and can be targeted for cancer therapy (Bauer, 2012).

In summary, targeting CIN and aneuploidy for cancer therapy has a therapeutic potential and further research is needed in identifying new approaches to manipulate CIN that can alter the fate of CIN cancer towards cell death. Moreover, assessing the state and level of chromosomal instability of a cancer cell could help in the selection and development of specific and more effective drugs for different types of CIN cancers. Furthermore, identification of genes that are required for CIN tolerance could serve as potential therapeutic targets that can specifically kill advanced and drug resistant tumours.

1.10- Animal models for chromosomal instability and cancer.

Genetic alteration that leads to misregulation of the cell cycle and defects in the cell's protection mechanisms can result in CIN and cancer. Chromosomal instability is one of the main mediators/facilitators of tumourigenesis, tumour progression and poor prognosis in cancer patients (Carter et al, 2006; Hanahan & Weinberg, 2011). Alternatively, massive CIN and aneuploidy also has tumour suppressive effects (Pfau & Amon, 2012). These properties of CIN make it a potent target for the treatment of cancer. To understand the causes, consequences and therapeutic potential of CIN, several studies have been done using different animal models and cell lines, which are briefly discussed in this section.

These models range from cancer cell lines, mouse, *Drosophila* and yeast, which have highly conserved cellular mechanisms controlling the integrity of cell cycle and the fate of the cells with chromosomal instability (Thompson et al, 2010).

For the identification of the causes and consequences of CIN, several genetic and proteomic profiling studies have been done on individual cancer samples and isolated cancer cell lines (Holland & Cleveland, 2012; McGranahan et al, 2012; Pfau & Amon, 2012). A panel of CIN cancer cell lines was also used for anti-cancer drug screening (Roschke & Kirsch, 2005; Roschke et al, 2005; Wallqvist et al, 2005). Although these cell line models provide a great understanding on the genetic background of CIN and its consequences, the main problem with them is that they already have a highly variable and unstable genome which makes it hard to differentiate whether any effect is due to the current CIN state or the previously disrupted genome. Specially, in order to identify mutations that are required for the survival and tolerance of CIN, it is necessary to have stable model system in which CIN be induced.

Several mouse models for CIN have been created by introducing changes in the expression of genes, which are mainly required for faithful segregation of sister chromatids during mitosis. Most of these mutations are related to weakening of mitotic checkpoint function, which is directly linked to CIN and cancer. Some alterations in genes (e.g. Cenp-E (Weaver & Cleveland, 2006), Mad2/Mad1 (Dobles et al, 2000; Iwanaga et al, 2007; Sotillo et al, 2007), Fzr1 (Artandi et al, 2000), Plk4 (Ko et al, 2005), Bub1 (Jeganathan et al, 2007), Cdc20 (Li et al, 2009), HEC1 (Diaz-Rodriguez et al, 2008), Aurora kinase A -AURKA (Wang et al, 2006), Trp53 and Kras (Hingorani et al, 2005)) are used to induce CIN which results in increased incidence of tumourigenesis in mice. Some mouse models for CIN (e.g. Bub1b, Bub3 and Rae1 (Kalitsis et al, 2000; Babu et al, 2003; Baker et al, 2004; Dai et al, 2004) showed increased sensitivity to carcinogen-induced tumours (For extensive reviews see (Foijer et al, 2008; Holland & Cleveland, 2009)). However, it is very difficult to do large scale screening for potential CIN specific drug targets in these models.

Aneuploid yeast strains (disomic for one chromosome) have been used for gene expression analysis to identify aneuploidy specific changes in cells (Torres et al, 2007). This model has identified the presence of aneuploidy related energy and proteotoxic stress which has the potential to specifically target aneuploid tumours (Pfau & Amon, 2012). A genome-wide RNAi screen was done in a multi-polar *Drosophila* S2 cell line model in order to identify the mutations that can induce lethality by altering the mechanisms which are required to tolerate multipolar division (Kwon et al, 2008).

However, these *Drosophila* cell lines have a highly variable and unstable genome which is not ideal for the identification of a CIN specific response.

In this study, *Drosophila* has been used as an *in vivo* CIN model system which allows the induction of CIN in an entirely wild type background. *Drosophila* provides a set of quick, easy and cost effective experimental tools, allowing tissue-specific knockdown and overexpression of genes that affect CIN cells (see chapter 2; (Shaukat et al, 2012)), which is not feasible in vertebrate models. The use of *Drosophila* as a model organism is not new: in 1921, Calvin Bridges presented the first characterization of aneuploidy and reported its deleterious effects in *Drosophila* (Bridges, 1921). Also, *Drosophila* is a highly recognized and well established model organism for cancer research (Brumby & Richardson, 2005; Manning et al, 2010; Dekanty et al, 2012). Several key pathways driving proliferation and metastasis were discovered and/or elucidated in this model organism, including the Ras, Hippo, Wnt and Notch pathways (Bier, 2005). Key elements of the spindle checkpoint were also first found in *Drosophila* (e.g. ZW10, Polo kinase, Aurora kinase), and *Drosophila* tumour models rapidly develop CIN (Caussinus & Gonzalez, 2005; Castellanos et al, 2008). The approach by which the induced-CIN model is generated in *Drosophila* for the screening and characterization of cell killers is further discussed in chapter 2 of this thesis.

1.11- Key points

In summary, the existing literature suggests that the CIN and aneuploidy phenotype are associated with the following properties:

- CIN and aneuploidy are hallmarks of cancer.
- CIN and aneuploidy are linked to tumourigenesis, progression, metastasis, low survival rate, drug resistance and relapse in cancer patients (need new therapies).
- CIN and aneuploidy are highly tolerated by cancer as compared to normal cells (can be used as a therapeutic target).
- CIN and aneuploidy are also linked to tumour suppression and cell death due to oxidative and proteotoxic effects (can be used as a target).
- CIN cancers are highly adaptive to internal and external stresses (can be used as a target).
- CIN is sensitive to alterations in DNA damage repair mechanism (can be targeted).
- Alteration in metabolic machinery prevents from the deleterious effects of CIN (can be targeted to make CIN cells sensitive to other therapies)
- Detailed screening and characterization of genes which are required for the survival of CIN cells, is highly desirable.
- A *Drosophila* model for CIN would be a useful tool for *in vivo* screening and characterization. The SAC is a well characterized cause of CIN and can be used to generate a *Drosophila* inducible CIN model.

1.12- Aims of the study

1. Generation of a CIN model system for the screening of CIN killers.
2. Screening of candidates whose knockdown can kill cells with chromosomal instability.
3. Characterization of screened candidates and their pathways which are involved in induction of CIN specific cell death.

AIM 1 and **AIM 2** are described in **Chapter 2** which is based on a published article and explains the generation of the *Drosophila* CIN model and the RNAi screening of

candidates whose knock down could potentially lead to cell death in cells with chromosomal instability.

AIM 3 is based on the characterization of selected candidates for the screening. **Chapter 3** explains the characterization of the JNK pathway candidates for their role in promoting CIN survival and the mechanism of cell death in JNK knockdown CIN cells. **Chapter 4** of this thesis also covers **Aim 3** of the study, and explains the effect of metabolic alterations on CIN cells which are already coping with cellular stresses.

Chapter 2

A Screen for Selective Killing of Cells with Chromosomal Instability Induced by a Spindle Checkpoint Defect

This chapter is based on the published article titled "*A screen for selective killing of cells with chromosomal instability induced by a spindle checkpoint defect*", which demonstrates the generation of a CIN model in *Drosophila* and the screening of candidates whose knockdown can induce cell death in cells with chromosomal instability.

Chromosomal instability is a common feature of cancer, specially advanced tumours which are resistant to conventional drugs (Mertens et al, 1994; Swanton et al, 2009). These cancer cells can tolerate high levels of CIN compared to normal cells, which offers an opportunity to specifically target these drug resistant tumours by targeting CIN. To identify possible targets for killing CIN cancer cells few large-scale screens have been done in yeast, *Drosophila* culture cells, and human cancer cell lines (Roschke & Kirsch, 2005; Roschke et al, 2005; Kwon et al, 2008). These CIN cell line model systems have always been unstable so it is difficult to analyse the separate effect of currently induced chromosomal missegregation from that of the already aberrant genome. To avoid that, a more direct approach is needed in which CIN is induced in an otherwise wild type background.

A range of mouse CIN models have been created by manipulating the expression of genes required for faithful mitosis (e.g. that are required for mitotic checkpoint), and have been used extensively to examine the link between CIN, aneuploidy and cancer. Inhibition of the SAC proteins Mad2 or BubR1 causes shorter metaphase, which leads to CIN, aneuploidy and tumour susceptibility in humans and mouse models. However, complete inhibition of SAC is lethal and requires p53 mutation for survival, which is not ideal because p53 is also involved in other cellular functions. Furthermore, no large scale screening for potential CIN specific targets has been carried out in these models, because it is not feasible using an *in vivo* mouse model. In this study, CIN was induced in *Drosophila melanogaster* by knocking down a SAC protein (Mad2). Mad2 knockdown is viable in *Drosophila* and results in shortening of metaphase (Buffin et al, 2007), giving cells less time to correctly orient their chromosomes before the onset of anaphase.This results in a high frequency of chromosomal bridges and lagging chromosomes (Shaukat et al, 2012).

To identify the potential targets for killing CIN cells, we did RNAi screening for genes required for the viability of cells with a CIN phenotype. Initial screening of kinase and

phosphatase identified 21 candidates whose knockdown induces apoptosis only in CIN cells. The rationale of this study is that for a therapy to be ideal and effective, the cell death should be restricted to the tumour, i.e. the cells that exhibit CIN. Genes identified included those involved in JNK signaling pathways, mitotic cytoskeletal regulation and metabolic pathways.

The outcome of the screen demonstrates that it is feasible to selectively kill cells with CIN without harming normal cells. The screen has identified candidates that are currently being pursued as cancer therapy targets (e.g. Nek2), confirming that the screen is able to identify promising drug targets of clinical significance. Further characterization of these candidates may contribute to identify novel mechanisms which help the cancer cells to acquire tolerance against the adverse effects of CIN and aneuploidy. Moreover, it can also help to specifically sensitize these drug resistant, CIN tumour cells to the conventional therapies.

Statement of Authorship

Title of Paper	A Screen for Selective Killing of Cells with Chromosomal Instability Induced by a Spindle Checkpoint Defect.
Publication Status	Published
Publication Details	Shaukat, Z., Wong, H.W.S., Nicolson, S., Saint, R.B., & Gregory, S.L. (2012) A Screen for Selective Killing of Cells with Chromosomal Instability Induced by a Spindle Checkpoint Defect. PLoS ONE 7(10): e47447. doi:10.1371/journal.pone.0047447 Corresponding E-mail: stephen.gregory@adelaide.edu.au

Author Contributions

By signing the Statement of Authorship, each author certifies that their stated contribution to the publication is accurate and that permission is granted for the publication to be included in the candidate's thesis.

Name of Principal Author	Zeeshan Shaukat		
Contribution to the paper	Conceived and designed the experiments Performed the experiments Analysed the data Contributed reagents/materials/analysis tools Wrote the paper		
Signature		Date	

Name of Co-Author	Heidi W. S. Wong		
Contribution to the paper	Conceived and designed the experiments Performed the experiments Contributed reagents/materials/analysis tools Analysed the data		
Signature		Date	6/5/2014

Name of Co-Author	Shannon Nicolson		
Contribution to the paper	Performed the experiments Analysed the data		
Signature		Date	

Name of Co-Author	Robert B. Saint		
Contribution to the paper	Conceived and designed the experiments Analysed the data Contributed reagents/materials/analysis tools		
Signature		Date	

Name of Co-Author	Stephen L. Gregory		
Contribution to the paper	Conceived and designed the experiments Performed the experiments Analysed the data Contributed reagents/materials/analysis tools Wrote the paper Correspondence		
Signature		Date	

OPEN ACCESS Freely available online

PLOS ONE

A Screen for Selective Killing of Cells with Chromosomal Instability Induced by a Spindle Checkpoint Defect

Zeeshan Shaukat[1], Heidi W. S. Wong[2], Shannon Nicolson[1], Robert B. Saint[2], Stephen L. Gregory[1]*

1 School of Molecular and Biomedical Sciences, University of Adelaide, Adelaide, South Australia, Australia, **2** Department of Genetics, University of Melbourne, Melbourne, Victoria, Australia

Abstract

Background: The spindle assembly checkpoint is crucial for the maintenance of a stable chromosome number. Defects in the checkpoint lead to Chromosomal INstability (CIN), which is linked to the progression of tumors with poor clinical outcomes such as drug resistance and metastasis. As CIN is not found in normal cells, it offers a cancer-specific target for therapy, which may be particularly valuable because CIN is common in advanced tumours that are resistant to conventional therapy.

Principal Findings: Here we identify genes that are required for the viability of cells with a CIN phenotype. We have used RNAi knockdown of the spindle assembly checkpoint to induce CIN in *Drosophila* and then screened the set of kinase and phosphatase genes by RNAi knockdown to identify those that induce apoptosis only in the CIN cells. Genes identified include those involved in JNK signaling pathways and mitotic cytoskeletal regulation.

Conclusions/Significance: The screen demonstrates that it is feasible to selectively kill cells with CIN induced by spindle checkpoint defects. It has identified candidates that are currently being pursued as cancer therapy targets (e.g. Nek2: NIMA related kinase 2), confirming that the screen is able to identify promising drug targets of clinical significance. In addition, several other candidates were identified that have no previous connection with mitosis or apoptosis. Further screening and detailed characterization of the candidates could potentially lead to the therapies that specifically target advanced cancers that exhibit CIN.

Citation: Shaukat Z, Wong HWS, Nicolson S, Saint RB, Gregory SL (2012) A Screen for Selective Killing of Cells with Chromosomal Instability Induced by a Spindle Checkpoint Defect. PLoS ONE 7(10): e47447. doi:10.1371/journal.pone.0047447

Editor: Barbara Jennings, University College London, United Kingdom

Received June 20, 2012; **Accepted** September 17, 2012; **Published** October 15, 2012

Copyright: © 2012 Shaukat et al. This is an open-access article distributed under the terms of the Creative Commons Attribution License, which permits unrestricted use, distribution, and reproduction in any medium, provided the original author and source are credited.

Funding: This work was funded in part by National Health and Medical Research Council grants 525477 and 1027878 (www.nhmrc.gov.au). No additional external funding was received for this study. The funders had no role in study design, data collection and analysis, decision to publish, or preparation of the manuscript.

Competing Interests: The authors have declared that no competing interests exist.

* E-mail: stephen.gregory@adelaide.edu.au

Introduction

Chromosomal INstability (CIN) is a common feature of nearly all solid tumors [1]. CIN results in ongoing numerical and structural aberrations of chromosomes as tumors proliferate, and is associated with poor clinical outcomes such as tumour metastasis and adaptability to environmental and chemical stresses [2,3]. Drug resistance and relapse is common in cancers with CIN as they evolve rapidly, making them difficult to target with regular therapies [4,5].

The most common errors seen in CIN cancer cells are lagging chromosomes and chromosomal bridges. The mechanisms proposed to be responsible for these errors include defects in: sister chromatid cohesion [6], kinetochore–spindle attachment [7], cytokinesis [8], and centrosome duplication [9]. Perhaps the best-characterized cause of chromosomal instability is weakening of the Spindle Assembly Checkpoint (SAC) [10,11].

The SAC is the only mechanism by which cells can detect aberrant kinetochore attachments in metaphase and delay the entry to anaphase until the problem is resolved, or otherwise induce apoptosis [12,13]. This mechanism is not perfect, so mutations that cause high rates of segregation defects or shorten the duration of the metaphase error checking can cause CIN and lead to tumorigenesis [10,11]. The list of mutations known to have effects on chromosomal segregation is long, and includes over- and under-expression of spindle checkpoint proteins and clinically relevant cancer mutations such as loss of Rb in retinoblastoma or Adenomatous Polyposis Coli (APC) in colorectal cancer [11,14]. Reduction of the SAC protein Mad2 (mitotic arrest deficient 2) or its partner proteins (e.g. BubR1: Budding uninhibited by benzimidazoles Related 1) have been shown to shorten metaphase, causing CIN, aneuploidy and tumour susceptibility in humans and mouse models [15–17]. However, even in those CIN cancers that retain a SAC capable of detecting gross spindle abnormalities [18], the checkpoint is not able to respond to the merotelic kinetochore attachments that cause instability [19]. Loss of function of p53, which is common in cancers [20], increases the tolerance level for such missegregation, allowing the continual reassortment of the genome seen in CIN tumours [21,22]. CIN levels are higher in malignant tumors than in benign ones [23,24] and CIN is not found in normal cells, so it offers an attractive target for a cancer-specific therapy. CIN is particularly common in tumour types that are most in need of new drugs (e.g. colorectal cancers). Targeting CIN could also help to limit the ability of cancer cells to evolve

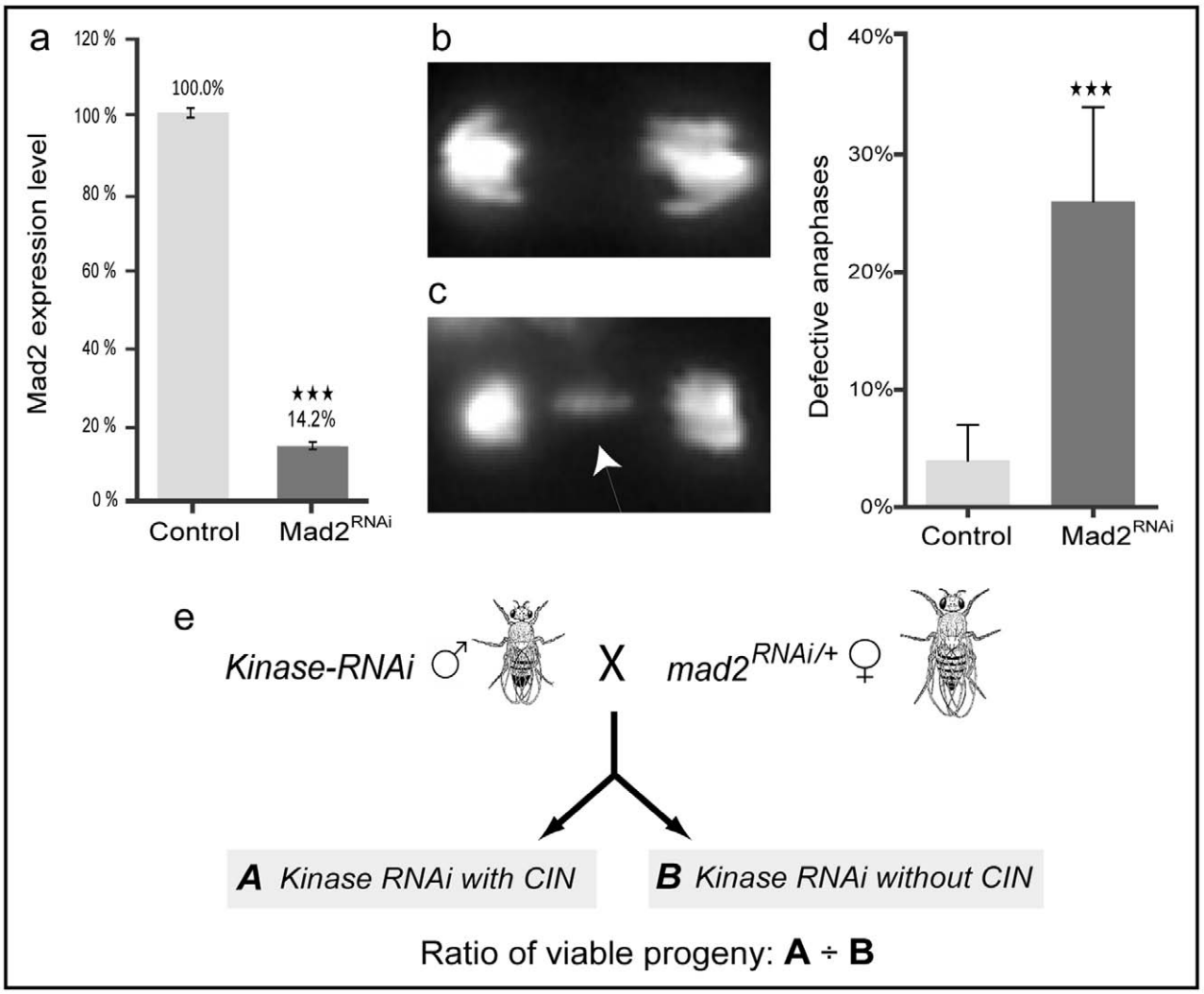

Figure 1. Establishment of a screening strategy using an induced-CIN model. (a) Reverse transcriptase-qPCR shows that the ubiquitous expression of UAS-*mad2* RNAi resulted in ~85% knocked down of *mad2* expression level (black bar) which is significantly less than the mad2 level in UAS-LacZ RNAi control (grey bar). Error bars represent SD. P-values are calculated by two-tailed Student's t-test: $p<0.001$ = ★★★. (b–c) Third instar larval brain cells stained with Hoechst 33342 to label DNA. (b) Normal segregation in a wild type anaphase. (c) Defective anaphase in an induced-CIN brain cell (*da*>*mad2*) resulting in a lagging chromosome (arrowed). (d) The fraction of defective anaphases (lagging chromosomes or bridges) observed in *mad2* knocked down (black bar) brain squashes and wild type controls (grey bar). Error bars represent 95% CIs. P-values are calculated by two-tailed Fisher's exact test: $p<0.001$ = ★★★. (e) Diagrammatic representation of viability screen crosses. Males with *Kinase-RNAi* (UAS-kinase^{dsRNA}) were crossed with females carrying the CIN background (UAS-*mad2*^{dsRNA}; *da-Gal4*). Progeny were double knockdown (A: *mad2* and *kinase*) or single knockdown (B: *kinase* only). The ratio of viable progeny A/B was used to rank candidates for further analysis.
doi:10.1371/journal.pone.0047447.g001

drug resistance and other poor clinical outcomes, which may increase the efficacy of current therapies.

Here we have used depletion of the SAC to induce CIN. We have then carried out a systematic genome-wide screen for kinase and phosphatase genes that, when depleted, can trigger apoptosis only in these genetically unstable cells, but not in normal cells. Our rationale is that for a therapy to be effective, cell death should be restricted to the tumour, i.e. the cells that exhibit CIN. We set up an assay system using *Drosophila melanogaster* in which we induced tissue-specific chromosomal instability in a wild type organism. We generated CIN by knocking down the SAC protein Mad2, which shortens metaphase, giving cells less time to correctly orient their chromosomes before the onset of anaphase [25], resulting in chromosomal bridges and lagging chromosomes. While there may be numerous defects that lead to CIN in a tumour, loss of Mad2 is found as a contributing factor in a range of CIN cancers [26,27] and more than 80% of colorectal cancers carry APC mutations that have been shown to sequester Mad2 [28] and BubR1 [29] at least in some cell lines [30].

Kinases and phosphatases are key regulatory enzymes controlling vital processes such as cell growth, differentiation, and survival [31]. Alteration in levels of these proteins can lead to abnormal cell growth and cell death mechanisms, which can result in tumorigenesis [32]. Many kinases and phosphatases are approved as good drug targets and currently they are the main focus of drug discovery efforts against cancer [33]. Our screening of kinase and phosphatase genes in a CIN background gave a set of potential candidates that reproducibly caused significant lethality via apoptosis in CIN flies compared to their non-CIN control siblings. The screen identified several groups of candidates including

centrosomal proteins such as Nek2, which is currently being pursued as a therapeutic target for cancer [34]. These results may contribute to the identification of novel targets that can specifically kill advanced, drug resistant, CIN tumor cells without harming normal cells.

Results

Screening for Candidate Knockdowns that Kill Cells with SAC-induced Chromosomal Instability

To generate a model system in which we could induce chromosomal instability we expressed dsRNA to knock down Mad2 and thereby weaken the SAC in *Drosophila*. Ubiquitous expression of *mad2* dsRNA in the whole organism gives ~85% reduction of Mad2 expression as compared to control *lacZ* dsRNA (Figure 1a). This depletion of Mad2 resulted in >25% of anaphases showing lagging chromosomes or chromosomal bridges in larval brains (Figure 1b–d), without compromising the overall viability of the organism. This survival, despite a significant rate of anaphase errors, is consistent with the viable amorphic *mad2* allele described by Buffin et al. [25]. We used this background to screen a set of gene knockdowns to identify candidates that could specifically kill cells with CIN but not normal dividing cells. We screened the *Drosophila* kinome, testing knockdown of 397 kinase and phosphatase genes for those that were lethal only in a CIN background (Figure 1e). This screening ranked the set of genes to identify those that when depleted in the whole organism, reproducibly caused the most lethality in CIN flies compared to their non-CIN control siblings (Table S1). The siblings vary only in whether or not they have induced CIN, so a deviation from the expected 1:1 ratio of CIN: non-CIN progeny indicated a CIN-specific effect of the candidate on viability. We observed the whole range of responses from complete lethality in a CIN background through to no effect, and we prioritized those candidates with the strongest CIN-specific lethality.

Screening for Cell Death

We investigated the cellular phenotypes of 26 kinases from the initial screen that gave more than 75% lethality in a CIN background, that is, more than four non-CIN for every one surviving CIN sibling. This lethality could have resulted from developmental or patterning failures, so we wished to test whether our candidates generated cell death in CIN cells. First, we examined the effect on wing development when candidates were depleted with or without *mad2* (Figure S1a), and these data were quantified by measuring the amount of tissue loss (notching) in the affected wing area (Figure S1b). 17 candidates resulted in significant cell loss in adult wings when Mad2 was reduced as compared to controls (Table 1). The most promising candidates identified from this screening included genes from some well characterized groups such as those involved in JNK (Jun N-terminal kinase) signaling and centrosomal regulation as well as others (e.g. PAS Kinase) with no previous connection to cell division.

Acridine Orange staining of larval wing discs showed significantly elevated levels of cell death when the candidates were knocked down in CIN cells (e.g. Figure 2), consistent with the wing tissue loss being caused by cell death in the affected region. Quantification of the Acridine Orange stains was carried out by measuring the average signal per unit area in each half of the disc and subtracting the background value (from the wild type, control half) from the RNAi affected half, to show the effect of the knockdown. This gave data consistent with the adult wing tissue loss results (complete data shown in Figures S2a and S2b). Note that loss of Mad2 by itself gave little cell death (Figure 2a'; [25]), as did depletion of the candidates alone (Figure 2b, 2c), consistent with these candidates only being required for the survival of genetically unstable cells. To validate our model we induced CIN by knocking down another SAC protein, BubR1 [35], and found that our candidates also induced cell death in this CIN background (e.g. Figure S4). Interestingly, not all candidates showing a high level of cell death in a CIN background were completely depleted by the candidate-RNAi. For example, *bsk* and *asp* knockdown still left 46% (±4%) and 63% (±3%) respectively of the wild type RNA levels when measured by qPCR. This partial knockdown was expected for essential genes like *bsk* and *asp*, because our original screen selected for candidate RNAi lines that were not lethal in normal cells. CIN cells must be highly sensitive to dosage variations in these candidates to give such strong phenotypes following modest candidate depletion, emphasizing the significant role these candidates have in cellular responses to CIN.

Apoptosis in CIN Cells

To confirm that the cell death observed was a result of the activation of apoptosis, we used antibody staining for the active form of effector caspase 3 (Figure 2e). Consistent with the results of Acridine Orange staining, knockdown of either Mad2 or a candidate alone showed little apoptosis-specific cleaved caspase 3 staining. However when we knocked down both *mad2* and a selected candidate (e.g. *asp: abnormal spindle*) we observed apoptosis in the affected area (dark staining in Fig. 2e''). Similar caspase results were seen for other candidates (data not shown). Together, these results suggest that knockdown of the candidates from our screen does not kill normal cells but does cause cell death by apoptosis in these CIN cells. This apoptosis could result if the candidate knockdowns generated CIN themselves, as high levels of CIN can be cell-lethal [36]. To test whether loss of our candidates induced apoptosis by increasing the level of CIN over a viability threshold, we tested whether their depletion induced CIN in normal cells by scoring mitotic cells from larval brains. We did not see any significant increase in anaphase errors (Figure S5), suggesting that depletion of the candidates alone does not generate CIN.

Involvement of DNA Damage

Because double-stranded DNA breaks are a well known cause of anaphase errors and are implicated in *p53* dependent cell death [37,38], we tested for DNA damage by anti-γH2aX antibody staining in knockdowns of selected candidates with and without Mad2 in larval wing discs (Figure 3). Depletion of *Pask, bsk, loki, Nek2, CG8878, asp, mbt or CG4041* in CIN cells gave an elevated level of DNA damage, compared to the *lacZ* RNAi negative control (Figure S3). Other candidates such as *aPKC*, when depleted in CIN cells, did not show a significantly elevated level of DNA damage as compared to the negative control (Figure S3), although they showed a high level of apoptosis (Figure S2A). In contrast, DNA damage in *Pask* (PAS kinase) depleted CIN cells was significantly higher than *aPKC* and *Nek2* (Figure 3 and S3), although *Pask* showed lower levels of apoptosis. Our results show that the CIN dependent apoptosis generated by candidate depletion was often, but not always, associated with an increase in double stranded DNA breaks.

P53 Dependence for Induced Cell Death in CIN Cells

Because P53 is commonly lost in tumours and has been implicated in their CIN tolerance [21,22], we tested the effect of P53 knockdown in several candidates from our screen. Specifical-

Table 1. Candidates giving CIN-dependent cell death.

Groups	Candidate symbol	Mammalian homolog	Functional association
Centrosomal	*Nek2*	NIMA-related kinase 2 (NEK2)	Cell cycle progression [61]
	lok	checkpoint homolog (Chk2)	DNA damage [62]
	asp	Abnormal spindle (Aspm)	Spindle organization [47]
	tefu	Ataxia telangiectasia mutated (ATM)	DNA damage response [62]
	bsk	JUN amino terminal kinase (JNK)	JNK signaling pathway [63]
JNK pathway	*bsk*	JUN amino terminal kinase (JNK)	JNK signaling pathway [63]
	pvr	PDGF/VEGF receptor	JNK activator [64]
	slpr	JUN kinase kinase kinase (JNKKK)	JNK signaling pathway [65]
	Pak3	p21 protein (Cdc42/Rac)-activated kinase 3 (PAK3)	JNK activator [66]
DNA damage	*lok*	checkpoint homolog (Chk2)	DNA damage [62]
	tefu	Ataxia telangiectasia mutated (ATM)	DNA damage response [62]
Wnt signaling pathway	*mbt*	p21 protein (Cdc42/Rac)-activated kinase 4 (PAK4)	Wnt signaling/cytoskeletal regulation [67]
	aPKC	Protein kinase C	Wnt signaling [68]
	Wnk	WNK lysine deficient protein kinase 1 (WNK1)	Ion regulation, cell cycle progression and adaptation [69]
Histone kinases	*CG8878*	vaccinia-related kinase (VRK)?	Histone kinase?
	ball	Nucleosomal histone kinase-1 (Nhk-1)	Histone kinase [70]
Others	*Pink1*	PTEN-induced putative kinase 1	apoptosis/mitophagy [71]
	lic	mitogen-activated protein kinase kinase 3 (MAP2K3)	MAP kinase-mediated signaling [72]
	CG4041	TBC1 domain containing kinase (TBCK)/Rab gtpase?	Unknown
	Pask	PAS kinase (PASKIN)	cellular energy homeostasis [52,53]

Candidates from the viability screening and cell death assay that gave the most CIN-dependent cell death. Some of the candidates are placed in more than one group on the basis of their associations.

doi:10.1371/journal.pone.0047447.t001

ly, we examined whether loss of P53 affected the ability of our candidates to induce cell death in a CIN background. Depletion of P53 suppressed the loss of tissue phenotype when *Pask* and *mad2* were both depleted in adult wings (data not shown) and significantly decreased the level of apoptosis in wing discs (Figure 4), suggesting that the cell death in this case was largely *p53* dependent. However for *asp*, depleting P53 had little effect in the double knockdown (*asp* and *mad2*) wing discs, showing that, in this case, the apoptosis induced by *asp* knockdown in CIN cells is largely P53 independent (Figure 4). Other candidates such as *bsk* (Jun kinase) gave a modest reduction in the level of cell death when P53 was depleted (data not shown), suggesting the involvement of both *p53* dependent and independent mechanisms in inducing cell death in this case.

Discussion

To identify targets that could be depleted to induce apoptosis in cells with chromosomal instability, we carried out RNAi screening of kinases and phosphatases in a CIN model system. We targeted CIN because it is common in cancers and CIN makes these cancers resistant to current therapies [3]. Using *Drosophila* as a model, we were able to induce CIN in a genetically stable background by depleting ~85% of Mad2, which weakens SAC function and shortens metaphase [25,39]. We found this gives an optimal level of CIN that is enough to screen against, but not so much that cells cannot survive. This approach has some advantages over using vertebrate CIN cell lines [40] which, by definition, have highly diverse and unstable genomes. In particular, we were able to test each candidate on genetically identical control tissues, which allowed us to be confident that any apoptosis was due to the effect of the checkpoint defect, not an artifact of a particular aberrant cell line.

The screen identified a significant group of candidates, including Nek2, JNK and Asp, that are directly or indirectly linked to the centrosome (Table 1). The centrosome is a regulatory hub of the major events during mitosis: alterations in centrosomal proteins and numbers result in segregation defects and CIN [41]. Extra centrosomes are common in cancer, and contribute to CIN by forming multi-polar spindles, which produce more merotely and lagging chromosomes and hence whole chromosome aneuploidy [42,43]. Our identification of Nek2, which is currently being pursued as therapeutic target for cancer [34], confirms that our screen has the potential to identify clinically significant drug targets for CIN tumors.

Members of the JNK pathway, which is known to promote apoptosis, DNA damage response, proliferation, migration and differentiation [44–46] were also found in our screen. Our results suggest a novel role for JNK in preventing cell death in response to mitotic errors. This may potentially explain the anti-apoptotic effect of JNK seen in HCC tumours and leukemia [44].

Abnormal spindle (Asp) binds at the minus end of microtubules, and is required for centrosome attachment [47] and possibly for down-regulating p53 [48]. In this respect it is interesting that we observed p53 independent cell death in *asp mad2* double depletions. This suggests that the apoptosis we observed was not simply a result of losing a negative regulator of p53. Further work will be required to determine what triggers cell death in this case.

Taken together, these results suggest that CIN cells are highly sensitive to centrosome disruption, responding by apoptosis to treatments that have no effect on normal dividing cells. One

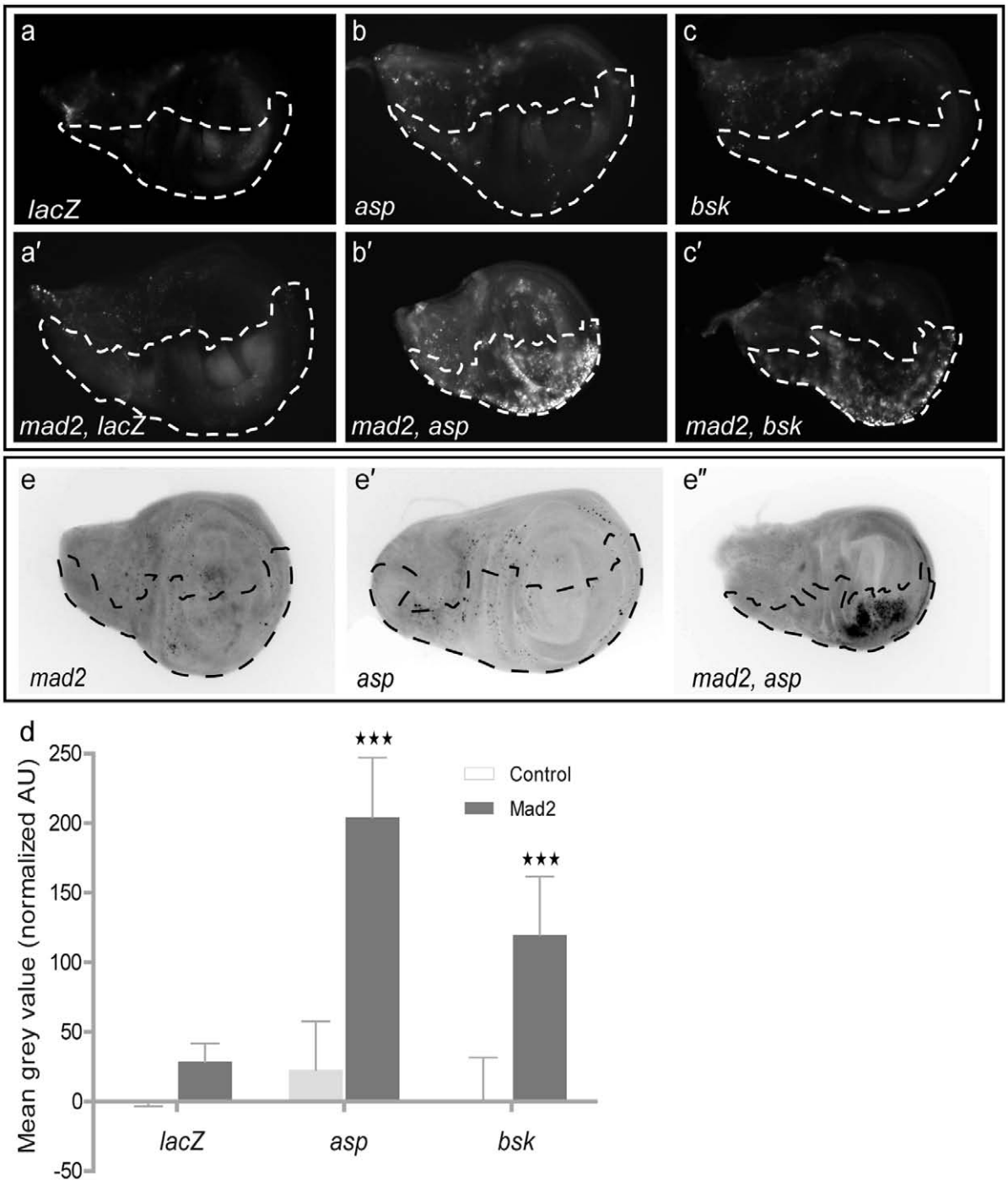

Figure 2. Cell death assays on larval wing discs. Dotted line shows the *en-CD8GFP* marked compartment or tester region in which genes were depleted. The other half of each wing disc expressed no transgenes and serves as an internal control. (a–c, a′–c′) Images of wing discs stained with Acridine Orange to show cell death. (a) Negative control (*lacZ RNAi*), (a′) *LacZ* and *mad2* RNAi, (b & c) Candidate RNAi (*asp* and *bsk*), (b′ & c′) double knockdown of candidate and Mad2. (d) Graph shows quantitation of Acridine Orange staining (above wild type) in control and candidate imaginal wing disc halves with or without *mad2* RNAi. Error bars represent 95% CIs, n≥8 in all cases. P-values were calculated by two-tailed t-tests with Welch's correction: $p<0.001$ = ★★★. (e-e′) Cleaved caspase 3 staining showing apoptosis in e: *mad2 RNAi,* e′: *asp RNAi* and double knockdown (e″: *asp RNAi* and *mad2 RNAi*).
doi:10.1371/journal.pone.0047447.g002

plausible hypothesis to explain this sensitivity was that the centrosome disruption by itself caused a certain rate of CIN, which when added to the CIN from Mad2 depletion, took the cells over a threshold of instability beyond which they were unviable [36]. Our data do not support this model, as we did not detect a significant rate of anaphase errors when any of our centrosomal candidates were depleted by themselves (Figure S5). An alternative explanation is that there is significant crosstalk between events at

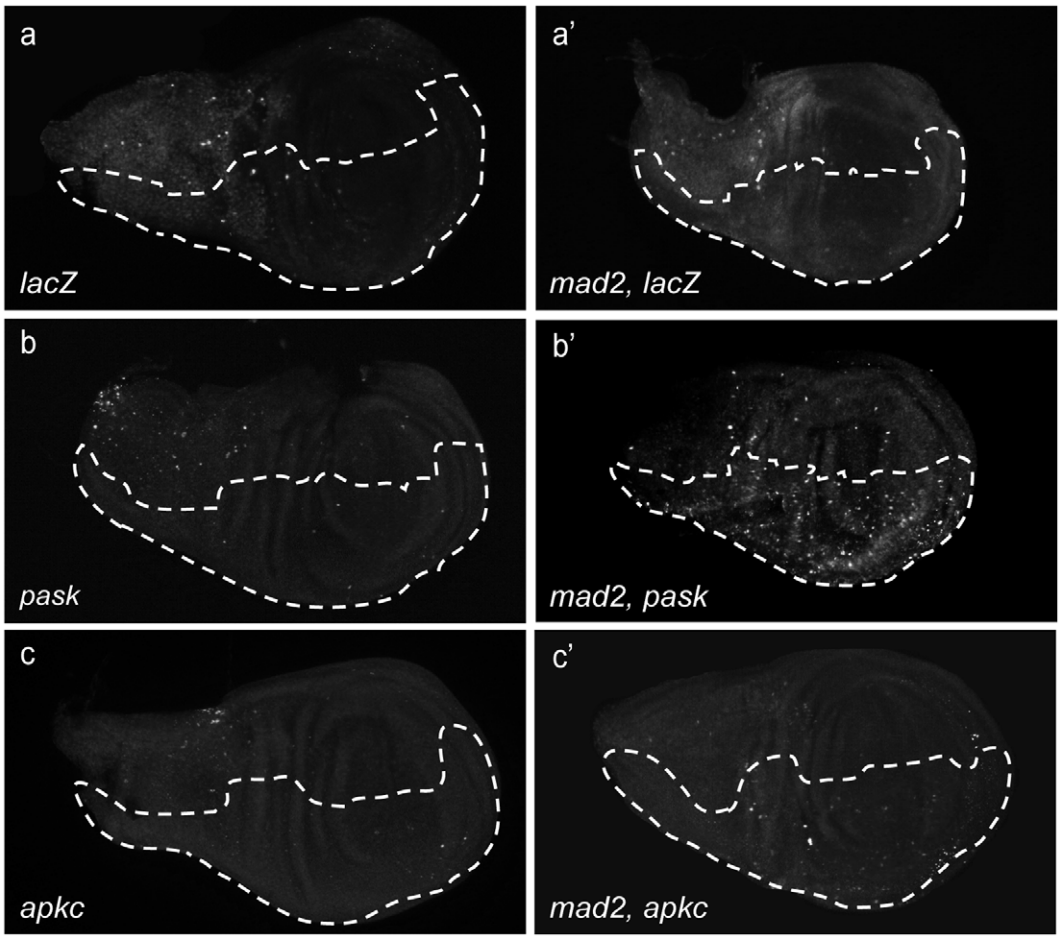

Figure 3. DNA damage (anti-P-H2AvD) staining of third instar larval wing discs. (a–c′) Dotted line shows the *en-CD8GFP* marked test region in which genes were depleted. The other half of each wing disc expressed no transgenes. (a, a′) Negative control (*LacZ RNAi*) with and without Mad2 (b, b′) PASK depletion with and without Mad2. (c, c′) aPKC depletion with and without Mad2. Significant induction of DNA damage in the depleted area is seen in *Pask, mad2* discs but not *LacZ, mad2* or *aPKC, mad2* discs.
doi:10.1371/journal.pone.0047447.g003

the centrosome and events at the kinetochore that renders SAC-deficient cells particularly dependent on centrosomal signals. This dependence may relate to the centrosomal localization of p53 [48,49], DNA damage repair proteins [50] or even Mad2 itself [51].

Several interesting candidates identified in our screen, however, are not localized on centrosomes (e.g. Pask and aPKC). Furthermore, some candidates have no reported connection of any kind with mitosis, indicating that we may have detected novel pathways that sense segregation defects and provide stability to cancer cells against CIN. For example, Pask is a serine/threonine kinase involved in sensing and regulating cellular energy homeostasis [52,53]. Here we show its novel role in preventing DNA damage and p53 dependent apoptosis in CIN cells. Our screen also isolated candidates that are involved in the DNA damage response (*tefu*, *lok*, *bsk*, and *pp1a*), suggesting a role for the DNA damage response pathway in responding to CIN. This is not surprising given the recent work showing that anaphase errors result in DNA damage [36,54] and the role of Mad2 in delaying anaphase onset to give time for repair [55].

It seems clear that the DNA damage we observed in our candidates in the presence of CIN is not simply part of the apoptotic program: we see strong apoptosis and little DNA damage in *aPKC* knockdown in CIN cells. Furthermore our highest levels of DNA damage were seen in *Pask mad2* double depletions, which gave no more apoptosis than *aPKC*. It is striking that none of our candidates alone, nor *mad2* alone, gives significant levels of DNA damage. Our interpretation of this is that the cellular DNA damage response can keep the level of damage below our detection sensitivity in any of the single depletions, and it is only when multiple checkpoint and repair mechanisms are depleted that we see unrepaired damage and widespread apoptosis.

Depletion of Asp or Bsk gives some P53 independent apoptosis in CIN cells, which could make them desirable therapeutic candidates in a clinical setting, where P53 is often absent [56], and indeed JNK inhibitors are currently in clinical trials [57]. Unfortunately, JNK is involved in many processes that make it problematic as a drug target [58]. However, the other candidates that regulate JNK signaling, (Hep: *hemipterous*/JNKK, Slpr: *slipper*/JNKKK, Pak3/Pak2 and Pvr: *PDGF/VEGF receptor*), may have potential as good CIN-specific targets.

In summary, we have used a new model for CIN in *Drosophila* to demonstrate the principle that it is possible to selectively kill CIN cells. Our RNAi knockdown identified candidates not previously known to have mitotic roles but whose depletion has the potential to kill proliferating CIN cells. Further characterization of screened candidates and their pathways may help to

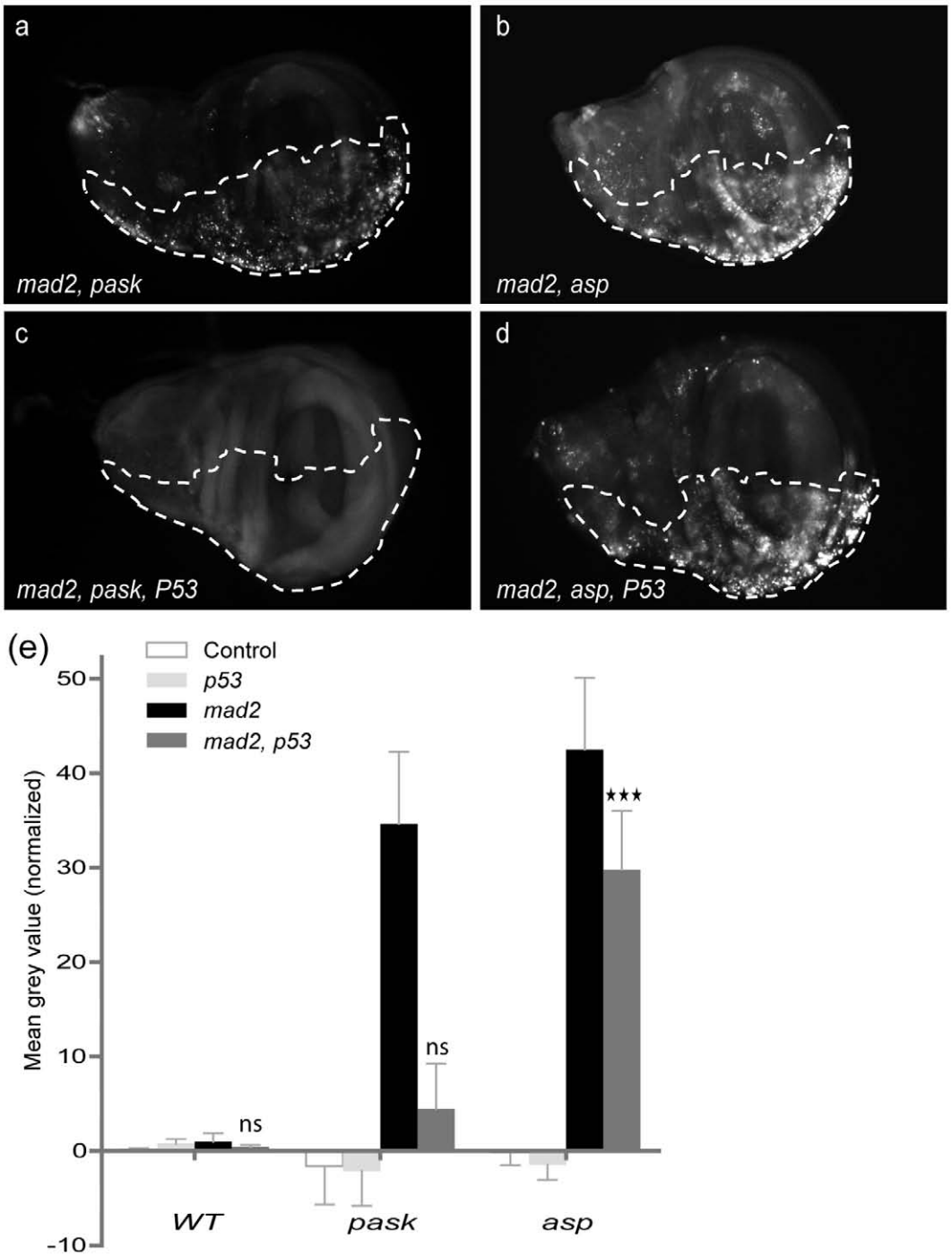

Figure 4. P53-dependent and p53-independent apoptosis. (a–d) Dotted line shows the *en>CD8GFP* marked test region and the other half expressed no transgenes. Acridine Orange staining on double (a–b: *Candidate* and *mad2*) and triple knockdown (c–d: *Candidate, mad2* and *p53*) wing discs. (e) Graph shows quantitation of Acridine Orange staining (above wild type) in control and candidate knocked down imaginal wing disc halves. The first bar of each group represents *candidate RNAi* alone (control), the second bar represents *candidate RNAi with p53RNAi* (P53), the third or black bar represents *Candidate* and *mad2* knocked down and the fourth bar represents triple knockdown (*Candidate, mad2* and *p53*). Error bars represent 95%CIs, n≥8 in all cases. P-values are calculated by two-tailed t-tests with Welch's correction: $p<0.001 = ★★★$ and $p>0.05 =$ ns (not significant). Tests compare *candidate mad2 p53* with *candidate* alone to test whether significant *p53*-independent cell death is seen when each candidate is co-depleted with Mad2. Significant levels of *p53*-independent cell death are seen for *asp, mad2* but not *Pask, mad2*.
doi:10.1371/journal.pone.0047447.g004

identify mechanisms by which cancer cells can tolerate the adverse effects of CIN and aneuploidy which in turn may lead to the identification of novel targets that can specifically kill advanced, drug resistant, CIN tumor cells without harming normal cells.

Materials and Methods

Stocks

All UAS-RNAi lines used, including 485 UAS- *Candidate RN*Ai (kinase and phosphatase) lines, were obtained from the Vienna *Drosophila* RNAi Centre. The *mad2-RNAi* line used was v47918. Ubiquitous expression was driven using *daughterless* (*da*)-*Gal4* and posterior wing disc expression was driven using *engrailed* (*en*)- or *hedgehog* (*hh*)-*Gal4* (Bloomington stock center).

Screening

In viability screening we have tested ubiquitous *(da>Gal4)* knockdown of candidates (the kinase and phosphatase genes, see Table S1) in the CIN background (*mad2 RNAi*): UAS>*mad2*-RNAi/CyO; *da>Gal4*/TM6 *tub>Gal80ts* × *UAS> candidate*-RNAi. The temperature of crosses was adjusted to give the best numbers of progeny while still getting effective knockdown (mostly 23°C). The ratio of the average viable fly count of double knockdown (*mad2* and *candidate*) over single knockdown (*candidate* only) progeny gave the level of viability of that candidate in CIN flies. Depletion of candidates that gave >75% lethality when *mad2* was co-depleted, compared to the candidate knockdown alone, were retested and, if reproducible, considered for further assays. This was measured by counting the number of surviving Cy versus non-Cy progeny from each cross, selecting those with a ratio of at least 4:1.

RNA Purification and Quantitative Real-time PCR (qPCR) Assays

For each genotype, thirty brains or sixty imaginal wing discs from third instar larvae were dissected in 1X PBS and quickly transferred and homogenized into pre-cooled Trizol reagent (Invitrogen). This was done in three biological replicates. Samples were then frozen in liquid nitrogen and kept in −80 C until RNA extraction. Total RNA was extracted with chloroform and precipitated with ethanol. RNA was further purified using the RNeasy Mini Kit (Qiagen).

The qPCR assays were carried out using protocols described in [59]. Each reaction was done in triplicate for all biological replicates. Superscript III (Invitrogen) was used to make cDNA and the relative quantitation was done by using the SYBR Green mix and ABI Prism 7000 Sequence Detection System (Applied Biosystems). The mRNA levels were normalized by the mRNA levels of house-keeping gene ribosomal protein 49 (rp49) from *Drosophila*.

Primers Pairs for Drosophila Mad2, Pask and Bsk qPCR Assay

mad2 F/R: GGCGACCAAAAACTGCATCA/GGTAAATTCCGCGTTGGAAGA, *bsk F/R:* GAATAGTATGCGCCGCTTACGA/ATTCCCTATATGCTCGCTTGGC, *asp F/R:* AGGCAAAGGCGGTAAACTCTGT/ACTCCGAACACCACATGAGCAG and (House-keeping gene) *rp49 F/R*: ATCGATATGCTAAGCTGTCGCAC/TGTCGATACCCTTGGGCTTG [59].

Histology

Loss of tissue in the posterior compartment of adult wings was scored by measuring the distance from where the fifth vein met the margin, to the fourth vein. Wings of adult females were dissected in ethanol and mounted in Aqua Poly/Mount (Polysciences, Inc.). Levels of CIN were tested by counting defective anaphases in fixed, Hoechst 33342 stained brain squashes as described [60]. Briefly, third instar larval brains were dissected in PBS, fixed for 30 minutes in 4% formaldehyde, then treated with 45% acetate for 30 seconds and put into a drop of 60% acetate for 3 minutes before squashing, freezing in liquid nitrogen and leaving in ethanol until staining with 5 ug/ml Hoechst 33342 in PBS plus 0.2% Tween20, then washing with PBST and mounting in 80% glycerol. All clear anaphases in each brain were photographed and scored as normal or defective. Defective included those with bridges, broken bridges or lagging chromosomes. Slides were coded and scored without knowing their genotype.

Cell death in 3rd instar larval imaginal wing discs was measured using a vital stain (Acridine Orange). Third instar larvae were selected and dissected, and imaginal discs were collected carefully in PBS. Imaginal wing discs were then incubated for 2 min in a 1 μM Acridine Orange solution and briefly rinsed in PBS before immediately mounting and imaging. The discs were transferred to a slide having double sided sticky tape on either side of the sample. This was done to prevent the squashing of discs when we placed a cover slip on top. Acridine staining was normalized by subtracting the mean intensity value of the wild type anterior compartment from the mean intensity value of the mutant posterior compartment (marked with *en>CD8GFP*), using ImageJ software. Before normalization, background noise was subtracted from all the images by setting the rolling ball radius at 10 pixels.

Cleaved caspase 3 immunostaining was performed on dissected wing imaginal discs. Single and double knockdown third instar larvae were selected and dissected in PBS and fixed in 4% formaldehyde for 20 minutes. Fixed discs were extensively washed with PBST (1xPBS+0.2% Tween) and then blocked by PBST containing 5% fetal calf serum (PBSTF) for 30 minutes. Discs were then incubated in primary antibody solution (1:100 Cleaved Caspase 3 Antibody from Cell Signaling in PBSTF) for 2.5 hrs at room temp or left overnight at 4°C followed by 2–3 quick washes with PBSTF and then 30 minutes in PBSTF. For secondary antibody staining, discs were incubated for 2 hrs in the dark at room temperature with 1:75 Anti rabbit CY-3 Antibody from Abacus/Jackson in PBST followed by 2–3 quick washes with PBST and then 30 minutes incubation in PBST. Mounting was done with 80% glycerol-PBS. DNA damage staining was done using the same method with rabbit anti-H2AvD P-Ser137 (1:700; Rockland) which is the *Drosophila* equivalent of vertebrate γH2aX, and anti-rabbit Cy3-conjugated secondary antibody (1:100; Abacus/Jackson). Quantitation of DNA damage staining *(anti-P-H2AvD)* was also done on normalized mean intensity value. Normalization was done by subtracting the mean intensity value of the wild type anterior compartment from the mean intensity value of the mutant posterior compartment (marked with *en>CD8GFP*), using ImageJ software. Before normalization, background noise was subtracted from all the images by setting the rolling ball radius at 5 pixels. All microscopy was done on a Zeiss Axioplan2 with Semrock Brightline filters and measurements and quantitation were done using Axiovision software (Carl Zeiss). Images were compiled using Axiovision (Carl Zeiss), Photoshop and Illustrator (Adobe) software.

Supporting Information

Figure S1 a. Loss of tissue in adult wings. *Engrailed*-driven single (*candidate-RNAi* only) and double (*candidate* and *mad2-RNAi*) knockdown in adult *Drosophila* wings. This driver depleted genes only in the posterior compartment of the wing, the lower half of each wing in this figure. We measured the loss of tissue by measuring the shortest distance from where the fifth longitudinal vein met the margin, to the fourth longitudinal vein (arrows).

Depletion of *Pask* shows posterior wing margin notching (arrowheads) along with shorter inter-vein distance (see Figure S1b), when co-depleted with *mad2* RNAi. ***Figure S1 b:*** *Quantification of loss of tissue in adult wings:* Graph shows the average distance between 4th and 5th vein of adult wings as in S1a, which measures loss of tissue in the *engrailed* test region. Light grey bars represent *candidate RNAi* alone, dark grey bars show double knockdowns (*candidate RNAi* with *mad2 RNAi*). Negative control (W^{1118}) showed no significant tissue loss with (black bar) or without CIN. The Y-axis starts from 250 µm, to improve resolution. dWNK was an outlier not included in this graph, showing an inter-vein distance without and with *mad2 RNAi* of 245 µm and 60 µm respectively. Error bars represent 95%CIs, n≥8 in all cases.
(PDF)

Figure S2 a:Quantitation of Acridine Orange staining on larval wing discs. Graph shows quantitation of Acridine Orange staining of control and candidate-RNAi imaginal wing discs. Quantification shows arbitrary grey value units normalized by subtracting the mean grey value of the wild type (anterior) region from the mean grey value of the affected (posterior) region for each disc. Negative control (*LacZ RNAi)* and *candidate RNAi* alone are represented in light grey bars and the double knockdowns of candidates with *mad2* are represented by dark grey bars, while double knockdown of *mad2* with the *LacZ* negative control is shown in black. Error bars indicate 95%CIs, n≥8 in all cases. P-values are calculated by two-tailed t-tests with Welch's correction: $p<0.001 = ★★★$, $p\ 0.001-0.01 = ★★$, $p\ 0.01-0.05 = ★$. All t-tests compare *candidate-RNAi mad2-RNAi* with *lacZ-RNAi mad2-RNAi.* **Figure S2. (b1–b4):Acridine Orange staining on larval wing discs (complete data).** All wing discs are stained with Acridine Orange and the dotted line shows the *en>CD8GFP* marked posterior compartment or test region in which the genes were depleted. The other half of each disc expressed no transgenes. Single knockdowns of each candidate are arranged on the right and the double knockdowns with *mad2* are on the left side. Representative discs for each genotype are shown; the level of variation for each genotype can be seen in Figure S2A.
(PDF)

Figure S3 DNA damage staining quantitation. Graph shows a quantitative analysis of DNA damage (anti-P-H2AvD staining). The Y-axis represents the level of P-H2AvD staining in the affected half normalized by subtracting the level in the control half for each disc. Light grey bars represent the candidate knockdown in wild type background and dark grey bars represent the double (*candidate* and *mad2*) knockdown. Error bars indicate 95%CIs, n≥8 in all cases. P-values are calculated by two-tailed t-tests with Welch's correction: $p<0.001 = ★★★$, $p\ 0.01-0.05 = ★$ and $p>0.05$ = ns (not significant).
(TIF)

Figure S4 Cell death assay for the validation of Mad2 results with BubR1. Dotted line shows the *en>CD8GFP* region or tester region and the other half expresses no transgenes (a-f) Images of wing discs stained with Acridine Orange. (a) *mad2* RNAi (d) *bubR1* RNAi. (b & e) *Pask* RNAi. Double knockdowns are (c): *Pask RNAi* and *mad2 RNAi* and (f): *Pask RNAi* and *bubR1 RNAi.*
(TIF)

Figure S5 CIN levels. Graph represents the frequency of defective anaphases in knockdowns of LacZ, Asp, Bsk, aPKC, Pask and Mad2 in brain cells. LacZ was used as a negative RNAi control and Mad2 is used as positive control to compare the level of CIN. None of the candidates show significantly elevated levels of CIN above the LacZ control. Error bars show 95%CIs, n>40 in all cases. P-values are calculated by two-tailed Fisher's exact test: $p<0.001 = ★★★$ (extremely significant) and $p>0.05$ = ns (not significant).
(TIF)

Table S1 List of kinases and phosphatases tested in the viability screening of our induced-CIN model. Columns show: the gene identifiers; number of replicate crosses carried out; total numbers of CyO (*kinase*-RNAi only) and non-CyO (*kinase*, *mad2* RNAi) progeny; Ratio of the average number of Cy/non-Cy progeny per cross used to rank the table; and probability of finding a cross this diverged or more diverged from a 50/50 ratio (the null hypothesis), out of this number of crosses (936), purely by chance.
(XLSX)

Acknowledgments

We thank the Bloomington and VDRC stock centers for provision of flies. We thank the University of Adelaide and University of Melbourne for providing facilities and student scholarships.

Author Contributions

Conceived and designed the experiments: RBS SLG. Performed the experiments: ZS HWSW SN SLG. Analyzed the data: ZS HWSW SN SLG. Wrote the paper: ZS SLG.

References

1. Mertens F, Johansson B, Mitelman F (1994) Isochromosomes in neoplasia. Genes, Chromosomes and Cancer 10: 221–230.
2. Gao C, Furge K, Koeman J, Dykema K, Su Y, et al. (2007) Chromosome instability, chromosome transcriptome, and clonal evolution of tumor cell populations. Proceedings of the National Academy of Sciences 104: 8995–9000.
3. Heilig CE, Löffler H, Mahlknecht U, Janssen JWG, Ho AD, et al. (2009) Chromosomal instability correlates with poor outcome in patients with myelodysplastic syndromes irrespectively of the cytogenetic risk group. Journal of Cellular and Molecular Medicine 14: 895–902.
4. Swanton C, Nicke B, Schuett M, Eklund AC, Ng C, et al. (2009) Chromosomal instability determines taxane response. Proceedings of the National Academy of Sciences 106: 8671–8676.
5. Sotillo R, Schvartzman J-M, Socci ND, Benezra R (2010) Mad2-induced chromosome instability leads to lung tumour relapse after oncogene withdrawal. Nature 464: 436–440.
6. Jallepalli PV, Waizenegger IC, Bunz F, Langer S, Speicher MR, et al. (2001) Securin Is Required for Chromosomal Stability in Human Cells. Cell 105: 445–457.
7. Thompson SL, Compton DA (2008) Examining the link between chromosomal instability and aneuploidy in human cells. The Journal of Cell Biology 180: 665–672.
8. Fukasawa K, Vande Woude GF (1997) Synergy between the Mos/mitogen-activated protein kinase pathway and loss of p53 function in transformation and chromosome instability. Molecular and Cellular Biology 17: 506–518.
9. Pihan GA, Purohit A, Wallace J, Malhotra R, Liotta L, et al. (2001) Centrosome Defects Can Account for Cellular and Genetic Changes That Characterize Prostate Cancer Progression. Cancer Research 61: 2212–2219.
10. Weaver BA, Cleveland DW (2006) Does aneuploidy cause cancer? Curr Opin Cell Biol 18: 658–667.
11. Thompson SL, Bakhoum SF, Compton DA (2010) Mechanisms of Chromosomal Instability. Current biology: CB 20: R285–R295.
12. Musacchio A, Salmon ED (2007) The spindle-assembly checkpoint in space and time. Nat Rev Mol Cell Biol 8: 379–393.
13. Rieder CL, Maiato H (2004) Stuck in division or passing through: what happens when cells cannot satisfy the spindle assembly checkpoint. Dev Cell 7: 637–651.
14. Cahill DP, Lengauer C, Yu J, Riggins GJ, Willson JKV, et al. (1998) Mutations of mitotic checkpoint genes in human cancers. Nature 392: 300–303.

15. Michel LS, Liberal V, Chatterjee A, Kirchwegger R, Pasche B, et al. (2001) MAD2 haplo-insufficiency causes premature anaphase and chromosome instability in mammalian cells. Nature 409: 355–359.
16. Hanks S, Coleman K, Reid S, Plaja A, Firth H, et al. (2004) Constitutional aneuploidy and cancer predisposition caused by biallelic mutations in BUB1B. Nat Genet 36: 1159–1161.
17. Schvartzman J-M, Sotillo R, Benezra R (2010) Mitotic chromosomal instability and cancer: mouse modelling of the human disease. Nat Rev Cancer 10: 102–115.
18. Wood LD, Parsons DW, Jones S, Lin J, Sjoblom T, et al. (2007) The Genomic Landscapes of Human Breast and Colorectal Cancers. Science 318: 1108–1113.
19. Cimini D, Howell B, Maddox P, Khodjakov A, Degrassi F, et al. (2001) Merotelic Kinetochore Orientation Is a Major Mechanism of Aneuploidy in Mitotic Mammalian Tissue Cells. The Journal of Cell Biology 153: 517–528.
20. Hollstein M, Sidransky D, Vogelstein B, Harris C (1991) p53 mutations in human cancers. Science 253: 49–53.
21. Burds AA, Lutum AS, Sorger PK (2005) Generating chromosome instability through the simultaneous deletion of Mad2 and p53. Proceedings of the National Academy of Sciences of the United States of America 102: 11296–11301.
22. Kasiappan R, Shih H-J, Chu K-L, Chen W-T, Liu H-P, et al. (2009) Loss of p53 and MCT-1 Overexpression Synergistically Promote Chromosome Instability and Tumorigenicity. Molecular Cancer Research 7: 536–548.
23. Yunis J (1983) The chromosomal basis of human neoplasia. Science 221: 227–236.
24. Mitelman F, Johansson B, Mandahl N, Mertens F (1997) Clinical significance of cytogenetic findings in solid tumors. Cancer Genetics and Cytogenetics 95: 1–8.
25. Buffin E, Emre D, Karess RE (2007) Flies without a spindle checkpoint. Nat Cell Biol 9: 565–572.
26. Prencipe M, McGoldrick A, Perry AS, O'Grady A, Phelan S, et al. (2010) MAD2 downregulation in hypoxia is independent of promoter hypermethylation. Cell Cycle 9: 2856–2865.
27. Furlong F, Fitzpatrick P, O'Toole S, Phelan S, McGrogan B, et al. (2012) Low MAD2 expression levels associate with reduced progression-free survival in patients with high-grade serous epithelial ovarian cancer. The Journal of Pathology 226: 746–755.
28. Zhang J, Neisa R, Mao Y (2009) Oncogenic Adenomatous Polyposis Coli Mutants Impair the Mitotic Checkpoint through Direct Interaction with Mad2. Molecular Biology of the Cell 20: 2381–2388.
29. Dikovskaya D, Schiffmann D, Newton IP, Oakley A, Kroboth K, et al. (2007) Loss of APC induces polyploidy as a result of a combination of defects in mitosis and apoptosis. The Journal of Cell Biology 176: 183–195.
30. Draviam VM, Shapiro I, Aldridge B, Sorger PK (2006) Misorientation and reduced stretching of aligned sister kinetochores promote chromosome missegregation in EB1- or APC-depleted cells. EMBO J 25: 2814–2827.
31. Hunter T (2000) Signaling–2000 and Beyond. Cell 100: 113–127.
32. Blume-Jensen P, Hunter T (2001) Oncogenic kinase signalling. Nature 411: 355–365.
33. Zhang J, Yang PL, Gray NS (2009) Targeting cancer with small molecule kinase inhibitors. Nat Rev Cancer 9: 28–39.
34. Suzuki K, Kokuryo T, Senga T, Yokoyama Y, Nagino M, et al. (2010) Novel combination treatment for colorectal cancer using Nek2 siRNA and cisplatin. Cancer Science 101: 1163–1169.
35. Weaver BAA, Cleveland DW (2009) The role of aneuploidy in promoting and suppressing tumors. The Journal of Cell Biology 185: 935–937.
36. Janssen A, Kops GJPL, Medema RH (2009) Elevating the frequency of chromosome mis-segregation as a strategy to kill tumor cells. Proceedings of the National Academy of Sciences 106: 19108–19113.
37. Mills KD, Ferguson DO, Alt FW (2003) The role of DNA breaks in genomic instability and tumorigenesis. Immunological Reviews 194: 77–95.
38. Kaye JA, Melo JA, Cheung SK, Vaze MB, Haber JE, et al. (2004) DNA Breaks Promote Genomic Instability by Impeding Proper Chromosome Segregation. Current Biology 14: 2096–2106.
39. Orr B, Bousbaa H, Sunkel CE (2007) Mad2-independent Spindle Assembly Checkpoint Activation and Controlled Metaphase–Anaphase Transition in Drosophila S2 Cells. Molecular Biology of the Cell 18: 850–863.
40. Roschke AV, Kirsch IR (2005) Targeting Cancer Cells by Exploiting Karyotypic Complexity and Chromosomal Instability. Cell Cycle 4: 679–682.
41. Duensing A, Duensing S (2010) Centrosomes, polyploidy and cancer. Adv Exp Med Biol 676: 93–103.
42. Mazzorana M, Montoya G, B. Mortuza G (2011) The Centrosome: A Target for Cancer Therapy. Current Cancer Drug Targets 11: 600–612.
43. Galimberti F, Thompson SL, Ravi S, Compton DA, Dmitrovsky E (2011) Anaphase Catastrophe Is a Target for Cancer Therapy. Clinical Cancer Research 17: 1218–1222.
44. Wagner EF, Nebreda AR (2009) Signal integration by JNK and p38 MAPK pathways in cancer development. Nat Rev Cancer 9: 537–549.
45. McEwen DG, Peifer M (2005) Puckered, a Drosophila MAPK phosphatase, ensures cell viability by antagonizing JNK-induced apoptosis. Development 132: 3935–3946.
46. Gutierrez GJ, Tsuji T, Cross JV, Davis RJ, Templeton DJ, et al. (2010) JNK-mediated Phosphorylation of Cdc25C Regulates Cell Cycle Entry and G2/M DNA Damage Checkpoint. Journal of Biological Chemistry 285: 14217–14228.
47. Wakefield JG, Bonaccorsi S, Gatti M (2001) The Drosophila Protein Asp Is Involved in Microtubule Organization during Spindle Formation and Cytokinesis. The Journal of Cell Biology 153: 637–648.
48. Lunardi A, Di Minin G, Provero P, Dal Ferro M, Carotti M, et al. (2010) A genome-scale protein interaction profile of Drosophila p53 uncovers additional nodes of the human p53 network. Proceedings of the National Academy of Sciences 107: 6322–6327.
49. Ma Z, Izumi H, Kanai M, Kabuyama Y, Ahn NG, et al. (2006) Mortalin controls centrosome duplication via modulating centrosomal localization of p53. Oncogene 25: 5377–5390.
50. Tritarelli A, Oricchio E, Ciciarello M, Mangiacasale R, Palena A, et al. (2004) p53 Localization at Centrosomes during Mitosis and Postmitotic Checkpoint Are ATM-dependent and Require Serine 15 Phosphorylation. Molecular Biology of the Cell 15: 3751–3757.
51. Liu Q, Hirohashi Y, Du X, Greene MI, Wang Q (2010) Nek2 targets the mitotic checkpoint proteins Mad2 and Cdc20: A mechanism for aneuploidy in cancer. Experimental and Molecular Pathology 88: 225–233.
52. Schläfli P, Borter E, Spielmann P, Wenger R (2009) The PAS-domain kinase PASKIN: a new sensor in energy homeostasis. Cellular and Molecular Life Sciences 66: 876–883.
53. MacDonald P, Rorsman P (2011) Per-arnt-sim (PAS) domain kinase (PASK) as a regulator of glucagon secretion. Diabetologia 54: 719–721.
54. Crasta K, Ganem NJ, Dagher R, Lantermann AB, Ivanova EV, et al. (2012) DNA breaks and chromosome pulverization from errors in mitosis. Nature advance online publication.
55. Dotiwala F, Harrison JC, Jain S, Sugawara N, Haber JE (2010) Mad2 Prolongs DNA Damage Checkpoint Arrest Caused by a Double-Strand Break via a Centromere-Dependent Mechanism. Current Biology 20: 328–332.
56. Petitjean A, Achatz MIW, Borresen-Dale AL, Hainaut P, Olivier M (2007) TP53 mutations in human cancers: functional selection and impact on cancer prognosis and outcomes. Oncogene 26: 2157–2165.
57. Bogoyevitch MA, Arthur PG (2008) Inhibitors of c-Jun N-terminal kinases" JuNK no more? Biochimica et Biophysica Acta (BBA) - Proteins & Proteomics 1784: 76–93.
58. Bogoyevitch MA, Ngoei KRW, Zhao TT, Yeap YYC, Ng DCH (2009) c-Jun N-terminal kinase (JNK) signaling: Recent advances and challenges. Biochimica et Biophysica Acta (BBA) - Proteins & Proteomics 1804: 463–475.
59. Lawlor KT, O'Keefe LV, Samaraweera SE, van Eyk CL, McLeod CJ, et al. (2011) Double-stranded RNA is pathogenic in Drosophila models of expanded repeat neurodegenerative diseases. Human Molecular Genetics 20: 3757–3768.
60. Williams BC, Goldberg ML (1994) Determinants of Drosophila zw10 protein localization and function. Journal of Cell Science 107: 785–798.
61. Sonn S, Oh GT, Rhee K (2011) Nek2 and its substrate, centrobin/Nip2, are required for proper meiotic spindle formation of the mouse oocytes. Zygote 19: 15–20.
62. Smith J, Mun Tho L, Xu N, A. Gillespie D (2010) The ATM-Chk2 and ATR-Chk1 pathways in DNA damage signaling and cancer. Advances in Cancer Research. 73–112.
63. Stronach B (2005) Dissecting JNK signaling, one KKKinase at a time. Developmental Dynamics 232: 575–584.
64. Ishimaru S, Ueda R, Hinohara Y, Ohtani M, Hanafusa H (2004) PVR plays a critical role via JNK activation in thorax closure during Drosophila metamorphosis. EMBO J 23: 3984–3994.
65. Polaski S, Whitney L, Barker BW, Stronach B (2006) Genetic Analysis of Slipper/Mixed Lineage Kinase Reveals Requirements in Multiple Jun-N-Terminal Kinase-Dependent Morphogenetic Events During Drosophila Development. Genetics 174: 719–733.
66. Liu RX, Wang WQ, Ye L, Bi YF, Fang H, et al. (2010) p21-Activated kinase 3 is overexpressed in thymic neuroendocrine tumors (carcinoids) with ectopic ACTH syndrome and participates in cell migration. Endocrine 38: 38–47.
67. Menzel N, Schneeberger D, Raabe T (2007) The Drosophila p21 activated kinase Mbt regulates the actin cytoskeleton and adherens junctions to control photoreceptor cell morphogenesis. Mechanisms of Development 124: 78–90.
68. De A (2011) Wnt/Ca2+ signaling pathway: a brief overview. Acta Biochimica et Biophysica Sinica 43: 745–756.
69. Moniz S, Jordan P (2010) Emerging roles for WNK kinases in cancer. Cellular and Molecular Life Sciences 67: 1265–1276.
70. Aihara H, Nakagawa T, Yasui K, Ohta T, Hirose S, et al. (2004) Nucleosomal histone kinase-1 phosphorylates H2A Thr 119 during mitosis in the early Drosophila embryo. Genes & Development 18: 877–888.
71. Kawajiri S, Saiki S, Sato S, Hattori N (2011) Genetic mutations and functions of PINK1. Trends in pharmacological sciences 32: 573–580.
72. Shiryaev A, Moens U (2010) Mitogen-activated protein kinase p38 and MK2, MK3 and MK5: Ménage à trois or ménage à quatre? Cellular Signalling 22: 1185–1192.

Figure S1

a

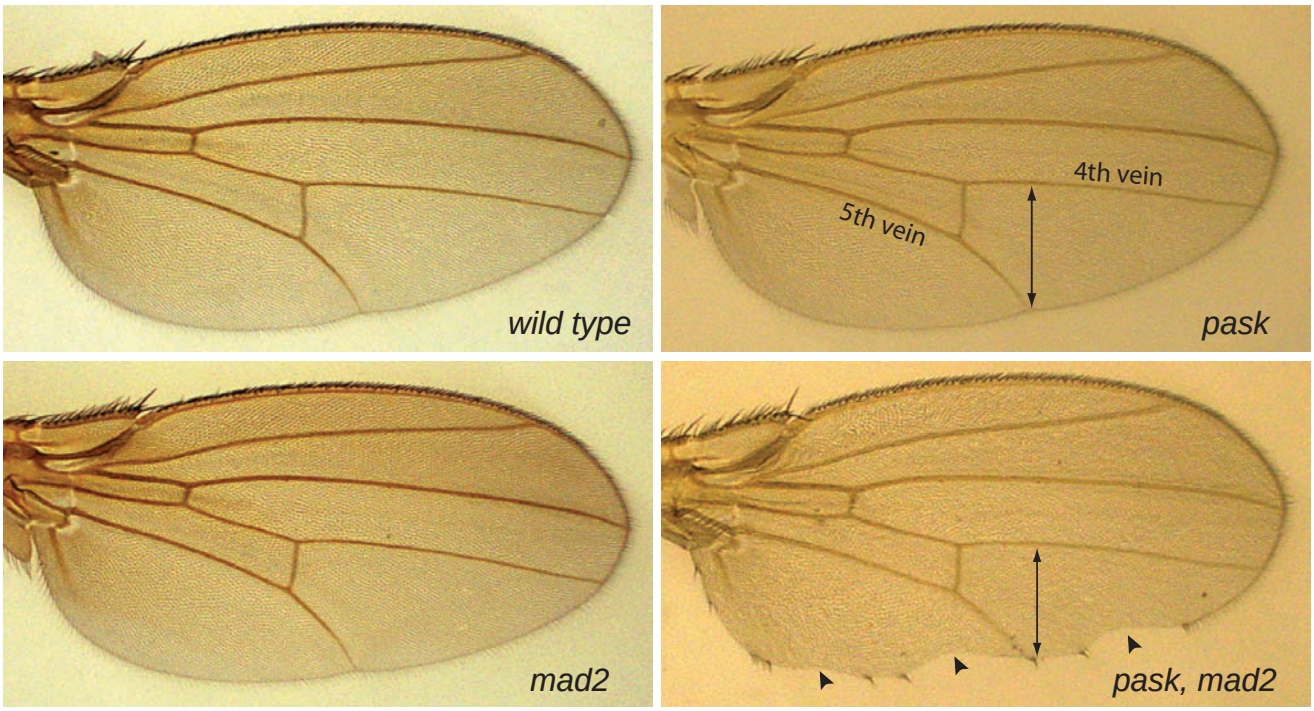

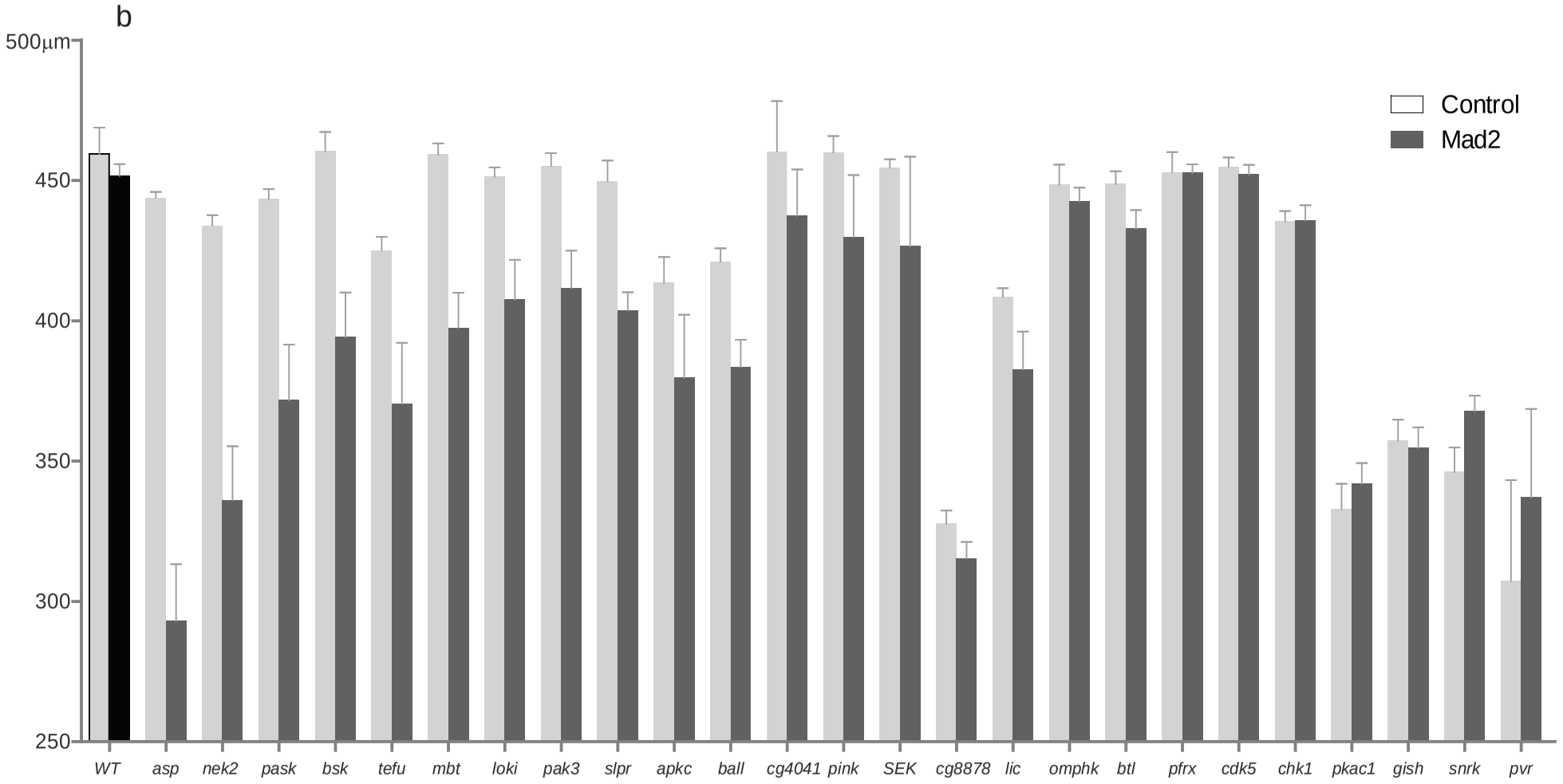
b
500µm
450
400
350
300
250
Control
Mad2
WT
asp
nek2
pask
bsk
tefu
mbt
loki
pak3
slpr
apkc
ball
cg4041
pink
SEK
cg8878
lic
omphk
btl
pfrx
cdk5
chk1
pkac1
gish
snrk
pvr

Figure S2

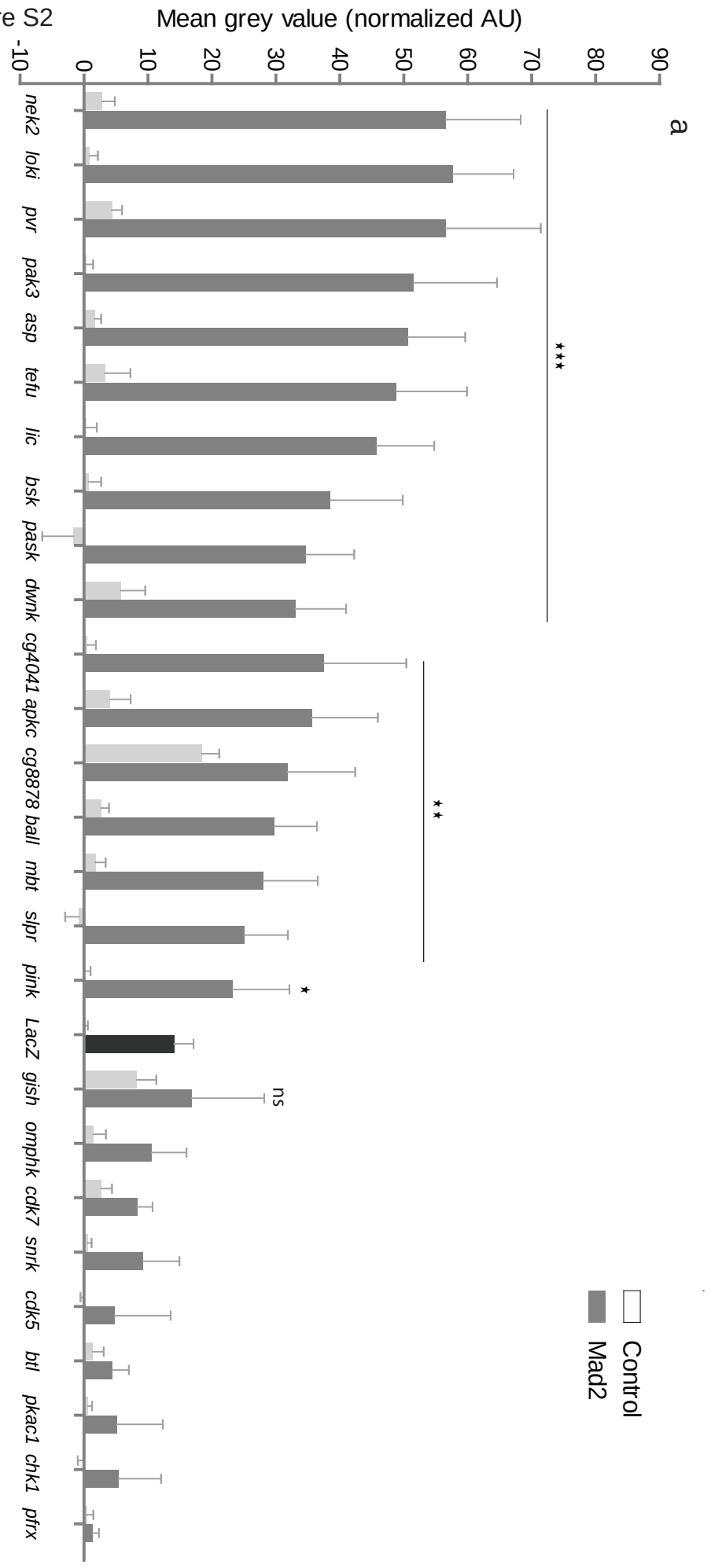
Mean grey value (normalized AU)
-10
0
10
20
30
40
50
60
70
80
90
a
***
**
*
ns
Control
Mad2
nek2
loki
pvr
pak3
asp
tefu
lic
bsk
pask
dwnk
cg4041
apkc
cg8878
ball
mbt
slpr
pink
LacZ
gish
omphk
cdk7
snrk
cdk5
btl
pkac1
chk1
pfrx

Figure S2

b (1)

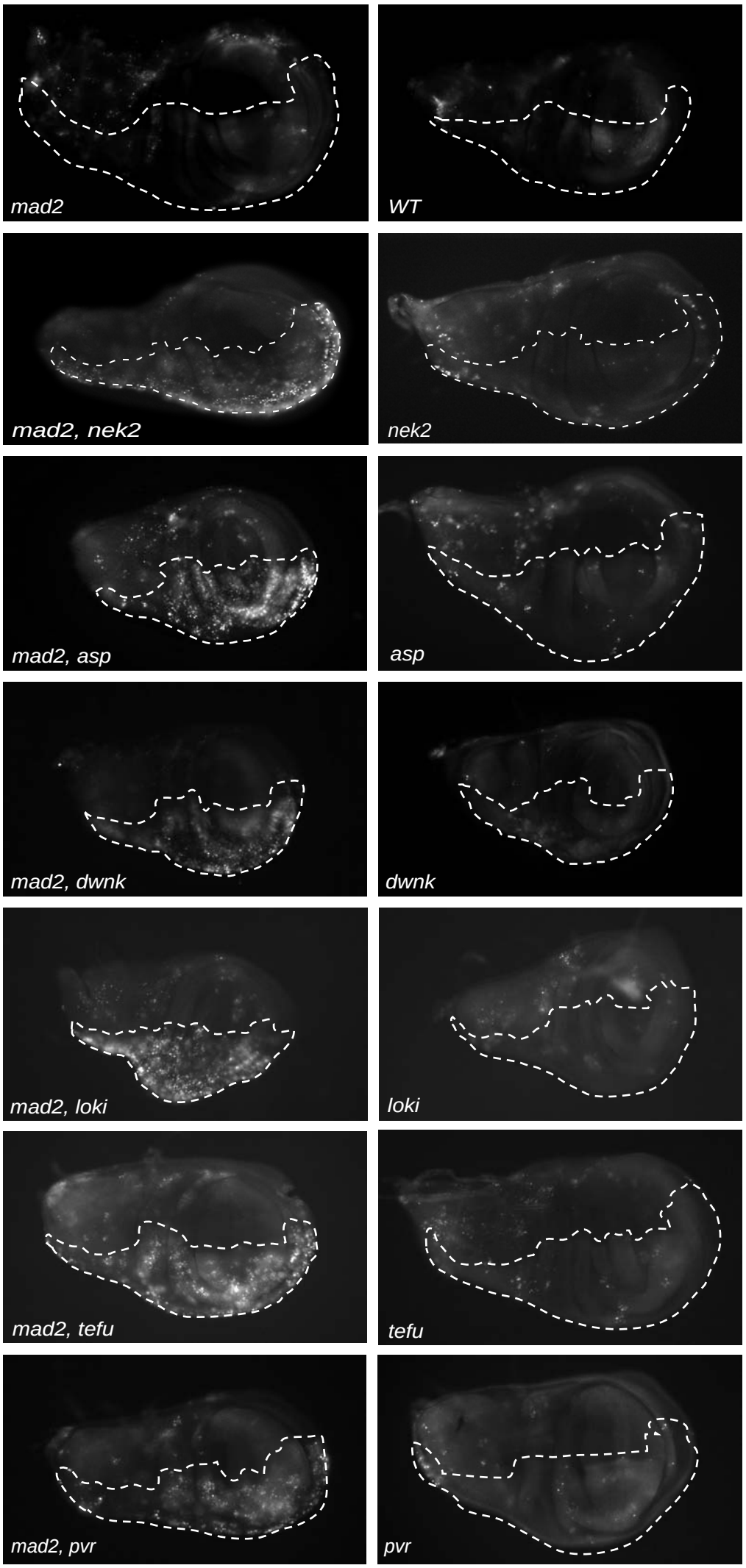
mad2
WT
mad2, nek2
nek2
mad2, asp
asp
mad2, dwnk
dwnk
mad2, loki
loki
mad2, tefu
tefu
mad2, pvr
pvr

b (2)

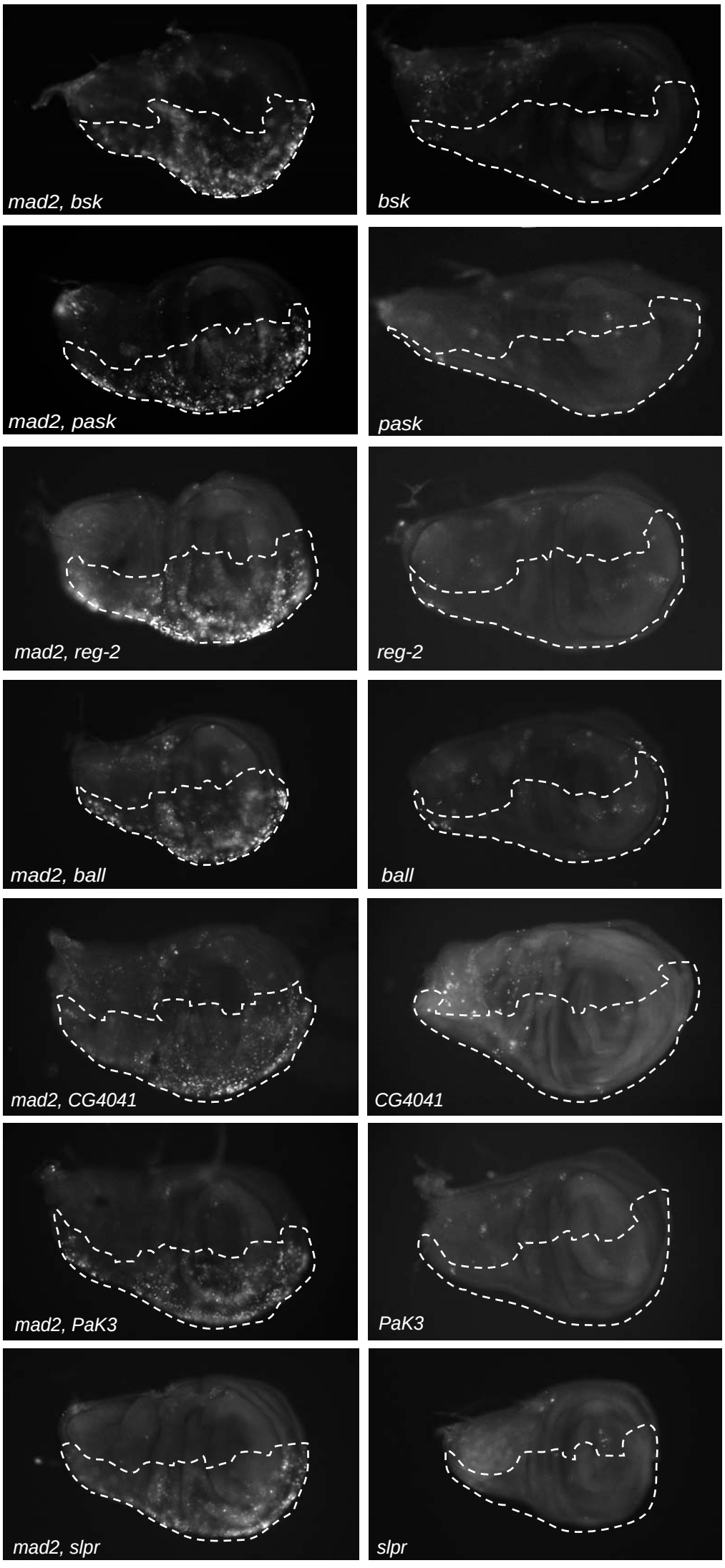
mad2, bsk
bsk
mad2, pask
pask
mad2, reg-2
reg-2
mad2, ball
ball
mad2, CG4041
CG4041
mad2, PaK3
PaK3
mad2, slpr
slpr

b (3)

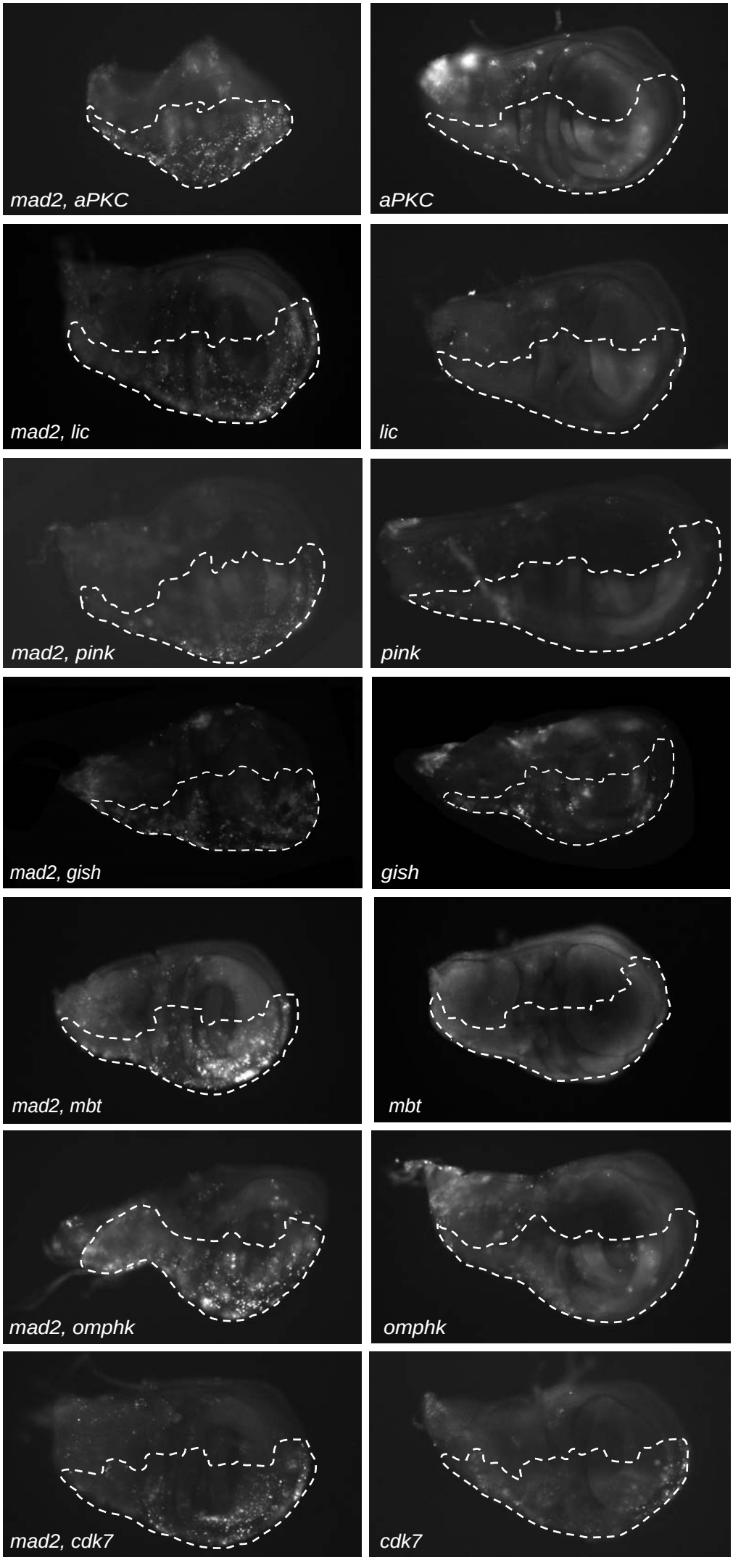
mad2, aPKC
aPKC
mad2, lic
lic
mad2, pink
pink
mad2, gish
gish
mad2, mbt
mbt
mad2, omphk
omphk
mad2, cdk7
cdk7

b (4)

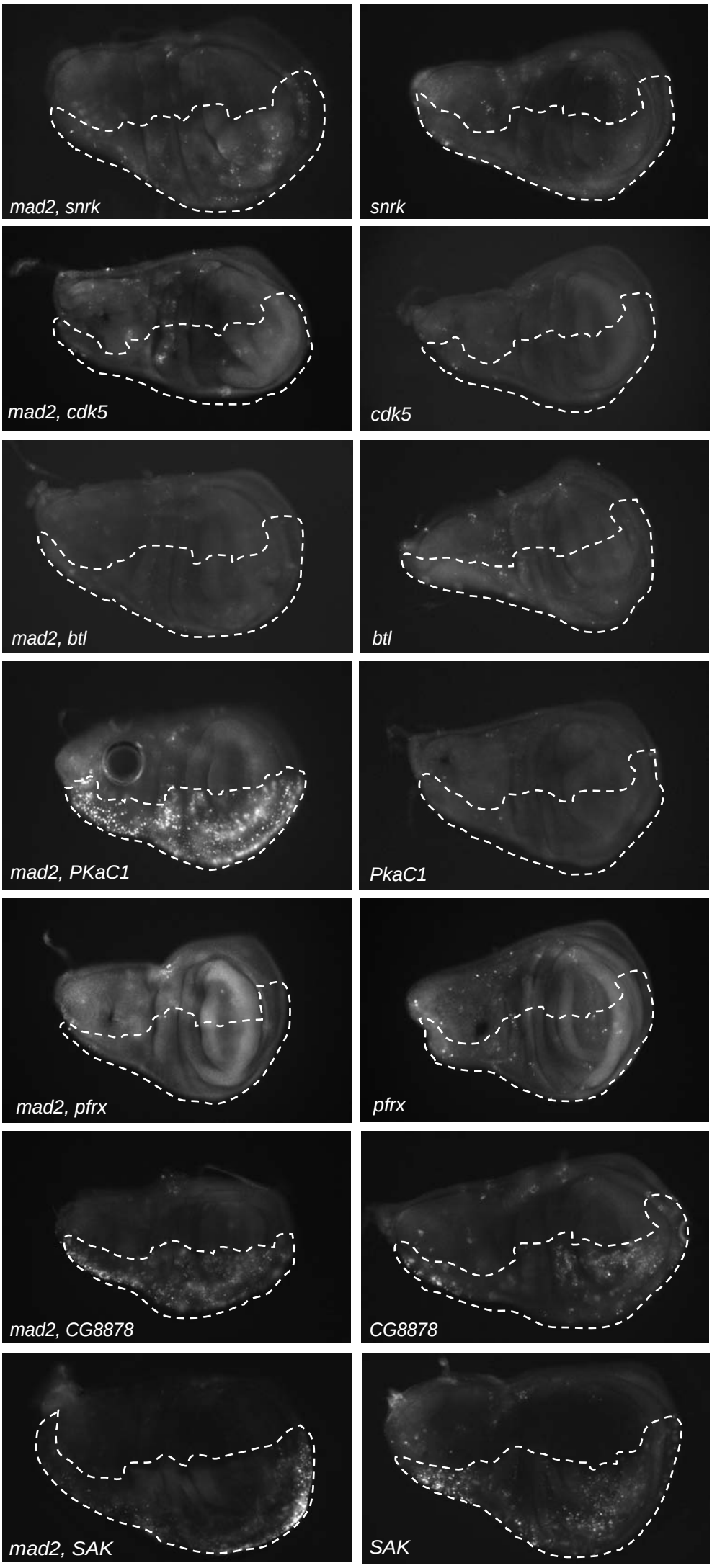
mad2, snrk
snrk
mad2, cdk5
cdk5
mad2, btl
btl
mad2, PKaC1
PkaC1
mad2, pfrx
pfrx
mad2, CG8878
CG8878
mad2, SAK
SAK

Figure S3

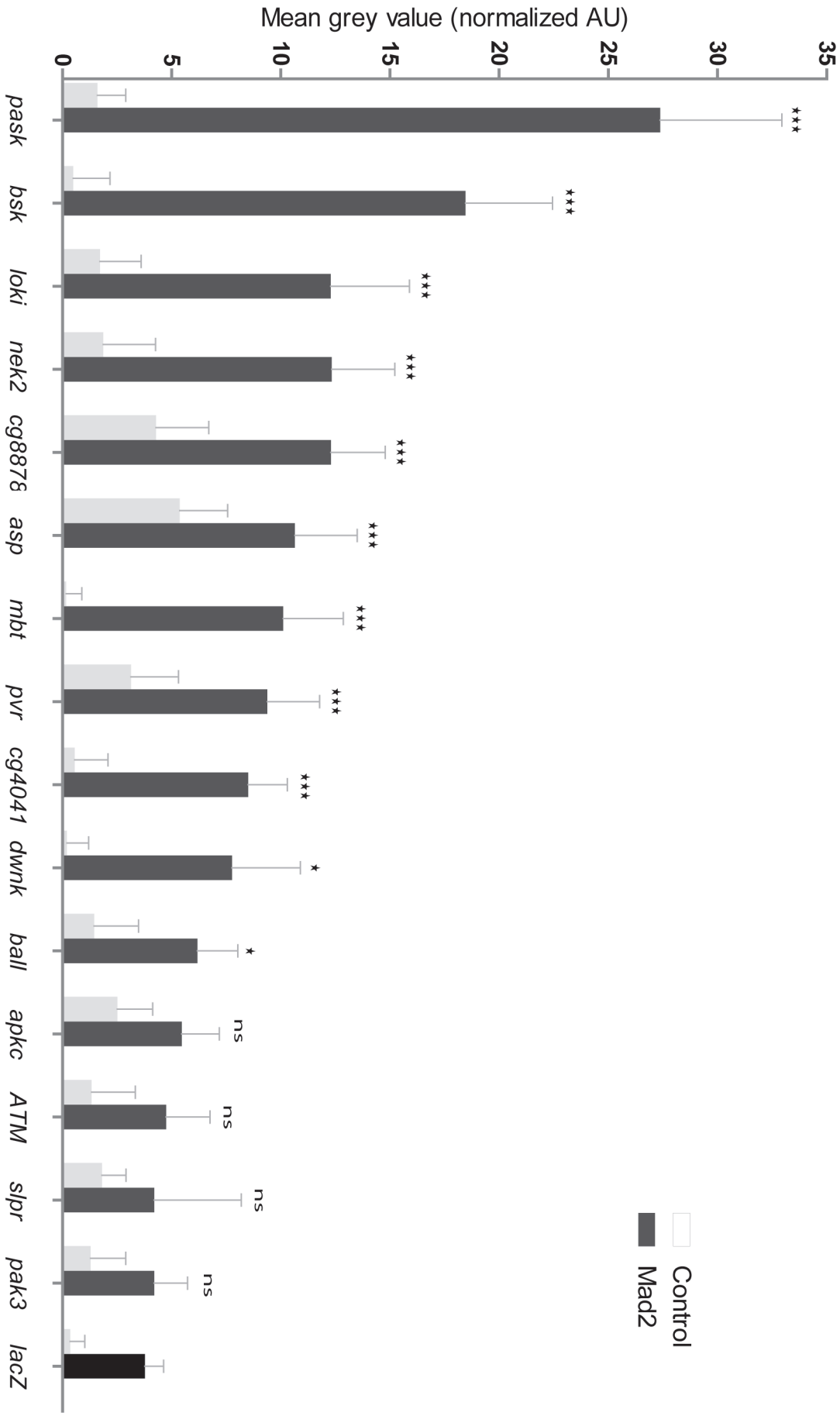
Mean grey value (normalized AU)
0
5
10
15
20
25
30
35
pask
bsk
loki
nek2
cg8878
asp
mbt
pvr
cg4041
dwnk
ball
apkc
ATM
slpr
pak3
lacZ
***
***
***
***
***
***
***
***
***
*
*
ns
ns
ns
ns
Control
Mad2

Figure S4

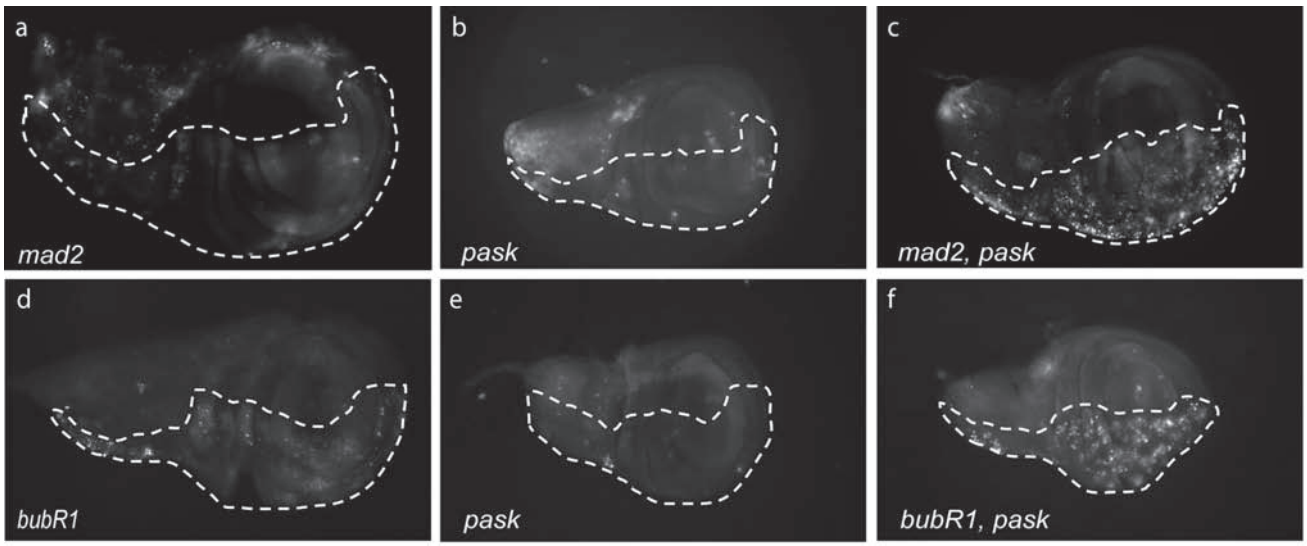

Figure S5

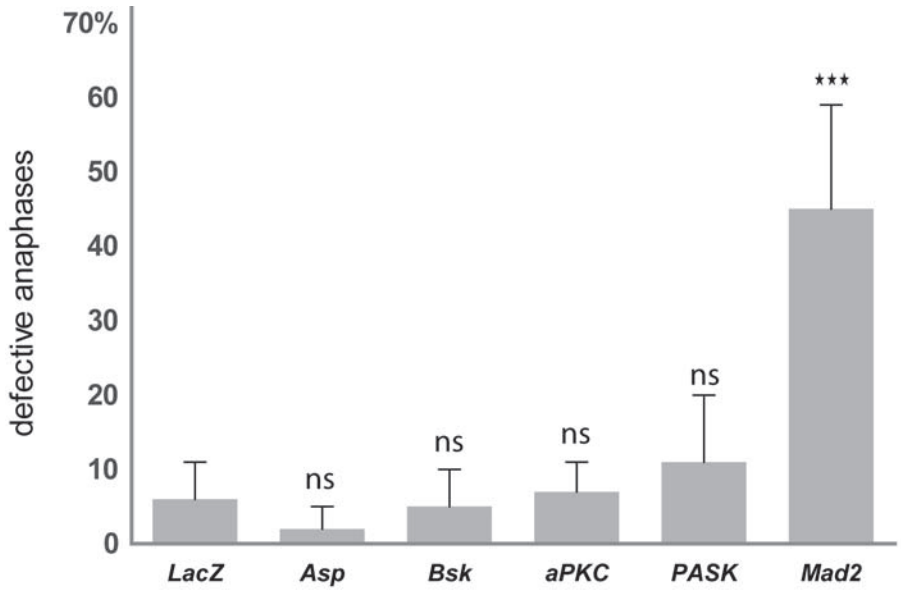
70%
60
50
40
30
20
10
0
defective anaphases
ns
ns
ns
***
LacZ
Asp
Bsk
aPKC
PASK
Mad2

VIABILITY SCREENING OF KINASES AND PHOSPHATASES IN CIN MODEL FLIES

total # crosses **936**

					progeny				
ID	**CG**	**Gene Symbol**	**Ratio of avg**	**# of crosses**	**Cumulative CyO**	**Cumulative nonCyO**	**Cumulative ratio**	**p[sum]**	**Gene Synonyms**
103408	17256	Nek2	23.5	2	47	0	47.0	3.6E-12	CG17256 , DmNek2 , NEK2 , Nek2 , Dm Nek2
107025	3105	PASK	13.3	2	53	4	13.3	1.4E-09	PAS-Kinase
26003	6963	gish see also 106826	12.5	2	25	2	12.5	1.3E-03	CG6963 , CKIgamma , Hrr25 , ms(3)89B , CKI-related , anon-WO0118547.425 , gish , CK1 , Gish , NEST:bs27c08
2907	10261	aPKC	12.3	6	74	1	68.0	1.0E-24	aPKC , aPKCzeta , DaPKC , aPKC-zeta , dapkc , psu , apkc , pkc-3 , CG10261 , l(2)k06403 , PKCl,i , daPKC , a-PKC
105102	7186	SAK	11.7	3	35	2	17.0	2.4E-06	PLK4 , Sak , SAK/PLK , CG7186 , SAK , sak
16334	11870	Omphk also 106088	11.7	2	35	3	11.7	1.5E-05	EMK/KIAA0537 , CG11871 , CG11870 , Omphk1
33518	2272	slpr JNKKK MLK	9.8	5	49	0	44.0	8.9E-13	dMLK , MLK2 , Mlk2 , dMLK2 , CG2272 , slpr , Slpr , JNKKK , MLK
105525	6593	PP1 alpha-96 A	9.8	5	49	0	48.0	8.9E-13	CG6593 , Pp1alpha-96A , Pp1-96A , DmPp1-96A , PP1alpha96A , PP1c , PP1 , PP1 96A , PP1alpha[[1]] , unnamed , 96A , PP1c 96A
4659	8657	DGKepsilon	9.1	5	109	12	8.9	1.0E-20	CG8657 , DGKepsilon , DGKe , unnamed , Dgkepsilon
101357	18492	tak	9.0	2	18	1	17.0	1.8E-02	dTAK1 , DTAK1 , TAK , D-tak , dTak1 , TAK-1 , dTAK , tak1 , TAK1 , tak , D10 , DmTak1 , CG18492 , CG1388 , DTak1 , DTak , Tak 1 , Tak1 , dTAK-1 , dTak
46043	18582	mbt (Pak4)	9.0	2	54	6	9.0	2.2E-08	DmPAK2 , DmMBT , Mbt , CG18582 , STE20 , Ste20 , unnamed , dPAK2 , anon-EST:fe1G7 , Pak2 , mbt
35939	8485	SNRK	8.5	2	17	0	17.0	3.8E-03	152964_at , SNRK , CG8485
34138	5680	jnk (bsk)	8.4	7	59	3	16.7	4.1E-12	bsk , JNK , DJNK , jnk , dJNK , DBSK/JNK , D-JNK , CG5680 , DJNK/bsk , JNK/SAPK , SAPKa , D-junk , Bsk , Junk
107185	3200	Reg-2 Pase	8.2	2	41	5	8.2	9.7E-06	CG3200 , Dreg-2 , Reg-2
106826	6963	gish	8.0	2	16	1	12.0	6.3E-02	CG6963 , CKIgamma , Hrr25 , ms(3)89B , CKI-related , anon-WO0118547.425 , gish , CK1 , Gish , NEST:bs27c08
34780	4041	rab gtpase kinase ?	7.2	2	79	11	7.2	1.7E-11	CG4041
101524	4379	PkaC1	6.8	4	41	6	6.2	3.8E-05	PKA , PKA Cl , DC0 , DCO , pka-C1 , Cos1 , pka-c1 , pka , PKAc , dPKA , Pka , Pka-C , PKAcA , pkA , PKA Cl , CG4379 , pKA , 6353 , PKA-C1 , Dc0 , l(2)01272 , C , dco , unnamed , Cos-1 , Dco , dcO , Cos , l(2)cos[[1]] , cos1 , l(2)s4402 , Dcpk , CdkA , Pka-C1 , PkaC1
947	32134	btl	6.4	3	32	5	6.4	1.6E-03	btl , dev , FGFR , D-FGFR , DFR2 , CT20816 , CG6714 , BTL/FGFR2 , dtk2 , DFGF-R1 , DmHD-311 , Dfr-2 , 0844/01 , Btl , FGFR1 , Fgf-r , fgf-r , dFGFR , l(3)00208 , Tk2 , HD-311 , Dtk2 , CG32134 , lambdatop
104697	31431	FGFR-like	6.1	3	85	14	6.1	3.0E-11	CT32770 , CG13414 , CG31431
106928	7177	dWNK (hyperploid)	6.0	4	24	1	21.0	3.7E-04	cg7177. wnk, dwnk
35988	8637	Trc	5.7	2	17	3	5.7	4.2E-01	dmTRC , NDR , CG8637 , Ndr , 0669/17 , l(3)S066917 , trc , Trc
49558	5169	GckIII also 107158	5.0	2	20	4	5.0	2.7E-01	GckIII , CG5169 , dGCKIII , GCKIII , STLK3
100396	5565	Pase	4.2	2	21	5	4.2	3.9E-01	CG5565
105484	15528	Pase	4.1	1	65	16	4.1	6.9E-06	CG15528
103413	3319	cdk7	4.0	4	80	20	4.0	2.1E-07	cdk7 , CDK7 , CG3319 , DmMO15 , p40[MO15] , DmCdk7 , Dmcdk7 , DmCDK7 , Cdk7 , cdk-7 , dCdk7
25958	3400	Pfrx	4.0	2	76	19	4.0	5.7E-07	CG3400 , Pfrx
22502	6535	tefu ATM	3.9	5	74	19	3.9	1.5E-06	tefu , ATM , CG6535 , dATM , atm , tef , unnamed , atm/tefu , Tefu
29965	30021	MaGuK	3.9	1	31	8	3.9	5.4E-02	CG18338 , CG13219 , CG30021 , skf, metro
30098	9784	IP Pase	3.8	3	90	24	3.8	6.6E-08	IPP , CG9784
21860	4523	pink1	3.7	2	26	7	3.7	2.2E-01	CG4523 , dPINK1 , BEST:GH23468 , Pink1 , PINK1 , pink1 , dPink1
36047	8822	PPD6 PP1	3.5	2	39	11	3.5	1.6E-02	CG8822 , D6 , PpD6 , PP1
27504	5757	CG5757	3.5	2	7	0	7.0	9.8E-01	CG5757
103739	4290	cg4290	3.4	1	24	7	3.4	4.6E-01	EG:22E5.8 , CG4290
2910	6875	asp	3.4	4	102	30	3.4	4.0E-08	CG6875 , Asp , abnormal spindle, abnormal spindle protein, anon-96Aa , anon-WO0118547.279 , asp , ASP , Dm Asp
858	31183	MAGuK/ GYC	3.3	1	65	20	3.3	1.8E-04	FBgn0038379 , GYC , CG4224 , CG11846 , CG31183
106180	10417	Pase	3.1	3	47	15	2.9	1.0E-02	PP2Cg , CG10417
106822	12244	mapkkk	3.1	3	37	12	3.1	7.9E-02	p38 , D-MKK3 , MEK3/MKK3 , CG12244 , DMKK3 , MKK3 , p38MAPKK , DMKK3/lic , DMEK3 , Mek3 , l(1)G0252 , Mpk3 , lic , dMKK3
9374	7497	CG7497	3.0	1	3	1	0.0	1.0E+00	CHED-related , BcDNA:GH27361 , anon-WO0170980.89 , anon-WO0170980.88 , CG7497
104663	7616	cg7616	3.0	2	42	14	3.0	3.9E-02	CG7616
100449	8565	SPRK2	3.0	1	18	6	3.0	9.8E-01	SPRK2 , CG8565
49772	33671	mevalonate kinase	3.0	1	18	6	3.0	9.8E-01	CG33009 , CG8810 , CG16804 , CG16804b , CG33009-ORFB , CG33671 , CG33009ORFB , Dromel_CG33672_FBtr0091651_mORF
104369	10539	S6K	3.0	2	59	20	3.0	2.2E-03	s6k , p70/S6K , S6K , dS6K , CG10539 , dS6k , ds6k , s6k11 , p70 S6K , DS6K , p70[S6kinase] , p70[S6 kinase] , fs(3)07084 , Dp70s6k , p70s6K , dps6k , dp70s6k , 7084 , p70[S6k] , p70S6K , Dp70[s6k] , Dp70S6k , dp70[S6k] , l(3)07084 , S6k
27346	1098	madm (secretion)	2.9	4	111	38	2.9	2.9E-07	CG1098 , dMADM , BcDNA:LD28657 , anon-WO0118547.406 , Madm
20655	18604	CG18604	2.8	4	65	23	2.8	1.4E-03	CG18604, CG15072, EMK/KIAA0999
44607	14895	Pak3 see 39844	2.8	2	44	16	2.8	6.3E-02	PaK3 , DmPAK3 , CG14895 , D-Pak3 , DPAK3 , pak3 , dPAK3 , PAK3 , anon-WO0118547.285 , Pak3 , DPak3
28970	8878	Vrk see 100985	2.7	2	43	16	2.7	9.1E-02	VRK , BcDNA:LD23371 , CG8878
41599	1578	CG1578	2.7	3	67	25	2.7	2.2E-03	CG1578
100985	8878	vrk-like	2.6	4	119	45	2.6	1.1E-06	VRK , BcDNA:LD23371 , CG8878
105173	33338	p38c non-MAPK	2.6	3	42	16	2.3	1.3E-01	CG33338 , p38c
14803	3135	shifted/shf	2.6	1	36	14	2.6	3.4E-01	D-Wif , DmWif , shf-ov , CT10514 , CG3135 , shf , DmWIF , Shf , CG3134, WNT inhibitory factor

104677	2096	flw	2.5	1	5	2	0.0	1.0E+00	PP1beta9C , flw , DmPp1-9C , PP1 b9C , PP1c , PP1 , PP19C , CG2096 , FLW/PP1B , Pp1beta-9C , PP1 9C , PP1beta , PP-1 , l(1)G0172 , anon-WO03040301.120 , FLW
107260	14895	Pak3	2.5	3	47	19	2.3	1.1E-01	PaK3 , DmPAK3 , CG14895 , D-Pak3 , DPAK3 , pak3 , dPAK3 , PAK3 , anon-WO0118547.285 , Pak3 , DPak3
48980	6386	ball	2.4	5	137	56	2.4	7.7E-07	nhk-1 , CG6386 , BcDNA:LD09009 , NHK-1 , VRK , ball , Ball , NHK1 , BALL , trip
35101	6498	MAST 205	2.4	1	22	9	2.4	9.9E-01	MAST 205 , CG6498
35473	10376	PP2C	2.4	2	66	27	2.4	9.8E-03	PP2C , CG10376
35855	8203	cdk5	2.4	4	171	70	2.4	9.3E-09	CDK5 , CG8203 , cdk5 , DmCdk5 , Cdk5
33198	2210	awd	2.4	1	17	7	2.4	1.0E+00	awd , Kpn , K-pn , CG2210 , NDPK , e(shi)A , eshiA , clone 2.27 , clone 2.28 , NDKB , 1084/08 , l(3)j2A4 , l(3)L8700 , anon-EST:Liang-2.28 , anon-EST:Liang-2.27 , BcDNA:RH27794 , BcDNA:GM19775 , anon-WO0172774.82 , anon-WO0172774.80 , Awd , Nm23/awd
36473	9962	CKIa like	2.4	1	17	7	2.4	1.0E+00	CG9962
34898	4803	Takl2 see also 104701	2.4	2	85	36	2.4	1.5E-03	CG4803 , TAK , Takl2
103353	13570	spag Pase	2.4	3	85	36	2.4	1.5E-03	l(2)k12101 , CG13570 , spag
42685	15743	CG15743	2.3	3	54	23	2.3	7.7E-02	CG15743
22675	8049	tec	2.3	1	42	18	2.3	3.3E-01	Btk29A , Tec29 , CG8049 , tec29 , Tec , Tec29A , fic , SRC 29A , CT41718 , CT2415 , DTec29 , DSrc28 , Dsrc29A , Dsrc28C , Src29A , Dm SRC2 , dsrc29A , c-src/fps , src28C , src-4 , src4 , src2 , Src2 , S13 , CG18355 , C-src4 , C-src2 , btk , btk29A
101997	12217	PpV	2.3	3	7	0	0.0	9.8E-01	DmPpV-6A , CG12217 , PPV , PPPV6A , PPV 6A , PpV
103725	8866	CG8866	2.3	3	35	15	2.3	6.3E-01	UNC 51-like , CG8866
6774	10917	fj	2.3	2	25	11	2.3	9.9E-01	CG10917 , fj , Fj
42599	11426	PI Pase	2.3	5	167	74	2.3	2.8E-07	Css1beta , WUN-like , CG11426
38647	1227	MPSK	2.2	1	20	9	2.2	1.0E+00	MPSK/PSK , CG1227
32476	1906	alph PP2Cb	2.2	1	31	14	2.2	9.1E-01	SK3-1 , alph , CG1906 , pp2c99B , PP2Cb
17957	10023	fak	2.2	1	33	15	2.2	8.6E-01	Fak56 , Fak , FAK , DFak , DFAK , CG10023 , CT28129 , DFak56 , Dfak , Dfak56 , DmFAK , Fak56D , fak
106071	14226	dome LIFR	2.2	3	48	22	2.2	3.0E-01	Dome , 142932_at , DOME , vsp , l(1)G0468 , l(1)G0217 , CG14226 , mom , CT33841 , l(1)G0441 , l(1)G0405 , l(1)G0367 , l(1)G0321 , l(1)G0264 , l(1)G0218 , l(1)G0282 , anon-18DEb , dome
34184	6703	caki	2.1	1	30	14	2.1	9.6E-01	DLin-2 , caki , Cmg , cmg , CAKI , CMG/CASK , CG6703 , CG13412 , CG13413 , CASK , CamGUK , Cask , Caki , Camguk , CMG , dCASK
9433	1891	sax	2.1	3	77	36	2.1	2.0E-02	sax , CG1891 , Sax , Bkr43E , Brk43E , STK-B , SAX
32249	1362	cdc2rk	2.1	1	17	8	2.1	1.0E+00	CG1362 , Dcdrk , cdc2rk
2895	6518	inaC PKC2	2.1	1	19	9	2.1	1.0E+00	InaC , PKC , INAC , CG6518 , eye PKC , PKCi , eye-PKC , PKC 53E , ePKC , unnamed , dPKC53E(ey) , Dpkc2 , pkc-2 , dPKC53E , Pkc2 , inaC
44980	10895	loki chk2	2.1	3	99	47	2.1	2.7E-03	CHK-2 , chk2 , CHK2 , chk2/lok , mnk , Chk2 , MNK , DmCHk2 , chk , Dmchk2 , DmChk2 , Dmnk , 38B.4 , LOKI/CHK2 , CG10895 , Dmnk-S , Dmnk-L , unnamed , lok
103808	10776	CG10776 wit	2.1	2	80	38	2.1	1.9E-02	CG10776 , STK-D , ALK3/BMPRII , l(3)64Aa , 1262/15 , SE20 , l(3)SH12 , l(3)S126215 , Stk-D , wit , Wit , WIT
21396	31692	fbp	2.1	2	42	20	2.1	6.3E-01	FbPase , CG10611 , CG31692 , fbp
107923	8637	trc	2.1	1	23	11	2.1	1.0E+00	dmTRC , NDR , CG8637 , Ndr , 0669/17 , l(3)S066917 , trc , Trc
104793	6703	Caki	2.1	1	29	14	2.1	9.9E-01	DLin-2 , caki , Cmg , cmg , CAKI , CMG/CASK , CG6703 , CG13412 , CG13413 , CASK , CamGUK , Cask , Caki , Camguk , CMG , dCASK
100039	17348	derailed	2.1	4	124	60	2.1	3.6E-04	derailed , lio , DRL , lin , lio/drl , CG17348 , CG10758 , unnamed , drl , Drl
43633	6027	cdi(limk-like, inhibits actin depo	2.1	2	33	16	2.1	9.5E-01	CG6027 , Cdi , unnamed , CDI/TSKI , l(3)07013 , B9.3 , 91F , cdi/TESK1 , cdi
28367	4012	gek MRCK	2.1	2	70	34	2.1	6.9E-02	MRCKalpha , CG4012 , dMRCK , l(2)09373 , Gek , anon-WO0200864.1 , Mrck , MdaPk , gek
107390	4141	PI3K	2.1	3	76	37	2.1	4.1E-02	Dp110 , PI3K , p110 , dp110 , dPI3K , type-1 PI3K , Dp110/PI3K , PI-3-K , Pi3Kp110 , PI(3)K , CG4141 , PI3K-92E/Dp110 , p120 , PI3K-92D , Dmp110 , rea , anon-92Ed , Pi3K92D , Pi3K92E , Pi3K , PI3K92E , PI3K-Dp110 , dP110 , PI-3 kinase , PI3K-dp110 , PI[[3]]K , PI3'K
27301	10673	CG10673	2.0	2	53	26	2.0	3.5E-01	CG10673
1101	1817	Ptp10D	2.0	2	65	32	2.0	1.3E-01	DPTP10D , ptp10D , CG1817 , PTP10D , Ptp10 , CT4920 , R-PTP 10D , DPTP , DPTP[[10D]] , Ptp10D , dptp
3170	3086	MAPk-Ak2	2.0	3	87	43	2.0	1.8E-02	MAPKAP , CG3086 , DmMAPKAPK-2 , MAPk-Ak2 , MK2 , MAPKAPK-2
17760	1395	string	2.0	1	10	5	2.0	1.0E+00	cdc25 , str/cdc25 , cdc25[string] , CDC25[string] , stg[cdc25] , Cdc25 , CG1395 , Cdc25[String] , String/Cdc25 , SY3-4 , l(3)01235 , clone 2.21 , Cdc25[stg] , 5473 , 1143/02 , 1089/08 , 1083/13 , 0980/06 , 0967/05 , 0896/05 , 0730/13 , 0439/22 , 0245/03 , 0224/06 , Cdc25[string] , S(rux)3A , EP1213 , l(3)s2213 , l(3)j3D1 , l(3)j1E3 , l(3)j1D3 , l(3)j10B9 , anon-EST:Liang-2.21 , stg , Stg , CDC25
104785	1696	Pase/ l(1)G0269	2.0	2	48	24	2.0	5.7E-01	CG1696 , BcDNA:LD08201 , anon-WO03040301.167 , l(1)G0269
108052	3277	CG3277	2.0	1	2	1	0.0	1.0E+00	CG3277
35105	6571	rdgc	2.0	3	70	35	2.0	1.0E-01	DmrdgC-77B , RDGC , CG6571 , RDGC/PP5 , RdgC 77B , rdgC , RdgC
107130	10079	Egfr	2.0	1	4	2	0.0	1.0E+00	Egfr , egfr , Elp-B1 , EGFR , DER , dEGFR , flb , der , d-egf-r , top , torpedo/egfr , EgfR , CG10079 , EGF-R , DER/EGFR , Der , D-EGFR , dEGFR1 , Egf-r , Elp , l(2)09261 , Egf , EK2-6 , c-erbB , DER/torpedo , unnamed , DmHD-33 , Elp-B1RB1 , Elp-1 , DER flb , top/DER , Torpedo/Egfr , D-Egf , Degfr , Torpedo/DER , torpedo/Egfr , EGFr , DER/faint little ball , DER/top , l(2)05351 , top/flb , l(2)57DEFa , l(2)57Ea , l(2)57EFa , HD-33 , El , C-erb , EFG-R , DEGFR
17991	10089	Pase	2.0	3	86	43	2.0	2.5E-02	CG10089
31264	10572	Cdk8	2.0	1	18	9	2.0	1.0E+00	Cdk8 , cdk8 , CDK8 , p58 , CG10572 , dTRAP56 , DmCdk8
106845	15224	CkIIbeta	2.0	1	2	0	0.0	1.0E+00	CKII , CK2 , CkII-beta , CK2beta , DmCKIIbeta , dCKII , DmCK2beta , CKIIbeta , CkIIbeta1 , betaCK2 , DmCkIIbeta , CKIIb , CG15224 , CK II , CKII-beta1 , mbu , CkII , And , CCK2 , CK-IIbeta , CK-II beta , CK-2 , Ds cas kin , CkIIbeta , Cask-II-b , dCK2beta , dCKII beta
100100	17028	IP Pase	1.9	3	93	48	1.9	2.3E-02	IMP , CG17028
104989	12746	WUN-like	1.9	1	27	14	1.9	1.0E+00	WUN-like , CG12746
101347	31140	CG31140	1.9	1	25	13	1.9	1.0E+00	CG5875 , DGKt , CG31452 , CG13600 , CG31140

38863	31349	pyd (GuK jnk)	1.9	2	59	31	1.9	4.1E-01	ZO-1 , CT36877 , pyd(Z01) , Tamou , Pyd/ZO-1 , CG9763 , ZO1 , Pyd , tam , dzo-1 , DZO-1 , xvt , Pch , CG9729 , CG12409 , CG11962 , CG11782 , CG31349 , pyd , polychaetoid
104388	14216	CG14216	1.9	1	36	19	1.9	9.8E-01	BEST:CK01830 , CG14216
9452	11437	Pase wun-like	1.9	3	81	43	1.9	9.6E-02	WUN-like , CG11437
31658	12147	CKIa-like	1.9	4	148	79	1.9	6.5E-04	CG12147, CKIa-like
105419	6214	MRP	1.9	1	13	7	1.9	1.0E+00	CG6214 , dMRP/CG6214 , dMRP , MRP
38326	10082	CG10082	1.9	1	13	7	1.9	1.0E+00	anon-WO0172774.149 , CG10082
45045	5790	CG5790	1.8	1	44	24	1.8	9.2E-01	CG5790
3018	7850	puc	1.8	2	11	6	1.8	1.0E+00	puc , Puc , CG7850 , PUC , PUC/MKP , l(3)A251.1 , hrt , 1351/08 , 0238/03 , l(3)84Eh , vco , l(3)j4E1
976	8222	Pvr	1.8	3	120	66	1.8	1.1E-02	VEGFR , PVR , pvr , CG8222 , VEGFR-A , Vegfr-c , Vegfr-b , stai , Vegfr , DmVEGFR , vgr1 , VGR1 , CT24332 , Vgr1 , Pvr
35482	10637	Nak	1.8	1	20	11	1.8	1.0E+00	CG10637 , nak , Nak
37216	9128	PI Pase	1.8	3	136	75	1.8	3.7E-03	sac1 , CG9128 , dsac1 , Sac1
104255	6800	cdk7-like	1.8	3	105	58	1.8	3.3E-02	AC014407 , CG6800
16057	10493	Phlpp	1.8	2	52	29	1.8	8.1E-01	CT29458 , PP2C , Phlpp , CG10493 , dPHLPP
108018	4317	Mipp2	1.8	2	25	14	1.6	1.0E+00	l(1)G0050 , l(1)G0303 , CG4317 , Mipp2
106421	7497	CG7497	1.8	4	66	37	1.8	4.8E-01	CHED-related , BcDNA:GH27361 , anon-WO0170980.89 , anon-WO0170980.88 , CG7497
26641	4839	CG4839	1.8	1	16	9	1.8	1.0E+00	CG4839
32822	17029	CG17029	1.8	3	62	35	1.8	6.1E-01	IMP , CG17029
13808	10776	wit	1.8	1	23	13	1.8	1.0E+00	CG10776 , STK-D , ALK3/BMPRII , l(3)64Aa , 1262/15 , SE20 , l(3)SH12 , l(3)S126215 , Stk-D , wit , Wit , WIT
33693	30274	CG30274	1.8	3	65	37	1.8	5.7E-01	CG13529 , CG30274
26216	3530	Pase	1.7	3	54	31	1.7	8.5E-01	BcDNA , BcDNA:GH04637 , CG18093 , CG3530
26929	9738	mkk4 sek	1.7	1	33	19	1.7	1.0E+00	SEK1/MKK4 , 142758_at , dMKK4 , mkk4 , MKK4 , CT27508 , CG9738 , JNKK2 , D-MKK4 , DMKK4 , Mpk4 , Mkk4
24308	8402	PpD3	1.7	2	45	26	1.7	9.8E-01	DmPpp5-85E , PP5 , CG8402 , Pp5-85E , DmPP5 , PP5 85E , D3 , PpD3
39844	14895	Pak3	1.7	3	64	37	1.7	6.6E-01	PaK3 , DmPAK3 , CG14895 , D-Pak3 , DPAK3 , pak3 , dPAK3 , PAK3 , anon-WO0118547.285 , Pak3 , DPak3
30105	9819	CanA-14F	1.7	2	83	48	1.7	2.7E-01	DmCanA-14F , CG9819 , canA-14F , PP2B , CnnA14D , unnamed , D27 , CnnA14D(l) , PpD27 , CanA-14F
102632	11489	CG11489	1.7	2	38	22	1.7	1.0E+00	CG11489 , SRPK , CG9085 , BEST:CK01209 , SRPK1 , CK01209
16133	10967	Atg1	1.7	6	131	76	1.7	1.7E-02	ATG1 , CG10967 , l(3)00305 , UNC 51-like , anon-WO0118547.287 , Atg1 , atg1
26574	4629	CG4629	1.7	1	31	18	1.7	1.0E+00	anon-WO0257455.15 , CG4629
33431	1951	CG1951	1.7	2	55	32	1.7	8.7E-01	CG1951
105549	3837	CG3837	1.7	3	48	28	1.7	9.6E-01	CG3837
25661	3105	PASK like 107025	1.7	2	44	26	1.7	9.9E-01	CG3105
34649	3573	ip5 phosphatase	1.7	3	110	65	1.7	8.6E-02	EG:86E4.5 , CG3573
35171	7109	mts	1.7	1	27	16	1.7	1.0E+00	mts , PP2 , DmPp2A-28D , PP2a , PP2Ac , PP2A , PP2a 28D , PP2A[[C]] , CG7109 , MTS/PP2A , dPP2A , 5559 , PP2A 28D , Pp2A-28D , Pp2A , ER2-6 , l(2)s5286 , l(2)02496 , PP2A C , PP2A-C , Mts
25760	31421	Takl1	1.7	3	81	48	1.7	4.0E-01	dTAK1 , DTAK1 , TAK , D-tak , dTak1 , TAK-1 , dTAK , tak1 , TAK1 , tak , D10 , DmTak1 , CG18492 , CG1388 , DTak1 , DTak , Tak 1 , Tak1 , dTAK-1 , dTak
35166	7097	GLK/KHS1	1.7	2	62	37	1.7	8.2E-01	GLK/KHS1 , anon-WO0153538.68 , CG7097, happyhour
36531	8767	mos	1.7	2	87	52	1.7	3.3E-01	dmos , DMOS , CG8767 , D-mos , MOS , mos
27843	7094	CKIa-like	1.7	1	15	9	1.7	1.0E+00	CG7094
105292	9151	acj6	1.7	3	98	59	1.7	2.2E-01	Acj6 , ACJ6 , CG9151 , I-POU , tl-POU , Ipou , acj6
107271	12151	pdp	1.7	2	33	20	1.7	1.0E+00	153332_at , Pdp , CG12151 , pdp , PDP
105621	31873	CG31873	1.6	1	23	14	1.6	1.0E+00	CG18162 , CG31873 , anon-31BCb
103740	1228	ptpmeg	1.6	2	54	33	1.6	9.7E-01	ptpmeg , scc , CG1228 , dMEG1 , MEG1 , anon-WO0118547.211 , Ptpmeg , PTP-meg
103580	7097	GLK/KHS1	1.6	3	44	27	1.6	1.0E+00	GLK/KHS1 , anon-WO0153538.68 , CG7097, happyhour
108071	9554	eya	1.6	2	62	39	1.6	9.5E-01	CG9554 , Eya , cli , cli/eya , CLIFT , EY2-1 , ey-2 , EYA , BcDNA:LD16029 , eya
100823	10951	niki	1.6	3	92	58	1.6	5.0E-01	CG10951 , Niki , NEK1 , niki
107728	6805	PI Pase	1.6	2	75	48	1.6	8.4E-01	IPP , CK01299 , BEST:CK01299 , CG6805
31500	11420	png	1.6	2	50	32	1.6	1.0E+00	Png , EG:8D8.5 , PNG , CG11420 , fs(1)M2 , pan-gnu , png
101376	4551	smi35A	1.6	1	28	18	1.6	1.0E+00	CG4551 , smi35A , dDYRK2 , Dyrk2 , DYRK , DYRK2 , BG:DS01523.3
52634	3008	CG3008	1.5	1	20	13	1.5	1.0E+00	CG3008
38349	10177	CG10177	1.5	1	20	13	1.5	1.0E+00	CG10177
16048	10426	CG10426	1.5	4	132	86	1.5	1.9E-01	IPP , CG10426
106525	8742	G cyclase	1.5	2	52	34	1.5	1.0E+00	Gyc76C , l(3)76BDl , DrGC-1 , GYC 76C , CG8742 , DGC1 , drgc , unnamed , CG32215 , l(3)L0090
104370	11217	calcineurin	1.5	3	76	50	1.5	9.1E-01	canB2 , CG11217 , CS2-1 , dCnB2 , dCNB2 , CanB2
46064	4965	twine cdc25	1.5	1	15	10	1.5	1.0E+00	twn , Cdc25 , CG4965 , TWINE , cdc25 , l(2)35Fh , BG:DS02740.1 , mat(2)synHB5 , mat(2)syn[HB5] , mat(2)syn-A , twe , Twe , twine
103561	5179	Cdk9	1.5	2	6	4	1.5	1.0E+00	P-TEFb , CDK9 , cdk9 , CG5179 , P-TEF , PTefb , Cdk9
103457	11516	CG11516 Ptp99A	1.5	1	36	24	1.5	1.0E+00	DPTP99A , CT6383 , R-PTP 99A , CG11516 , CG2005 , PTP99A , dptp99A , DPTP[[99A]] , CG11515 , CG11517 , Ptp99A
32854	17090	CG17090	1.5	1	15	10	1.5	1.0E+00	HIPK , CG17090
103806	34344	rdgA	1.5	1	21	14	1.5	1.0E+00	rdgA , CG34344 , DGK , CG10966 , dDGK2 , DGK2 , x35 , CG12660
45120	11533	Asator tubulin kinase	1.5	2	100	67	1.5	6.9E-01	CG11533 , CK I , CKI-like , Asator
102772	34359	IP3K2	1.5	3	73	49	1.5	9.7E-01	dmIP[[3]]beta , CG1630 , IP[[3]]K2 , CG34359 , dmIP3Kbeta , dmIP3K2 , DIP3K2 , D-IP3K2 , IP3K2 , CG12724

30658	12066	PKA-C2	1.5	2	64	43	1.5	9.9E-01	PKA C2 , PKA , CG12066 , DC1 , DC1a , CdkB , Pka-C2
103410	8789	wnd	1.5	2	31	21	1.5	1.0E+00	DLK/ZPK , wnd , CG8789 , MAPKKK , DLK
100163	11221	CG11221	1.5	3	93	63	1.5	8.3E-01	PKN , CG11221
107836	4993	PRL-1	1.5	2	28	19	1.4	1.0E+00	PRL , CG4993 , BG:DS07473.3 , BcDNA:RE40268 , PRL-1 , PrL-1
103513	3324	Pkg21D	1.5	2	25	17	1.5	1.0E+00	PKG-21D , dg1 , PKG 21D , CG3324 , DG1 , PKG , cGMP , Pkg1 , Dg1 , Pkg21D
9404	7115	CG7115	1.5	1	25	17	1.5	1.0E+00	PP2C , BcDNA:LD21794 , CG7115
102192	3915	Drl-2	1.5	3	47	32	1.5	1.0E+00	dnl , DNT-like , CG12463 , CG3915 , Drl-2 , drl-2
3691	10702	CG10702	1.5	1	22	15	1.5	1.0E+00	CG10702
12680	17161	grp chk1	1.5	5	51	35	1.5	1.0E+00	grp , Grp , CHK1/Grapes , Chk1 , CG17161 , CHK1 , dChk1 , lemp , 1C , Pk?1 , Pk36A , DmChk1 , grps , chk1
47280	18069	CG18069 CaMKII	1.5	1	16	11	1.5	1.0E+00	CaMKII , CAMKII , CaMK-II , dCaMKII , Calcium/calmodulin-dependent protein kinase , camKII , CaM KII , CamKII , CaM II , CG18069 , CAMKIId , CDPK1 , Ca2+/calmodulin-dependent protein kinase II , calcium/calmodulin-dependent protein kinase II , DCK , CaMK II , CaM , CamKIIalpha , Cam , CAMKIIalpha
107048	18085	sev / v107048	1.4	1	23	16	1.4	1.0E+00	Sev , CT3980 , CG18085 , DROSEV1 , DmHD-265 , sev(AC)[[14]] , DROSEV , 7less , 7LES , HD-265 , sev , SEV
107429	31003	gskt	1.4	2	56	39	1.4	1.0E+00	CG31003 , NGSK , GSK3b , CT4237 , CG11338 , mjl , BEST:GH16447 , NEST:bs22e06 , Gsk3b , BcDNA:AT21229 , gskt
26109	7838	BubR1	1.4	1	10	7	1.4	1.0E+00	BubR1 , bubr1 , CG 7838 , CG7838 , bub1 , BUB1 , Dmbub1 , DmBUB1 , l(2)k06109 , dBUB1 , 31/13 , l(2)k03113 , BcDNA:LD23835 , Bub1 , bubR1 , BUBR1 , Mad3
104374	34099	map Pase	1.4	3	78	55	1.4	9.9E-01	CG34099 , CG7042 , DMKP , Mkp
101437	5725	fbl	1.4	3	56	40	1.4	1.0E+00	CG5725 , fbl , dPANK
35024	5650	PP1-87B	1.4	2	21	15	1.4	1.0E+00	DmPp1-87B , PP1alpha87B , Su(var)3-6 , PP1-87B , PP1c , PP1 , PP187B , CG5650 , PP1 87B , Pp1-87Bb , Su-var(3)6 , Su(Var)3-6 , l(3)j6E7 , Pp1 , Suvar(3)6 , su-var(3)6 , ck19 , Su(var)(3)6 , PP1A87B , PP1alpha[[2]] , PP-1alpha , l(3)ck19 , l(3)87Bg , Pp-1alpha , Pp1-87B , Ppl-87B , 87B , PP1c 87B , Pp1alpha-87B
36053	8874	Fps85D	1.4	1	7	5	1.4	1.0E+00	FER , CG8874 , Dfer , fer , DFER , FPS , DmHD-179 , dfps 85D , dFer , Dfps , DFer , Dm FPS , Fer , dfps85D , fps , dfps , fps85D , HD-179 , Fps85D , dfer
16096	10930	PpY-55A	1.4	1	14	10	1.4	1.0E+00	DmPpY-55A , PPY 55A , CG10930 , PPY , D19 , PpD19 , PpY-55A
105185	34357	CG34357	1.4	1	21	15	1.4	1.0E+00	CG34357 , CG14652 , CG12585 , CG12584 , CG41467 , GYC , CG9783
104147	4965	twe	1.4	3	99	71	1.4	9.5E-01	twn , Cdc25 , CG4965 , TWINE , cdc25 , l(2)35Fh , BG:DS02740.1 , mat(2)synHB5 , mat(2)syn[HB5] , mat(2)syn-A , twe , Twe , twine
25343	1848	limk	1.4	3	163	117	1.4	1.5E-01	LIM-kinase 1 , Dlimk , CG1848 , D-LIMK1 , LIMK , Limk , dLIMK , DLIMK , limk , DLIMK1 , LIMK1 , D-Limk , dLIMK1
100842	10702	CG10702	1.4	1	25	18	1.4	1.0E+00	CG10702
7005	2621	sgg	1.4	1	18	13	1.4	1.0E+00	GSK3beta/SGG , Zw3 , GSK , zw3 , GSK3beta , GSK3 , Gsk3 , GSK-3 , GSKbeta , GSK-3beta , ZW3 , CG2621 , EG:155E2.3 , Zw3-sh , DMSGG3 , Sgg , SGG/GSK3b , Zw3/GSK3 , sgg46 , sgg39 , sgg10 , DMZ3K25Z , sgg-zw3 , l(1)3Ba , zw-3 , Zw-3 , zw3[sgg] , Zw3[sgg] , zw3/sgg , sgg/zw3 , zw[3] , zw3(sgg) , l(1)zw3 , ZW-3 , l(1)G0055 , l(1)G0183 , l(1)G0263 , l(1)G0335 , EG:BACR7C10.8 , anon-WO03040301.254 , sgg , gsk3 , Dmsgg3 , SGG , Sgg/Zw3/GSK3 , Gsk-3 , GSK-3B , GSK3betagr;
104701	4803	Takl2	1.4	2	54	39	1.4	1.0E+00	CG4803 , TAK , Takl2
102633	8914	CKIIb2	1.4	2	62	45	1.4	1.0E+00	CK2 , CKIIbeta' , CK2beta' , DmCKIIbeta' , CKIIb2 , CG8914 , CkIIbeta2 , DmCK2beta'
102021	10930	Pase like PpY-55A	1.4	3	84	61	1.4	1.0E+00	DmPpY-55A , PPY 55A , CG10930 , PPY , D19 , PpD19 , PpY-55A
49408	12798	SEK1/MKK4	1.4	2	56	41	1.4	1.0E+00	SEK1/MKK4 , CT38386 , CG12798
106824	10579	CG10579	1.4	1	15	11	1.4	1.0E+00	PFTAIRE , cdc2-63E , L63 , CG10579 , Eip63E
102071	14297	CG14297	1.4	2	30	22	1.4	1.0E+00	LMW-PTP , CG14297
45121	11533	Asator also 45120	1.4	1	34	25	1.4	1.0E+00	CG11533 , CK I , CKI-like , Asator
100777	15912	CG15912	1.4	1	19	14	1.4	1.0E+00	CG15912
104211	8822	PPD6 PP1	1.4	2	23	17	1.1	1.0E+00	CG8822 , D6 , PpD6 , PP1
101545	7892	like nemo	1.3	1	31	23	1.3	1.0E+00	Nlk , CG7892 , Nemo , NEMO/NLK , NEMO , adk , clone 2.43 , anon-WO0172774.138 , anon-EST:Gibbs3 , anon-EST:Liang-2.43 , anon-WO0140519.256 , anon-WO0118547.332 , nmo , nemo
102060	3245	PpN58A	1.3	3	90	67	1.3	1.0E+00	PpN-58A , DmPpN-58A , PPN 58A , CG3245 , PPN , PpN58A
103563	7207	CG7207	1.3	2	63	47	1.3	1.0E+00	BcDNA:GH07688 , CG7207
102484	5475	Mpk2	1.3	1	8	6	1.3	1.0E+00	p38 alpha , D-p38a , P38 , D-p38 , p38 , p38a , Dp38 , p38A , CG5475 , D-P38a , D-MPK2 , DmMPK2 , dMPK2 , DMPK2 , group 2 , Erk2 , Mpk2 , dp38
104774	10371	Plip	1.3	2	40	30	1.3	1.0E+00	150466_at , PLIP , CG10371 , Plip
100265	18069	CaMKII	1.3	2	28	21	1.3	1.0E+00	CaMKII , CAMKII , CaMK-II , dCaMKII , Calcium/calmodulin-dependent protein kinase , camKII , CaM KII , CamKII , CaM II , CG18069 , CAMKIId , CDPK1 , Ca2+/calmodulin-dependent protein kinase II , calcium/calmodulin-dependent protein kinase II , DCK , CaMK II , CaM , CamKIIalpha , Cam , CAMKIIalpha
37436	9181	Ptp61F	1.3	2	37	28	1.3	1.0E+00	PTP61F , ptp61F , DPTP61F , R-PTP 61F , CG9181 , dPTP61F , dptp61F , CG9178 , BEST:LP01280 , anon-WO0118547.297 , anon-WO0140519.98 , Ptp61F
11251	4252	mei-41 ATR	1.3	2	58	44	1.3	1.0E+00	mei-41 , ATR , CG4252 , meiP41 , mus104 , mei41 , mus103 , MEI41/FRP1 , Mei-41 , MEI41 , mus-104 , mus(1)104 , fs(1)M37 , mus(1)103 , mus-103 , atr , mei-195 , DmATR
23719	12069	CG12069	1.3	1	25	19	1.3	1.0E+00	CG12069
105630	5483	lrrk	1.3	3	80	61	1.3	1.0E+00	lrrk , CT17358 , CG5483 , LRRK
18736	1210	Pk61C	1.3	1	13	10	1.3	1.0E+00	Pk61C , PDK1/Pk61C , PDK , PDK1 , dSTPK61 , Pdk1 , DSTPK61 , Dstpk61 , CG1210 , PDK-1 , dPDK1 , CG1201 , dPDK-1 , serine/threonine protein kinase. , Pk61C/PDK1
25529	7717	CG7717 Mekk1	1.3	1	13	10	1.3	1.0E+00	Mekk1/4 , D-MEKK1 , D-Mekk1 , dMEKK4 , dMEKK , mekk1b , mekk1a , MEKK4 , MEKK , DmMEKK1 , mekk1 , CG7717 , Mekk1 , dMEKK1 , MEKK1

103037	11425	CG11425	1.3	1	26	20	1.3	1.0E+00	WUN-like , CG11425
103804	4007	Nrk	1.3	2	58	45	1.3	1.0E+00	CG4007 , DmHD-434 , Dnrk , nrtk_dros , DNRK , l(2)k14301 , HD-434 , anon-WO2004063362.79 , Nrk
101257	12169	Ppm1	1.3	2	58	45	1.3	1.0E+00	PP2C , Ppm1 , CG12169 , dPPM1
165427	2087	PEK	1.3	1	18	14	1.3	1.0E+00	EIF2-like , CG2087 , DPERK , DmPEK , Perk , PERK , PEK
26035	7156	CG7156	1.3	3	46	36	1.3	1.0E+00	CG7156
105884	17698	CG17698	1.3	2	23	18	1.3	1.0E+00	CAMKIIB , CAMKIIb , CG40297 , CG17698
101475	5671	Pten	1.3	1	28	22	1.3	1.0E+00	pten , PTEN , dPTEN , DPTEN , PTEN3 , CG5671 , Pten , dPten
7560	31795	ia2	1.3	2	56	44	1.3	1.0E+00	R-PTPX/1A2 , unnamed , CG4355 , CG11344 , CG31795 , anon-WO0153538.69 , ia2
106497	11486	CG11486	1.3	1	19	15	1.3	1.0E+00	CG11486
100987	6772	slob	1.3	2	62	49	1.3	1.0E+00	slob , CG6772 , Slob
107386	8402	PpD3	1.3	2	24	19	1.2	1.0E+00	DmPpp5-85E , PP5 , CG8402 , Pp5-85E , DmPP5 , PP5 85E , D3 , PpD3
26879	7525	Tie	1.3	2	39	31	1.3	1.0E+00	tie , RTK , CG7525 , DPR1 , Tie
17477	14305	CG14305	1.3	1	15	12	1.3	1.0E+00	CG14305
27368	5182	Pk34A	1.2	2	51	41	1.2	1.0E+00	GSK3a , CG5182 , Pk34A
47027	3682	PIP5K59B	1.2	1	41	33	1.2	1.0E+00	CG3682 , PIP5K 59B , CG17281 , PIP5K59B
101719	6518	inaC PKC2	1.2	2	67	54	1.2	1.0E+00	InaC , PKC , INAC , CG6518 , eye PKC , PKCi , eye-PKC , PKC 53E , ePKC , unnamed , dPKC53E(ey) , Dpkc2 , pkc-2 , dPKC53E , Pkc2 , inaC
27719	6697	CG6697	1.2	2	62	50	1.2	1.0E+00	BcDNA:LD21504 , CG6697
101018	32484	CG32484	1.2	3	57	46	1.1	1.0E+00	CG32484 , CG2159 , Sphk2 , SK2 , Sk2
105706	18247	Shark	1.2	2	47	38	1.2	1.0E+00	Shark , SHARK , CG18247 , SYK/SHARK , dtk7 , l(2R)W4 , l(2)W4 , Tk7 , Dtk7 , shark
104427	32697	onX Ypase or l(1)G0232	1.2	5	70	57	1.2	1.0E+00	CG3101 , CG3102 , MEG2 , unnamed , CG32697 , l(1)G0232
932	4926	Ror	1.2	2	54	44	1.2	1.0E+00	Dror , CG4926 , DmHD-2 , ROR , DRor , HD-2 , Ror
42592	11440	Laza	1.2	4	114	93	1.2	1.0E+00	WUN-like , laza , Laza , CG11440
103270	17027	CG17027	1.2	3	60	49	1.2	1.0E+00	152392_at , IMP , CG17027
27591	6355	fab-1	1.2	1	11	9	1.2	1.0E+00	EG:52C10.5 , fab1 , CG6355 , Fab1 , fab-1 , PIKfyve
105249	2984	PP2C1	1.2	4	111	91	1.2	1.0E+00	PP2C , CG2984 , PP2C1 , dpp2c1 , anon-WO03040301.132 , Pp2C1
25615	3028	Ipp	1.2	2	34	28	1.2	1.0E+00	ipp , CG3028 , anon-WO02059370.48 , Ipp
104259	9222	CG9222	1.2	3	80	66	1.2	1.0E+00	CG9222
107998	6238	ssh	1.2	2	63	53	1.2	1.0E+00	Ssh , MKP , CG6238 , Mkph , l(3)01207 , ssh
46070	6562	synj	1.2	1	19	16	1.2	1.0E+00	CG6562 , Synj , IPP , synj
103354	7115	CG7115 like 9404	1.2	2	26	22	1.0	1.0E+00	PP2C , BcDNA:LD21794 , CG7115
43783	4527	slik	1.2	3	32	27	1.2	1.0E+00	Plkk1 , CG4527 , DPlkk1 , slk , SLK , slik , dPlkk/Slik , Plkk/Slik , Slk , Slik , PLKK1
44663	9389	CG9389	1.2	2	34	29	1.2	1.0E+00	142336_at , IMP , CG9389
102397	7180	CG7180	1.2	2	62	53	1.2	1.0E+00	R-PTPk , CG7180
100296	5373	Pi3K59F	1.2	2	35	30	1.0	1.0E+00	PI3K , dPI3K , CG5373 , PI(3)K , PI3K-59F , PI3K_59F , DmVps34 , VPS34 , Pi3K59F , Vps34 , PI[[3]]K , Pi3K_59F
107537	34123	CG34123	1.2	3	57	49	1.2	1.0E+00	CG30079 , CG30078 , TrpM , TRPM , CG16805 , BcDNA:GH04950 , CG34123
101096	14030	bub1	1.2	2	57	49	1.2	1.0E+00	Bub1 , BUB1 , CG14030/Bub1 , BUB1-like , BubR1 , CG14030 , bub1
51995	17216	KP78b	1.2	2	51	44	1.2	1.0E+00	CG17216 , Kp78B , KP78B , KP78b
24683	4945	CG4945	1.2	2	22	19	1.2	1.0E+00	PKN , CT15864 , CG4945
6446	8804	wun	1.2	1	23	20	1.2	1.0E+00	CG8804 , Wunen , l(2)k16806 , wun
25817	3172	twf	1.1	2	63	55	1.1	1.0E+00	CG3172 , A6 , twf
17576	14411	CG14411	1.1	2	41	36	1.1	1.0E+00	CG14411
107996	10443	Dlar	1.1	3	33	29	1.0	1.0E+00	Dlar , LAR , DLAR , dlar , DLar , CG10443 , PTP38A , Lar
105471	2577	CG2577	1.1	1	25	22	1.1	1.0E+00	CG2577
51616	6715	CG6715 KP78a	1.1	1	34	30	1.1	1.0E+00	CG6715 , Kp78A , KP78A , KP78a
29024	9096	cycD	1.1	3	77	68	1.1	1.0E+00	cycD, CycD, cyclinD, Cyclin-dependent Kinase interactor 3, dcycD, cdi3
106088	11870	Omphk1 like16334	1.1	2	52	46	1.1	1.0E+00	EMK/KIAA0537 , CG11871 , CG11870 , Omphk1
101634	4123	CG34123	1.1	2	35	31	1.1	1.0E+00	CG30079 , CG30078 , TrpM , TRPM , CG16805 , BcDNA:GH04950 , CG34123
100178	17746	PP2C	1.1	3	55	49	1.1	1.0E+00	PP2C , CG17746
26496	4290	CG4290	1.1	1	28	25	1.1	1.0E+00	EG:22E5.8 , CG4290
1827	3051	SNF1a	1.1	4	67	60	1.1	1.0E+00	AMPK , snf1a , DmAMPK alpha , FBgn0023169 , EG:132E8.2 , CG3051 , Gprk-4 , Gprk4 , SNF1A , dAMPKa , AMPKalpha , ampk&aagr;
105753	34361	Dgk	1.1	2	48	43	1.1	1.0E+00	CG34361 , DGKb , CG18654 , unnamed , dDGK , CG1535 , Dgk , CG12820
1016	1389	tor	1.1	2	82	74	1.1	1.0E+00	CG1389 , Tor , splc , tor , Torso , TOR
32955	17598	CG17598	1.1	2	21	19	1.1	1.0E+00	PP2C , CG17598
23723	9391	CG9391	1.1	2	32	29	1.1	1.0E+00	142335_at , IMP , CG9391
100717	6114	MRP	1.1	2	43	39	1.1	1.0E+00	CG6214 , dMRP/CG6214 , dMRP , MRP
107303	4268	pitslre	1.1	3	70	64	1.1	1.0E+00	PITSLRE , CG4268 , group 3 , Gta , Gat , Pitslre , cdk11
26915	8914	CG8914 CkIIbeta2	1.1	1	12	11	1.1	1.0E+00	CK2 , CKIIbeta' , CK2beta' , DmCKIIbeta' , CKIIb2 , CG8914 , CkIIbeta2 , DmCK2beta'
105157	32417	Myt1	1.1	2	36	33	1.0	1.0E+00	myt1 , Dmyt1 , MYT 1 , dMyt1 , CG10569 , CG32417 , Myt1
105324	18741	DopR2	1.1	5	111	101	1.1	1.0E+00	CG18741 , DOPR99B , DAMB , DopR99B , CG7569 , Dar2 , DopRII , DopD1 , DopR2

40576	5072	cdk4	1.1	8	156	144	0.9	1.0E+00	Cdk4/6 , cdk4 , CDK4 , l(2)0671 , l(2)sh0671 , cdk4/6 , CG5072 , CDK4/6 , l(2)s4639 , l(2)k06503 , l(2)05428 , DmCdk4 , 8-6 , Pk?7 , Pk53C , Cdk4
23179	3705	aay	1.1	2	41	38	1.1	1.0E+00	0423/14 , CG3705 , anon-WO0172774.117 , aay
104491	8203	cdk5	1.1	2	14	13	0.8	1.0E+00	CDK5 , CG8203 , cdk5 , DmCdk5 , Cdk5
107848	10177	CG10177	1.1	2	44	41	1.1	1.0E+00	CG10177
101380	1495	CaMKI	1.1	3	60	56	1.1	1.0E+00	caMKI , Calcium/calmodulin-dependent protein kinase , CamKI , CG1495 , camKI , dCKI , CaMKI
1214	31127	Wsck	1.1	1	15	14	1.1	1.0E+00	WSCK , CG31127 , BcDNA:SD05152 , BcDNA:LD25626 , Wsck
12553	10295	Pak	1.1	2	46	43	1.1	1.0E+00	PAK1 , DPAK , DmPAK1 , pak , dpak , pak1 , dPak , Pak1 , PAK , Dpak , DPak , PaK , dPAK1 , PAK2 , CG10295 , Dpak1 , D-Pak , p65[PAK] , dPAK , Pak , dpak1
106056	17559	dnt	1.1	2	49	46	1.1	1.0E+00	CG17559 , dnt
105661	8173	CG8173	1.1	2	18	17	1.1	1.0E+00	CG8173
29032	9115	CG9115	1.1	2	18	17	1.1	1.0E+00	MTM1 , CG9115 , unnamed , dMTMH1 , mtm
100241	13035	cg13035	1.1	2	56	53	1.1	1.0E+00	cg13035
4771	1511	Eph	1.1	2	60	57	1.1	1.0E+00	Eph , eph , Dek , Deph , DEK , CT3831 , CG1511 , dek , Dek7 , RPTK Dek7 , Ek7
31672	12170	CG12170	1.0	2	22	21	0.8	1.0E+00	anon-WO0118547.367 , CG12170
43824	13688	CG13688	1.0	2	27	26	1.0	1.0E+00	CG13688 , dmIpk2 , Ipk2
17282	3682	PIP5K 59B	1.0	1	29	28	1.0	1.0E+00	CG3682 , PIP5K 59B , CG17281 , PIP5K59B
106268	18604	CG18604	1.0	2	46	45	1.0	1.0E+00	CG18604
100886	12069	CG12069	1.0	3	74	73	1.0	1.0E+00	CG12069
9241	2048	dco	1.0	1	1	0	0.0	1.0E+00	dco , DBT , dbt , Dbt , CKIepsilon , CK1epsilon , DBT/CK1epsilon , ddbt , ck1epsilon , DCO/CKIe , CG2048 , l(3)j3B9 , l(3)discs overgrown , l(3)S144701 , l(3)S053813 , 1460/09 , 1447/01 , 1396/02 , 0915/10 , 0538/13 , l(3)dco , dco-1 , l(3)discs overgrown-1 , l(3)dco-1 , l(3)rK215 , dCKIepsilon , Dco/CK1 , DCO , Dco
33516	2272	slpr JNKKK MLK	1.0	1	1	0	0.0	1.0E+00	dMLK , MLK2 , Mlk2 , dMLK2 , CG2272 , slpr , Slpr , JNKKK , MLK
106449	2272	slpr JNKKK MLK	1.0	1	23	23	1.0	1.0E+00	dMLK , MLK2 , Mlk2 , dMLK2 , CG2272 , slpr , Slpr , JNKKK , MLK
107985	3216	CG3216	1.0	2	58	58	1.0	1.0E+00	GYC , CG3216
34594	3324	Pkg21D	1.0	1	1	0	0.0	1.0E+00	PKG-21D , dg1 , PKG 21D , CG3324 , DG1 , PKG , cGMP , Pkg1 , Dg1 , Pkg21D
2897	4032	abl	1.0	1	6	6	1.0	1.0E+00	D-abl , abl , Ableson , AblK , CG4032 , DROTKABL3 , ABL , Ddash/abl , DAbl , c-abl , 4674 , Dash , Am ABL , Dabl , l(3)04674 , cAbl , D-ash , l(3)c-abl , l(3)73Ba , abl1 , Dsrc7 , C-abl , Abl1 , Abl , dAbl
21611	4209	CanB	1.0	2	50	50	1.0	1.0E+00	Calcineurin B , canB-4F , CNB , dCnB1 , BcDNA:RH11383 , Can , CG4209 , CanB
103739	4290	cg4290	1.0	1	23	23	1.0	1.0E+00	EG:22E5.8 , CG4290
106329	4488	wee1	1.0	1	23	23	1.0	1.0E+00	Wee1 , dwee1 , Dwee , wee1 , Dwee1 , Wee 1 , dWee1 , WEE1 , CG4488 , Wee , wee
106130	5363	cdc2	1.0	2	9	9	1.0	1.0E+00	cdk1 , Cdk1 , Cdc2 , CDK1 , CG5363 , Dmcdc2 , CDK1/CDC2 , DmCdk1 , DmCdc2 , cdc , CDCDm , Dm cdc2 , Dcdc2 , CDC2 , group 4 , cdc2Dm , l(2)31Eh , cdc2
101539	5830	CG5830	1.0	1	21	21	1.0	1.0E+00	CG5830
27696	6622	Pkc53E	1.0	1	8	8	1.0	1.0E+00	PKC-53B , PKC-53E , PKC , PKC 53B , CG6622 , PKC 53E , dPKC53E(br) , Dpkc1 , PKC1 , DPKC , dPKC , Pkc1 , Pkc53E , PKC53E
106098	7378	CG7378	1.0	2	11	11	1.0	1.0E+00	BcDNA:RH25447 , CG7378
25528	7717	mekk1	1.0	1	1	0	0.0	1.0E+00	Mekk1/4 , D-MEKK1 , D-Mekk1 , dMEKK4 , dMEKK , mekk1b , mekk1a , MEKK4 , MEKK , DmMEKK1 , mekk1 , CG7717 , Mekk1 , dMEKK1 , MEKK1
3002	7892	nemo see also 101545	1.0	1	14	14	1.0	1.0E+00	Nlk , CG7892 , Nemo , NEMO/NLK , NEMO , adk , clone 2.43 , anon-WO0172774.138 , anon-EST:Gibbs3 , anon-EST:Liang-2.43 , anon-WO0140519.256 , anon-WO0118547.332 , nmo , nemo
107083	8250	Alk	1.0	2	41	41	1.0	1.0E+00	ALK , mili , DAlk , dALK , DAlk53 , CG8250 , Alk
107187	10572	Cdk8	1.0	1	7	7	1.0	1.0E+00	Cdk8 , cdk8 , CDK8 , p58 , CG10572 , dTRAP56 , DmCdk8
38541	11597	PP4	1.0	1	1	0	0.0	1.0E+00	CG11597 , PP4
106253	12252	CG12252	1.0	2	2	0	0.0	1.0E+00	CG12252
104884	14211	CG14211	1.0	2	39	39	1.0	1.0E+00	CG14211
32378	15224	CG15224 CkIIbeta	1.0	1	1	0	0.0	1.0E+00	CKII , CK2 , CkII-beta , CK2beta , DmCKIIbeta , dCKII , DmCK2beta , CKIIbeta , CkIIbeta1 , betaCK2 , DmCkIIbeta , CKIIb , CG15224 , CK II , CKII-beta1 , mbu , CkII , And , CCK2 , CK-IIbeta , CK-II beta , CK-2 , Ds cas kin , CkIIbeta , Cask-II-b , dCK2beta , dCKII beta
991	18402	inr	1.0	2	2	1	0.0	1.0E+00	dInR , dinr , InsR , Inr , DInr , dInr , DInR , DIR , insulin/insulin-like growth factor receptor , inr , CG18402 , dIR , INR , l(3)05545 , IR , dir , DIRbeta , DIRH , DIHR , dInsR , DILR , dIRH , er10 , l(3)er10 , l(3)93Dj , Inr-beta , Inr-alpha , Dir-b , Dir-a , InR , dINR
105762	32156	Mbs	1.0	1	1	1	0.0	1.0E+00	MBS , DMBS , l(3)72Dd , DMYPT , DMbs , CG5891 , l(3)03802 , 0573/06 , 0953/04 , l(3)S095304 , l(3)S005331b , l(3)S057306 , l(3)S057306b , l(3)j7A1 , l(3)j3B4 , Mypt , CG5600 , CG32156 , Mbs , mbs
32813	17026	CG17026	1.0	2	59	60	1.0	1.0E+00	CG17026
103976	1609	Gcn2	1.0	3	50	51	1.0	1.0E+00	DGCN2 , EIF2 , CG1609 , GCN2 , dGCN2 , Gcn2
107458	15072	EMK	1.0	2	47	48	1.0	1.0E+00	EMK/KIAA0999 , CG15072
20909	2845	phl	1.0	3	41	42	0.9	1.0E+00	raf , phl , Raf , D-Raf , RAF , Draf , draf , l(1)polehole/draf , raf-1 , D-raf , DRaf , EG:BACH48C10.3 , CG2845 , l(1)pole hole , Draf1 , D-RAF , l(1)phl , l(1)2Fe , Raf1 , raf1 , rafl , D-raf1 , l(1)polehole , l(1)ph , ph , C110 , 11-29 , l(1)raf , Draf-1 , l(1)G0475 , Phl , Raf/phl
104688	8967	otk	1.0	2	41	42	0.9	1.0E+00	OTK , Otk , Dtrk , dTrk , CT25769 , OFT/TRK , CG8967 , DTrk , Trk48D , Tk48D , IGGtyk , Dtkr , anon-WO2004063362.81 , otk
105568	6036	CG6036	1.0	4	67	69	1.0	1.0E+00	PP2Cb , CG6036
39561	4583	ire	1.0	2	33	34	1.0	1.0E+00	CG4583 , dire-1 , IRE-like , ire-1 , IRE1 , Ire1 , Ire-1
46076	6562	synj	1.0	1	29	30	1.0	1.0E+00	

26427	4201	ird5	1.0	2	27	28	0.8	1.0E+00	ird , dIKK-beta , IKK , IKK-beta , dIKK , IKKB , DmIKKb , DmIkkbeta , dmIKKbeta , ird5/Dmlkk[beta] , DmIKKbeta , CG4201 , DmIKK , Dmikkbeta , DmIKKBeta , dLak , Ird-5 , Ik , ikk , LRK , DLAK , DIK , unnamed , anon-89Bd , Lak , IK , ird5 , IKKbeta , IKKb , Ird5 , IRD-5
104081	32812	CG32812	1.0	2	27	28	1.0	1.0E+00	EG:114D9.1 , CG11408 , CG32812
25458	2929	Pi4KIIalpha	1.0	2	23	24	1.0	1.0E+00	CG2929 , PI4KIIalpha , Pi4KIIalpha , PI4KII
107652	31097	CG31097	1.0	2	68	71	1.0	1.0E+00	CG13665 , CG31097
1012	6899	Ptp4E	1.0	2	21	22	1.0	1.0E+00	PTP4E , CG6899 , CT21187 , R-PTP 4E , DPTP4E , unnamed , Ptp4E , PtP4E
103749	10082	CG10082	0.9	2	77	82	0.9	1.0E+00	anon-WO0172774.149 , CG10082
107001	6297	JIL-1	0.9	2	44	48	0.9	1.0E+00	JIL1 , JIL-1 , MSK , JIL , CG6297 , Jil-1 , 2Ab17 , unnamed , Jil1 , Su(var)3-1 , Su(var)3-103 , Su-var(3)103 , Su-var(3)1 , anon-WO0118547.379 , IL-1
103416	8174	SRPK	0.9	2	33	36	0.9	1.0E+00	dSRPK1 , CG8174 , dSRPK , BcDNA:SD03158 , SRPK , srpk
101875	12147	CKIa-like	0.9	2	11	12	0.8	1.0E+00	CG12147, CKIa-like
101624	9985	sktl	0.9	4	32	35	0.9	1.0E+00	PIP5K 57B6 , CG9985 , l(2)k12405 , l(2)05475 , 25/17 , ski , fam , sktl , PIP5K
106919	7693	fray	0.9	2	42	46	0.9	1.0E+00	STE20-like/SPAK , CG7693 , l(3)07551 , lag , 4624 , fray , dSTRAD
102179	7001	Pk17E	0.9	2	30	33	0.9	1.0E+00	BIN4 , Bin4 , CG7001 , bin4 , 3-10 , Pk?4 , Pk17E
103774	5974	pelle	0.9	4	69	76	0.8	1.0E+00	CG5974 , PELLE/IL-1 , p11 , pll
106255	7125	PKD	0.9	2	67	74	0.9	1.0E+00	PKD , 150131_at , PKCm , CG7125 , dPKD
40719	8726	CG8726	0.9	2	46	51	0.9	1.0E+00	CG8726
103828	3008	CG3008	0.9	1	9	10	0.9	1.0E+00	CG3008
38930	18069	CaMKII	0.9	1	9	10	0.9	1.0E+00	CaMKII , CAMKII , CaMK-II , dCaMKII , Calcium/calmodulin-dependent protein kinase , camKII , CaM KII , CamKII , CaM II , CG18069 , CAMKIId , CDPK1 , Ca2+/calmodulin-dependent protein kinase II , calcium/calmodulin-dependent protein kinase II , DCK , CaMK II , CaM , CamKIIalpha , Cam , CAMKIIalpha
19275	1973	CG1973	0.9	2	41	46	0.9	1.0E+00	CG1973
27662	6551	fu	0.9	2	40	45	0.9	1.0E+00	fu , Fu , CG6551 , fu[mel] , Dm fu , l(1)fu , FU , dFu
107071	7904	put	0.9	2	40	45	0.9	1.0E+00	atrII , CG7904 , Punt , TGF-B , Atr-II , l(3)10460 , STK-C , pun , TGF-beta , l(3)j5A5 , dlhC , Tgf-r , AtrII , Atr , Atr88CD , Act-r , put , Put , punt
104555	14212	CG14212	0.9	2	23	26	0.9	1.0E+00	CG14212
107849	8584	CG8584	0.9	2	30	34	0.9	1.0E+00	BEST:LP01468 , CG8584
105752	14903	CG14903	0.9	2	30	34	0.9	1.0E+00	CG14903
107266	8874	Fps85D	0.9	2	37	42	0.9	1.0E+00	FER , CG8874 , Dfer , fer , DFER , FPS , DmHD-179 , dfps 85D , dFer , Dfps , DFer , Dm FPS , Fer , dfps85D , fps , dfps , fps85D , HD-179 , Fps85D , dfer
107042	7028	CG7028	0.9	3	42	48	0.9	1.0E+00	FBgn0027587 , BcDNA:GH04978 , PRP4 , prp4 , CG7028
107648	14396	Ret	0.9	2	62	71	0.9	1.0E+00	MEN2 , dRet , dRET , RET , Dret , CG14396 , CG1061 , ret , D-ret , DmHD-59 , DRET , Reto , HD-59 , Ret
106331	15771	CG15771	0.9	2	38	44	0.9	1.0E+00	CR33074 , CG15771
100999	4839	CG4839	0.9	2	42	49	0.9	1.0E+00	CG4839
107158	5169	GckIII	0.9	2	36	42	0.9	1.0E+00	GckIII , CG5169 , dGCKIII , GCKIII , STLK3
100863	13850	CG13850	0.9	1	6	7	0.9	1.0E+00	GH07286p , CG13850
103144	9842	PP2B-14D	0.9	2	58	68	0.9	1.0E+00	DmPp2B-14D , canA , PP2B 14D , CG9842 , Pp12-14D , CnnA14D , calcium/calmodulin regulated protein phosphatase 2B , PP2B , D33 , PpD33 , Pp2B-14DF , CanA14D , Pp2B-14D
104452	10138	PpD5	0.8	2	21	25	0.8	1.0E+00	CG10138 , D5 , anon-WO0140519.107 , PpD5
104814	12484	CG12484	0.8	2	51	61	0.8	1.0E+00	CG12484 , CG33041 , CT32777 , CG30143
104348	8024	ltd	0.8	3	64	77	0.8	1.0E+00	ltd , Rab-RP1/CG8024 , CG8024 , Rab-RP1 , RabRP1 , Rab32 , DmRab32 , DrabRP1 , DRABR1 , Rab-r1 , anon-WO0118547.106 , RAB-RP1 , Rab32/RP1
101154	1389	tor	0.8	1	29	35	0.8	1.0E+00	CG1389 , Tor , splc , tor , Torso , TOR
104489	8057	alc	0.8	2	24	29	0.7	1.0E+00	FBgn0033383 , alc , CG8057
100169	3969	PR2	0.8	2	47	57	0.8	1.0E+00	DPR2 , PR2/ACK , CG3969 , DmHD-11 , DRODPR2 , dACK , Rp2 , HD-11 , PR2
101451	17596	s6kII	0.8	2	37	45	0.8	1.0E+00	RSK , ign , dRSK , CG17596 , S6KII , Rsk , S6kII
106267	33519	Unc-89	0.8	2	37	45	0.8	1.0E+00	CG33519 , CG30171 , CG18020 , CG3901 , CG18021 , CT40326 , CT40322 , CT12925 , BEST:HL01080 , CG18019 , CG30175 , Unc-89 , UNC-89
101242	18734	Fur2	0.8	1	23	28	0.8	1.0E+00	154521_at , fur2 , Furin , Dfur2 , FUR2 , DMH#11 , furin , CG4235 , CG18734 , Fur2
104729	11597	PP4	0.8	3	90	111	0.8	1.0E+00	CG11597 , PP4
107770	9156	Pp1-13C	0.8	1	17	21	0.8	1.0E+00	DmPp1-13C , pp1-13C , PP1alpha13C , PP1c , PP1 , PP1 13C , CG9156 , PP13C , Pp1 , unnamed , Pp1-13C , 13C
27359	5125	ninaC	0.8	2	37	46	0.8	1.0E+00	Nina C , NINAC , NinaC , Dm NinaC , CG5125 , NINA C , CT42491 , CT16120 , CG54125 , 2.2 , DRONINAC , ninaC
101335	10376	PP2C	0.8	2	37	46	0.8	1.0E+00	PP2C , CG10376
38460	11236	CG11236	0.8	2	37	46	0.8	1.0E+00	CG11236
105483	1906	alph PP2Cb	0.8	1	20	25	0.8	1.0E+00	SK3-1 , alph , CG1906 , pp2c99B , PP2Cb
35252	7524	Src64B	0.8	2	22	28	0.7	1.0E+00	Src64 , Src , src64 , src64B , CG7524 , src64b , dSrc , DSrc64B , Dsrc64B , SRC 64B , src , DSrc64 , DmHD-358 , dsrc , Dsrc64 , Dm SRC1 , DSRC64 , DSrc , Src1 , Dsrc , D-src , c-src , src1 , HD-358 , C-src1 , Src64B
25304	18247	shark	0.8	1	7	9	0.8	1.0E+00	Shark , SHARK , CG18247 , SYK/SHARK , dtk7 , l(2R)W4 , l(2)W4 , Tk7 , Dtk7 , shark
26933	8174	SRPK	0.8	1	13	17	0.8	1.0E+00	dSRPK1 , CG8174 , dSRPK , BcDNA:SD03158 , SRPK , srpk
101463	17998	Gprk2	0.8	2	16	21	0.7	1.0E+00	154978_at , gprk2 , CG17998 , Gprk-2 , Gprk2
106210	17269	Fancd2	0.8	2	35	46	0.8	1.0E+00	dmFANCD2 , CG17269 , CG31194 , FANCD2 , CG31192 , Fancd2

100800	12091	CG12091	0.8	1	22	29	0.8	1.0E+00	CG12091
106092	8224	baboon activin-R	0.8	2	3	4	0.0	1.0E+00	babo , Bab , CG8224 , ATR-I , l(2)k16912 , ATR-1 , Atr-1 , Atr-I , AtrI , Atr45A , STK-E , atr-I , Gprk-3 , Babo , l(2)44Fd , Gprk3 , Atf1 , BABO
106774	5408	trbl	0.7	2	40	54	0.7	1.0E+00	trbl , CG5408 , unnamed
33054	1830	CG1830	0.7	2	24	33	0.7	1.0E+00	unnamed , CG1830 , DPhK-gamma , anon-sts6 , ESTS:194B3T , EP779 , PhKgamma
105265	17216	KP78b like 51995	0.7	1	8	11	0.7	1.0E+00	CG17216 , Kp78B , KP78B , KP78b
104569	5680	jnk (bsk)	0.7	2	13	18	0.5	1.0E+00	bsk , JNK , DJNK , jnk , dJNK , DBSK/JNK , D-JNK , CG5680 , DJNK/bsk , JNK/SAPK , SAPKa , D-junk , Bsk , Junk
101758	1098	madm (secretion)	0.7	2	5	7	0.0	1.0E+00	CG1098 , dMADM , BcDNA:LD28657 , anon-WO0118547.406 , Madm
16239	11621	Pi3K68D	0.7	1	10	14	0.7	1.0E+00	Pi3K , PI3K , dPI3K , PI3K_68D , CG11621 , PI(3)K , cpk , PI3K 68D , PI3K-68D/E , Cpk , PI3K 68_D , PI3K-68D , dPIK , BcDNA:LD15217 , Pi3K68D , PI3K68D , PI[[3]]K
50642	33747	primo-2	0.7	1	5	7	0.0	1.0E+00	LMW-PTP , CG9599 , primo , CG31311 , CG33747 , primo-2
101274	12078	CG12078	0.7	2	39	55	0.7	1.0E+00	CG12078
101146	5182	Pk34A	0.7	2	29	41	0.7	1.0E+00	GSK3a , CG5182 , Pk34A
100257	16910	key	0.7	3	53	77	0.7	9.8E-01	key , dIKK-gamma , IKKgamma , Kenny , IKK-gamma , DmIKKgamma , dIKK , dmIKKgamma , CG16910 , Dmikkgamma , DmIKK-gamma , IKKg , Key , kenny
100299	1362	cdc2rk	0.7	3	75	110	0.7	6.6E-01	CG1362 , Dcdrk , cdc2rk
105674	5026	CG5026	0.7	2	19	28	0.7	1.0E+00	CG5026
107766	2845	phl	0.7	3	57	85	0.7	8.8E-01	raf , phl , Raf , D-Raf , RAF , Draf , draf , l(1)polehole/draf , raf-1 , D-raf , DRaf , EG:BACH48C10.3 , CG2845 , l(1)pole hole , Draf1 , D-RAF , l(1)phl , l(1)2Fe , Raf1 , raf1 , rafl , D-raf1 , l(1)polehole , l(1)ph , ph , C110 , 11-29 , l(1)raf , Draf-1 , l(1)G0475 , Phl , Raf/phl
101345	1216	mri	0.7	1	14	21	0.7	1.0E+00	CG1216 , mri
105122	13197	CG13197	0.7	1	12	18	0.7	1.0E+00	BcDNA:RE27552 , CG13197
101550	16708	CG16708	0.7	2	44	66	0.7	9.9E-01	CG16708 , DCERK
103642	32944	CG32944	0.7	1	10	15	0.7	1.0E+00	CG9818 , CG10532 , CG32944
102830	1594	hop	0.7	3	19	29	0.6	1.0E+00	Hop , JAK , d-jak , Jak , Tum-1 , CG1594 , DmHD-160 , Hop1 , Dm JAK , l(1)10Be , l(1)hop , Tum , l(1)L4 , 4 , L4 , msvl , l(1)G18 , HD-160 , hop , HOP , hopscotch
862	14026	tkv	0.7	1	13	20	0.7	1.0E+00	tkv , Tkv , TKV , CG14026 , Brk25D2 , Brk25D1 , dtfr , Atkv , l(2)04415 , str , Brk25D , l(2)25Da , STK-A , Dtfr , Atr25D , tkv1
2968	4353	hep	0.6	5	16	25	0.5	1.0E+00	HEP/MKK7 , DJNKK , HEP , JNKK , MKK7 , DHEP/MKK7 , CG2190 , CG4353 , DMKK7 , hp , l(1)G0107 , l(1)G0208 , l(1)7P1 , hem , hep , Hep , MAPKK
100685	32717	stardust	0.6	3	62	97	0.6	4.9E-01	CG12657 , Sdt , PALS1 , Std , CG15341 , CG15339 , std , anon-EST:fe2E6 , l(1)7Ef , CG1617 , CG15340 , CG12658 , CG15342 , CG32717 , sdt , pal1 , Pals1
29406	30295	CG30295	0.6	2	23	36	0.6	1.0E+00	CG30295 , dmIpk1 , CG15230 , CG15229 , CG15228 , Ipk1
101538	2621	sgg	0.6	2	15	24	0.4	1.0E+00	GSK3beta/SGG , Zw3 , GSK , zw3 , GSK3beta , GSK3 , Gsk3 , GSK-3 , GSKbeta , GSK-3beta , ZW3 , CG2621 , EG:155E2.3 , Zw3-sh , DMSGG3 , Sgg , SGG/GSK3b , Zw3/GSK3 , sgg46 , sgg39 , sgg10 , DMZ3K25Z , sgg-zw3 , l(1)3Ba , zw-3 , Zw-3 , zw3[sgg] , Zw3[sgg] , zw3/sgg , sgg/zw3 , zw[3] , zw3(sgg) , l(1)zw3 , ZW-3 , l(1)G0055 , l(1)G0183 , l(1)G0263 , l(1)G0335 , EG:BACR7C10.8 , anon-WO03040301.254 , sgg , gsk3 , Dmsgg3 , SGG , Sgg/Zw3/GSK3 , Gsk-3 , GSK-3B , GSK3betagr;
100269	3724	pgd	0.6	1	13	21	0.6	1.0E+00	6PGDH , 6-Pgd , 6-PGD , CG3724 , EG:87B1.4 , 6-pgd , Pdg , 6Pgdh , l(1)G0385 , 6Pgd , l(1)Pgd , 6PGD , PGD , l(1)2De , l(1)2Dc , l35 , N1 , l(1)A7 , A7 , l(1)Pgd-A , l(1)N3[90] , l(1)N1 , Pgd , pgd , 6pgdh
41735	30388	Magi	0.6	2	16	26	0.5	1.0E+00	ima , Ima , D-MAGI , CG4117 , CG15656 , CG30388 , Magi
103624	4252	mei-41 ATR	0.6	4	96	157	0.6	1.5E-02	mei-41 , ATR , CG4252 , meiP41 , mus104 , mei41 , mus103 , MEI41/FRP1 , Mei-41 , MEI41 , mus-104 , mus(1)104 , fs(1)M37 , mus(1)103 , mus-103 , atr , mei-195 , DmATR
5702	17596	s6kII	0.6	1	15	25	0.6	1.0E+00	RSK , ign , dRSK , CG17596 , S6KII , Rsk , S6kII
104902	32742	l(1)G0148	0.6	1	18	32	0.6	1.0E+00	CG32742 , cdc7-related , CG8655 , l(1)G0149 , CT25076 , l(1)G0461 , CG8656 , anon-WO03040301.250 , l(1)G0148
10347	11516	Ptp99A	0.6	2	33	59	0.6	6.5E-01	DPTP99A , CT6383 , R-PTP 99A , CG11516 , CG2005 , PTP99A , dptp99A , DPTP[[99A]] , CG11515 , CG11517 , Ptp99A
105732	34412	tlk (spindle defects, EP is E(pble	0.6	3	10	18	0.5	1.0E+00	CG34412 , tlk , CG32782 , CG2829 , BcDNA:GH07910 , l(1)G0054 , CG33219 , dtlk , anon-WO03040301.116 , anon-WO03040301.114 , CG32781 , EP1413 , EP(X)1413 , CG12462 , Tlk
101655	13311	CG13311	0.5	1	27	51	0.5	6.7E-01	BcDNA:RE29808 , CG13311
21756	3954	csw	0.5	3	36	70	0.5	1.5E-01	csw , Csw , EG:BACN25G24.2 , CG3954 , Csw/Shp2 , l(1)2Db , E(sev)1A , CSW , l(1)G0170 , l(1)2Dd , l(1)csw , 19-106 , l(1)GA114 , anon-WO03040301.219 , anon-WO03040301.209 , anon-WO03040301.207 , Shp2/csw
16182	1107	aux	0.5	2	1	0	0.0	1.0E+00	auxilin , CG1107 , GAK , anon-WO0118547.393 , aux , auxillin , dAux
106200	3051	SNF1a	0.5	2	9	18	0.4	1.0E+00	AMPK , snf1a , DmAMPK alpha , FBgn0023169 , EG:132E8.2 , CG3051 , Gprk-4 , Gprk4 , SNF1A , dAMPKa , AMPKalpha , ampk&aagr;
103387	6292	CycT	0.5	2	1	0	0.0	1.0E+00	P-TEFb , dT , p124 , Dmcyclin T , unnamed , anon-74EFc , CG6292 , CycT
103452	8805	wun2	0.5	1	3	6	0.0	1.0E+00	N14 , wun-2 , CG8805 , Tunen , WUN-like , Pap2G , DrPAP2[G] , CK02248 , BEST:CK02248 , wun2
3793	9774	rok	0.5	2	1	1	0.0	1.0E+00	ROCK , Drok , Rok , DROK , ROK , ROKalpha/beta , drok , Rock , RhoK , dROK , dRok , DRhk , ROCK1 , CG9774 , unnamed , Rhk , rok , ROCK-1
105614	10260	CG10260	0.5	2	1	1	0.0	1.0E+00	EG:BACR7C10.2 , PI4K , CG10260
104959	10498	cdc2c	0.5	2	1	1	0.0	1.0E+00	Cdk2 , cdk2 , CDK2 , Cdc2c , CG10498 , CDK2/CDC2c , S(Sev-CycE)3A , DmCdk2 , Dmcdc2c , DmCdc2 , Dcdc2c , CDC2c , cdc2c
105834	14026	tkv	0.5	2	1	0	0.0	1.0E+00	tkv , Tkv , TKV , CG14026 , Brk25D2 , Brk25D1 , dtfr , Atkv , l(2)04415 , str , Brk25D , l(2)25Da , STK-A , Dtfr , Atr25D , tkv1
3116	18243	Ptp52F	0.4	3	25	56	0.4	1.0E-01	DPTP52F , CT18044 , CG18243 , Ptp52F , PTP52F
105610	1227	MPSK	0.4	2	5	12	0.0	1.0E+00	MPSK/PSK , CG1227
33434	1954	PKC98E	0.4	1	14	36	0.4	3.4E-01	PKC-98F , PKC , PKC 98F , CG1954 , 98F , dPKC98F , Dpkc3 , PKC d98F , nPKC , Pkc3 , Nc98F , Pkc98E

101406	5643	wdb	0.4	3	7	18	0.3	1.0E+00	PP2A , CG5643 , PP2-AB , BcDNA:LD34343 , EP3559 , l(3)S031807 , LD02456 , 0318/07 , BEST:LD02456 , wdb , dPP2A , dB56-2 , PP2a
106962	8049	tec	0.3	4	8	23	0.0	8.4E-01	Btk29A , Tec29 , CG8049 , tec29 , Tec , Tec29A , fic , SRC 29A , CT41718 , CT2415 , DTec29 , DSrc28 , Dsrc29A , Dsrc28C , Src29A , Dm SRC2 , dsrc29A , c-src/fps , src28C , src-4 , src4 , src2 , Src2 , S13 , CG18355 , C-src4 , C-src2 , btk , btk29A
104169	11228	hpo	0.3	1	1	3	0.0	1.0E+00	CG11228 , dMST , MST2 , hpo , Hpo
102481	34384	CG34384	0.3	1	3	10	0.0	1.0E+00	CG34384 , CG14462 , DGKd , CG9851 , CG2667 , CG31187
105353	8222	Pvr	0.3	6	43	145	0.3	7.0E-12	VEGFR , PVR , pvr , CG8222 , VEGFR-A , Vegfr-c , Vegfr-b , stai , Vegfr , DmVEGFR , vgr1 , VGR1 , CT24332 , Vgr1 , Pvr
1089	10244	FGFR1-like	0.3	1	1	4	0.0	1.0E+00	HD-14 , DCad96Ca , CG10239 , CG10244 , CT28779 , FGFR1-like , DmHD-14 , Cad96Ca , Dm Cad96Ca
103426	1107	aux	0.0	2	0	0	0.0	1.0E+00	auxilin , CG1107 , GAK , anon-WO0118547.393 , aux , auxillin , dAux
32283	1455	CanA1	0.0	1	0	0	0.0	1.0E+00	DmCanA1-100B , canA , CG1455 , CAN A1/PP2B , unnamed , pMY4 , CNA1 , PP2B , PP2B 21EF , CnnA21EF , D14 , PpD14 , Can , CanA1
107991	1634	CG1634 Nrg	0.0	1	0	0	0.0	1.0E+00	CT4318, l(1)7Fa, l(1)G0099, neuroglian, Ngl, nrg, NRG, RA35, ceb, central brain deranged
41134	1725	dlg1	0.0	1	0	0	0.0	1.0E+00	dlg , DLG , Dlg , Discs-large , Dlg-A , anon-EST:Posey93 , Dlg1 , dlg-A , misb , CG1725 , DLG-A , DlgA , dlgA , dlg-1 , Drodlg , l(1)dlg1 , l(1)dlg , l(1)10Bf , l(1)d.lg-1 , l(1)discs large , l(1)bwn , l(1)dlg-1 , d. lg.-1 , l(1)L11 , 11 , l(1)lpr-2 , l(1)d.lg.-1 , l(1)G0276 , l(1)G0342 , l(1)G0456 , l(1)l.pr.-2 , l(1)G19 , CG1730 , anon-WO03040301.258 , anon-WO03040301.268 , anon-WO03040301.260 , dlg1 , CPD , SAP97 , PSD95
42457	1891	CG1891 sax	0.0	1	0	0	0.0	1.0E+00	sax , CG1891 , Sax , Bkr43E , Brk43E , STK-B , SAX
13664	2028	CK1a	0.0	1	0	0	0.0	1.0E+00	CK1 , CK1alpha , CKIalpha , CKI , CK1a , CkIa , CKIa , CG2028 , CK I , dmckI , dmCK1 , CkIalpha , l(1)G0492 , anon-WO03040301.95 , anon-WO03040301.93 , ck1alpha , CKI alpha , ck1a , PKA-C
2964	2096	flw	0.0	1	0	0	0.0	1.0E+00	PP1beta9C , flw , DmPp1-9C , PP1 b9C , PP1c , PP1 , PP19C , CG2096 , FLW/PP1B , Pp1beta-9C , PP1 9C , PP1beta , PP-1 , l(1)G0172 , CG15305 , anon-WO03040301.120 , FLW
51227	2252	fs(1)h	0.0	3	0	2	0.0	1.0E+00	l(1)7Da , fsh , clone 1.81 , rnc , fst(1)h , fs(1)1456 , N72 , fs(1)M16 , l(1)G0093 , l(1)G0495 , anon-EST:fe1G2 , fs(1)R10.4 , fs(1)26/26A , anon-EST:Liang-1.81 , CG2252 , fs(1)h
41693	2577	CG2577	0.0	1	0	0	0.0	1.0E+00	CG2577
103748	2615	ik2	0.0	1	0	0	0.0	1.0E+00	ik2 , l(2)38Ea , DmIKKepsilon , APTX7 , CG2615 , IKKepsilon , Ik2 , Ik2/DmIKK , dIKK , IK2 , 38D.31 , DmIKKepsilon/dIK2 , Dmik2 , DIK2 , dik2 , Dik2 , IKK
106695	3608	CG3608	0.0	2	0	1	0.0	1.0E+00	CG3608
103703	4006	Akt	0.0	4	0	5	0.0	1.0E+00	dAkt1 , AKT , Akt , RAC , PKB , dAKT/dPKB , dAkt , PKB/AKT , PKB/Akt , PKB/dAKT , dPKB , Dakt1 , Akt/PKB , DAKT1/PKB , dAkt/PKB , Dakt , D-Akt , AKT/PKB , akt , l(3)89Bq , CG4006 , DAkt1 , l(3)04226 , DRAC-PK66; DRAC-PK85 , DAKT1 , dakt1 , DPKB , DRAC-PK , RacPK , Akt1 , dakt , dAKT1 , DAkt , pAkt , akt1
34891	4720	pk92b ASK1	0.0	1	0	0	0.0	1.0E+00	DASK1 , ASK1 , DPk92B/ASK1 , Ask1 , DASK , MEKK5/ASK1 , CG4720 , Pk92B , dASK
34915	5026	CG5026	0.0	0	0	0	0.0	1.0E+00	CG5026
30448	5179	cdk9	0.0	1	0	0	0.0	1.0E+00	P-TEFb , CDK9 , cdk9 , CG5179 , P-TEF , PTefb , Cdk9
41838	5363	cdc2	0.0	1	0	0	0.0	1.0E+00	cdk1 , Cdk1 , Cdc2 , CDK1 , CG5363 , Dmcdc2 , CDK1/CDC2 , DmCdk1 , DmCdc2 , cdc , CDCDm , Dm cdc2 , Dcdc2 , CDC2 , group 4 , cdc2Dm , l(2)31Eh , cdc2
34990	5387	cdk5a	0.0	1	0	0	0.0	1.0E+00	p35 , P35 , Dp35 , CG5387 , Cdk5a , dCdk5alpha , p35-31C , Cdk5alpha , Dmp35
22225	6114	CG6114	0.0	1	0	0	0.0	1.0E+00	CG6114
104167	6235	tws	0.0	1	0	0	0.0	1.0E+00	l(3)S049902 , tws/aar , PP2A , aar , CG6235 , B/PR55 , v158 , PR55 , 2414 , l(3)02414 , DPR55 , tw , l(3)S061805 , 1466/06 , l(3)S146606 , l(3)S141309 , l(3)S134601a , l(3)S132907 , l(3)S119908 , l(3)S111515 , l(3)S110815 , l(3)S110008a , l(3)S105605 , l(3)S101413b , l(3)S091905 , l(3)S088513 , l(3)S080409 , l(3)S076415 , l(3)S075902b , l(3)S075515b , l(3)S075110 , l(3)S069206a , l(3)S067915 , l(3)S067109b , l(3)S066813 , l(3)S066017 , l(3)S063110 , l(3)S061915 , l(3)S060804 , l(3)S060203 , l(3)S053011 , l(3)S052810 , l(3)S048507 , l(3)S048013 , l(3)S048006 , l(3)S046918 , l(3)S045519 , l(3)S043029 , l(3)S043008b , l(3)S042630 , l(3)S042629 , l(3)S035505b , l(3)S033903 , l(3)S032708c , l(3)S032303 , l(3)S031006 , l(3)S029701a , l(3)S029403 , l(3)S029110 , l(3)S028707 , l(3)S027313 , l(3)S027127 , l(3)S026326 , l(3)S026226 , l(3)S025913 , l(3)S025832 , l(3)S025806 , l(3)S024838 , l(3)S024834a , l(3)S024455 , l(3)S023938 , l(3)S023309 , l(3)S023206 , l(3)S023141a , l(3)S023013 , l(3)S022440 , l(3)S022361 , l(3)S022205b , l(3)s1801 , l(3)j11C8 , l(3)01436 , Pp2A-85F , tws , dPP2A , dPR55 , PP2a
104051	6620	aurB	0.0	2	0	5	0.0	1.0E+00	Aurora-B , aurora B , AurB , IAL1 , DmAurB , DmAuroraB , aurB , CG6620 , IAL , DmAIRK2 , ial , Ial
27785	7004	fwd	0.0	1	0	0	0.0	1.0E+00	CG7004 , PI4K , anon-WO0118547.259 , fwd
27808	7028	CG7028	0.0	1	0	0	0.0	1.0E+00	FBgn0027587 , BcDNA:GH04978 , PRP4 , prp4 , CG7028
6692	7223	htl	0.0	1	0	0	0.0	1.0E+00	Htl , heartless , FGFR , CG7223 , i79 , i100 , i150 , j372 , EMS2 , DFR1 , CT39172 , CT22273 , HTL/FGFR1 , dtk1 , DmHD-38 , Dfr-1 , DTRK(FR1) , FGF-R2 , DFGF-R1 , FR1 , DFR1/DFGF-R2 , DFGF-R2 , DFR-1 , FGFR2 , DPR3 , Tk1 , HD-38 , Fr1 , Dtk1 , Dfr1 , htl
25508	7597	CG7597	0.0	1	0	0	0.0	1.0E+00	AC017581 , anon-WO0140519.165 , CG7597 , gi24668141
26019	7873	Src42A	0.0	1	0	0	0.0	1.0E+00	src42A , Src42 , DSrc42A , Src , src42 , Dsrc42A , SRC 42A , CG7873 , SK2-4 , src , Dsrc41 , dtk5 , DmHD-29 , Src41 , Su(Raf)1 , Su1 , Dm SRC41 , dtk-5 , Su(phl)1 , Su(D-raf)1 , SRC42A , l(2)k10108 , Tk5 , HD-29 , Dtk5 , Src42A , dSrc
100708	7873	Src42A	0.0	2	0	0	0.0	1.0E+00	src42A , Src42 , DSrc42A , Src , src42 , Dsrc42A , SRC 42A , CG7873 , SK2-4 , src , Dsrc41 , dtk5 , DmHD-29 , Src41 , Su(Raf)1 , Su1 , Dm SRC41 , dtk-5 , Su(phl)1 , Su(D-raf)1 , SRC42A , l(2)k10108 , Tk5 , HD-29 , Dtk5 , Src42A , dSrc
37279	7904	put	0.0	1	0	0	0.0	1.0E+00	atrII , CG7904 , Punt , TGF-B , Atr-II , l(3)10460 , STK-C , pun , TGF-beta , l(3)j5A5 , dlhC , Tgf-r , AtrII , Atr , Atr88CD , Act-r , put , Put , punt
35845	8173	CG8173	0.0	1	0	0	0.0	1.0E+00	CG8173
853	8224	baboon activin-R	0.0	1	0	18	0.0	1.9E-03	babo , Bab , CG8224 , ATR-I , l(2)k16912 , ATR-1 , Atr-1 , Atr-I , AtrI , Atr45A , STK-E , atr-I , Gprk-3 , Babo , l(2)44Fd , Gprk3 , Atf1 , BABO
28895	8351	Tcp-1eta	0.0	1	0	0	0.0	1.0E+00	Tcp-1eta , CG8351 , Tcp-1-eta1
4176	8805	wun2	0.0	1	0	0	0.0	1.0E+00	N14 , wun-2 , CG8805 , Tunen , WUN-like , Pap2G , DrPAP2[G] , CK02248 , BEST:CK02248 , wun2

104860	9311	CG9311	0.0	1	0	0	0.0	1.0E+00	CG9311 , mop
106938	9358	Phk-3	0.0	1	0	0	0.0	1.0E+00	CG9358 , BcDNA:RE09339 , Phk-3
40743	9493	pez	0.0	1	0	0	0.0	1.0E+00	CG9493 , PTPD1 , Pez
104675	9774	rok	0.0	1	0	0	0.0	1.0E+00	ROCK , Drok , Rok , DROK , ROK , ROKalpha/beta , drok , Rock , RhoK , dROK , dRok , DRhk , ROCK1 , CG9774 , unnamed , Rhk , rok , ROCK-1
46873	9842	PP2B-14D	0.0	1	0	0	0.0	1.0E+00	DmPp2B-14D , canA , PP2B 14D , CG9842 , Pp12-14D , CnnA14D , calcium/calmodulin regulated protein phosphatase 2B , PP2B , D33 , PpD33 , Pp2B-14DF , CanA14D , Pp2B-14D
6229	9985	sktl	0.0	1	0	0	0.0	1.0E+00	PIP5K 57B6 , CG9985 , l(2)k12405 , l(2)05475 , 25/17 , ski , fam , sktl , PIP5K
38319	10033	for	0.0	1	0	0	0.0	1.0E+00	for , FOR/PKG , 142251_at , dg2 , CG10033 , DG2 , PKG , l(2)06860 , Pkg24A , Pkg2 , Dg2 , BcDNA:GM08338 , anon-WO02059370.47 , anon-WO0140519.260
105624	10261	aPKC like 2907	0.0	1	0	0	0.0	1.0E+00	aPKC , aPKCzeta , DaPKC , aPKC-zeta , dapkc , psu , apkc , pkc-3 , CG10261 , l(2)k06403 , PKCl,i , daPKC , a-PKC
104761	10975	Ptp69D	0.0	1	0	0	0.0	1.0E+00	DPTP69D , PTP69D , dptp69D , Ptp69d , Dptp69D , PTPase , CT30751 , R-PTP 69D , CG10975 , ptp69D , DPTP , Ptp , Ptp69D , dptp69d
42947	11221	CG11221	0.0	1	0	0	0.0	1.0E+00	PKN , CG11221
105395	11660	CG11660	0.0	1	0	0	0.0	1.0E+00	CG11660
47401	11859	CG11859	0.0	1	0	0	0.0	1.0E+00	CG11859
106174	12072	wts	0.0	2	0	0	0.0	1.0E+00	wts , Lats/Warts , Warts/Lats , lats , Dlats , Warts , dmLATS , LATS , lts , WTS/LATS , CG12072 , warts/lats , Lats , l(3)100Aa , wart , Wts/Lats , wts/lats , warts , Wts , MENE (3R)-G
20177	12306	Polo	0.0	4	0	4	0.0	1.0E+00	polo , Polo , POLO , POLO/PLK1 , CG12306 , l(3)01673 , 1324/08 , 0256/04 , l(3)77Aa , l(3)S132408 , l(3)S025604 , anon-WO0172774.3
43123	12559	rl	0.0	1	0	0	0.0	1.0E+00	ERK , MAPK , MAP-k , dpERK , dERK , ERKA , D-ERK , CG12559 , dpErk , erk , dp-ERK , Erk , pERK , ERK-A , DERK , dpMAPK , CT39192 , CT34260 , mapk , EK2-1 , DmERK-A , Dsor2 , EY2-2 , DmErk , Erk1 , Mapk , DmMAPK , Erk/Map kinase , Sem , ERKa , DERK-A , SR2-1 , rll , E(sina)7 , rl/MAPK , DmERKA , l(2R)EMS45-39 , GroupII , l(2)41Ac , Su(Raf)2B , ErkA , BcDNA:RE08694 , CG18732 , rl , DpErk , Rl
17432	14217	Tao	0.0	0	0	0	0.0	1.0E+00	CG14217 , dTao-1 , AAF48973 , TAO1 , Tao-1 , tao-1 , MARKK
107645	14217	Tao	0.0	1	0	0	0.0	1.0E+00	CG14217 , dTao-1 , AAF48973 , TAO1 , Tao-1 , tao-1 , MARKK
39857	14992	Ack	0.0	1	0	0	0.0	1.0E+00	DACK , DAck , p145 , ACK , CG14992 , ACK2 , BcDNA:GH10777 , Ack
39864	15072	EMK	0.0	1	0	0	0.0	1.0E+00	EMK/KIAA0999 , CG15072
32377	15224	CkIIbeta	0.0	1	0	0	0.0	1.0E+00	CKII , CK2 , CkII-beta , CK2beta , DmCKIIbeta , dCKII , DmCK2beta , CKIIbeta , CkIIbeta1 , betaCK2 , DmCkIIbeta , CKIIb , CG15224 , CK II , CKII-beta1 , mbu , CkII , And , CCK2 , CK-IIbeta , CK-II beta , CK-2 , Ds cas kin , CkIIbeta , Cask-II-b , dCK2beta , dCKII beta
40026	15793	Dsor1 mek	0.0	1	0	0	0.0	1.0E+00	Dsor , DSor1 , MEK , MEK1/2 , DSORT , sor/MEK1 , DRODSOR1 , SOR , CG15793 , mek , EK1-1 , sor , MAPKK , Mek , D-SOR , DSOR1 , D-sor , D-MEK/Dsor , Su(Raf)34B , Dmek , DSor , D-MEK , dsor1 , D-Mek , D-mek , D-sor-1 , DMEK-1 , Dsor1 , Sor , dSor , dMEK , MEK/Dsor1 , D-Sor
107276	15793	Dsor1 mek	0.0	2	0	0	0.0	1.0E+00	Dsor , DSor1 , MEK , MEK1/2 , DSORT , sor/MEK1 , DRODSOR1 , SOR , CG15793 , mek , EK1-1 , sor , MAPKK , Mek , D-SOR , DSOR1 , D-sor , D-MEK/Dsor , Su(Raf)34B , Dmek , DSor , D-MEK , dsor1 , D-Mek , D-mek , D-sor-1 , DMEK-1 , Dsor1 , Sor , dSor , dMEK , MEK/Dsor1 , D-Sor
101517	16973	msn	0.0	3	0	0	0.0	1.0E+00	MSN , Msn , DMSN , NIK , CG16973 , MESR5 , l(3)6286 , msm , 6286 , l(3)06946 , unnamed , l(3)j1E2 , l(3)03349 , Nik , msn , HGK , JNKKKK
49671	17291	Pp2A-29B	0.0	3	0	0	0.0	1.0E+00	CG13383 , Pp2A , PP2A , A/PR65 , PP2A-29B , DPR65 , PR65 , CG33297 , CG17291 , Pp2A-29B , PP2A A
32885	17342	Lk6	0.0	1	0	0	0.0	1.0E+00	CG17342 , LK6 , lk6 , MNK/LK6 , MESR8 , CG6929 , anon-WO0172774.84 , Lk6
106119	17603	Taf1	0.0	1	0	0	0.0	1.0E+00	TAF[[II]]230 , dmTAF1 , dTAF[[II]]250 , TAF250/230 , TAF , TFIID , TAF250 , dmTAF[[II]]230 , TAF[[II]] , TAF[[II]]250 , TAF[II]250 , TAF1 , dTAFII250 , dTAF230 , TAFII250 , TFIID TAF250 , d230 , TAFII-250 , CG17603 , dTAF[[II]]230 , SR3-5 , Taf250 , TAF[[II]]250/230 , dTAF250 , TAF230 , cell , p230 , Taf230 , Taf[[II]]250 , unnamed , l(3)84Ab , TAF200 , cel , EfW1 , Taf200 , BG:DS00004.13 , Taf1 , Taf1p
46252	32019	bent titin	0.0	1	0	0	0.0	1.0E+00	bt , 39c-18 , CG32019 , CT8086 , CT3598 , CG1479 , unnamed , titin , l(4)PT-2 , l(4)23 , l(4)2 , l(2)23 , l(2)2 , l(4)38 , l(4)37 , l(4)21 , l(4)102CDa , Prj , CG10285 , bent
52268	32491	mod(mdg4)	0.0	0	0	0	0.0	1.0E+00	mod(mdg4) , CG32491 , mod , E(var)3-93D , Mod(mdg4) , mod(mdg4)67.2 , doom , MOD(MDG4)56.3 , pf-2 , CG15500 , CG7836 , Mod(mdg)4 , E-(var)3-93D , bpd , Doom , Mod[mdg4] , mod(mdg-4) , l(3)L3101 , E-var(3)1 , BcDNA:GH07769 , mod2.2 , mod(gypsy) , l(3)j2B7 , l(3)03852 , E-var(3)3 , E(var)93D , E(var)129 , CG7859 , CG8076 , CG18151 , CG15802 , CG15501 , BcDNA:SD03001 , mnm , mod[mdg4] , Mod(mdg4)2.2 , mnn , Mod(mdg4)-67.2
25317	32505	CG32505 Pp4-19C	0.0	1	0	0	0.0	1.0E+00	PPP4c , DmPpp4-19C , PP4 , CG1459 , pp4 , PP4 19C , PPX , PpX , CG18339 , CG1596 , CG32505 , Pp4-19C , PP1
107263	32666	CG32666	0.0	2	0	0	0.0	1.0E+00	CG1760 , EP(X)1452 , CG11713 , EP1452 , CG32666

Chapter 3

JNK signaling is needed to tolerate Chromosomal instability

This chapter is based on the published article titled "*JNK signaling is needed to tolerate Chromosomal instability*", which demonstrates that the DNA damage response and G2 timing is critical for the tolerance of chromosomal instability.

Chromosomal instability is a common feature of advanced tumours, is linked to poor clinical outcomes such as drug resistance, low survival rate, metastasis and relapse. This makes CIN as a valuable target to treat these resistant tumours. Chromosomal missegregation also leads to aneuploidy, stress and DNA damage, which activates cellular stress responses. JNK is a key stress response mediator involved in DNA damage repair, autophagy, antioxidant production and apoptosis (Karin & Gallagher, 2005; Wagner & Nebreda, 2009). Currently, many DNA damage based cancer therapies are effective, but they are not ideal because of their side effects on normal proliferating cells, so finding a target that induces DNA damage or cell death only in CIN cells could be highly significant for therapy.

From the initial screening we identified candidates form DNA damage and c-Jun N terminal kinase (JNK) pathway, whose knockdown induces apoptosis only in CIN cells (Shaukat et al, 2012).This is interesting because the JNK pathway is known to mediate apoptosis, but our results suggest that JNK is also required for the survival of cells with chromosomal instability. Further screening and characterization of JNK pathway showed that the induction of CIN results in DNA damage and the activation of JNK, knock down of JNK leads to an increase in CIN specific DNA damage and cell death. Moreover, lengthening of G2 rescues the CIN specific-JNK knockdown phenotype which suggests that the JNK is required for pre-mitotic delay of cell cycle in response to DNA damage which has significant impact on DNA damage repair and the survival of CIN cells. Consistently, shortening of G2 mimics the effect of JNK knockdown. This study shows that JNK knock down in CIN cell causes caspase mediated apoptosis through a p53-independent mechanism, which is clinically significant as many tumours lack p53. This CIN specific effect of G2 length and JNK knockdown suggests that CIN cells are sensitive to unrepaired DNA damage.

Statement of Authorship

Title of Paper	JNK signaling is needed to tolerate chromosomal instability
Publication Status	Published
Publication Details	Wong, H.W., Shaukat, Z., Wang, J., Saint, R. & Gregory, S.L. (2014) JNK signaling is needed to tolerate chromosomal instability. Cell Cycle, 13(4): 622–631. doi:10.4161/cc.27484 Corresponding E-mail: robert.saint@adelaide.edu.au; stephen.gregory@adelaide.edu.au

Author Contributions

By signing the Statement of Authorship, each author certifies that their stated contribution to the publication is accurate and that permission is granted for the publication to be included in the candidate's thesis.

Name of Principal Author	Heidi W. S. Wong		
Contribution to the paper	Conceived and designed the experiments Performed the experiments Analysed the data Contributed reagents/materials/analysis tools Wrote the paper		
Signature		Date	6/5/2014

Name of Co-Author	Zeeshan Shaukat		
Contribution to the paper	Performed the experiments Analysed the data Contributed reagents/materials/analysis tools		
Signature		Date	9/5/2014

Name of Co-Author	Jianbin Wang		
Contribution to the paper	Performed the experiments Analysed the data		
Signature		Date	

Name of Co-Author	Robert Saint		
Contribution to the paper	Conceived and designed the experiments Analysed the data Contributed reagents/materials/analysis tools Correspondence		
Signature		Date	12/5/14

Name of Co-Author	Stephen L. Gregory		
Contribution to the paper	Conceived and designed the experiments Performed the experiments Analysed the data Contributed reagents/materials/analysis tools Wrote the paper Correspondence		
Signature		Date	9/5/14

Wong, H.W-S., Shaukat, Z, Wang, J., Saint, R. & Gregory, S.L. (2014) JNK signaling is needed to tolerate chromosomal instability.
Cell Cycle, v. 13(4), pp. 622-631

NOTE:
This publication is included on pages 67-80 in the print copy of the thesis held in the University of Adelaide Library.

It is also available online to authorised users at:

http://doi.org/10.4161/cc.27484

Chapter 4

Chromosomal Instability Causes Sensitivity to Metabolic Stress.

Cancer cells often make adjustments to metabolic pathways in order to support cell growth and division under stressed conditions. Cancer cells use a high rate of glycolysis and lactic acid fermentation to fulfil their high energy and macromolecule demands. Normal cells use a comparatively lower rate of glycolysis followed by pyruvate oxidation in mitochondria (Warburg, 1956). This metabolic shift was first reported by Otto Warburg in 1925, is now an important hallmark and diagnostic marker of cancer (Warburg, 1925; Warburg et al, 1927; Warburg, 1956; Delbeke, 1999). This may be an adaptation of cancer cells to high macromolecule demand for proliferation or to low-oxygen environment. Moreover, this change in metabolism may be used to avoid the excessive use of mitochondria which are involved in apoptosis (Lopez-Lazaro, 2008).

Metabolism in cancer cells is reprogrammed both by mutational regulation of certain metabolic enzymes or by oncogene signaling (Yuneva et al, 2007; Yun et al, 2009; Puzio-Kuter, 2011; Pfau & Amon, 2012). Enhanced glycolysis levels and increased production of lactate is a specific characteristic of many cancers which distinguish them from their normal counterparts and this difference is widely considered as a potential anti-cancer target (Kaplan et al, 1990; Clem et al, 2008; Holen et al, 2008; Jiralerspong et al, 2009; Gross et al, 2010; Le et al, 2010; Michelakis et al, 2010; Tennant et al, 2010). These alterations in metabolic pathways support cellular growth and proliferation, and also provide resistance to cellular and environmental stresses (Pfau & Amon, 2012). On the other hand, numerous studies have shown the significance of targeting metabolism for the treatment of cancer. Currently, drugs that inhibit glycolysis, lactate synthesis and transport, fatty acid synthesis, nucleotide biosynthesis, mTORC1, HIF signaling, PI3K signaling synthesis are in clinical trials and show effectiveness against wide variety of tumours (Tennant et al, 2010).

Moreover, chromosomal instability and aneuploidy are common in cancers and are linked to metabolic adaptations under cellular and environmental stresses (Komarova, 2006; Yuneva et al, 2007; Pavelka et al, 2010). These alterations are likely the result of continuous genomic reshuffling and high mutation rates in CIN cells, which can also produce cells with a growth advantage, adaptation to the environment and resistance to chemotherapies (Swanton et al, 2009; Sotillo et al, 2010). These acquired adaptations also provide potential to target them for anti-cancer therapy (Raj et al, 2011). Furthermore, aneuploidy can act as an inhibitor of tumour growth and progression (Weaver et al, 2007; Galimberti et al, 2010). This growth retardation in aneuploid cells

is linked to energy burden, proteotoxic and metabolic stress (Torres et al, 2007; Pfau & Amon, 2012). Increasing the levels of CIN and aneuploidy above the threshold level could lead to cell death and an increased sensitivity to conventional drugs (Weaver et al, 2007).

There is a strong relationship between CIN levels and poor prognosis (Walther et al, 2008; Choi et al, 2009), CIN can also lead to multi-drug resistance, metastasis, low survival rate and relapse (Duesberg et al, 2000; Nakamura et al, 2003; Jonkers et al, 2005; Li et al, 2005; Swanton et al, 2009; Sotillo et al, 2010; Lee et al, 2011). Similar to metabolism, chromosomal instability also represents a potential target that is specific to cancer cells, particularly late-stage cancers that are typically genetically diverse and drug resistant.

In this study we show that the induction of CIN in cells makes them vulnerable to certain metabolic changes, some of them do not affect normal cells and can potentially be used as drug targets. We demonstrate that this is because the CIN and aneuploidy cause redox stress that pushes these cells close to their stress tolerance limits. Further screening of metabolic candidates was done in a *Drosophila* CIN model to identify metabolic pathways that can be targeted to specifically induce cell death in these unstable cells. These studies also explored the possible mechanisms which sensitize CIN cells and push them towards cell death.

Statement of Authorship

Title of Paper	Chromosomal instability makes cells sensitive to metabolic stress.
Publication Status	Submitted, under review for Oncogene.
Publication Details	Zeeshan Shaukat, Dawei Liu, Amanda Choo, Rashid Hussain, Louise O'Keefe, Robert Richards, Robert Saint and Stephen Gregory Affiliations: School of Molecular and Biomedical Sciences, University of Adelaide, Adelaide, SA, Australia Corresponding E-mail: stephen.gregory@adelaide.edu.au

Author Contributions

By signing the Statement of Authorship, each author certifies that their stated contribution to the publication is accurate and that permission is granted for the publication to be included in the candidate's thesis.

Name of Principal Author	Zeeshan Shaukat		
Contribution to the paper	Conceived and designed the experiments Performed the experiments Analysed the data Contributed reagents/materials/analysis tools Wrote the paper		
Signature		Date	

Name of Co-Author	Dawei Liu		
Contribution to the paper	Performed the experiments Analysed the data		
Signature		Date	

Name of Co-Author	Amanda Choo		
Contribution to the paper	Performed the experiments Analysed the data Contributed reagents/materials/analysis tools		
Signature		Date	

Name of Co-Author	Rashid Hussain		
Contribution to the paper	Performed the experiments		
Signature		Date	

Name of Co-Author	Louise O'Keefe		
Contribution to the paper	Analysed the data Contributed reagents/materials/analysis tools		
Signature		Date	

Name of Co-Author	Robert Richards		
Contribution to the paper	Conceived and designed the experiments Contributed reagents/materials/analysis tools		
Signature		Date	

Name of Co-Author	Robert Saint		
Contribution to the paper	Conceived and designed the experiments Contributed reagents/materials/analysis tools		
Signature		Date	

Name of Co-Author	Stephen Gregory		
Contribution to the paper	Conceived and designed the experiments Performed the experiments Analysed the data Contributed reagents/materials/analysis tools Wrote the paper Correspondence		
Signature		Date	

Title: *Chromosomal Instability Causes Sensitivity to Metabolic Stress.*

Authors: Zeeshan Shaukat, Dawei Liu, Amanda Choo, Rashid Hussain, Louise O'Keefe, Robert Richards, Robert Saint and Stephen L. Gregory*

Affiliations: School of Molecular and Biomedical Sciences, University of Adelaide, Adelaide, SA, Australia

***Corresponding Author**

Email: stephen.gregory@adelaide.edu.au

Running Title: CIN Causes Sensitivity to Metabolic Stress

Keywords/Subject Areas: chromosomal instability/ aneuploidy/ metabolism/ apoptosis/ oxidative stress.

ABSTRACT

Chromosomal instability (CIN), a hallmark of cancer, refers to cells with an increased rate of gain or loss of whole chromosomes or chromosome parts. Chromosomal instability is linked to the progression of tumors with poor clinical outcomes such as drug resistance. CIN can give tumours the diversity to resist therapy, but it comes at the cost of significant stress to tumour cells. To tolerate this, cancer cells must modify their energy use to provide adaptation against genetic changes as well as to promote their survival and growth. In this study, we have demonstrated that CIN induction causes sensitivity to metabolic stress. We show that mild metabolic disruption that does not affect normal cells, can lead to high levels of oxidative stress and subsequent cell death in CIN cells because they are already managing elevated stress levels. Altered metabolism is a differential characteristic of cancer cells, so our identification of key regulators that can exploit these changes to cause cell death may provide cancer-specific drug targets, especially for advanced cancers that exhibit CIN.

Introduction

Cancer is a large group of diseases caused by failure to control the cell cycle, which leads to aberrant cell growth and division. Cancer is one of the leading causes of death and many current anti-cancer therapies are not ideal because they have adverse effects on the normal proliferating cells of the body. Moreover, these drugs are ineffective in advanced tumors because of drug resistance that often leads to relapses, and these clinical problems have been linked to chromosomal instability (Carter *et al*, 2006; Walther *et al*, 2008; Swanton *et al*, 2009; Bakhoum *et al*, 2011; McGranahan *et al*, 2012).

Chromosomal INstability (CIN), a common feature of nearly all solid tumors (Mertens *et al*, 1994), is defined as the ongoing propensity of a cell to gain or lose whole or parts of chromosomes with each cell division. The resulting aneuploidy can influence tumour evolution (Thompson & Compton, 2008; Weaver & Cleveland, 2007; Sotillo *et al*, 2010; Wassmann & Benezra, 2001; Baker *et al*, 2009). Continuous chromosomal reshuffling and high mutation rates lead to heterogeneity, which can produce cells with a growth advantage, adaptation to the environment and resistance to chemotherapy (Swanton *et al*, 2009; Sotillo *et al*, 2010). CIN is also linked to metastasis and low survival rates in cancer patients (Carter *et al*, 2006). Furthermore, a high level of CIN is a characteristic of cancer cells that is not common in normal cells, so CIN can potentially be used as a tumour specific target for

therapy. Consequently, there is a strong need to explore the mechanism by which CIN is acquired by cancer cells and how it affects tolerance and adaptation to cellular and environmental stresses.

We have previously used an induced-CIN model in *Drosophila* to carry out a genetic screen to identify genes that, when knocked down, induce cell death specifically in CIN cells and thus represent potential therapeutic targets for advanced tumors (Shaukat *et al*, 2012). We induced chromosomal instability by weakening the spindle checkpoint, using $mad2^{RNAi}$, which shortens mitosis and gives less time to correct any chromosome misorientation at metaphase (Buffin *et al*, 2007) resulting in a significantly higher rate of chromosome segregation errors, i.e. CIN (Shaukat *et al*, 2012).

That screen tested all the kinases and phosphatases in *Drosophila* to identify candidates whose knockdown could trigger apoptosis in cells with induced CIN, while not killing control cells without CIN (Shaukat *et al*, 2012). The kinome was tested as phosphorylation regulates key processes such as proliferation and survival, and because kinases make good drug targets. A set of genes was identified that affected the survival of CIN cells without affecting the levels of chromosomal instability. Amongst these were some metabolism related kinases (PAS Kinase, Phosphofructokinase), which were of particular interest because altered metabolism is a hallmark cancer cells (Warburg, 1956). Metabolism in cancer cells is reprogrammed both by mutational regulation of certain metabolic enzymes and by oncogene signalling (Yun *et al*, 2009; Yuneva *et al*, 2007; Puzio-Kuter, 2011). These modifications in metabolic machinery provide advantages over normal cells in terms of cellular growth, proliferation and resistance to cellular and environmental stresses (Pfau & Amon, 2012). In addition, there has been a long standing interest in using differences in metabolism as a potential target to specifically kill cancer cells (Clem *et al*, 2008; Le *et al*, 2010; Michelakis *et al*, 2010; Kaplan *et al*, 1990; Jiralerspong *et al*, 2009; Gross *et al*, 2010; Holen *et al*, 2008).

These considerations led us to investigate whether CIN cells might be particularly sensitive to metabolic changes. Here we describe a screen for candidates from a range of metabolic pathways, to identify whether these could be targeted to induce CIN-specific cell death without affecting normal cells. We find that several metabolic pathways can impact CIN cell survival, particularly those affecting mitochondrial output and effective antioxidant responses. We demonstrate that *mad2* knockdown, which leads to CIN and aneuploidy (Shaukat *et al*, 2012), also results in metabolic stress and sensitivity to alterations in oxidative

stress response genes. We propose, therefore, that CIN cells are close to the limits of redox tolerance, and so are unable to effectively buffer further oxidative stress. Knockdown of our metabolic candidates led to elevated levels of energy use, increased mitochondrial output and the production of reactive oxygen species. In CIN cells, this resulted in oxidative damage, DNA double strand breaks and apoptosis, suggesting that increased metabolic flux represents a promising opportunity for selectively targeting CIN cells.

Results

Screening metabolic pathways for CIN specific lethality: Previous screening of kinases and phosphatases identified a metabolic regulatory gene (PAS Kinase) that could be targeted to promote cell death in cells with induced chromosomal instability [12]. PASK was known to affect glucose usage (Schläfli *et al*, 2009; Hao & Rutter, 2008), but had not previously been implicated in cell death or proliferation. In order to further explore metabolic pathways that could be involved in regulating the fate of CIN cells, we tested 93 genes from across the range of known metabolic pathways by a similar screening method. Using RNA interference (RNAi) to decrease gene expression we found that 22 out of the 93 gene knockdowns gave strongly decreased (< 50%) survival of CIN flies compared to non-CIN control siblings, which suggested that CIN cells are sensitive to certain metabolic disruptions, while others have no effect. The metabolic candidates identified from these screens are listed in Table 1 along with their functional associations, especially in terms of stress related responses. The full list of genes screened is given in Supplementary Table 1.

Screening for Cell Death/Apoptosis: Acridine orange staining was used to test whether knockdown of the selected candidates led to cause cell death specifically in cells with induced CIN. We used RNAi to knock down these metabolic genes in a proliferating tissue: the third instar larval wing disc with or without induced chromosomal instability. We detected little or no cell death in the control (empty vector) discs or in control discs with induced-CIN ($mad2^{RNAi}$) (Figure 1A). Similarly, knockdown of a metabolic gene alone ($pask^{RNAi}$) also induced little or no cell death. In contrast, double knockdown of our metabolic candidate with Mad2 gave significant levels of cell death (Figure 1A iv). Quantitation of the cell death signal from a range of metabolic candidates with and without CIN (Figure 1B) showed strong induction of CIN-specific cell death. Representative images of the Acridine Orange staining on all candidates are shown in Supplementary Figure 1.

These results showed that metabolic candidate knockdowns led to significant increases in CIN-specific cell death compared to negative controls, consistent with the CIN-specific lethality observed for these knockdowns in the original screen (Supplementary Table 1). Candidates such as PASK, phosphoenolpyruvate carboxykinase (PEPCK) and glucose-6-phosphate dehydrogenase (G6PD) affect glucose usage; Catalase (Cat) and superoxide dismutase (Sod1) affect oxidative stress responses and isocitrate dehydrogenase (Idh) and Wwox effects include the TCA cycle (O'Keefe *et al*, 2011; Stanton, 2012; Hao & Rutter, 2008), so we have found that a range of metabolic processes can impact on CIN cell survival.

We have previously demonstrated that the CIN-specific cell death induced by several candidate knockdowns was brought about by the onset of apoptosis (Shaukat *et al*, 2012; Wong *et al*, 2013). To test whether metabolic disruption also induced apoptosis in CIN cells, we tested for cleaved caspase 3 staining in $pask^{RNAi}$ $mad2^{RNAi}$ cells, which confirmed the induction of CIN specific apoptosis (Figure 1C). Cell death assays on Pask knocked down in different CIN models i.e. *BubR1* (Shaukat *et al*, 2012), *Rb* and *Rad21* (Supplementary Figure 4) gave similar increases in CIN specific cell death.

Nutrient use: We identified candidates that are thought to affect nutrient usage through glycolysis, gluconeogenesis and the pentose phosphate pathway, so we tested them for an effect on nutrient levels. Vertebrates store lipid and glycogen in the liver as energy sources that can be utilized in case of nutrient shortage. In *Drosophila,* the fat body serves as storage for glycogen and lipids. The amount of lipid stored in fat body cells can be monitored by staining them with Nile red stain (Iijima *et al*, 2009). In starved conditions, knockdown of our metabolic candidates showed significantly less lipid storage compared to wild type (Table 2); the knockdown animals can also be noticeably lean and translucent. This inability to retain energy stores under starvation suggests higher energy usage, and is consistent with *PASK* deficient mice which have increased glucose use and lower lipid storage (Hao *et al*, 2007). Increased energy usage can be detrimental to cells, causing mitochondrial defects and cell stress (Hockenbery, 2010).

Mitochondrial dysfunction: Mitochondria are the powerhouse of the cell, and during the process of energy production they generate reactive oxygen species (ROS) which, if not neutralized, cause oxidative damage to proteins, lipids and DNA (Gogvadze *et al*, 2008). Damaged or defective mitochondria have a decreased membrane potential and fail to sequester the positively charged dye tetramethylrhodamine ethyl ester (TMRE), as shown by

knockdown of the mitochondrial complex I gene *ND42* (Figure 2b). In contrast, over-active mitochondria are hyperpolarized and accumulate more TMRE than normal mitochondria as shown by blocking ATP translocation using $sesB^{RNAi}$ (Figure 2c). Single knockdown of selected metabolic candidates did not alter levels of accumulation of TMRE (Figure 2d-j). In contrast, knockdown of candidates in induced-CIN cells showed significantly higher levels of TMRE accumulation (Figure 2d'-g', i') compared to the WT region and normal controls (Figure 2a'), suggesting hyperpolarization of mitochondria. Hyperpolarization is seen when mitochondria are overactive, and can lead to oxidative stress (Terhzaz *et al*, 2010). Catalase was the only candidate knockdown that showed no change in TMRE staining in CIN cells (Figure 2h'). This is consistent with the absence of Catalase expression in mitochondria (Radyuk *et al*, 2010); its relevance for CIN cell survival is investigated further below.

Activation of the oxidative stress response: Having observed mitochondrial hyperpolarization, we wished to test the cellular anti-oxidant response. We hypothesized that a robust antioxidant response might be particularly needed in CIN cells because CIN inevitably causes aneuploidy, and aneuploidy has been shown to generate redox stress (Sheltzer *et al*, 2012). Reduced glutathione (GSH) is the major antioxidant of a cell, produced in response to oxidative stress (Coe *et al*, 2002; Wu & Cederbaum, 2005). ThiolTracker™ staining of wing discs from selected metabolic candidates showed that knockdown of candidates alone did not change the GSH signal, similar to the negative control RNAi (Figure 3a, d-j). In contrast, knockdown of candidates in cells with induced CIN produced significantly higher levels of GSH compared to the negative RNAi control (Figure 3d'-j'), but similar to controls (*ND42* and *sesB*, Figure 3b-c) that disrupt mitochondria to generate oxidative stress (Owusu-Ansah & Banerjee, 2009; Terhzaz *et al*, 2010). These results indicated that metabolic candidate knockdown in CIN cells led to activation of oxidative stress responses that were not seen in normal cells.

Generation of reactive oxygen species: The detection of hyperpolarized mitochondria in CIN cells depleted of our metabolic candidates strongly suggests that a major source of oxidative stress in these cells was likely to be reactive oxygen species from the overactive mitochondria (Miwa *et al*, 2003). CellROX staining of knockdowns for the metabolic candidates alone showed no detectable level of ROS signal (Figure 4c-g) above the control (Figure 4a). In contrast, candidate knockdown in CIN cells showed a significant level of ROS signals (Figure 4c'-g'), similar to the positive control *sesB* (Figure 4b) and clearly different from

wild type controls or metabolically unperturbed CIN cells at 25^{o}C (Figure 4a, a'). These results show that CIN cells are vulnerable to metabolic interventions that increase redox stress, and that this stress can be generated either by depleting normal antioxidant levels (e.g. *Catalase* knockdown) or by metabolic interventions that drive mitochondria to generate ROS.

CIN also causes oxidative stress: We found that *Catalase* knockdown revealed oxidative stress and ROS production in CIN cells (Figure 3h', 4f'), but not normal cells (Figure 3h, 4f). This suggested that the CIN cells are generating additional ROS, though not enough to be detected unless Catalase was removed. A plausible mechanism for the generation of this ROS in CIN cells is through the metabolic stress imposed by aneuploidy. If aneuploid cells survive, they typically show proteotoxic and metabolic stress, thought to be brought about by the gene dosage disruptions (Oromendia *et al*, 2012; Sheltzer *et al*, 2012). If this model is correct, then a higher level of CIN and aneuploidy should generate significant levels of ROS by itself without the need for additional metabolic disruption. We have shown that $mad2^{RNAi}$ at 25^{o}C gives defective anaphases and a low rate of apoptosis without a detectable level of ROS or DNA damage (Figure 4a', (Shaukat *et al*, 2012)). However, increasing the knockdown of *mad2*, either by increasing the temperature (30^{o}C) or by overexpressing the RNAi enzyme *Dicer2*, resulted in significantly increased levels of ROS (Figure 4a"), DNA damage (Figure 5a) and apoptosis (Figure 5b) compared to *mad2* knockdown at 25^{o}C. These results suggest that CIN does generate oxidative stress, though it is normally limited by cellular antioxidants such as Catalase. However, if the CIN level is increased or the antioxidants compromised, potentially damaging levels of ROS can result.

Oxidative Damage: Normal cells maintain the ratio between the generation and neutralization of ROS because increased ROS levels can lead to permanent oxidative damage to lipids, proteins, and DNA (Liu *et al*, 1996). ROS are known to cause double-strand DNA breaks, particularly in replicating cells (Tanaka *et al*, 2008). Consistent with this, we see increased numbers of cells marked with the double stranded break binding protein γH2aX when our candidates are knocked down in CIN cells (Figure 6A). Some damage was seen in normal cells when Catalase was depleted, suggesting an endogenous level of ROS production, but this was greatly increased in CIN cells, consistent with our model for CIN causing ROS (Figure 5). Because DNA breaks in CIN cells could be caused by non-oxidative mechanisms (Janssen *et al*, 2011; Crasta *et al*, 2012), we specifically tested for the formation of oxidative DNA damage. 8-hydroxy-2'-deoxyguanosine (8-oxoG), is the most common

oxidative damage caused in nuclear and mitochondrial DNA (Kasai & Nishimura, 1984). 8-oxoG antibody staining was not increased relative to controls when either PASK or Mad2 were depleted alone (Figure 6B a', b). However, elevated levels of 8-oxoG antibody staining in $pask^{RNAi}$ $mad2^{RNAi}$ cells (Figure 6B b') confirmed the presence of oxidative damage to DNA, consistent with the generation of damaging levels of ROS in these cells (Figure 4).

Elevated levels of ROS should also lead to lipid peroxidation, which we tested using the peroxidation state dependent fluorescence (non-peroxidised: red; peroxidised: green) of BODIPY$^{581/591}$ - C_{11}. Wing discs knocked down for a metabolic candidate alone ($pask^{RNAi}$) gave similar staining to wild type controls. In contrast, knockdown of PASK in cells with induced CIN gave a significant increase in green fluorescence compared to wild type controls (Figure 6C). Similar increases were seen in positive control ($ND42^{RNAi}$) and pro-oxidant menadione treated discs (Supplementary Figure 2), indicating the presence of oxidative damage to macromolecules as a result of excessive ROS generation.

Oxidative damage is responsible for the death of CIN cells: Previously we reported that knockdown of *Pask* in CIN cells resulted DNA damage and apoptosis (Shaukat *et al*, 2012), and here we have seen that these are found with an increase in oxidative stress and ROS (Figures 2-4). To assess whether oxidative stress was responsible for the observed cell death, we tested whether the cell death phenotype of $pask^{RNAi}$ $mad2^{RNAi}$ could be rescued by overexpression of antioxidant enzymes (Figure 7). Overexpression of Catalase, Superoxide dismutase 1, Superoxide dismutase 2, or Glucose-6-Phosphate Dehydrogenase in $pask^{RNAi}$ $mad2^{RNAi}$ discs significantly reduced the level of cell death (p-value <0.001 for each). Taken together, our data indicate that metabolic changes can generate oxidative stress specifically in CIN cells that results in oxidative DNA damage and cell death.

Discussion

Chromosomal instability and abnormal chromosome numbers (aneuploidy) are frequent in solid tumors (Kops *et al*, 2005). Aneuploidy can have a range of effects including aberrant cell growth, proliferation, proteotoxic and oxidative stress (Oromendia *et al*, 2012). Survival through ongoing gain or loss of chromosomes requires adaptation to these stresses, making cellular stress responses a plausible target to induce cancer specific apoptosis. However, as well as causing stress, CIN also generates massive genetic diversity, which could drive rapid evolution to select cells that can tolerate high stress conditions. The question then is whether

the constraints of high energy use, ROS generation, proliferation and ongoing genotoxic stress inevitably push CIN cells close to their tolerance threshold. In our experiments, we have found that the induction of CIN makes cells highly vulnerable to oxidative stress, showing DNA damage and apoptosis in response to metabolic changes that do not damage normal cells. While some fraction of CIN cells may survive metabolic intervention, the rate of apoptosis generated in CIN cells by our metabolic knockdowns is high, and compares favourably with most of the alternative approaches to killing CIN cells that we have identified (Shaukat *et al*, 2012). As with all therapies against a diverse cell population, targeting disparate pathways is likely to be most effective, and we have identified several, including glycolysis, NADPH production, and antioxidant enzymes.

Altered metabolism in cancer cells is thought to provide growth and proliferative advantages and can be specifically targeted to limit their adaptability against external and internal stresses (DeBerardinis *et al*, 2008). Although CIN is known to be a highly adaptive feature of tumours (Pfau & Amon, 2012), our results suggest that CIN also places significant metabolic constraints on the cell in addition to those imposed by the demands of proliferation. The range of processes that we found to be sensitive to disruption in CIN cells included glycolysis, TCA cycle, fat metabolism, gluconeogenesis and oxidative stress responses (Table 1). Our data suggest that the CIN cells are sensitive to alteration in the cellular redox status or antioxidant capacity because they are already coping with elevated levels of stress. However, the increased levels of GSH and DNA damage we observed could have been a result of the onset of apoptosis rather than a cause of it. We have rejected this model because blocking apoptosis by p35 expression did not decrease the DNA damage levels seen in metabolically disrupted CIN cells (Supplementary Figure 3). In addition, overexpressing antioxidant enzymes rescued the apoptosis in $pask^{RNAi}$ $mad2^{RNAi}$ cells (Figure 7), consistent with redox stress causing the apoptosis rather than the reverse.

Cancer cells utilize elevated glycolytic flux and low TCA flux to meet their high energy and macromolecule demands with minimized oxidative stress (Warburg, 1956; Vander Heiden *et al*, 2009). Many of the candidates that we found could be knocked down to kill CIN cells affected glucose metabolism in some way (Table 1), and those that we tested had a decreased ability to store energy, suggesting an increased metabolic flux. Consistent with this, we observed that in CIN cells, most of these knockdowns gave an elevated mitochondrial membrane potential. In normal cells the knockdowns did not give a detectable increase in

membrane potential, which may reflect the degree of uncoupling available to deal with variation in flux (Miwa *et al*, 2003). Cells with induced CIN (Li *et al*, 2010) or aneuploidy (Torres *et al*, 2007; Williams *et al*, 2008) have been shown to have increased glucose usage, which combined with the effect of our metabolic knockdowns was sufficient to generate a significant excess in membrane potential, with the consequent production of reactive oxygen species and oxidative damage that we observed.

Glucose metabolism not only provides energy, it also maintains the redox potential of the cell by producing NADPH, especially through the pentose phosphate pathway which is used to maintain anti-oxidant levels (Stanton, 2012). G6PD is a key enzyme for NADPH production and we found that reduction of G6PD in CIN cells leads to oxidative stress, DNA damage and apoptosis. In this case not only was glycolytic flux increased, causing ROS generation in the mitochondria, but the cell's ability to counteract the ROS with GSH and Catalase was limited by the block in NADPH synthesis. Consistent with this explanation, G6PD levels are high in some cancers (Wang *et al*, 2012), overexpression increases tumorigenesis (Kuo *et al*, 2000) and its reduction sensitizes cancerous cells to radiotherapy and chemical oxidants (Zhang *et al*, 2014). We would predict that the significant human population with G6PD deficiency (Howes *et al*, 2012) may have some resistance to CIN tumours, though to our knowledge this has never been tested (Manganelli *et al*, 2013). Similarly, reduced levels of PEPCK (a key enzyme of gluconeogenesis) in our CIN model also resulted in oxidative stress and damage which led to apoptosis. Gluconeogenesis provides substrates for the pentose phosphate pathway, and knockdown of PEPCK results in low NADPH and reduced glutathione levels (Zhang, 2007). Other sources of NADPH are malate and citrate (Cairns *et al*, 2011) and depletion of the relevant enzymes (IDH or malic enzyme) in our CIN model also gives DNA damage and apoptosis. Malic enzyme is also overexpressed in tumors and its knockdown inhibits the progression of these tumors (Ren *et al*, 2010). Our model for all of these enzymes is that the effect of excess glucose usage on mitochondrial ROS levels is compounded by a defect in anti-oxidant capacity, resulting in DNA damage and apoptosis in CIN cells that are already near their limits of oxidative tolerance.

PAS kinase has no previously described role in mitosis, apoptosis or tumour progression. Pask mutant mice have an increased metabolic rate and decreased lipid storage (Hao *et al*, 2007), consistent with the lipid storage and mitochondrial phenotype enhancement we have observed in *Drosophila*. We found that Pask knockdown in CIN cells caused oxidative stress

(Figure 2), increased mitochondrial membrane potential (Figure 3), elevated ROS level (Figure 4), which leads to oxidative damage to DNA (Figure 6a, b) and resulted in p53 dependent apoptosis (Shaukat *et al*, 2012). These results suggested that induction of oxidative stress was the main cause of apoptosis, which was confirmed by rescuing apoptosis in *pask*^{RNAi} *mad2*^{RNAi} cells by overexpressing antioxidant enzymes. Similar results were obtained when we reduced the level of the tumour suppressor Wwox, which we have shown results in metabolic disruption that includes downregulation of PEPCK (O'Keefe *et al*, 2011). While Wwox affects a wide range of metabolic targets, a null mutant for this gene (O'Keefe *et al*, 2011), like *pask* (Beumer *et al*, 2008), is viable and fertile, underlining the fact that these metabolic changes are within the tolerance range of normal animals, although lethal to CIN cells.

The other main group of candidates identified by our screening relates to the oxidative stress response mechanism of the cell. The primary oxidative threat to cells is the production of reactive oxygen species. Superoxide is highly reactive and mainly produced in mitochondria where superoxide dismutase converts it to less reactive hydrogen peroxide. Hydrogen peroxide leaks into the cytoplasm where the Fenton reaction can convert it to highly reactive OH radicals that result in oxidative damage to DNA lipids and proteins (Reuter *et al*, 2010). Enzymes such as Catalase, Peroxiredoxins, and Thioredoxin Peroxidase protect the cell from oxidative damage from peroxides. These antioxidant enzymes regulate pro-survival mechanisms in response to oxidative stress and can be targeted for cancer therapy (Bauer, 2012). Table 1 suggests that several antioxidant enzymes (SOD1, catalase, xanthine dehydrogenase/oxidase, sulfiredoxin and peroxiredoxin) are required for CIN tolerance, which is consistent with the results showing that inhibition of SOD can kill Rad54 deficient CIN and colorectal cancer cells by inducing DNA damage (Sajesh *et al*, 2013). DNA damage inducing drugs have been effectively used for cancer therapy, but with unavoidable side-effects (Cheung-Ong *et al*, 2013). Here we showed that by metabolic intervention we could induce oxidative stress and DNA damage only in CIN cells without damaging normal proliferating cells. Oxidative stress and stress response pathways are considered plausible targets for cancer therapy (Smart *et al*, 2004; Ozben, 2007; Fang *et al*, 2007) and metabolic intervention that generates oxidative stress and cytotoxicity is currently in clinical trials for cancer therapy (Kaplan *et al*, 1990; Le *et al*, 2010; Sotgia *et al*, 2013). From our data we would anticipate that these approaches will be most successful on CIN positive cell types

because they suffer ongoing genomic disruption that pushes cell stress responses near to their limits of tolerance.

In summary, we have demonstrated that the CIN cells are particularly sensitive to metabolic alteration. Metabolic disruption leads to high levels of oxidative stress in CIN cells, which are already managing elevated ROS levels. Therefore, metabolic interventions are potentially a highly effective way of killing CIN cells without affecting normal dividing cells. These potential therapeutic targets are clinically highly desirable because of their effects on CIN tumours that are typically refractory to current therapy.

Materials and Methods

Drosophila stocks: All stocks (Gal4 drivers, balancers, RNAi and overexpression lines) were raised and tested at 25°C, and unless otherwise noted, were obtained from the Vienna *Drosophila* Resource Center or Bloomington stock center. Stocks are listed in supplementary Table 1.

Screening

We used viability screening as previously described (Shaukat *et al*, 2012), to identify further metabolic candidates whose knockdown gave lethality only in CIN (Mad2 knockdown) flies. Depletion of candidates that gave <50% survival when *mad2* was co-depleted, compared to the candidate knockdown alone, were retested and selected for further assays.

Cell death assay

Acridine Orange (Invitrogen) was used to identify the level of cell death in the *engrailed* or *hedgehog* driven third instar larval wing discs as previously described (Shaukat *et al*, 2012). Imaginal wing discs were selected and dissected in PBS, then stained for 2 min in a 1μM Acridine Orange solution, rinsed briefly, mounted and imaged in PBS. For quantitation, the stain was normalized by subtracting the average Acridine Orange signal of the wild type anterior compartment from the average Acridine Orange signal in the *engrailed*-Gal4 driven mutant posterior compartment (marked with m*CD8-GFP*), using ImageJ software. To reduce noise, background subtraction (rolling ball radius at 10 pixels) was done in all the images (Shaukat *et al*, 2012). For Supplementary Figure 1, a representative disc was selected from at least nine for each experiment shown and contrast, brightness and gamma levels were

adjusted in Photoshop to most clearly reproduce the signal while retaining enough background to visualize the tissue.

Nile Red staining for lipid storage. To identify lipid storage levels we used Nile Red staining on third instar larval fat bodies. For starvation, approximately equal aged late-second instar larvae were selected and starved for 48hrs at 25^{o}C before dissection. Fat body tissue was dissected out in the Nile Red solution (2 μg/mL Nile Red (Sigma-Aldrich), 1.2μg/mL Hoechst33342 (Life Technologies) and 75% glycerol in PBS) from normally fed or 48hrs starved larvae and incubated for 30 min before mounting it on a glass slide. Fat depleted vs normally stained cells were counted using Axiovision software.

Reduced Glutathione assay:

ThiolTracker™ Violet dye reacts with reduced thiols and can be used to detect the level of reduced glutathione (GSH) in live cells. Imaginal wing discs from third instar larvae were dissected in PBS, and then placed in 9μM ThiolTracker for 20 minutes in the dark at room temperature. Discs were then quickly washed in PBS and briefly fixed in 3.7% formaldehyde for 5 minutes. Fixed discs were then mounted using 80% glycerol. For figures, a region (400 x 400 pixels) on an anterior/posterior boundary was cropped from a representative disc (from at least nine for each experiment shown) and processed as for Acridine stainings.

Mitochondrial stress

Mitochondrial stress was interrogated by identifying the change in mitochondrial membrane potential in live cells using TMRE (tetramethylrhodamine, ethyl ester). TMRE is a positively charged, cell permeant dye which readily labels negatively charged mitochondria. Depolarized or inactive mitochondria have decreased membrane potential and fail to sequester TMRE. In contrast, hyperpolarized mitochondria accumulate more TMRE and gives brighter red signal compared to normal mitochondria (Ehrenberg *et al*, 1988). Imaginal wing discs from third instar larvae were selected and dissected in PBS. Discs were then incubated for 10 min in a 0.05μM TMRE (Invitrogen) solution and washed for 10 min in PBS. Mounting and imaging was done similar to Acridine orange staining described previously (Shaukat *et al*, 2012). For figures, a region (400 x 400 pixels) on an anterior/posterior boundary was cropped from a representative disc and processed as described above.

Oxidative stress assay

Oxidative stress in the cell was measured by the fluorogenic probe CellROX (Life Technologies) that detects reactive oxygen species (ROS) in live cells. CellROX is a cell-permeable non-fluorescent reagent in its reduced state and upon oxidation exhibits strong infrared fluorescence. Imaginal wing discs from third instar larvae were dissected in D22 media (pH 6.8), then placed in 5μM CellROX in D22 media (D22 insect culture medium: pH 6.8) for 15 minutes in the dark at room temperature. Discs were then quickly washed in PBS and fixed in 3.7% formaldehyde for 5 minutes. Fixed discs were then mounted using 80% glycerol and observed under a fluorescence microscope. For figures, a region (650 x 300 pixels) on an anterior/posterior boundary was cropped from a representative disc and processed as described above.

Oxidative damage assays

***Lipid peroxidation*:** Lipid peroxidation detection in *engrailed*-driven single and double knockdown larval wing discs was carried out using an oxidation-sensitive fluorescent lipid probe (C_{11}-BODIPY$^{581/591}$, Invitrogen™) which is easily incorporated into membranes. In a normal non peroxidised state it gives red fluorescence but turns green upon oxidation by ROS (Pap *et al*, 1999). Imaginal wing discs from third instar larvae were dissected in PBS and then placed in 5μM C_{11}-BODIPY solution for 25 minutes in the dark at room temperature. Discs were then washed three times in PBS and the fixed in 3.7% formaldehyde for 5 minutes. Fixed discs were then mounted using 80% glycerol and imaged under a fluorescence microscope. For a positive control, C_{11}-BODIPY stained discs were treated with 200μM menadione (Sigma-Aldrich) for 20 min in the dark and washed twice in PBS before fixation and mounting.

***Oxidative damage to DNA**:* Oxidative damage to DNA was detected by using antibody staining against 8-hydroxy-2'-deoxyguanosine (8-oxoG) as well as staining of double stranded breaks using a ɣ-H2AX antibody (Rockland anti-P-H2AvD).

Immunostainings were performed on imaginal discs of third instar larvae using protocols as described (Shaukat *et al*, 2012). Primary antibodies used were: Rabbit anti-P-H2AvD (Rockland: 1:700) and mouse anti-8-oxoG (Abcam 15A3 1:100) for DNA damage, Rabbit

anti-cleaved caspase 3 (Cell signalling: 1:100) for Apoptosis, Secondary antibodies used were: Goat anti-Rabbit CY3 (Invitrogen 1:100).

Quantification of DNA damage staining was done by counting the number of ɣ-H2AX positive cells in the engrailed driven posterior half of wing pouch. Signals from each disc were normalized by subtracting the number of ɣ-H2AX positive cells of wild type half from the number of ɣ-H2AX positive cells of engrailed driven mutant half of wing disc (Wong *et al*, 2013). Imaging for all the experiments was carried out on a Zeiss Axioplan2 microscope with AxioCam MRm camera using AxioVision software.

Acknowledgements

We thank the Bloomington and VDRC stock centers for providing fly stocks, the Australian *Drosophila* Biomedical Research Support Facility (OzDros) for import services and the University of Adelaide. Helpful comments and advice were given by Michael Murray. This work was supported by NHMRC project grants 1027878 and 525447.

Author Contributions

Conceived and designed the experiments: ZS RR RS SG. Performed the experiments: ZS DL AC RH. Analyzed the data: ZS DL AC LOK SG. Contributed reagents/materials/analysis tools: ZS AC LOK RR RS SG. Wrote the paper: ZS SG.

Conflict of interest

The authors have declared that no competing interests exist.

References

Baker DJ, Jin F, Jeganathan KB & van Deursen JM (2009) Whole chromosome instability caused by Bub1 insufficiency drives tumorigenesis through tumor suppressor gene loss of heterozygosity. *Cancer Cell* **16:** 475–86

Bakhoum SF, Danilova O V, Kaur P, Levy NB & Compton D (2011) Chromosomal instability substantiates poor prognosis in patients with diffuse large B-cell lymphoma. *Clin. Cancer Res.* **17:** 7704–11

Bauer G (2012) Tumor cell-protective catalase as a novel target for rational therapeutic approaches based on specific intercellular ROS signaling. *Anticancer Res.* **32:** 2599–2634

Beumer KJ, Trautman JK, Bozas A, Liu J-L, Rutter J, Gall JG & Carroll D (2008) Efficient gene targeting in Drosophila by direct embryo injection with zinc-finger nucleases. *Proc. Natl. Acad. Sci. U. S. A.* **105:** 19821–6

Buffin E, Emre D & Karess RE (2007) Flies without a spindle checkpoint. *Nat Cell Biol* **9:** 565–572

Cairns R, Harris IS & Mak TW (2011) Regulation of cancer cell metabolism. *Nat. Rev. Cancer* **11:** 85–95

Carter SL, Eklund AC, Kohane IS, Harris LN & Szallasi Z (2006) A signature of chromosomal instability inferred from gene expression profiles predicts clinical outcome in multiple human cancers. *Nat Genet* **38:** 1043–1048

Cheung-Ong K, Giaever G & Nislow C (2013) DNA-damaging agents in cancer chemotherapy: serendipity and chemical biology. *Chem. Biol.* **20:** 648–59

Clem B, Telang S, Clem A, Yalcin A, Meier J, Simmons A, Rasku MA, Arumugam S, Dean WL, Eaton J, Lane A, Trent JO & Chesney J (2008) Small-molecule inhibition of 6-phosphofructo-2-kinase activity suppresses glycolytic flux and tumor growth. *Mol. Cancer Ther.* **7:** 110–20

Coe JP, Rahman I, Sphyris N, Clarke AR & Harrison DJ (2002) Glutathione and p53 independently mediate responses against oxidative stress in ES cells. *Free Radic. Biol. Med.* **32:** 187–96

Crasta K, Ganem NJ, Dagher R, Lantermann AB, Ivanova E V, Pan Y, Nezi L, Protopopov A, Chowdhury D & Pellman D (2012) DNA breaks and chromosome pulverization from errors in mitosis. *Nature* **482:** 53–58

DeBerardinis RJ, Lum JJ, Hatzivassiliou G & Thompson CB (2008) The biology of cancer: metabolic reprogramming fuels cell growth and proliferation. *Cell Metab.* **7:** 11–20

Ehrenberg B, Montana V, Wei MD, Wuskell JP & Loew LM (1988) Membrane potential can be determined in individual cells from the nernstian distribution of cationic dyes. *Biophys. J.* **53:** 785–94

Fang J, Nakamura H & Iyer AK (2007) Tumor-targeted induction of oxystress for cancer therapy. *J. Drug Target.* **15:** 475–86

Gogvadze V, Orrenius S & Zhivotovsky B (2008) Mitochondria in cancer cells: what is so special about them? *Trends Cell Biol.* **18:** 165–73

Gross S, Cairns RA, Minden MD, Driggers EM, Bittinger MA, Jang HG, Sasaki M, Jin S, Schenkein DP, Su SM, Dang L, Fantin VR & Mak TW (2010) Cancer-associated metabolite 2-hydroxyglutarate accumulates in acute myelogenous leukemia with isocitrate dehydrogenase 1 and 2 mutations. *J. Exp. Med.* **207:** 339–44

Hao H-X, Cardon CM, Swiatek W, Cooksey RC, Smith TL, Wilde J, Boudina S, Abel ED, McClain D a & Rutter J (2007) PAS kinase is required for normal cellular energy balance. *Proc. Natl. Acad. Sci. U. S. A.* **104:** 15466–71

Hao H-X & Rutter J (2008) The role of PAS kinase in regulating energy metabolism. *IUBMB Life* **60:** 204–9

Vander Heiden MG, Cantley LC & Thompson CB (2009) Understanding the Warburg effect: the metabolic requirements of cell proliferation. *Science* **324:** 1029–33

Hockenbery DM (2010) Targeting mitochondria for cancer therapy. *Environ. Mol. Mutagen.* **51:** 476–89

Holen K, Saltz LB, Hollywood E, Burk K & Hanauske A-R (2008) The pharmacokinetics, toxicities, and biologic effects of FK866, a nicotinamide adenine dinucleotide biosynthesis inhibitor. *Invest. New Drugs* **26:** 45–51

Howes RE, Piel FB, Patil AP, Nyangiri OA, Gething PW, Dewi M, Hogg MM, Battle KE, Padilla CD, Baird JK & Hay SI (2012) G6PD deficiency prevalence and estimates of affected populations in malaria endemic countries: a geostatistical model-based map. *PLoS Med.* **9:** e1001339

Iijima K, Zhao L, Shenton C & Iijima-Ando K (2009) Regulation of energy stores and feeding by neuronal and peripheral CREB activity in Drosophila. *PLoS One* **4:** e8498

Janssen A, van der Burg M, Szuhai K, Kops GJ & Medema RH (2011) Chromosome segregation errors as a cause of DNA damage and structural chromosome aberrations. *Science* **333:** 1895–1898

Jiralerspong S, Palla SL, Giordano SH, Meric-Bernstam F, Liedtke C, Barnett CM, Hsu L, Hung M-C, Hortobagyi GN & Gonzalez-Angulo AM (2009) Metformin and pathologic complete responses to neoadjuvant chemotherapy in diabetic patients with breast cancer. *J. Clin. Oncol.* **27:** 3297–302

Kaplan O, Navon G, Lyon RC, Faustino PJ, Straka EJ & Cohen JS (1990) Effects of 2-deoxyglucose on drug-sensitive and drug-resistant human breast cancer cells: toxicity and magnetic resonance spectroscopy studies of metabolism. *Cancer Res.* **50:** 544–51

Kasai H & Nishimura S (1984) Hydroxylation of deoxyguanosine at the C-8 position by ascorbic acid and other reducing agents. *Nucleic Acids Res.* **12:** 2137–45

Kops GJPL, Weaver B & Cleveland DW (2005) On the road to cancer: aneuploidy and the mitotic checkpoint. *Nat. Rev. Cancer* **5:** 773–85

Kuo W, Lin J & Tang TK (2000) Human glucose-6-phosphate dehydrogenase (G6PD) gene transforms NIH 3T3 cells and induces tumors in nude mice. *Int. J. Cancer* **85:** 857–64

Le A, Cooper CR, Gouw AM, Dinavahi R, Maitra A, Deck LM, Royer RE, Vander Jagt DL, Semenza GL & Dang C V (2010) Inhibition of lactate dehydrogenase A induces oxidative stress and inhibits tumor progression. *Proc. Natl. Acad. Sci. U. S. A.* **107:** 2037–42

Li M, Fang X, Baker DJ, Guo L, Gao X, Wei Z, Han S, van Deursen JM & Zhang P (2010) The ATM-p53 pathway suppresses aneuploidy-induced tumorigenesis. *Proc. Natl. Acad. Sci. U. S. A.* **107:** 14188–93

Liu J, Wang X, Shigenaga MK, Yeo HC, Mori A & Ames BN (1996) Immobilization stress causes oxidative damage to lipid, protein, and DNA in the brain of rats. *FASEB J.* **10:** 1532–8

Manganelli G, Masullo U, Passarelli S & Filosa S (2013) Glucose-6-phosphate dehydrogenase deficiency: disadvantages and possible benefits. *Cardiovasc. Hematol. Disord. Drug Targets* **13:** 73–82

McGranahan N, Burrell R a, Endesfelder D, Novelli MR & Swanton C (2012) Cancer chromosomal instability: therapeutic and diagnostic challenges. *EMBO Rep.* **13:** 528–38

Mertens F, Mandahl N, Mitelman F & Heim S (1994) Cytogenetic analysis in the examination of solid tumors in children. *Pediatr. Hematol. Oncol.* **11:** 361–77

Michelakis ED, Sutendra G, Dromparis P, Webster L, Haromy A, Niven E, Maguire C, Gammer T-L, Mackey JR, Fulton D, Abdulkarim B, McMurtry MS & Petruk KC (2010) Metabolic modulation of glioblastoma with dichloroacetate. *Sci. Transl. Med.* **2:** 31ra34

Miwa S, St-Pierre J, Partridge L & Brand MD (2003) Superoxide and hydrogen peroxide production by Drosophila mitochondria. *Free Radic. Biol. Med.* **35:** 938–948

O'Keefe L V, Colella A, Dayan S, Chen Q, Choo A, Jacob R, Price G, Venter D & Richards RI (2011) Drosophila orthologue of WWOX, the chromosomal fragile site FRA16D tumour suppressor gene, functions in aerobic metabolism and regulates reactive oxygen species. *Hum. Mol. Genet.* **20:** 497–509

Oromendia AB, Dodgson SE & Amon A (2012) Aneuploidy causes proteotoxic stress in yeast. *Genes Dev.* **26:** 2696–708

Owusu-Ansah E & Banerjee U (2009) Reactive oxygen species prime Drosophila haematopoietic progenitors for differentiation. *Nature* **461:** 537–41

Ozben T (2007) Oxidative stress and apoptosis: impact on cancer therapy. *J. Pharm. Sci.* **96:** 2181–96

Pap E, Drummen G & Winter V (1999) Ratio-fluorescence microscopy of lipid oxidation in living cells using C11-BODIPY 581/591. *FEBS Lett.* **453:** 278–282

Pfau SJ & Amon A (2012) Chromosomal instability and aneuploidy in cancer: from yeast to man. *EMBO Rep* **13:** 515–527

Puzio-Kuter AM (2011) The Role of p53 in Metabolic Regulation. *Genes Cancer* **2:** 385–91

Radyuk SN, Rebrin I, Klichko VI, Sohal BH, Michalak K, Benes J, Sohal RS & Orr WC (2010) Mitochondrial peroxiredoxins are critical for the maintenance of redox state and the survival of adult Drosophila. *Free Radic. Biol. Med.* **49:** 1892–902

Ren J-G, Seth P, Everett P, Clish CB & Sukhatme VP (2010) Induction of erythroid differentiation in human erythroleukemia cells by depletion of malic enzyme 2. *PLoS One* **5:** e12520

Reuter S, Gupta SC, Chaturvedi MM & Aggarwal BB (2010) Oxidative stress, inflammation, and cancer: how are they linked? *Free Radic. Biol. Med.* **49:** 1603–16

Sajesh B V, Bailey M, Lichtensztejn Z, Hieter P & McManus KJ (2013) Synthetic lethal targeting of superoxide dismutase 1 selectively kills RAD54B-deficient colorectal cancer cells. *Genetics* **195:** 757–67

Schläfli P, Borter E, Spielmann P & Wenger RH (2009) The PAS-domain kinase PASKIN: a new sensor in energy homeostasis. *Cell. Mol. Life Sci.* **66:** 876–83

Shaukat Z, Wong HW, Nicolson S, Saint RB & Gregory SL (2012) A screen for selective killing of cells with chromosomal instability induced by a spindle checkpoint defect. *PLoS One* **7:** e47447

Sheltzer JM, Torres EM, Dunham MJ & Amon A (2012) Transcriptional consequences of aneuploidy. *Proc Natl Acad Sci U S A* **109:** 12644–12649

Smart DK, Ortiz KL, Mattson D, Bradbury CM, Bisht KS, Sieck LK, Brechbiel MW & Gius D (2004) Thioredoxin reductase as a potential molecular target for anticancer agents that induce oxidative stress. *Cancer Res.* **64:** 6716–24

Sotgia F, Martinez-Outschoorn UE & Lisanti MP (2013) Cancer metabolism: new validated targets for drug discovery. *Oncotarget* **4:** 1309–16

Sotillo R, Schvartzman JM, Socci ND & Benezra R (2010) Mad2-induced chromosome instability leads to lung tumour relapse after oncogene withdrawal. *Nature* **464:** 436–440

Stanton RC (2012) Glucose-6-phosphate dehydrogenase, NADPH, and cell survival. *IUBMB Life* **64:** 362–9

Swanton C, Nicke B, Schuett M, Eklund AC, Ng C, Li Q, Hardcastle T, Lee A, Roy R, East P, Kschischo M, Endesfelder D, Wylie P, Kim SN, Chen JG, Howell M, Ried T, Habermann JK, Auer G, Brenton JD, et al (2009) Chromosomal instability determines taxane response. *Proc Natl Acad Sci U S A* **106:** 8671–8676

Tanaka T, Halicka HD, Huang X, Traganos F & Darzynkiewicz Z (2008) Constitutive Histone H2AX Phosphorylation and ATM Activation, the Reporters of DNA Damage by Endogenous Oxidants. *Cell Cycle* **5:** 1940–1945

Terhzaz S, Cabrero P, Chintapalli VR, Davies S-A & Dow J a T (2010) Mislocalization of mitochondria and compromised renal function and oxidative stress resistance in Drosophila SesB mutants. *Physiol. Genomics* **41:** 33–41

Thompson SL & Compton DA (2008) Examining the link between chromosomal instability and aneuploidy in human cells. *J. Cell Biol.* **180:** 665–72

Torres EM, Sokolsky T, Tucker CM, Chan LY, Boselli M, Dunham MJ & Amon A (2007) Effects of aneuploidy on cellular physiology and cell division in haploid yeast. *Science* **317:** 916–24

Walther A, Houlston R & Tomlinson I (2008) Association between chromosomal instability and prognosis in colorectal cancer: a meta-analysis. *Gut* **57:** 941–50

Wang J, Yuan W, Chen Z, Wu S, Chen J, Ge J, Hou F & Chen Z (2012) Overexpression of G6PD is associated with poor clinical outcome in gastric cancer. *Tumour Biol.* **33:** 95–101

Warburg O (1956) On the origin of cancer cells. *Science* **123:** 309–14

Wassmann K & Benezra R (2001) Mitotic checkpoints: from yeast to cancer. *Curr. Opin. Genet. Dev.* **11:** 83–90

Weaver B & Cleveland DW (2007) Aneuploidy: instigator and inhibitor of tumorigenesis. *Cancer Res.* **67:** 10103–5

Williams B, Prabhu V & Hunter K (2008) Aneuploidy affects proliferation and spontaneous immortalization in mammalian cells. *Science* **322:** 703–709

Wong HW-S, Shaukat Z, Wang J, Saint R & Gregory SL (2013) JNK signaling is needed to tolerate chromosomal instability. *Cell Cycle* **13:** 1–10

Wu D & Cederbaum AI (2005) Oxidative stress mediated toxicity exerted by ethanol-inducible CYP2E1. *Toxicol. Appl. Pharmacol.* **207:** 70–6

Yun J, Rago C, Cheong I, Pagliarini R, Angenendt P, Rajagopalan H, Schmidt K, Willson JK V, Markowitz S, Zhou S, Diaz LA, Velculescu VE, Lengauer C, Kinzler KW, Vogelstein B & Papadopoulos N (2009) Glucose deprivation contributes to the development of KRAS pathway mutations in tumor cells. *Science* **325:** 1555–9

Yuneva M, Zamboni N, Oefner P, Sachidanandam R & Lazebnik Y (2007) Deficiency in glutamine but not glucose induces MYC-dependent apoptosis in human cells. *J. Cell Biol.* **178:** 93–105

Zhang C, Zhang Z, Zhu Y & Qin S (2014) Glucose-6-phosphate dehydrogenase: a biomarker and potential therapeutic target for cancer. *Anticancer. Agents Med. Chem.* **14:** 280–9

Zhang J (2007) Suppression of phosphoenolpyruvate carboxykinase gene expression by reduced endogenous glutathione level. *Biochim. Biophys. Acta* **1772:** 1175–81

Figure Legends

***Figure 1. The effect of CIN on cell death in larval wing discs knocked down for metabolic candidates*. (A)** Acridine Orange staining of third instar larval wing discs. The dotted line shows the *en>CD8GFP* marked posterior compartment or test region in which the indicated genes were knocked down. The other half of each disc expressed no transgenes and acted as a wild type control. (i) Negative control (*lacZ*^{RNAi}), (ii) *LacZ*^{RNAi} *mad2*^{RNAi}, (iii) *pask*^{RNAi}, and (iv) *pask*^{RNAi} *mad2*^{RNAi} discs showed elevated levels of cell death only when Pask was depleted in CIN cells. **(B)** Quantitation of Acridine Orange staining of control and candidate-RNAi imaginal wing discs. Quantification shows grey value units normalized by subtracting the mean grey value of the wild type (anterior) region from the mean grey value of the affected (posterior) region for each disc. Negative control (*LacZ*^{RNAi}*)* and *candidate*^{RNAi} alone are represented in light grey bars and the knockdowns of candidates in CIN cells (*mad2*^{RNAi}) are represented by black bars. Knockdown of these candidates caused significant cell death in CIN cells but not normal cells. Error bars indicate 95% CIs, n≥10 in all cases. P-values are calculated by two-tailed t-tests with Welch's correction: p<0.001 = ***. All t-tests compare *candidate*^{RNAi} *mad2*^{RNAi} with *lacZ*^{RNAi} *mad2*^{RNAi}. **(C)** Cleaved caspase 3 staining. Third instar larval wing discs were stained for apoptosis using cleaved caspase 3 antibodies. As in 1A, genotypes tested were (i) Negative control (*lacZ*^{RNAi}), (ii) *LacZ*^{RNAi} *mad2*^{RNAi}, (iii) *pask*^{RNAi}, and (iv) *pask*^{RNAi} *mad2*^{RNAi}. Caspase-driven apoptosis was detected when Pask was depleted in CIN cells. Contrast, brightness and gamma levels were adjusted to show tissue outlines.

Figure 2. The effect of CIN on mitochondrial responses to metabolic disruption: Third instar larval wing discs were stained with TMRE to show mitochondrial membrane potential. Each image shows the anterior/posterior boundary of a representative wing disc from each genotype (a-j, a', d'-j'). Left of the dotted line is the region in which the indicated genes were knocked down, where (a-j) are single knockdowns and (a',d'-j') are knockdowns in CIN cells (*mad2*^{RNAi}). On each image, right of the dotted line is a wild type control (WT). (a) Negative control. (a') Negative control in CIN cells (b) Control showing reduced mitochondrial membrane potential (*ND42*^{RNAi}). (c) Control showing elevated mitochondrial membrane potential (*sesB*^{RNAi}). The candidate metabolic knockdowns caused elevated levels of mitochondrial membrane potential in CIN cells with no effect on normal cells.

Figure 3. Oxidative stress responses to metabolic intervention in CIN cells: Third instar larval wing discs were stained with ThiolTracker to show increased levels of GSH in

response to oxidative stress. (k) The dotted line shows the *en>CD8GFP* marked region in which the indicated genes were knocked down. The other half of each disc expressed no transgenes and is a wild type control. The marked region on the anterior/posterior boundary was cropped from a representative disc of each genotype (a-j, a'-h'). Left of the dotted line is the *engrailed*-driven tester region labelled with the knocked down gene name, where (a-j) are single knock downs and (a', d'-j') are knock downs in CIN cells (*mad2*^{RNAi}). On each image, right of the dotted line is a wild type control (WT). (a) Negative control (a') Negative control in CIN cells (b, c) positive controls showing oxidative stress induced by mitochondrial dysfunction. The candidate metabolic knockdowns caused an oxidative stress response in CIN cells but not normal cells.

Figure 4. CIN increased ROS levels in metabolic knockdowns: Third instar larval wing discs were stained with CellRox to show levels of reactive oxygen species. Images show the anterior/posterior boundary of a representative wing disc from each genotype. The dotted line shows the *engrailed*-driven knockdown area in each cropped image; right of the dotted line is wild type tissue (WT). (b-g) are candidate gene knockdowns; (c'-g') are candidate gene knockdowns in CIN cells (*mad2*^{RNAi}). (a, a') Negative controls. (b) positive control showing ROS generated by hyperpolarized mitochondria (*sesB*^{RNAi}). The candidate metabolic knockdowns caused significantly elevated levels of reactive oxygen species in CIN cells. Elevated CIN levels (Dicer 2 overexpression with *mad2*^{RNAi}) also gave ROS (a").

Figure 5. CIN causes DNA damage and apoptosis. **(A)** The effects of different levels of induced CIN on DNA damage (anti-P-H2AvD staining) using increased temperature or expression of *Dicer2* to give stronger knockdown of Mad2. The Y-axis shows the number of γ-H2aX stained cells in the engrailed driven region normalized by subtracting the number of stained cells in the control region for each disc. **(B)** The effects of different levels of induced CIN on cell death (Acridine Orange staining) using increased temperature or expression of *Dicer2* to give stronger knockdown of Mad2. The Y-axis shows the Acridine Orange signal normalized by subtracting the mean value of the wild type (anterior) region from the mean value of the affected (posterior) region for each disc. Light grey bars represent the control^{RNAi} or Dcr2 overexpression. Dark grey bars represent *mad2*^{RNAi} or *Dcr2 mad2*^{RNAi}. Error bars indicate 95% CIs, n≥10 in all cases. P-values are calculated by two-tailed t-tests with Welch's correction: $p<0.001$ = ***, $p<0.01$ = **.

Figure 6. Metabolic disruption damages DNA and lipids in CIN cells. **(A)** A quantitative analysis of DNA damage (anti-γ-H2aX staining) in third instar larval wing discs knocked down for metabolic genes. The Y-axis shows the number of γ-H2aX stained cells in the *engrailed*-driven knockdown region (normalized by subtracting the number of stained cells in the control region for each disc). Light grey bars represent the candidate knockdown in wild type background and dark grey bars represent the candidate knockdown in CIN cells (*mad2*^{RNAi}). Error bars indicate 95% CIs, n≥10 in all cases. P-values are calculated by two-tailed t-tests with Welch's correction: p<0.001 = ***. **(B)** Oxidative damage to DNA. Third instar larval wing discs were stained with 8-oxoG antibody. Each image shows the anterior posterior/boundary of a representative wing disc from each genotype (dotted line). Left from the dotted line is the *engrailed*-driven test region labelled with the knocked down gene name, where (a, b) are single knockdowns and (a'-b') are knockdowns of candidates in CIN cells (*mad2*^{RNAi}). On each image, right of the dotted line is a wild type control (WT). Contrast, brightness and gamma levels were adjusted for clarity. Oxidative damage to DNA was seen when CIN cells were metabolically disrupted (b'). **(C)** Oxidative damage to lipids. Third instar larval wing discs were stained with the marker lipid C_{11}-BODIPY$^{581/591}$, which increases in green fluorescence when oxidised. Left of the dotted line is the region knocked down for the indicated gene in each panel: (a) negative control, (b) *Pask* knockdown alone and (c) *mad2* knockdown alone show no lipid oxidation compared to the wild type regions (right of the dotted line). (d) Metabolic disruption in CIN cells (*pask*^{RNAi} *mad2*^{RNAi}) shows oxidative damage to lipids.

Figure 7. Oxidative damage was responsible for cell death in metabolically disrupted CIN cells. Levels of cell death (Acridine Orange) were measured in positive control third instar wing discs knocked down for Pask and Mad2 (Control). The Y-axis shows the cell death signal normalized by subtracting the mean value of the wild type (anterior) region from the mean value of the affected (posterior) region for each disc. Error bars indicate 95% CIs, n≥8 in all cases. The cell death caused by Pask depletion in CIN cells could be significantly reduced by the overexpression of antioxidant enzymes: Calatase (Cat), Superoxide Dismutases (Sod1 or Sod2), or Glucose-6-P-Dehydrogenase (G6PD). P-values were calculated by two-tailed t-tests with Welch's correction: p<0.001 = ***.

Tables

	Gene	Functional associations
1	Phosphoenlopyruvate carboxykinase (PEPCK)	Gluconeogenesis
2	Fructose 1,6-bisphosphatase	
3	PAS Kinase (PASK)	Glucose and lipid metabolism
4	Glucose 6 phosphatase	Glycolysis, PP pathway
5	Galactose 1-phosphate uridylyltranferase	Galactose to glucose and glycogen
6	Glucose 6-phosphate dehydrogenase (G6PD)	PP pathway, NADPH production
7	Phosphoglycerate mutase 5	Glycolysis
8	Wwox	Glucose metabolism, TCA cycle
9	Isocitrate dehydrogenase (Idh)	TCA cycle, NADPH production
10	Malic enzyme B	
11	Superoxide dismutase 1	Oxidative stress response, antioxidants
12	Catalase	
13	Xanthine dehydrogenase	
14	Peroxiredoxin	
15	Sulfiredoxin	
16	Thioredoxin peroxidase 1	
17	Glutathione S transferase D2	
18	NADPH oxidase	Immune response, ROS production
19	Type III alchohol dehydrogenase	Alcohol to acetaldehyde to lipid
20	Acyl- Coenzyme A oxidase at 57D distal	Beta-oxidation
21	MTPα	
22	Mfe2	

Table 1: Candidates required for CIN tolerance.

Candidate knockdowns that gave less than 50% survival in CIN animals, compared to their control siblings, are listed along with their expected function. Further details of the screening results are given in Supplementary Table 1.

	Knockdown	# animals	Total # of fat cells	Fat depleted	percentage
1	Pask	25	5973	2210	37 %
2	PEPCK	5	1022	671	66%
3	G6PD	4	943	219	23%
4	Mad2	12	2981	12	0.4%
5	control	30	7865	364	5%

Table 2: Effect of candidate knockdowns on energy stores.

Third instar larvae were starved for two days and their remaining fat stores at that time are indicated by the percentage of fat body cells that have been depleted of lipid, detected by Nile Red staining. After two days fasting, the tested metabolic candidate knockdowns have significantly depleted energy stores in the fat body, while control or CIN animals show a low level of lipid depletion.

Expanded View:

Supplementary Table 1. List of metabolic candidates tested by viability screening in our induced-CIN model. Columns show: The RNAi line ID, the affected gene identifiers; the number of replicate crosses carried out; the ratio of the total number of Cy/non-Cy progeny (*Candiate*^{RNAi} only/*Candidate*^{RNAi} and *mad2*^{RNAi}) used to rank the Table; and probability of finding a result this diverged or more diverged from a 50/50 ratio (the null hypothesis), out of this number of crosses (280), purely by chance.

Supplementary Figure 1 (A-D). Acridine Orange staining on larval wing discs (complete data). All wing discs are stained with Acridine Orange and the dotted line shows the *en>CD8GFP* marked posterior compartment or test region in which the genes were depleted. The other half of each disc expressed no transgenes and serves as an internal control. Single knockdowns of each candidate are arranged on the left and the *candidate*^{RNAi} *mad2*^{RNAi} are on the right side. Representative discs for each genotype are shown; the level of variation for selected genotypes can be seen in Figure 1 of the main paper.

Supplementary Figure 2. Staining for lipid oxidation (positive controls). Third instar larval wing discs were stained with the lipid marker C_{11}-BODIPY$^{581/591}$, which increases in green fluorescence when oxidised. To demonstrate that C_{11}-BODIPY signal is increased directly by reactive oxygen species (without mitochondrial or metabolic mutations), wild type discs were either untreated (a) or treated with the pro-oxidant menadione (b). Menadione treated discs show strongly increased levels of green fluorescence from C_{11}-BODIPY. A similar increase in lipid oxidation is seen in the affected tissue when ROS are induced by mitochondrial disruption (*ND42*^{RNAi}) (d) compared to control discs (c).

Supplementary Figure 3. DNA damage in metabolically disrupted CIN cells is not a result of apoptosis. Third instar larval wing discs were stained for DNA damage (anti-γ-H2aX staining). Metabolic disruption of CIN cells (*PEPCK*^{RNAi} *mad2*^{RNAi}) (a), causes DNA damage in the affected tissue (outlined) that is not reduced by overexpression of the apoptosis inhibitor p35 (b). The tissue overgrowth in (b) is consistent with cell death inhibition and the effect of undead cells.

Supplementary Figure 4. Cell death by metabolic disruption is consistent in different CIN models. Quantitation of Acridine Orange staining in third instar imaginal wing discs.

Quantification shows grey value units normalized by subtracting the mean grey value of the wild type (anterior) region from the mean grey value of the affected (posterior) region for each disc. (a). Knockdown of *Pask* or *Pepck* in cells with CIN induced by *Rb* knockdown caused significant cell death compared to $LacZ^{RNAi}$ in CIN cells. (b) Knockdown of *Pask* in cells with CIN induced by $Rad21^{RNAi}$ with Dicer overexpression showed significant cell death above the $LacZ^{RNAi}$ control. Error bars indicate 95% CIs, n≥10 in all cases. P-values are calculated by two-tailed t-tests with Welch's correction: $p<0.001$ = ***. The t-tests compare $candidate^{RNAi}$ with $lacZ^{RNAi}$ in each CIN model.

Figure 1

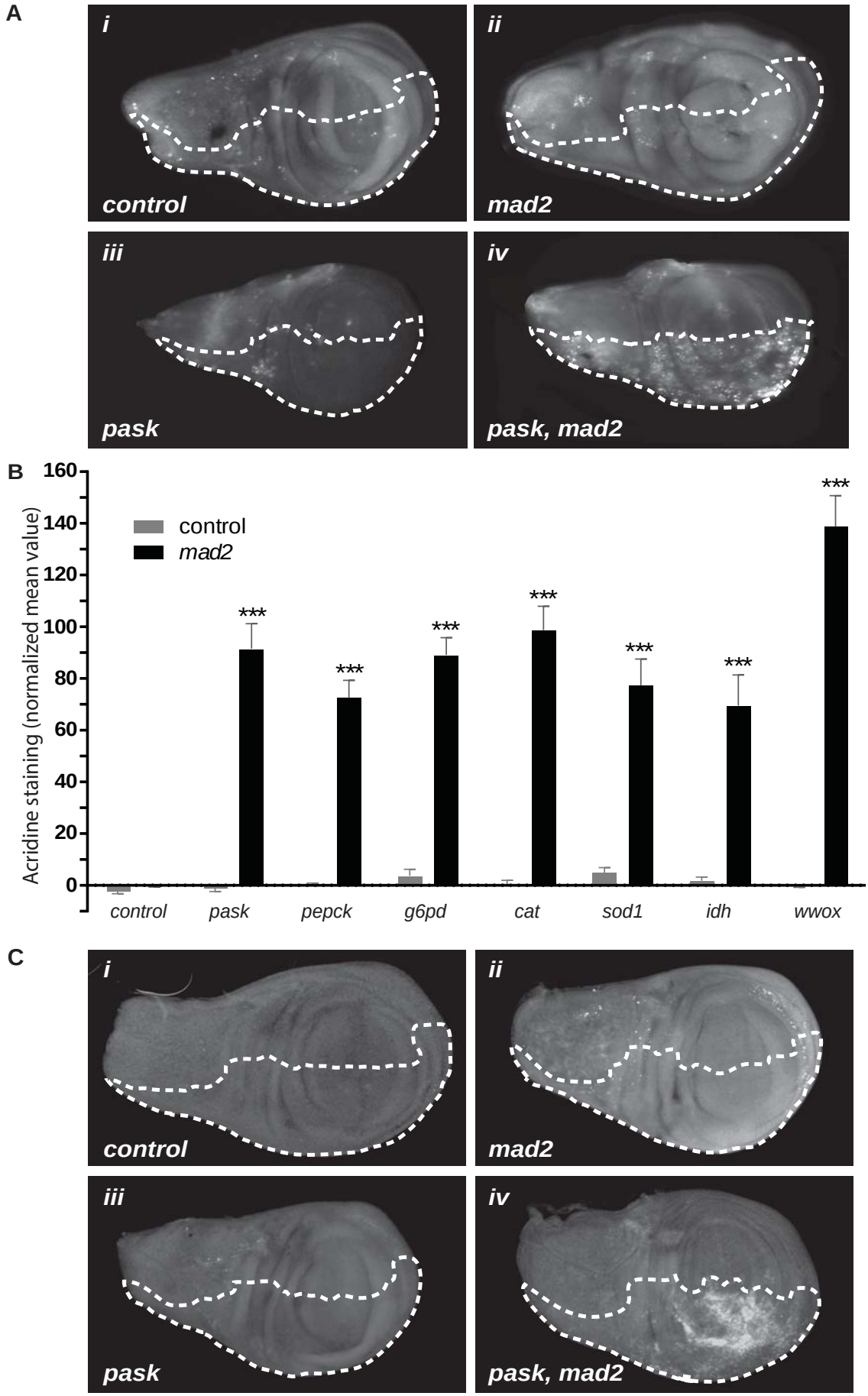
A
i
control
ii
mad2
iii
pask
iv
pask, mad2
B
Acridine staining (normalized mean value)
160
140
120
100
80
60
40
20
0
control
mad2
***
control
pask
pepck
g6pd
cat
sod1
idh
wwox
C
i
control
ii
mad2
iii
pask
iv
pask, mad2

Figure 2 TMRE

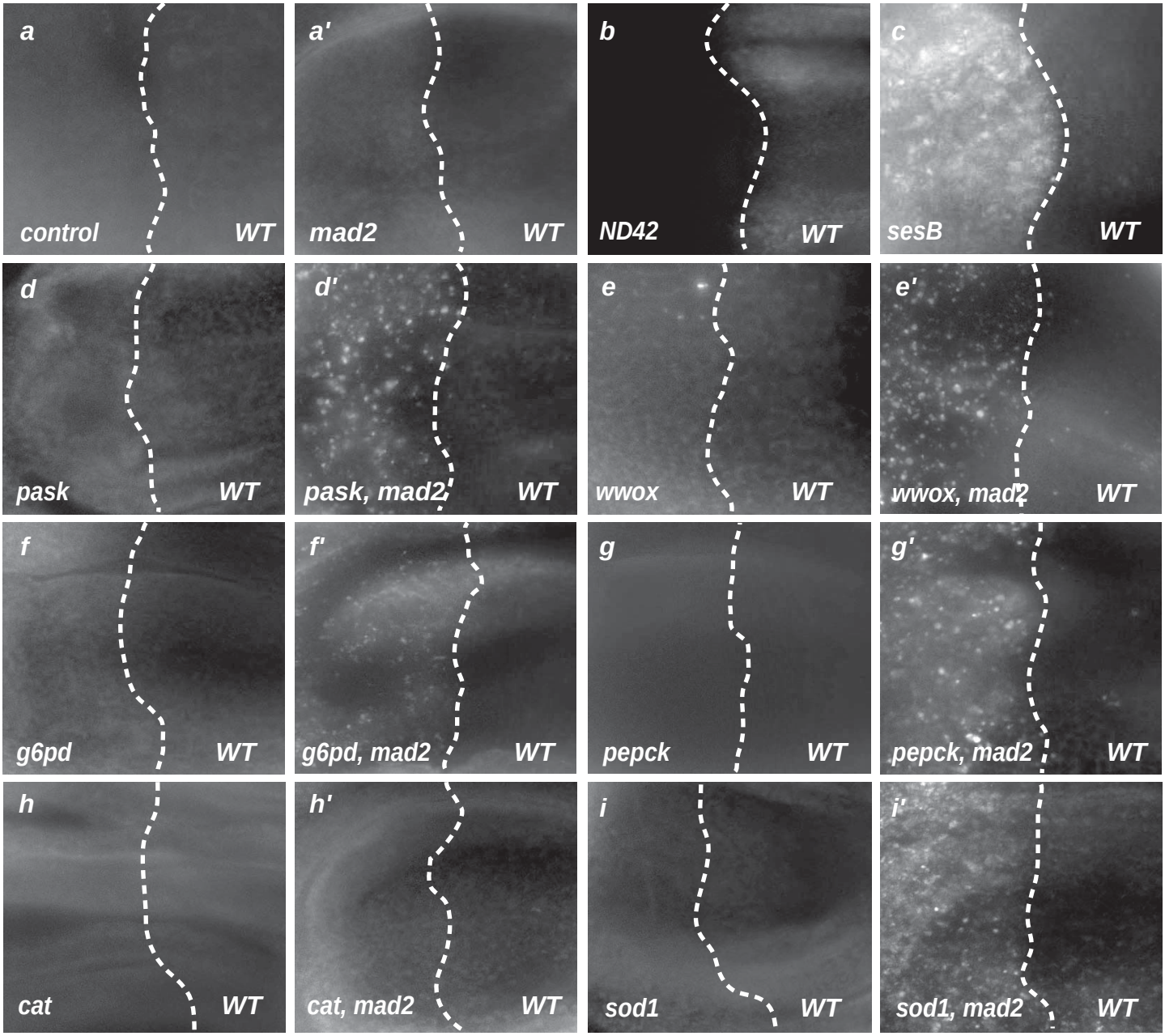

Figure 3 GSH

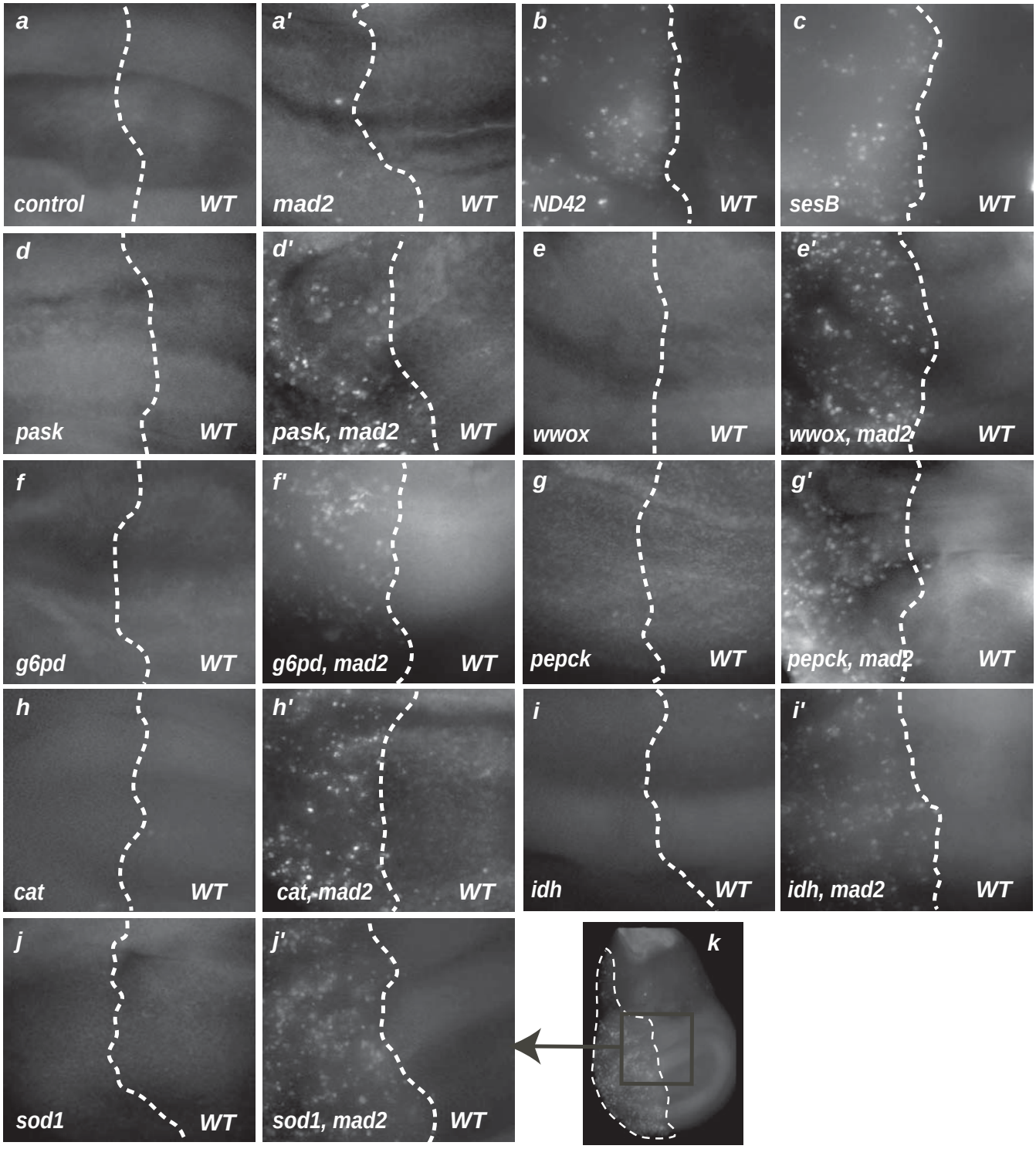
a
control
WT
a'
mad2
WT
b
ND42
WT
c
sesB
WT
d
pask
WT
d'
pask, mad2
WT
e
wwox
WT
e'
wwox, mad2
WT
f
g6pd
WT
f'
g6pd, mad2
WT
g
pepck
WT
g'
pepck, mad2
WT
h
cat
WT
h'
cat, mad2
WT
i
idh
WT
i'
idh, mad2
WT
j
sod1
WT
j'
sod1, mad2
WT
k

Figure 4 ROS

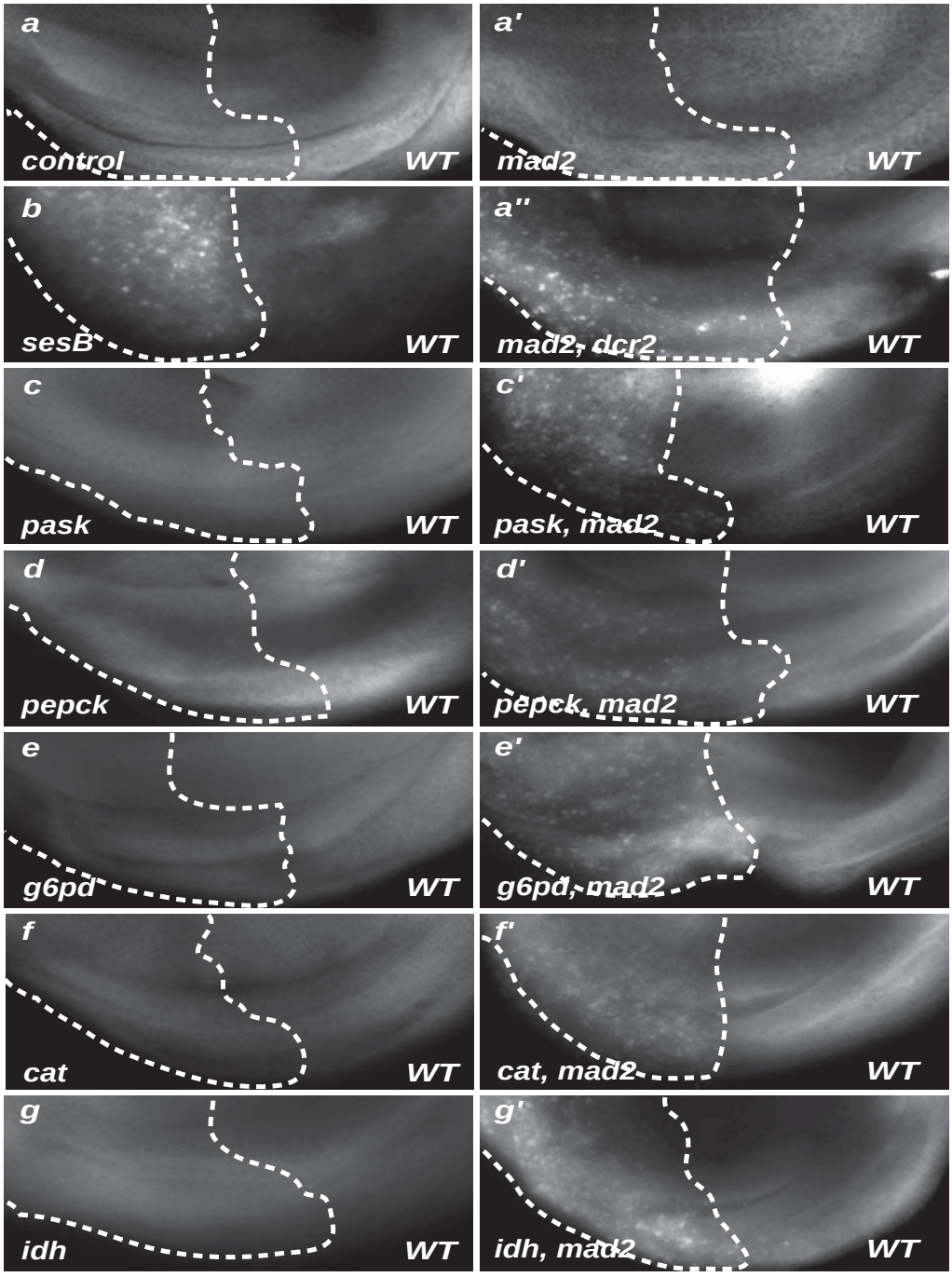
a
control
WT
a'
mad2
WT
b
sesB
WT
a''
mad2, dcr2
WT
c
pask
WT
c'
pask, mad2
WT
d
pepck
WT
d'
pepck, mad2
WT
e
g6pd
WT
e'
g6pd, mad2
WT
f
cat
WT
f'
cat, mad2
WT
g
idh
WT
g'
idh, mad2
WT

Figure 5

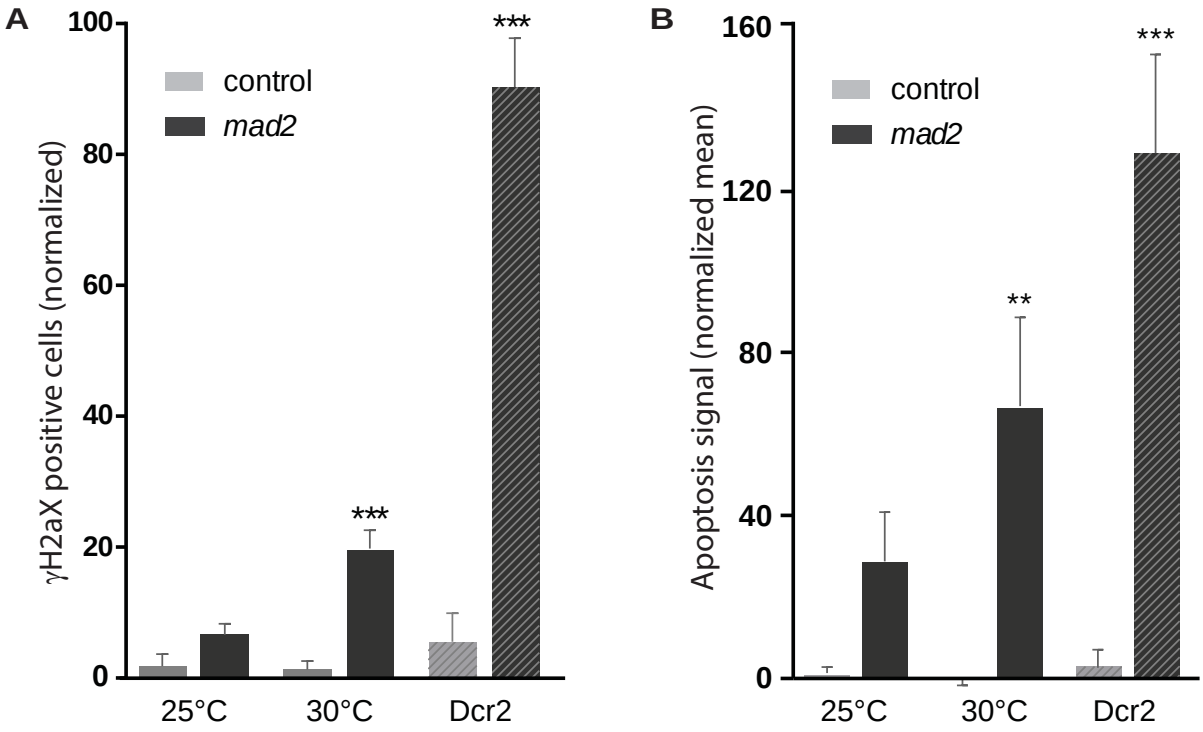
A
100
80
60
40
20
0
γH2aX positive cells (normalized)
control
mad2
***
***
25°C
30°C
Dcr2
B
160
120
80
40
0
Apoptosis signal (normalized mean)
control
mad2
**
***
25°C
30°C
Dcr2

Figure 6 - oxidative damage

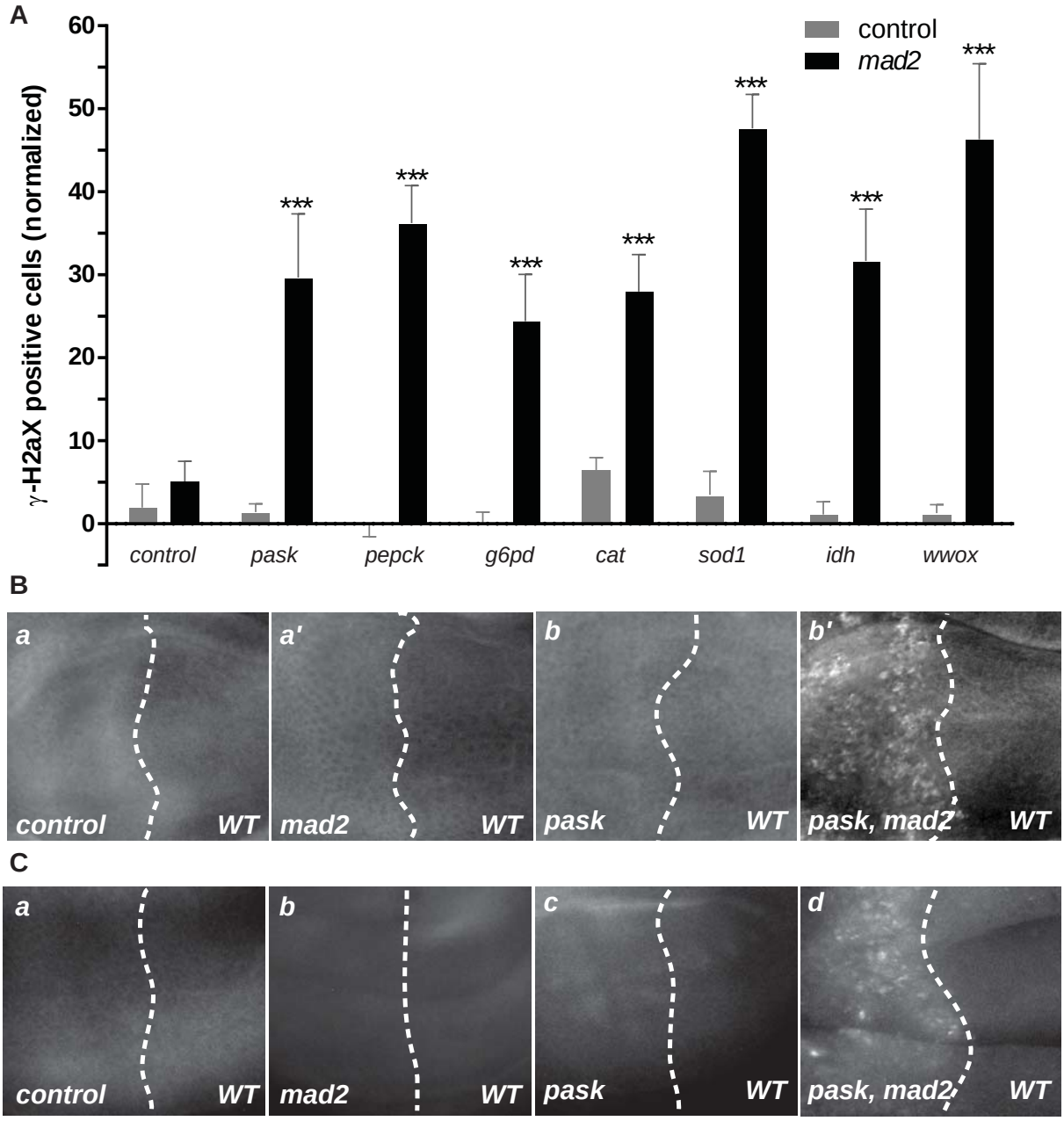

Figure 7 - Anti-oxidant rescue

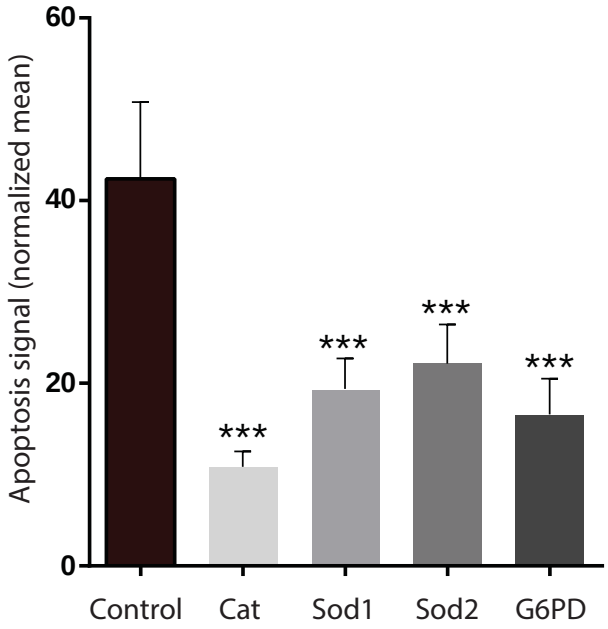

Supplementary figure 1A

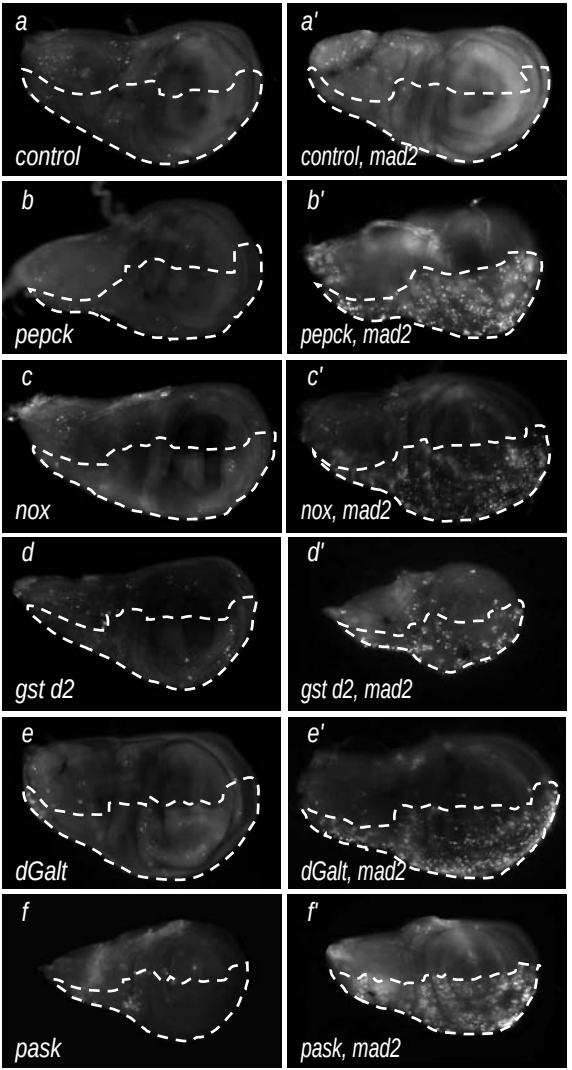

Supplementary figure 1B

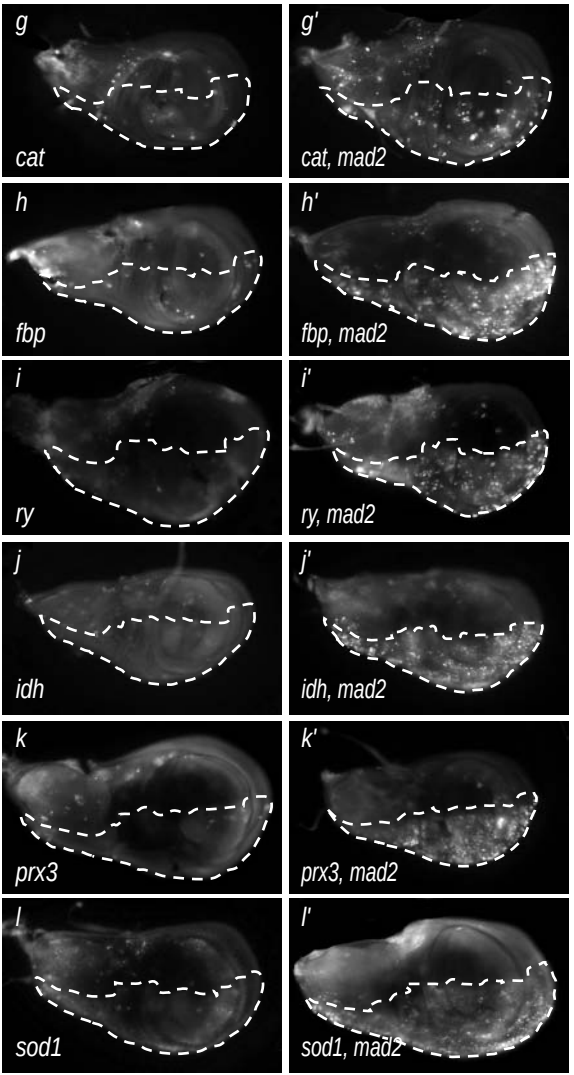

Supplementary figure 1C

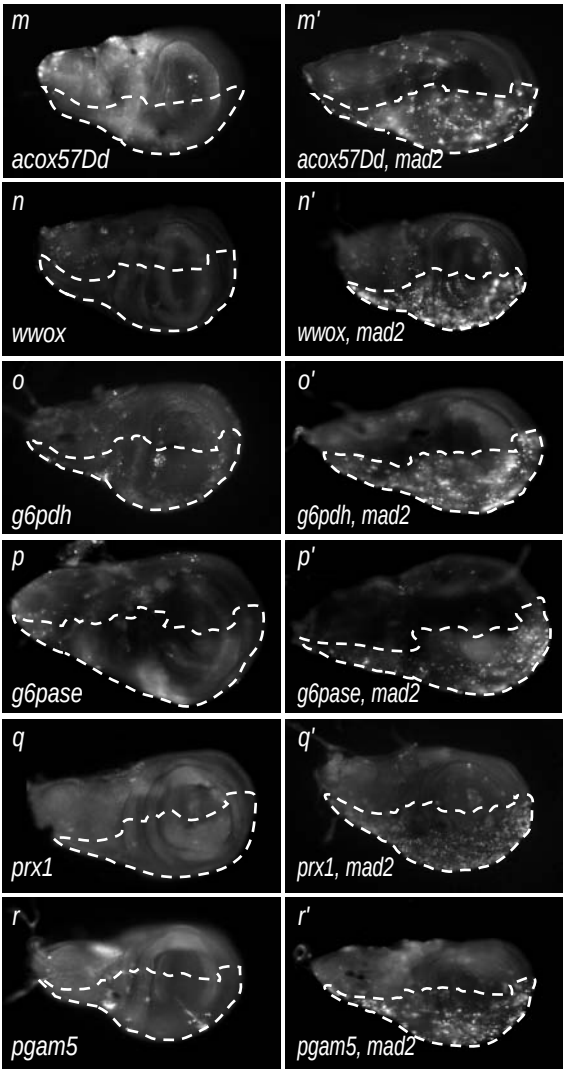

Supplementary figure 1D

Supplementary Figure 2

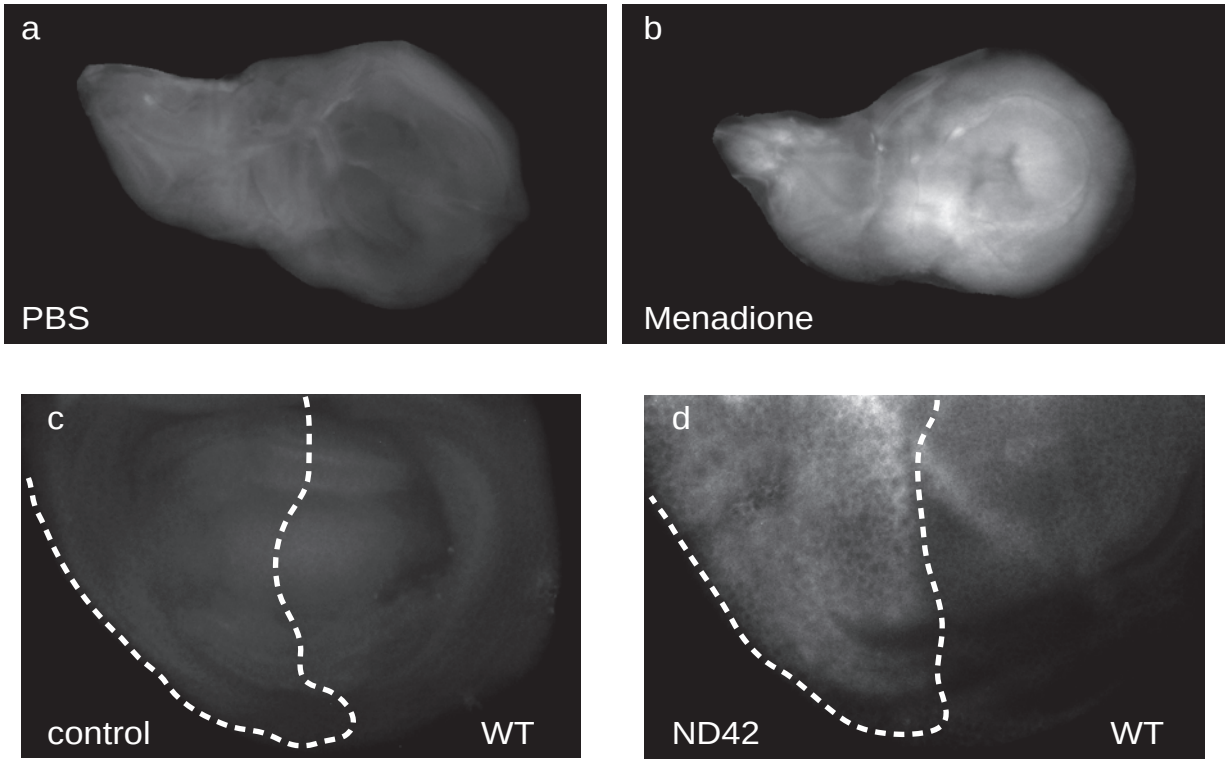

Supplementary Figure 3

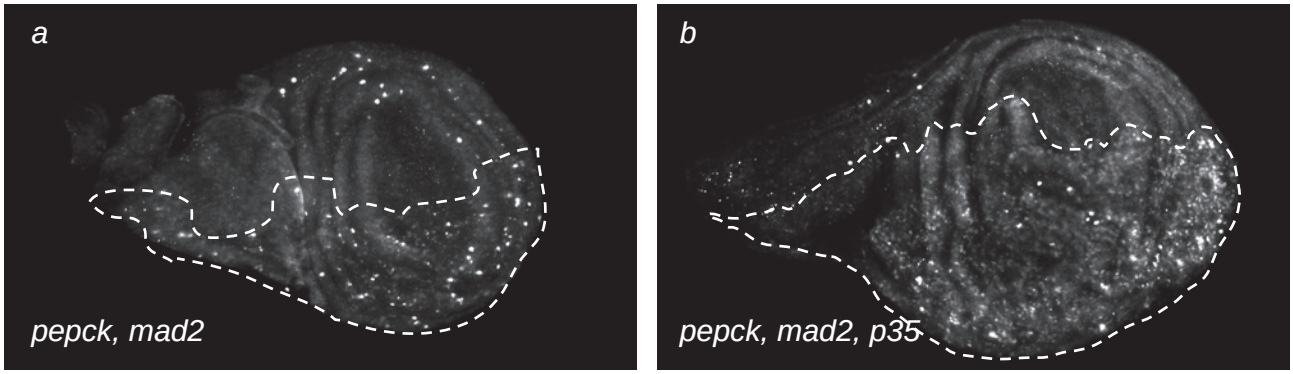

Supplementary figure 4

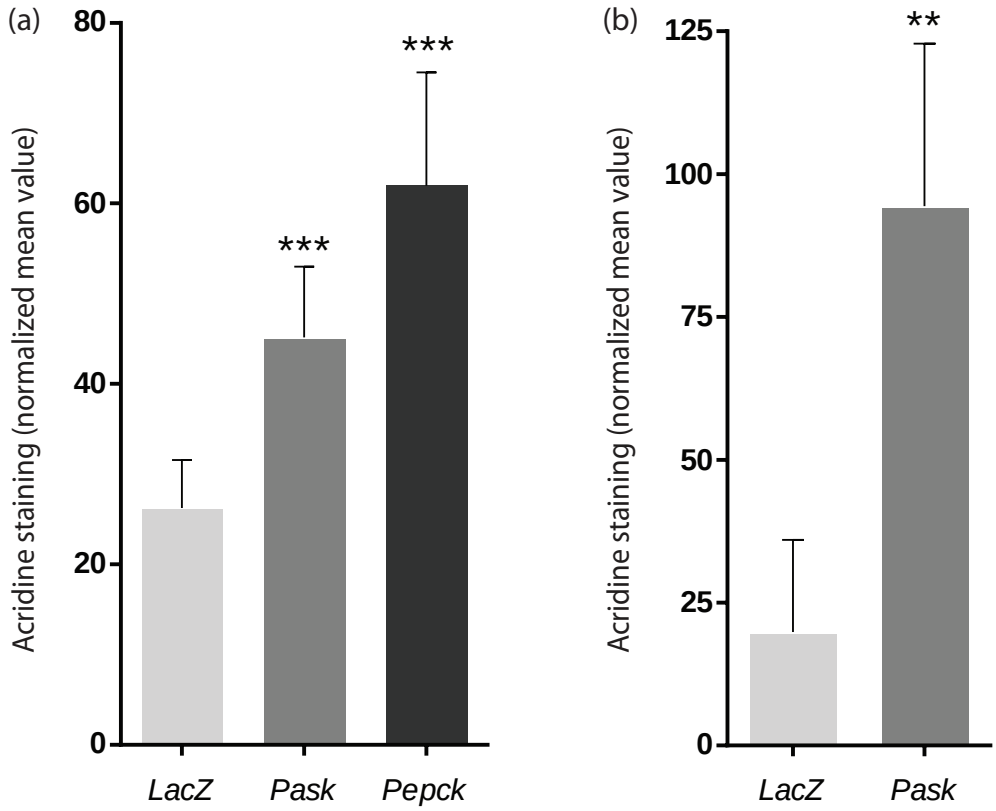

ID	CG	Gene	#crosses	Cumulative ratio	p[sum]
20529	17725	phosphoenlopyruvate carboxykinase (PEPCK)	4	126.00	0.000E+00
102559	34399	NADPH oxidase NOX	4	95.00	0.000E+00
2907	42783	apkc (POSITIVE CONTROL)	2	56.00	6.883E-15
109123	4181	glutathione S transferase D2 (GstD2)	4	52.00	1.110E-13
100025	9232	Galactose 1-phosphate uridylyltransferese	2	49.00	2.220E-11
107025	3105	PASK kk	2	29.50	3.968E-13
103591	6871	catalase	4	25.75	0.000E+00
108554	31692	Fructose- 1,6- bisphosphatase	4	12.60	0.000E+00
106995	7642	Xanthine dehydrogenase (rosy, ry)	4	12.43	0.000E+00
100554	7176	Isocitrate dehydrogenase	5	12.20	1.766E-11
105617	5826	peroxoredoxin	4	11.54	0.000E+00
103408	17256	nek2 (POSITIVE CONTROL)	2	11.00	5.195E-05
108307	11793	Superoxide dismutase SOD1	3	9.82	0.000E+00
106733	9709	Acyl- Coenzyme A oxidase at 57D distal	4	9.77	0.000E+00
100627	6762	Sulfiredoxin	4	6.58	0.000E+00
26190	3425	Type III alchohol dehydrogenase (T3dh)	2	6.33	2.508E-07
108350	7221	WWOX	3	5.42	7.709E-13
100021	4389	Mtp-a	2	5.25	1.720E-01
101507	12529	G6PDH	3	5.12	3.387E-10
7261	15400	Glucose 6 phosphatase	2	4.31	3.274E-05
25661	3105	PASK GD	4	3.89	5.483E-13
109514	1633	Thioredoxin peroxidase 1, prx1	4	3.44	1.998E-07
27535	5889	malic enzyme b:	3	3.04	1.094E-04
104016	10120	malic enzyme	3	2.82	1.406E-06
101809	31075	has aldehyde dehydrogenase NAD activity	2	2.78	2.135E-02
108880	3415	Mfe2	2	2.70	7.188E-01
110219	14816	phosphoglyceratemutase 5 /cyo	3	2.00	2.381E-01
110190	10160	Ecdysone-inducible gene L3: L-lactate dehydrogenase	2	1.83	9.544E-01
100269	3724	phosphogluconate dehydrogenase: pgd	2	1.63	9.998E-01
42162	8905	SOD2	3	1.54	1.000E+00
15007	13334	L-lactate dehydrogenase activity	2	1.49	9.997E-01
109423	30499	ribulose-phosphate 3-epimerase	2	1.47	1.000E+00
109391	34067	Mitochondrial cytochrome C oxidase subunit 1	3	1.46	1.000E+00
103829	14290	Mitochondrial pyruvate carrier: Mpc1: pyruvade dehydrogenase phosphate	2	1.39	9.992E-01
108954	12390	defective in the avoidance of repellents (dare)	4	1.28	1.000E+00
35135	7070	pyruate kinase	3	1.21	1.000E+00
35337	8094	HexC	3	1.20	1.000E+00
100812	5889	Malate dehydrogenase	3	1.19	1.000E+00
105666	4001	phosphofructokinase	3	1.19	1.000E+00
104680	3001	Hexokinase HexA	3	1.13	1.000E+00
22536	7221	WWOX	7	1.09	3.423E-01
102109	18418	oxoglutarate:malate antiporter activity: Transmembrane transporter activity	2	1.09	1.000E+00
107642	3861	Citrate synthase	3	1.06	1.000E+00
105359	9042	Glycerol 3 phosphate dehydrogenase	2	1.04	1.000E+00
103616	8251	phosphoglucose isomerase	3	1.00	1.000E+00
25634	2171	Triose phosphate isomerase	3	1.00	1.000E+00
103616	8251	Phosphoglucoisomerase	2	1.00	1.000E+00
		LacZ (NEGATIVE CONTROL)	7	0.99	1.000E+00
106641	8808	Pyruvate dehydrogenase kinase	3	0.97	1.000E+00
101339	6058	fructose biphosphate aldolase	3	0.97	1.000E+00
107820	12262	Acyl-CoA dehydrogenase	4	0.96	1.000E+00
107164	1065	succinyl-CoA synthetase	3	0.96	1.000E+00
107209	7010	pyruvate dehydrogenase	3	0.90	1.000E+00
100734	17333	6-phosphogluconolactonase activity	2	0.89	1.000E+00
105936	1516	Pyruate carboxylase	3	0.83	1.000E+00
105128	3425	Type III alchohol dehydrogenase (T3dh)	2	0.78	1.000E+00
106562	8893	gapdh2	3	0.76	1.000E+00
		empty vector 68E (NEGATIVE CONTROL)	5	0.73	2.740E-01
29015	9042	Glycerol 3 phosphate dehydrogenase	2	0.71	1.000E+00
BL15666	7254	Glycogen phosphorylase	2	0.71	9.995E-01
103809	9244	Aconitase	3	0.70	1.000E+00
15508	12140	Preducted homolog of ETFDH	3	0.70	1.000E+00
109278	34069	Mitochondrial cytochrome C oxidase subunit II	3	0.69	1.000E+00
110081	3127	phosphoglycerate kinase	3	0.65	1.000E+00
110440	17246	succinic dehydrogenase A	3	0.65	9.998E-01
21832	4347	UG Pase	2	0.63	1.000E+00
104606	30491	Thioredoxin peroxidase 2	2	0.59	4.708E-01
110090	17654	enolase	3	0.53	1.000E+00
6031	6666	succinic dehydrogenase B	3	0.25	5.771E-01
108457	2014	NADH-coenzyme Q oxidoreductase (complex1)	3	0.11	8.596E-05
BL29581	3105	PASK	4	0.00	1.000E+00
106126	7430	dihydrolipoamide dehydrogenase	2	0.00	1.000E+00
105680	4094	Fumarase	3	0.00	1.000E+00
101371	7580	there is a UQCRQ	3	0.00	1.000E+00
21748	3944	NADH: ubiquonone reductase 23KD precursor	3	0.00	1.000E+00
14444	6343	NADH: ubiquonone reductase 42KD precursor	3	0.00	1.000E+00
100733	2286	NADH: ubiquonone reductase 75KD precursor	3	0.00	1.000E+00
106717	15116	Glutathione peroxidase	4	0.00	1.000E+00
107110	11140	Aldehyde dehydrogenase type III (Aldh-III)	4	0.00	1.000E+00

50970	3481	Alchohol Dehydrogenase (Adh)	2	0.00	1.000E+00
108920	13221	von Hippel-Lindau (Vhl)	4	0.00	1.000E+00
106308	2827	Trans aldolase: sedoheptulose-7-phosphate:D-glyceraldehyde-3-phosphate glyceronetransfe	2	0.00	1.000E+00
105633	8036	transketolase activity	2	0.00	1.000E+00
100275	30410	Ribose-5-phosphate isomerase: Rpi	2	0.00	1.000E+00
100747	13369	ribokinase activity: Carbohydrate/puine kinase	2	0.00	1.000E+00
100783	4747	3-hydroxyisobutyrate dehydrogenase	2	0.00	1.000E+00
109812	1210	Phosphoinositide-dependent kinase 1: pdk1	2	0.00	1.000E+00
103023	7514	oxoglutarate:malate antiporter activity; transmembrane transporter activity.	2	0.00	1.000E+00
105936	1516	pyruvate carboxylase activity	2	0.00	1.000E+00
109632	4347	UDP-glucose pyrophosphorylase	2	0.00	1.000E+00
107110	11140	Aldehyde dehydrogenase type III	2	0.00	1.000E+00
Bl34930	6904	Glycogen synthase	2	0.00	1.000E+00
1110802	7113	Scu	2	0.00	1.000E+00
30557	3143	FOXO	2	0.00	1.000E+00

total # crosses #REF! p< 5E10-5

BL = Bloomington
other = VDRC

Chapter 5

DISCUSSION

Chromosomal instability and aneuploidy are frequent in solid tumours (Mertens et al, 1994; Kops et al, 2005) and linked to tumour heterogeneity which leads to high tolerance of internal and external stresses. CIN is also linked to tumourigenesis, metastasis, a low survival rate, relapse and drug resistance. There is a strong need to explore new therapeutic targets (Carter et al, 2006). CIN as a characteristic of drug resistant tumours presents a therapeutic potential against these unstable cancers. Targeting CIN provides an opportunity to make these resistant cells sensitive to current therapies without affecting normal cells.

A CIN model in *Drosophila* was generated by depleting Mad2, which weakens the SAC function and results in lagging chromosomes and chromosomal bridges (Chapter 2 - Figure 1; Buffin et al, 2007; Orr et al, 2007). Mad2 deficiency leads to increased merotely and lagging chromosomes, which results in aneuploidy (Michel et al, 1994; Michel et al, 2001; Lee et al, 2008). Mad2 is also required to facilitate centrosomal clustering in multi polar mitosis, mainly by giving more time in mitosis (Kwon et al, 2008). The induction of CIN in a stable tissue has some advantages over vertebrate cell line models, which have highly diverse and unstable genomes (Roschke & Kirsch, 2005). Screening for candidates that can kill CIN cells using this model allowed us to confidently compare the effects of candidates, which is not possible in cell lines with a varied genetic background.

The initial genome-wide screening of kinases and phosphatases identified a significant group of potential candidates that can kill cells exhibiting CIN. This includes candidates linked to the centrosome (Nek2, JNK and Asp; Chk2, ATM etc. Chapter 2, Table 1), which is a structural and regulatory hub of mitotic events. Errors in the centrosomal machinery and control are common in cancers and can lead to CIN (Duensing & Duensing, 2010; Galimberti et al, 2011; Mazzorana et al, 2011). Identification of Nek2 in the screen confirms that this screen has potential to identify clinically significant drug targets for CIN tumours because Nek2 is currently being pursued as therapeutic target for cancer (Suzuki et al, 2010). In addition, Kwon et al also showed that Asp is required to reduce the chances of merotely by facilitating centrosomal clustering in multi polar mitosis (Kwon et al, 2008). Therefore, in our induced-CIN model Asp may have a role in protecting the cell from chromosomal missegregation.

Some candidates were directly or indirectly involved in the DNA damage response, which is interesting because many current therapies for cancer rely on DNA damage but they are not ideal to use because of their side effects on normal proliferating cells (Cheung-Ong et al, 2013). By contrast, these candidates can cause DNA damage specifically in CIN cells, which would be highly desirable clinically.Enhancement of CIN above a threshold level can increase the efficiency of conventional therapies and also decrease cellular fitness which can lead to cell death in tumours (Dome et al, 2005; Stewenius et al, 2007). In our screening we expected to get candidates which are involved in CIN enhancement (e.g. other SAC and cell cycle proteins). The results from viability screening showed that SAK/Plk4 (Snk akin kinase/polo-like kinase 4) knockdown induces lethality only in CIN cells, which may be through CIN enhancement. Measuring CIN level in these knockdowns is needed to confirm this hypothesis. In the case of Aurora B and Polo, their knockdowns induce lethality also in normal cells and therefore were not selected as candidates. This suggests that the knockdown of these proteins alone can generate enough CIN to induce cell death or disturbs other cellular function which can further reduce the cellular fitness. In contrast, Bub1 knockdown has no effects on either normal or CIN cells, presumably due to inefficient RNAi knockdown. Using RNAi screening is an efficient approach but it shows variable gene silencing which may be disadvantageous in some cases.

The other interesting candidates identified were some metabolism related kinases (i.e. PAS Kinase, Phosphofructokinase), which were further screened and characterized (Chapter 4) in order to identify the possible link between two hallmarks of Cancer (i.e. altered metabolism and CIN) (Warburg, 1956; Mertens et al, 1994).

Further screening and characterization of the JNK pathway suggested the involvement of a typical JNK signaling cascade from a MAPKKK through to the JNK targets FOXO and Jun in CIN tolerance (Chapter 3, (Wong et al, 2014)). Reduction of JNK in CIN cells resulted in caspase-mediated apoptosis, which is partly independent of p53. The results show the presence of high levels of DNA damage in JNK reduced CIN cells, which is consistent with the role of JNK in DNA damage repair and the production of antioxidants (Karin & Gallagher, 2005; Wagner, E. F. & Nebreda, Á. R., 2009). In support for the role of efficient DNA damage repair in CIN tolerance, we also demonstrated that the shortening of G2 phase (but not G1 phase) induces apoptosis in

CIN cells. This is consistent with the findings that JNK signaling is involved in promoting efficient DNA damage repair via AP1 (MacLaren et al, 2004; Christmann et al, 2006). Furthermore, shortening of G2 enhances the level of cell death in JNK-reduced CIN cells, while lengthening the G2 phase suppresses the levels of cell death. This suggests that cells require more time for repair if the level of DNA damage is high or the repair mechanism is slightly compromised. However, the DNA damage checkpoint does not give enough time in JNK-reduced CIN cells, which accumulate unrepaired DNA damage during the cell cycle. Failure to repair damage before mitosis can lead to anaphase chromatin bridges and subsequent tetraploidy or bridge-breakage-fusion cycles that perpetuate the damage (Ganem & Pellman, 2012).

The role of JNK in tolerating chromosomal instability might appear surprising given the amount of data showing that signaling through JNK can lead to apoptosis (Weston & Davis, 2007). While the activation of JNK is an essential feature of some apoptotic responses such as to irradiation (McEwen & Peifer, 2005; Luo et al, 2007), other treatments have been shown to induce JNK-independent cell death (Umemori et al, 2009; Ma et al, 2012), which suggests that JNK activation is not the only mechanism for triggering apoptosis. Consistent with our finding that JNK signaling is required to promote cell survival in CIN cells, knockdown of JNK sensitizes cells to CD95-mediated apoptosis (Kuntzen et al, 2005), and phosphorylation of FOXO by JNK is needed for a wide range of stress survival responses (Ventura et al, 2006; Storz, 2011). Moreover, JNK is needed in *Drosophila* for effective stress tolerance (Biteau et al, 2008) and in our case the stress involved is imposed by the induction of CIN and aneuploidy, which leads to a high rate of anaphase errors, oxidative stress and DNA damage (Chapter 2 & 4). Consistently, aneuploidy can cause proteotoxic stress, JNK activation, and DNA damage sensitivity (Pavelka et al, 2010; Sheltzer et al, 2011; Dekanty et al, 2012). Moreover, the loss of JNK has been reported to reduce the incidence of tumours in several mouse models and elevated levels of JNK expression are common in many tumours (Wagner & Nebreda, 2009).

Cancer cells also reprogram their metabolic pathways in order to achieve an advantage over normal cells in terms of cellular growth, proliferation and resistance to cellular and environmental stresses (Yuneva et al, 2007; Yun et al, 2009; Puzio-Kuter, 2011; Pfau & Amon, 2012). Consequently, there has been a long standing interest in using differences

in metabolism as a potential target to specifically kill cancer cells (Kaplan et al, 1990; Clem et al, 2008; Holen et al, 2008; Jiralerspong et al, 2009; Gross et al, 2010; Le et al, 2010; Michelakis et al, 2010). Metabolic adaptations are more frequent and efficient in CIN tumours (Pfau & Amon, 2012) and our screening and characterization of metabolic candidates suggests that CIN cells are sensitive to metabolic alterations, specially those which are involved in stress responses and maintaining the redox status of the cell (Chapter 4 - Table 1). Furthermore, an increased level of CIN and aneuploidy also affects cell growth, proliferation, proteotoxic and oxidative stress (Oromendia et al, 2012) so any alteration that increases the existing cellular stress is a plausible target to induce cancer specific apoptosis.

Our results showed that the induction of CIN makes cells highly vulnerable to oxidative stress, showing DNA damage and apoptosis in response to metabolic changes that do not damage normal cells. The data suggest that CIN cells are sensitive to alterations in the cellular redox status or antioxidant capacity because they are already coping with elevated levels of stress. Consistent with this, overexpression of antioxidant enzymes rescued the apoptosis caused by metabolic candidate knockdown in CIN cells (Chapter 4 - Figure 7). In addition, one of the main groups of candidates identified by the screening was related to the oxidative stress response mechanism of the cell (Chapter 4 – Table 1) which protects DNA, lipids and proteins from oxidative damage (Reuter et al, 2010). Our results shows that these antioxidant enzymes (SOD1, catalase, xanthine dehydrogenase/oxidase, sulfiredoxin and peroxiredoxin) are required for CIN tolerance, which is consistent with the results showing that inhibition of SOD can kill Rad54 deficient CIN and colorectal cancer cells by inducing DNA damage (Sajesh et al, 2013).

Another group of metabolic candidates that induced CIN specific apoptosis was involved in glucose metabolism (Chapter 4 -Table 1), which provides energy and also maintains the redox potential of the cell via NADPH production (Stanton, 2012). Consistent with this, enzymes (G6PD, malic enzyme, IDH, etc.) that are involved in NADPH production are overexpressed in cancers (Cairns et al, 2011; Wang et al, 2012) and their reduction sensitizes the cancerous cells to conventional therapies (Zhang et al, 2014) and inhibits the progression of these tumours (Ren et al, 2010). Furthermore, cancer cells utilize elevated glycolytic flux and low TCA flux to meet their high energy and macromolecule demands with minimized oxidative stress (Warburg, 1956; Vander

Heiden et al, 2009). Induction of CIN or aneuploidy leads to increased glucose usage (Torres et al, 2007; Williams et al, 2008; Li et al, 2010), and our results show that the metabolic knockdowns in these cells lead to increased mitochondrial membrane potential, with the consequent production of reactive oxygen species and oxidative damage. In contrast, no detectable effect on membrane potential was observed in normal cells with these metabolic knockdowns (Chapter 4), suggesting the possibility to utilize these genes as a specific target for CIN cancers.

PAS kinase is an interesting candidate for CIN related effects because it had not previously been implicated in cell death or proliferation. PASK knockdown is linked to increase metabolic rate and decreased lipid storage [(Hao et al, 2007), Chapter 4]. In CIN cells, PASK knockdown enhanced the oxidative stress, mitochondrial membrane potential and ROS level, which led to an increase in DNA damage and resulted in p53 dependent apoptosis (Chapter 2 & Chapter 4). Rescuing apoptosis in $pask^{RNAi}mad2^{RNAi}$ cells by overexpressing antioxidant enzymes confirms the involvement of oxidative stress in this CIN specific cell death [Chapter 4]. PASK has been implicated as a therapeutic target for type 2 diabetes and metabolic syndrome (da Silva Xavier et al, 2004; Grose & Rutter, 2010; da Silva Xavier et al, 2011) but in this study we proposed a novel role of PASK as target for CIN specific anti-cancer therapy, having identified its effect on mitochondria and oxidative stress in CIN cells. Consistent with our results, oxidative stress and stress response pathways are considered plausible targets for cancer therapy (Smart et al, 2004; Fang et al, 2007; Ozben, 2007) and metabolic intervention that generates oxidative stress and cytotoxicity is currently in clinical trials for cancer therapy (Le et al, 2010; Michelakis et al, 2010; Sotgia et al, 2013).

In summary, we have used a new model for CIN in *Drosophila* to demonstrate the principle that it is possible to selectively kill CIN cells. Our RNAi screening identified candidates whose depletion has the potential to induce apoptosis only in CIN cells. Further characterization of screened candidates in CIN cells found that CIN cells, which are already coping with oxidative and proteotoxic stress, are sensitive to alterations in the cell's stress response mechanisms. Although tumours are highly resistant to apoptosis, they still have a need to manage high levels of DNA damage generated by CIN and ROS by maintaining the antioxidant capacity of the cell. Our results suggest that JNK signaling and metabolic alterations (to maintain the anti-oxidant capacity and

the redox potential of the cell) are needed to tolerate CIN. Therefore, these interventions present a highly effective way of killing CIN cells without affecting normal dividing cells. These potential therapeutic targets are clinically highly desirable because of their effects on CIN tumours that are typically refractory to current therapy.

Current Model and Future work

Chromosomal instability and aneuploidy leads to genomic and proteomic imbalance which results in the formation of aberrant protein complexes and metabolic disruptions which cause proteotoxic and metabolic stress. These stresses lead to self-amplifying ROS production and DNA damage. Oxidative response pathways and DNA damage repair mechanisms are critical for the survival of these stressed cells, because CIN cells are already close to their limits in buffering metabolic stress. If damage is unrepaired, it leads to high levels of oxidative stress and DNA damage which can result in apoptosis. Due to the continuous reshuffling of genomic material under stress conditions CIN cells generate modification in pathways which are required for stress tolerance. These CIN specific adaptations can be targeted to make these cells sensitive to those alterations (stress and damage response pathways), which have no effects on normal cells.

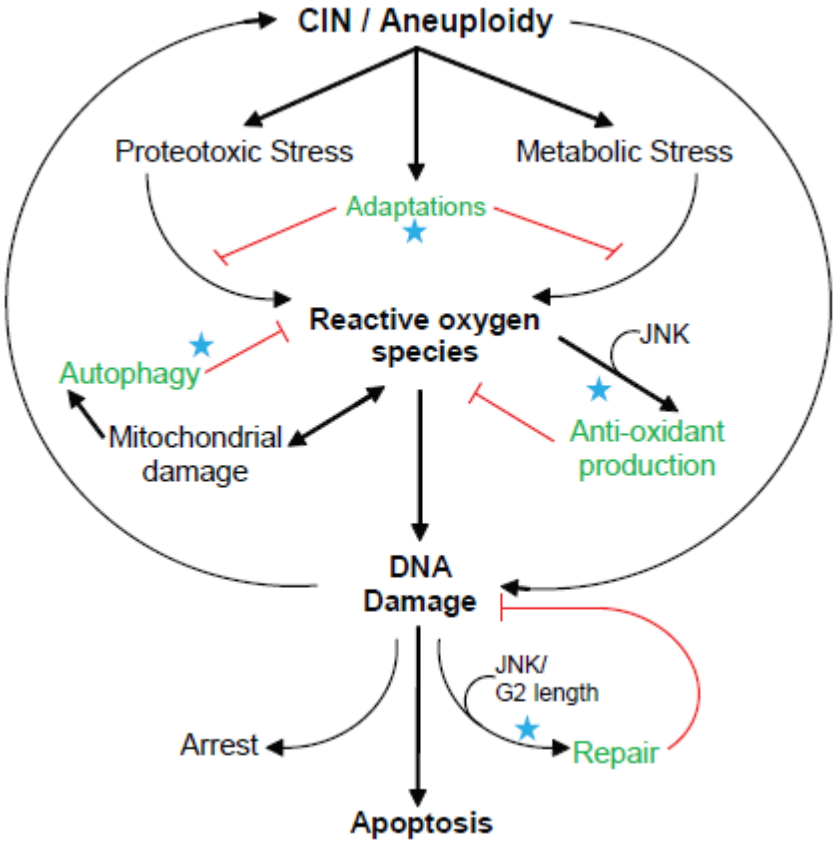

Figure 5.1: *Model for the effect of CIN on cell fates. CIN induces adaptations in the mechanisms which are involved in CIN tolerance and can be targeted (green).*

The JNK pathway has been implicated in the production of anti-oxidants and DNA repair and our results showed that JNK is highly activated in CIN cells, which is required for CIN tolerance. Similarly, timing in G2 is also crucial to manage high levels of DNA damage generated by oxidative stress. JNK is activated at centrosome where the major DNA damage repair and mitotic control proteins are present. This requires further investigation to explore the role of JNK in DNA repair and mitotic control. Identification of physical and functional interactions between JNK and DNA damage repair proteins could explain the direct involvement of JNK into this process.

Mad2 deficiency leads to increased merotelic attachments and lagging chromosomes which results in aneuploidy and facilitates the acquisition of more mutations and heterogeneity. Lagging chromosomes in anaphase have been reported to get DNA double strand breaks or tend to form micronuclei, which leads to further damage and CIN in the subsequent mitosis. Analysing the cause of DNA damage in lagging chromosomes may provide a useful link between DNA damage and CIN.

CIN and aneuploidy cause oxidative stress, which generates mitochondrial damage and the production of more ROS. Autophagy is a known mediator which protects a cell from further damage by clearing these defective mitochondria. Initial results from our lab suggest that the autophagy is required for CIN tolerance and can be targeted to specifically kill them (Dawei Liu – PhD thesis). Further investigation is required to identify the mediators of autophagy in CIN cells and to identify the mechanism by which cell can sense the presence of chromosomal instability.

Our results suggested that CIN cells are sensitive to metabolic alterations that are linked to oxidative stress, so further investigation is required to explore the effects of oxidative stress on the proliferation of CIN cells and what adaptations are acquired by the CIN cells to tolerate high levels of oxidative stress. Proteomics and metabolomics on different CIN models can help to identify generalized and specific effects of CIN. Moreover, the results show that CIN can itself cause oxidative stress which may be through aneuploidy but further investigation is required to explore the direct effects of CIN on metabolism and oxidative stress related pathways.

Significance

Cancer is one of the leading causes of premature death. Every year, approximately 14 million people are diagnosed with cancer worldwide. In 2012, 8.2 million deaths from cancer are reported worldwide. In Australia, more than 14,000 new cases of colorectal cancer alone are diagnosed each year, with a mortality of around 30% (Cancer Council of Australia). More than 80% of such tumours and many lung cancers have chromosomal instability and resistance to multiple chemotherapeutics, so there is a clear and pressing need for novel therapies that can specifically kill these resistant tumours. Here we provide a model for the identification and characterization of candidates that can be targeted to kill cells with CIN. The candidates are selected on the basis of their specificity against CIN cells to avoid the usual side effects of conventional chemotherapies. Identification of pathways that can be targeted to induce apoptosis in CIN cells is already a significant conceptual advance. We also broadly explained how our candidates affect the mechanism of CIN tolerance; this requires more detailed investigation of pathways and the adaptation of CIN. Further characterization and validation of selected candidates in other *in vivo* animal models and cell lines will provide a way to select the best protein/pathway that can be used as a therapeutic target for unstable tumours which are highly resistant to current treatments.

References

Anderhub, S.J., Krämer, A. & Maier, B. (2012) Centrosome amplification in tumorigenesis. *Cancer Lett*, 322 (1), 8-17.

Artandi, S.E., Chang, S., Lee, S.-L., Alson, S., Gottlieb, G.J., Chin, L. & DePinho, R.A. (2000) Telomere dysfunction promotes non-reciprocal translocations and epithelial cancers in mice. *Nature*, 406 (6796), 641-645.

Arzimanoglou, I.I., Gilbert, F. & Barber, H.R. (1998) Microsatellite instability in human solid tumors. *Cancer*, 82 (10), 1808-1820.

Babu, J.R., Jeganathan, K.B., Baker, D.J., Wu, X., Kang-Decker, N. & van Deursen, J.M. (2003) Rae1 is an essential mitotic checkpoint regulator that cooperates with Bub3 to prevent chromosome missegregation. *J Cell Biol*, 160 (3), 341-353.

Baker, D.J., Jeganathan, K.B., Cameron, J.D., Thompson, M., Juneja, S., Kopecka, A., . . . Roche, P. (2004) BubR1 insufficiency causes early onset of aging-associated phenotypes and infertility in mice. *Nat genet*, 36 (7), 744-749.

Baker, D.J., Jin, F., Jeganathan, K.B. & van Deursen, J.M. (2009) Whole chromosome instability caused by Bub1 insufficiency drives tumorigenesis through tumor suppressor gene loss of heterozygosity. *Cancer cell*, 16 (6), 475-486.

Bakhoum, S.F. & Compton, D.A. (2012) Chromosomal instability and cancer: a complex relationship with therapeutic potential. *J Clin. Invest.*, 122 (4), 1138-1143.

Bakhoum, S.F., Genovese, G. & Compton, D.A. (2009) Deviant kinetochore microtubule dynamics underlie chromosomal instability. *Curr Biol*, 19 (22), 1937-1942.

Bakhoum, S.F., Thompson, S.L., Manning, A.L. & Compton, D.A. (2009b) Genome stability is ensured by temporal control of kinetochore-microtubule dynamics. *Nat Cell Biol*, 11 (1), 27-35.

Barber, T.D., McManus, K., Yuen, K.W., Reis, M., Parmigiani, G., Shen, D., . . . Markowitz, S. (2008) Chromatid cohesion defects may underlie chromosome instability in human colorectal cancers. *Proc Natl Acad Sci U S A*, 105 (9), 3443-3448.

Baritaud, M., Boujrad, H., Lorenzo, H.K., Krantic, S. & Susin, S.A. (2010) Histone H2AX. *Cell Cycle*, 16, 3166-3173.

Basto, R., Brunk, K., Vinadogrova, T., Peel, N., Franz, A., Khodjakov, A. & Raff, J.W. (2008) Centrosome amplification can initiate tumorigenesis in flies. *Cell*, 133 (6), 1032-1042.

Basu, J., Bousbaa, H., Logarinho, E., Li, Z., Williams, B.C., Lopes, C., . . . Goldberg, M.L. (1999) Mutations in the essential spindle checkpoint gene bub1 cause chromosome missegregation and fail to block apoptosis in *Drosophila*. *J Cell Biol*, 146 (1), 13-28.

Bauer, G. (2012) Tumor cell-protective catalase as a novel target for rational therapeutic approaches based on specific intercellular ROS signaling. *Anticancer Res*, 32 (7), 2599-2624.

Bettencourt-Dias, M., Giet, R., Sinka, R., Mazumdar, A., Lock, W., Balloux, F., . . . Carthew, R. (2004) Genome-wide survey of protein kinases required for cell cycle progression. *Nature*, 432 (7020), 980-987.

Bier, E. (2005) Drosophila, the golden bug, emerges as a tool for human genetics. *Nat. Rev. Genet.*, 6 (1), 9-23.

Birkbak, N.J., Eklund, A.C., Li, Q., McClelland, S.E., Endesfelder, D., Tan, P., . . . Swanton, C. (2011) Paradoxical relationship between chromosomal instability and survival outcome in cancer. *Cancer Res*, 71 (10), 3447-3452.

Biteau, B., Hochmuth, C.E. & Jasper, H. (2008) JNK Activity in Somatic Stem Cells Causes Loss of Tissue Homeostasis in the Aging *Drosophila* Gut. *Cell stem cell*, 3 (4), 442-455.

Bouwman, P. & Jonkers, J. (2012) The effects of deregulated DNA damage signalling on cancer chemotherapy response and resistance. *Nat Rev Cancer*, 12 (9), 587-598.

Boveri, T. (1914) *Zur Frage der Entstehung maligner Tumorin.* Germany, Jena, Gustav Fisher Verlag.

Bridges, C.B. (1921) Genetical and cytological proof of non-disjunction of the fourth chromosome of Drosophila melanogaster. *Proc Natl Acad Sci U S A*, 7 (7), 186.

Brinkley, B.R. (2001) Managing the centrosome numbers game: from chaos to stability in cancer cell division. *Trends Cell Biol*, 11 (1), 18-21.

Bristow, R.G. & Hill, R.P. (2008) Hypoxia and metabolism: hypoxia, DNA repair and genetic instability. *Nat Rev Cancer*, 8 (3), 180-192.

Brumby, A.M. & Richardson, H.E. (2005) Using Drosophila melanogaster to map human cancer pathways. *Nat Rev Cancer*, 5 (8), 626-639.

Buecher, B., Cacheux, W., Rouleau, E., Dieumegard, B., Mitry, E. & Lièvre, A. (2013) Role of microsatellite instability in the management of colorectal cancers. *Digest Liver Dis*, 45 (6), 441-449.

Buffin, E., Emre, D. & Karess, R.E. (2007) Flies without a spindle checkpoint. *Nat Cell Biol*, 9 (5), 565-572.

Burrell, R.A.,McClelland, S.E.,Endesfelder, D.,Groth, P.,Weller, M.C.,Shaikh, N., . . . Swanton, C. (2013) Replication stress links structural and numerical cancer chromosomal instability. *Nature*, 494 (7438), 492-496.

Cahill, D.P., Lengauer, C., Yu, J., Riggins, G.J., Willson, J.K., Markowitz, S.D., . . . Vogelstein, B. (1998) Mutations of mitotic checkpoint genes in human cancers. *Nature*, 392 (6673), 300-303.

Cairns, R.A., Harris, I.S. & Mak, T.W. (2011) Regulation of cancer cell metabolism. *Nat Rev Cancer*, 11 (2), 85-95.

Caley, A. & Jones, R. (2012) The principles of cancer treatment by chemotherapy. *Surgery (Oxford)*, 30 (4), 186-190.

Campbell, P.J.,Yachida, S.,Mudie, L.J.,Stephens, P.J.,Pleasance, E.D.,Stebbings, L.A., . . . Futreal, P.A. (2010) The patterns and dynamics of genomic instability in metastatic pancreatic cancer. *Nature*, 467 (7319), 1109-1113.

Carmena, M., Ruchaud, S. & Earnshaw, W.C. (2009) Making the Auroras glow: regulation of Aurora A and B kinase function by interacting proteins. *Curr Opin Cell Biol*, 21 (6), 796-805.

Carter, S.L., Eklund, A.C., Kohane, I.S., Harris, L.N. & Szallasi, Z. (2006) A signature of chromosomal instability inferred from gene expression profiles predicts clinical outcome in multiple human cancers. *Nat Genet*, 38 (9), 1043-1048.

Castellanos, E., Dominguez, P. & Gonzalez, C. (2008) Centrosome Dysfunction in *Drosophila* Neural Stem Cells Causes Tumors that Are Not Due to Genome Instability. *Curr Biol*, 18 (16), 1209-1214.

Caussinus, E. & Gonzalez, C. (2005) Induction of tumor growth by altered stem-cell asymmetric division in Drosophila melanogaster. *Nat Genet*, 37 (10), 1125-1129.

Cheung-Ong, K., Giaever, G. & Nislow, C. (2013) DNA-damaging agents in cancer chemotherapy: serendipity and chemical biology. *Chem Biol*, 20 (5), 648-659.

Choi, C.-M., Seo, K.W., Jang, S.J., Oh, Y.-M., Shim, T.-S., Kim, W.S., . . . Lee, S.-D. (2009) Chromosomal instability is a risk factor for poor prognosis of adenocarcinoma of the lung: Fluorescence in situ hybridization analysis of paraffin-embedded tissue from Korean patients. *Lung Cancer*, 64 (1), 66-70.

Christmann, M., Tomicic, M.T., Aasland, D. & Kaina, B. (2006) A role for UV-light-induced c-Fos: stimulation of nucleotide excision repair and protection against sustained JNK activation and apoptosis. *Carcinogenesis*, 28 (1), 183-190.

Cimini, D. (2007) Detection and correction of merotelic kinetochore orientation by Aurora B and its partners. *Cell Cycle*, 6 (13), 1558.

Cimini, D. (2008) Merotelic kinetochore orientation, aneuploidy, and cancer. *BBA-Rev Cancer*, 1786 (1), 32-40.

Cimini, D., Howell, B., Maddox, P., Khodjakov, A., Degrassi, F. & Salmon, E. (2001) Merotelic kinetochore orientation is a major mechanism of aneuploidy in mitotic mammalian tissue cells. *J Cell Biol*, 153 (3), 517-528.

Cimini, D., Wan, X., Hirel, C.B. & Salmon, E. (2006) Aurora kinase promotes turnover of kinetochore microtubules to reduce chromosome segregation errors. *Curr Biol*, 16 (17), 1711-1718.

Cleaver, J.E. (2011) γH2Ax: biomarker of damage or functional participant in DNA repair "all that glitters is not gold!". *Photochem Photobiol*, 87 (6), 1230-1239.

Clem, B., Telang, S., Clem, A., Yalcin, A., Meier, J., Simmons, A., . . . Eaton, J. (2008) Small-molecule inhibition of 6-phosphofructo-2-kinase activity suppresses glycolytic flux and tumor growth. *Mol Cancer Ther*, 7 (1), 110-120.

Colombo, R., Caldarelli, M., Mennecozzi, M., Giorgini, M.L., Sola, F., Cappella, P., . . . Cucchi, U. (2010) Targeting the mitotic checkpoint for cancer therapy with NMS-P715, an inhibitor of MPS1 kinase. *Cancer Res*, 70 (24), 10255-10264.

Compton, D.A. (2011) Mechanisms of aneuploidy. *Curr Opin Cell Biol*, 23 (1), 109-113.

da Silva Xavier, G., Farhan, H., Kim, H., Caxaria, S., Johnson, P., Hughes, S., . . . Birzele, F. (2011) Per-arnt-sim (PAS) domain-containing protein kinase is downregulated in human islets in type 2 diabetes and regulates glucagon secretion. *Diabetologia*, 54 (4), 819-827.

da Silva Xavier, G., Rutter, J. & Rutter, G.A. (2004) Involvement of Per–Arnt–Sim (PAS) kinase in the stimulation of preproinsulin and pancreatic duodenum homeobox 1 gene expression by glucose. *Proc Natl Acad Sci U S A*, 101 (22), 8319-8324.

Dai, W., Wang, Q., Liu, T., Swamy, M., Fang, Y., Xie, S., . . . Rao, C.V. (2004) Slippage of mitotic arrest and enhanced tumor development in mice with BubR1 haploinsufficiency. *Cancer Res*, 64 (2), 440-445.

DeBerardinis, R.J., Lum, J.J., Hatzivassiliou, G. & Thompson, C.B. (2008) The biology of cancer: metabolic reprogramming fuels cell growth and proliferation. *Cell Metab*, 7 (1), 11-20.

Decordier, I., Cundari, E. & Kirsch-Volders, M. (2008) Mitotic checkpoints and the maintenance of the chromosome karyotype. *Mutat Res*, 651, 3-13.

Dekanty, A., Barrio, L., Muzzopappa, M., Auer, H. & Milan, M. (2012) Aneuploidy-induced delaminating cells drive tumorigenesis in Drosophila epithelia. *Proc Natl Acad Sci U S A*, 109 (50), 20549-20554.

Delbeke, D. (1999) Oncological applications of FDG PET imaging: brain tumors, colorectal cancer, lymphoma and melanoma. *J Nucl Med*, 40 (4), 591.

DeLuca, J.G., Gall, W.E., Ciferri, C., Cimini, D., Musacchio, A. & Salmon, E. (2006) Kinetochore microtubule dynamics and attachment stability are regulated by Hec1. *Cell*, 127 (5), 969-982.

Diaz-Rodriguez, E., Sotillo, R., Schvartzman, J.-M. & Benezra, R. (2008) Hec1 overexpression hyperactivates the mitotic checkpoint and induces tumor formation in vivo. *Proc Natl Acad Sci U S A*, 105 (43), 16719-16724.

Dikovskaya, D., Schiffmann, D., Newton, I.P., Oakley, A., Kroboth, K., Sansom, O., . . . Näthke, I.S. (2007) Loss of APC induces polyploidy as a result of a combination of defects in mitosis and apoptosis. *J Cell Biol*, 176 (2), 183-195.

Dobles, M., Liberal, V., Scott, M.L., Benezra, R. & Sorger, P.K. (2000) Chromosome missegregation and apoptosis in mice lacking the mitotic checkpoint protein Mad2. *Cell*, 101 (6), 635-645.

Dome, J.S., Bockhold, C.A., Li, S.M., Baker, S.D., Green, D.M., Perlman, E.J., . . . Breslow, N.E. (2005) High telomerase RNA expression level is an adverse prognostic factor for favorable-histology Wilms' tumor. *J Clin Oncol*, 23 (36), 9138-9145.

Dorsett, D. (2011) Cohesin: genomic insights into controlling gene transcription and development. *Curr Opini Genet Dev*, 21 (2), 199-206.

Draviam, V., Shapiro, I., Aldridge, B. & Sorger, P. (2006) Misorientation and reduced stretching of aligned sister kinetochores promote chromosome missegregation in EB1- or APC-depleted cells. *EMBO J*, 25 (12), 2814-2827.

Duensing, A. & Duensing, S. (2010). Centrosomes, polyploidy and cancer. Polyploidization and Cancer, Springer**:** 93-103.

Duesberg, P., Stindl, R. & Hehlmann, R. (2000) Explaining the high mutation rates of cancer cells to drug and multidrug resistance by chromosome reassortments that are catalyzed by aneuploidy. *Proc Natl Acad Sci U S A*, 97 (26), 14295-14300.

Duker, N.J. (2002) Chromosome breakage syndromes and cancer. *Am J Med Gen*, 115 (3), 125-129.

Emanuele, M.J., Lan, W., Jwa, M., Miller, S.A., Chan, C.S. & Stukenberg, P.T. (2008) Aurora B kinase and protein phosphatase 1 have opposing roles in modulating kinetochore assembly. *J Cell Biol*, 181 (2), 241-254.

Fang, J., Nakamura, H. & Iyer, A. (2007) Tumor-targeted induction of oxystress for cancer therapy. *J Drug Target*, 15 (7-8), 475-486.

Fenech, M., Kirsch-Volders, M., Natarajan, A., Surralles, J., Crott, J., Parry, J., . . . Thomas, P. (2011) Molecular mechanisms of micronucleus, nucleoplasmic bridge and nuclear bud formation in mammalian and human cells. *Mutagenesis*, 26 (1), 125-132.

Florl, A.R. & Schulz, W.A. (2008) Chromosomal instability in bladder cancer. *Arc Toxicol*, 82 (3), 173-182.

Foijer, F., Draviam, V.M. & Sorger, P.K. (2008) Studying chromosome instability in the mouse. *BBA-Rev Cancer*, 1786 (1), 73-82.

Fujiwara, T., Bandi, M., Nitta, M., Ivanova, E.V., Bronson, R.T. & Pellman, D. (2005) Cytokinesis failure generating tetraploids promotes tumorigenesis in p53-null cells. *Nature*, 437 (7061), 1043-1047.

Galimberti, F., Thompson, S.L., Liu, X., Li, H., Memoli, V., Green, S.R., . . . Settleman, J. (2010) Targeting the cyclin E-Cdk-2 complex represses lung cancer growth by triggering anaphase catastrophe. *Clin Cancer Res*, 16 (1), 109-120.

Galimberti, F., Thompson, S.L., Ravi, S., Compton, D.A. & Dmitrovsky, E. (2011) Anaphase catastrophe is a target for cancer therapy. *Clin Cancer Res*, 17 (6), 1218-1222.

Ganem, N.J., Godinho, S.A. & Pellman, D. (2009) A mechanism linking extra centrosomes to chromosomal instability. *Nature*, 460 (7252), 278-282.

Ganem, N.J. & Pellman, D. (2012) Linking abnormal mitosis to the acquisition of DNA damage. *J Cell Biol*, 199 (6), 871-881.

Gao, C., Furge, K., Koeman, J., Dykema, K., Su, Y., Cutler, M.L., . . . Woude, G.F.V. (2007) Chromosome instability, chromosome transcriptome, and clonal evolution of tumor cell populations. *Proc Natl Acad Sci U S A*, 104 (21), 8995-9000.

Gascoigne, K.E. & Taylor, S.S. (2008) Cancer cells display profound intra-and interline variation following prolonged exposure to antimitotic drugs. *Cancer cell*, 14 (2), 111-122.

Geigl, J.B., Obenauf, A.C., Schwarzbraun, T. & Speicher, M.R. (2008) Defining 'chromosomal instability'. *Trends Genet*, 24 (2), 64-69.

Gisselsson, D., Bjork, J., Hoglund, M., Mertens, F., Dal Cin, P., Akerman, M. & Mandahl, N. (2001) Abnormal nuclear shape in solid tumors reflects mitotic instability. *Am J Pathol*, 158 (1), 199-206.

Gisselsson, D., Jonson, T., Petersen, A., Strombeck, B., Dal Cin, P., Hoglund, M., . . . Mandahl, N. (2001) Telomere dysfunction triggers extensive DNA fragmentation and evolution of complex chromosome abnormalities in human malignant tumors. *Proc Natl Acad Sci U S A*, 98 (22), 12683-12688.

Gisselsson, D., Pettersson, L., Hoglund, M., Heidenblad, M., Gorunova, L., Wiegant, J., . . . Mandahl, N. (2000) Chromosomal breakage-fusion-bridge events cause genetic intratumor heterogeneity. *Proc Natl Acad Sci U S A*, 97 (10), 5357-5362.

Goa, K.L. & Faulds, D. (1994) Vinorelbine. A review of its pharmacological properties and clinical use in cancer chemotherapy. *Drugs Aging*, 5, 200-234.

Gollin, S.M. (2005). Mechanisms leading to chromosomal instability. Seminars in cancer biology, Elsevier.

Goshima, G. & Vale, R.D. (2003) The roles of microtubule-based motor proteins in mitosis comprehensive RNAi analysis in the Drosophila S2 cell line. *J Cell Biol*, 162 (6), 1003-1016.

Grabsch, H., Takeno, S., Parsons, W.J., Pomjanski, N., Boecking, A., Gabbert, H.E. & Mueller, W. (2003) Overexpression of the mitotic checkpoint genes BUB1, BUBR1, and BUB3 in gastric cancer- association with tumour cell proliferation. *J Pathol*, 200 (1), 16-22.

Gregan, J., Polakova, S., Zhang, L., Tolic-Norrelykke, I.M. & Cimini, D. (2011) Merotelic kinetochore attachment: causes and effects. *Trends Cell Biol*, 21 (6), 374-381.

Grose, J.H. & Rutter, J. (2010) The role of PAS kinase in PASsing the glucose signal. *Sensors*, 10 (6), 5668-5682.

Gross, S., Cairns, R.A., Minden, M.D., Driggers, E.M., Bittinger, M.A., Jang, H.G., . . . Su, S.M. (2010) Cancer-associated metabolite 2-hydroxyglutarate accumulates in acute myelogenous leukemia with isocitrate dehydrogenase 1 and 2 mutations. *J Exp Med*, 207 (2), 339-344.

Gurtler, U., Tontsch-Grunt, U., Jarvis, M., Zahn, S., Boehmelt, G., Adolf, G. & Solca, F. (2010) Effect of BI 811283, a novel inhibitor of Aurora B kinase, on tumor senescence and apoptosis. *J Clin Oncol*, 28, e13632.

Hanahan, D. & Weinberg, R.A. (2000) The hallmarks of cancer. *Cell*, 100 (1), 57-70.

Hanahan, D. & Weinberg, R.A. (2011) Hallmarks of cancer: the next generation. *Cell*, 144 (5), 646-674.

Hanks, S., Coleman, K., Reid, S., Plaja, A., Firth, H., FitzPatrick, D., . . . Robin, N. (2004) Constitutional aneuploidy and cancer predisposition caused by biallelic mutations in BUB1B. *Nat Genet*, 36 (11), 1159-1161.

Hansemann, D. (1891) Ueber pathologische Mitosen. *Virchows Archiv*, 123 (2), 356-370.

Hao, H.-X., Cardon, C.M., Swiatek, W., Cooksey, R.C., Smith, T.L., Wilde, J., . . . Rutter, J. (2007) PAS kinase is required for normal cellular energy balance. *Proc Natl Acad Sci U S A*, 104 (39), 15466-15471.

Harrison, M.R., Holen, K.D. & Liu, G. (2009) Beyond taxanes: a review of novel agents that target mitotic tubulin and microtubules, kinases, and kinesins. *Clin Adv Hematol Oncol*, 7 (1), 54.

Hartwell, L.H. & Smith, D. (1985) Altered fidelity of mitotic chromosome transmission in cell cycle mutants of S. cerevisiae. Genetics, 110(3), 381-395.

Hastie, N.D. & Allshire, R.C. (1989) Human telomeres: fusion and interstitial sites. *Trends Genet*, 5, 326-330.

Heilig, C.E., Loffler, H., Mahlknecht, U., Janssen, J.W., Ho, A.D., Jauch, A. & Kramer, A. (2009) Chromosomal instability correlates with poor outcome in patients with myelodysplastic syndromes irrespectively of the cytogenetic risk group. *J Cell Mol Med*, 14 (4), 895-902.

Heinimann, K. (2013) Toward a molecular classification of colorectal cancer: the role of microsatellite instability status. *Front Oncol*, 3.

Hingorani, S.R., Wang, L., Multani, A.S., Combs, C., Deramaudt, T.B., Hruban, R.H., . . . Tuveson, D.A. (2005) Trp53R172H and KrasG12D cooperate to promote chromosomal instability and widely metastatic pancreatic ductal adenocarcinoma in mice. *Cancer cell*, 7 (5), 469-483.

Holen, K., Saltz, L.B., Hollywood, E., Burk, K. & Hanauske, A.-R. (2008) The pharmacokinetics, toxicities, and biologic effects of FK866, a nicotinamide adenine dinucleotide biosynthesis inhibitor. *Invest New Drugs*, 26 (1), 45-51.

Holland, A.J. & Cleveland, D.W. (2009) Boveri revisited: chromosomal instability, aneuploidy and tumorigenesis. *Nat Rev Mol Cell Biol*, 10 (7), 478-487.

Holland, A.J. & Cleveland, D.W. (2012) Losing balance: the origin and impact of aneuploidy in cancer. *EMBO Rep*, 13 (6), 501-514.

Hoyt, M.A., Totis, L. & Roberts, B.T. (1991) S. cerevisiae genes required for cell cycle arrest in response to loss of microtubule function. *Cell*, 66, 507-517.

Ionov, Y., Peinado, M.A., Malkhosyan, S., Shibata, D. & Perucho, M. (1993) Ubiquitous somatic mutations in simple repeated sequences reveal a new mechanism for colonic carcinogenesis. *Nature*, 363 (6429), 558-561.

Ivachtchenko, A.V., Kiselyov, A.S., Tkachenko, S.E., Ivanenkov, Y.A. & Balakin, K.V. (2007) Novel mitotic targets and their small-molecule inhibitors. *Curr Cancer Drug Targets*, 7, 776-784.

Iwaizumi, M., Shinmura, K., Mori, H., Yamada, H., Suzuki, M., Kitayama, Y., . . . Watanabe, Y. (2009) Human Sgo1 downregulation leads to chromosomal instability in colorectal cancer. *Gut*, 58 (2), 249-260.

Iwanaga, Y., Chi, Y.-H., Miyazato, A., Sheleg, S., Haller, K., Peloponese, J.-M., . . . Jeang, K.-T. (2007) Heterozygous Deletion of Mitotic Arrest-Deficient Protein 1 (MAD1) Increases the Incidence of Tumors in Mice. *Cancer Res*, 67 (1), 160-166.

Jallepalli, P.V., Waizenegger, I.C., Bunz, F., Langer, S., Speicher, M.R., Peters, J.-M., . . . Lengauer, C. (2001) Securin is required for chromosomal stability in human cells. *Cell*, 105 (4), 445-457.

Janssen, A., Kops, G.J. & Medema, R.H. (2009) Elevating the frequency of chromosome mis-segregation as a strategy to kill tumor cells. *Proc Natl Acad Sci U S A*, 106 (45), 19108-19113.

Janssen, A. & Medema, R. (2011) Mitosis as an anti-cancer target. *Oncogene*, 30 (25), 2799-2809.

Janssen, A. & Medema, R.H. (2013) Genetic instability: tipping the balance. Oncogene, 32: 4459–4470.

Janssen, A., van der Burg, M., Szuhai, K., Kops, G.J. & Medema, R.H. (2011) Chromosome segregation errors as a cause of DNA damage and structural chromosome aberrations. *Science*, 333 (6051), 1895-1898.

Jeganathan, K., Malureanu, L., Baker, D.J., Abraham, S.C. & van Deursen, J.M. (2007) Bub1 mediates cell death in response to chromosome missegregation and acts to suppress spontaneous tumorigenesis. *J Cell Biol*, 179 (2), 255-267.

Jiralerspong, S., Palla, S.L., Giordano, S.H., Meric-Bernstam, F., Liedtke, C., Barnett, C.M., . . . Gonzalez-Angulo, A.M. (2009) Metformin and pathologic complete responses to neoadjuvant chemotherapy in diabetic patients with breast cancer. *J Clin Oncol*, 27 (20), 3297-3302.

Jonkers, Y., Claessen, S., Perren, A., Schmid, S., Komminoth, P., Verhofstad, A., . . . Ramaekers, F. (2005) Chromosomal instability predicts metastatic disease in patients with insulinomas. *Endocr-Relat Cancer*, 12 (2), 435-447.

Kabeche, L. & Compton, D.A. (2012) Checkpoint-independent stabilization of kinetochore-microtubule attachments by Mad2 in human cells. *Curr Biol*, 22 (7), 638-644.

Kalitsis, P., Earle, E., Fowler, K.J. & Choo, K.A. (2000) Bub3 gene disruption in mice reveals essential mitotic spindle checkpoint function during early embryogenesis. *Genes Dev*, 14 (18), 2277-2282.

Kaneko, Y. & Knudson, A.G. (2000) Mechanism and relevance of ploidy in neuroblastoma. *Gene Chromosome Canc*, 29 (2), 89-95.

Kaplan, O., Navon, G., Lyon, R.C., Faustino, P.J., Straka, E.J. & Cohen, J.S. (1990) Effects of 2-deoxyglucose on drug-sensitive and drug-resistant human breast cancer cells: toxicity and magnetic resonance spectroscopy studies of metabolism. *Cancer Res*, 50 (3), 544-551.

Karin, M. & Gallagher, E. (2005) From JNK to pay dirt: jun kinases, their biochemistry, physiology and clinical importance. *IUBMB life*, 57 (4‐5), 283-295.

Kato, T., Daigo, Y., Aragaki, M., Ishikawa, K., Sato, M., Kondo, S. & Kaji, M. (2011) Overexpression of MAD2 predicts clinical outcome in primary lung cancer patients. *Lung Cancer*, 74 (1), 124-131.

Kawamura, E., Fielding, A.B., Kannan, N., Balgi, A., Eaves, C.J., Roberge, M. & Dedhar, S. (2013) Identification of novel small molecule inhibitors of centrosome clustering in cancer cells. *Oncotarget*, 4 (10), 1763.

Kelland, L. (2007) The resurgence of platinum-based cancer chemotherapy. *Nat. Rev. Cancer*, 7, 573–584.Kim, H.-S., Park, K.H., Kim, S.A., Wen, J., Park, S.W., Park, B., . . . Kim, H.K. (2005) Frequent mutations of human *Mad2*, but not *Bub1*, in gastric cancers cause defective mitotic spindle checkpoint. *Mutat Res-Fund Molecular M*, 578 (1), 187-201.

Ko, M.A., Rosario, C.O., Hudson, J.W., Kulkarni, S., Pollett, A., Dennis, J.W. & Swallow, C.J. (2005) Plk4 haploinsufficiency causes mitotic infidelity and carcinogenesis. *Nat Genet*, 37 (8), 883-888.

Kolodner, R.D., Cleveland, D.W. & Putnam, C.D. (2011) Aneuploidy drives a mutator phenotype in cancer. *Science*, 333 (6045), 942.

Komarova, N. (2006) Does Cancer Solve an Optimization Problem? *Cell Cycle*, 3 (7), 838-842.

Kops, G.J., Foltz, D.R. & Cleveland, D.W. (2004) Lethality to human cancer cells through massive chromosome loss by inhibition of the mitotic checkpoint. *Proc Natl Acad Sci U S A*, 101 (23), 8699-8704.

Kops, G.J., Weaver, B.A. & Cleveland, D.W. (2005) On the road to cancer: aneuploidy and the mitotic checkpoint. *Nat Rev Cancer*, 5 (10), 773-785.

Korzeniewski, N., Hohenfellner, M. & Duensing, S. (2013) The centrosome as potential target for cancer therapy and prevention. *Expert Opin Ther Tar*, 17 (1), 43-52.

Kufe, D.W., Pollock, R.E., Weichselbaum, R.R., Bast, R.C. & Gansler, T.S. (2003) *Holland-Frei cancer medicine*, BC Decker Hamilton, ON.

Kuntzen, C., Sonuc, N., De Toni, E.N., Opelz, C., Mucha, S.R., Gerbes, A.L. & Eichhorst, S.T. (2005) Inhibition of c-Jun-N-terminal-kinase sensitizes tumor cells to CD95-induced apoptosis and induces G2/M cell cycle arrest. *Cancer Res*, 65 (15), 6780-6788.

Kuukasjarvi, T., Karhu, R., Tanner, M., Kahkonen, M., Schaffer, A., Nupponen, N., . . . Isola, J. (1997) Genetic heterogeneity and clonal evolution underlying development of asynchronous metastasis in human breast cancer. *Cancer Res*, 57 (8), 1597-1604.

Kwon, M., Godinho, S.A., Chandhok, N.S., Ganem, N.J., Azioune, A., Thery, M. & Pellman, D. (2008) Mechanisms to suppress multipolar divisions in cancer cells with extra centrosomes. *Genes Dev*, 22 (16), 2189-2203.

Lampson, M.A., Renduchitala, K., Khodjakov, A. & Kapoor, T.M. (2004) Correcting improper chromosome-spindle attachments during cell division. *Nat Cell Biol*, 6 (3), 232-237.

Le, A., Cooper, C.R., Gouw, A.M., Dinavahi, R., Maitra, A., Deck, L.M., . . . Dang, C.V. (2010) Inhibition of lactate dehydrogenase A induces oxidative stress and inhibits tumor progression. *Proc Natl Acad Sci U S A*, 107 (5), 2037-2042.

Lee, A.J., Endesfelder, D., Rowan, A.J., Walther, A., Birkbak, N.J., Futreal, P.A., . . . Howell, M. (2011) Chromosomal instability confers intrinsic multidrug resistance. *Cancer Res*, 71 (5), 1858-1870.

Lee, S.H., Sterling, H., Burlingame, A. & McCormick, F. (2008) Tpr directly binds to Mad1 and Mad2 and is important for the Mad1–Mad2-mediated mitotic spindle checkpoint. Genes & Dev., 22, 2926-2931.

Lengauer, C., Kinzler, K. & Vogelstein, B. (1997) Genetic instability in colorectal cancers. *Nature*, 386 (6625), 623-627.

Lengauer, C., Kinzler, K. W. & Vogelstein, B. (1998) Genetic instabilities in human cancers. Nature, 396, 643-649.Li, G.Q., Li, H. & Zhang, H.F. (2003) Mad2 and p53 expression profiles in colorectal cancer and its clinical significance. *World J Gastroenterol*, 9, 1972-1975.

Li, M., Fang, X., Baker, D.J., Guo, L., Gao, X., Wei, Z., . . . Zhang, P. (2010) The ATM-p53 pathway suppresses aneuploidy-induced tumorigenesis. *Proc Natl Acad Sci U S A*, 107 (32), 14188-14193.

Li, M., Fang, X., Wei, Z., York, J.P. & Zhang, P. (2009) Loss of spindle assembly checkpoint - mediated inhibition of Cdc20 promotes tumorigenesis in mice. *J Cell Biol*, 185 (6), 983-994.

Li, R. & Murray, A. W. (1991) Feedback Control of Mitosis in Budding Yeast. Cell, 66; 519-531.

Li, R., Hehlman, R., Sachs, R. & Duesberg, P. (2005) Chromosomal alterations cause the high rates and wide ranges of drug resistance in cancer cells. *Cancer Genet Cytogenet*, 163 (1), 44-56.

Li, Y. & Benezra, R. (1996) Identification of a human mitotic checkpoint gene: hsMAD2. *Science*, 274 (5285), 246-248.

Lingle, W.L., Barrett, S.L., Negron, V.C., D'Assoro, A.B., Boeneman, K., Liu, W., . . . Salisbury, J.L. (2002) Centrosome amplification drives chromosomal instability in breast tumor development. *Proc Natl Acad Sci U S A*, 99 (4), 1978-1983.

Liu, D., Vader, G., Vromans, M.J., Lampson, M.A. & Lens, S.M. (2009) Sensing chromosome bi-orientation by spatial separation of aurora B kinase from kinetochore substrates. *Science*, 323 (5919), 1350-1353.

Lobert, S. (1997) Neurotoxicity in cancer chemotherapy: vinca alkaloids. *Crit Care Nurse*, 17 (4), 71-79.

Longley, D. & Johnston, P. (2005) Molecular mechanisms of drug resistance. *J Pathol*, 205 (2), 275-292.

Lopez-Lazaro, M. (2008) The warburg effect: why and how do cancer cells activate glycolysis in the presence of oxygen? *Anticancer Agents Med Chem*, 8 (3), 305-312.

Luo, X., Puig, O., Hyun, J., Bohmann, D. & Jasper, H. (2007) Foxo and Fos regulate the decision between cell death and survival in response to UV irradiation. *EMBO J*, 26 (2), 380-390.

M'kacher, R., Andreoletti, L., Flamant, S., Milliat, F., Girinsky, T., Dossou, J., . . . Koscielny, S. (2010) JC human polyomavirus is associated to chromosomal instability in peripheral blood lymphocytes of Hodgkin's lymphoma patients and poor clinical outcome. *Ann Oncol*, 21 (4), 826-832.

Ma, X., Huang, J., Yang, L., Yang, Y., Li, W. & Xue, L. (2012) NOPO modulates Egr-induced JNK-independent cell death in Drosophila. *Cell Res*, 22 (2), 425-431.

MacLaren, A., Black, E.J., Clark, W. & Gillespie, D.A. (2004) c-Jun-deficient cells undergo premature senescence as a result of spontaneous DNA damage accumulation. *Mol Cell Biol*, 24 (20), 9006-9018.

Malumbres, M. & Barbacid, M. (2007) Cell cycle kinases in cancer. *Curr Opin Genet Dev*, 17 (1), 60-65.

Manning, A.L., Longworth, M.S. & Dyson, N.J. (2010) Loss of pRB causes centromere dysfunction and chromosomal instability. *Genes Dev*, 24 (13), 1364-1376.

Mannini, L. & Musio, A. (2011) The dark side of cohesin: the carcinogenic point of view. *Mutat Res-Rev Mutat*, 728 (3), 81-87.

Masuda, A., Maeno, K., Nakagawa, T., Saito, H. & Takahashi, T. (2003) Association between mitotic spindle checkpoint impairment and susceptibility to the induction of apoptosis by anti-microtubule agents in human lung cancers. *Am J Pathol*, 163 (3), 1109-1116.

Masuda, A. & Takahashi, T. (2002) Chromosome instability in human lung cancers: possible underlying mechanisms and potential consequences in the pathogenesis. *Oncogene*, 21 (45), 6884-6897.

Matsuura, S., Matsumoto, Y., Morishima, K.i., Izumi, H., Matsumoto, H., Ito, E., . . . Kajiwara, Y. (2006) Monoallelic BUB1B mutations and defective mitotic‐spindle checkpoint in seven families with premature chromatid separation (PCS) syndrome. *Am J Med Genet Part A*, 140 (4), 358-367.

Mazzorana, M., Montoya, G. & B Mortuza, G. (2011) The centrosome: a target for cancer therapy. *Curr Cancer Drug*, 11 (5), 600-612.

McClintock, B. (1938) The production of homozygous deficient tissues with mutant characteristics by means of the aberrant mitotic behavior of ring-shaped chromosomes. *Genetics*, 23 (4), 315.

McClintock, B. (1941) The stability of broken ends of chromosomes in Zea mays. *Genetics*, 26 (2), 234.

McEwen, D.G. & Peifer, M. (2005) Puckered, a Drosophila MAPK phosphatase, ensures cell viability by antagonizing JNK-induced apoptosis. *Development*, 132 (17), 3935-3946.

McGranahan, N., Burrell, R.A., Endesfelder, D., Novelli, M.R. & Swanton, C. (2012) Cancer chromosomal instability: therapeutic and diagnostic challenges. *EMBO Rep*, 13 (6), 528-538.

Mertens, F., Johansson, B. & Mitelman, F. (1994) Isochromosomes in neoplasia. *Gene Chromosome Cancer*, 10 (4), 221-230.

Meyer, R., Fofanov, V., Panigrahi, A., Merchant, F., Zhang, N. & Pati, D. (2009) Overexpression and mislocalization of the chromosomal segregation protein separase in multiple human cancers. *Clin Cancer Res*, 15 (8), 2703-2710.

Michel, L.S., Liberal, V., Chatterjee, A., Kirchwegger, R., Pasche, B., Gerald, W., . . . Benezra, R. (2001) MAD2 haplo-insufficiency causes premature anaphase and chromosome instability in mammalian cells. *Nature*, 409 (6818), 355-359.

Michelakis, E., Sutendra, G., Dromparis, P., Webster, L., Haromy, A., Niven, E., . . . Fulton, D. (2010) Metabolic modulation of glioblastoma with dichloroacetate. *Sci Transl Med*, 2 (31), 31ra34-31ra34.

Minotti, G., Menna, P., Salvatorelli, E., Cairo, G., & Gianni, L. (2004) Anthracyclines: molecular advances and pharmacologic developments in antitumor activity and

cardiotoxicity. *Pharmacol. Rev*. 56, 185–229.Mitelman, F., Johansson, B., Mandahl, N. & Mertens, F. (1997) Clinical significance of cytogenetic findings in solid tumors. *Cancer Genet Cytogen*, 95 (1), 1-8.

Mitelman, F., Johansson, B. & Mertens, F. (2012) Mitelman database of chromosome aberrations and gene fusions in cancer. *Mitelman F, Johansson B, Mertens F, editors*.

Miura, M., Miura, Y., Padilla-Nash, H.M., Molinolo, A.A., Fu, B., Patel, V., . . . Baker, C.C. (2006) Accumulated chromosomal instability in murine bone marrow mesenchymal stem cells leads to malignant transformation. *Stem cells*, 24 (4), 1095-1103.

Musacchio, A., Salmon, E.D. (2007) The spindle-assembly checkpoint in space and time. *Nat Rev Mol Cell Biol*, 8, 379-393.

Nakamura, H., Saji, H., Idiris, A., Kawasaki, N., Hosaka, M., Ogata, A., . . . Kato, H. (2003) Chromosomal instability detected by fluorescence in situ hybridization in surgical specimens of non-small cell lung cancer is associated with poor survival. *Clin Cancer Res*, 9 (6), 2294-2299.

Nasmyth, K. (2011) Cohesin: a catenase with separate entry and exit gates? *Nat Cell Biol*, 13 (10), 1170-1177.

Natarajan, A.T. & Palitti, F. (2008) DNA repair and chromosomal alterations. *Mutat Res-Gen Tox En*, 657 (1), 3-7.

Nezi, L. & Musacchio, A. (2009) Sister chromatid tension and the spindle assembly checkpoint. *Curr Opin Cell Biol*, 21 (6), 785-795.

Nishizaki, T., Chew, K., Chu, L., Isola, J., Kallioniemi, A., Weidner, N. & Waldman, F.M. (1997) Genetic alterations in lobular breast cancer by comparative genomic hybridization. *Int J Cancer*, 74 (5), 513-517.

Nishizaki, T., DeVries, S., Chew, K., Goodson, W.H., Ljung, B.-M., Thor, A. & Waldman, F.M. (1997) Genetic alterations in primary breast cancers and their metastases: direct comparison using modified comparative genomic hybridization. *Gene Chromosome Canc*, 19 (4), 267-272.

Nowak, M.A., Komarova, N.L., Sengupta, A., Jallepalli, P.V., Shih, I.-M., Vogelstein, B. & Lengauer, C. (2002) The role of chromosomal instability in tumor initiation. *Proc Natl Acad Sci U S A*, 99 (25), 16226-16231.

Nowell, C. (1962) The minute chromosome (Ph 1) in chronic granulocytic leukemia. *Ann Hematol*, 8 (2), 65-66.

Oda, S., Maehara, Y., Ikeda, Y., Oki, E., Egashira, A., Okamura, Y., . . . Miyashita, K. (2005) Two modes of microsatellite instability in human cancer: differential connection of defective DNA mismatch repair to dinucleotide repeat instability. *Nucleic acids Res*, 33 (5), 1628-1636.

Oromendia, A.B., Dodgson, S.E. & Amon, A. (2012) Aneuploidy causes proteotoxic stress in yeast. *Genes Dev*, 26 (24), 2696-2708.

Orr, B., Bousbaa, H. & Sunkel, C.E. (2007) Mad2-independent spindle assembly checkpoint activation and controlled metaphase - anaphase transition in Drosophila S2 cells. *Mol Biol Cell*, 18 (3), 850-863.

Ozben, T. (2007) Oxidative stress and apoptosis: impact on cancer therapy. *J Pharm Sci*, 96 (9), 2181-2196.

Parker, W.B. & Cheng, Y.C. (1990) Metabolism and mechanism of action of 5-fluorouracil, *Pharmacol. Ther*. 48, 381–395.

Paulsson, K. & Johansson, B. (2009) High hyperdiploid childhood acute lymphoblastic leukemia. *Gene Chromosome Canc*, 48 (8), 637-660.

Pavelka, N., Rancati, G., Zhu, J., Bradford, W.D., Saraf, A., Florens, L., . . . Li, R. (2010) Aneuploidy confers quantitative proteome changes and phenotypic variation in budding yeast. *Nature*, 468 (7321), 321-325.

Payton, M., Bush, T.L., Chung, G., Ziegler, B., Eden, P., McElroy, P., . . . Hodous, B.L. (2010) Preclinical evaluation of AMG 900, a novel potent and highly selective pan-aurora kinase inhibitor with activity in taxane-resistant tumor cell lines. *Cancer Res*, 70 (23), 9846-9854.

Percy, M.J., Myrie, K.A., Neeley, C.K., Azim, J.N., Ethier, S.P. & Petty, E.M. (2000) Expression and mutational analyses of the human MAD2L1 gene in breast cancer cells. *Gene Chromosome Canc*, 29 (4), 356-362.

Pfau, S.J. & Amon, A. (2012) Chromosomal instability and aneuploidy in cancer: from yeast to man. *EMBO Rep*, 13 (6), 515-527.

Pihan, G.A. (2013) Centrosome dysfunction contributes to chromosome instability, chromoanagenesis, and genome reprograming in cancer. *Front Oncol*, 3.

Pihan, G.A., Purohit, A., Wallace, J., Knecht, H., Woda, B., Quesenberry, P. & Doxsey, S.J. (1998) Centrosome defects and genetic instability in malignant tumors. *Cancer Res*, 58 (17), 3974-3985.

Pinsky, B.A., Kung, C., Shokat, K.M. & Biggins, S. (2006) The Ipl1-Aurora protein kinase activates the spindle checkpoint by creating unattached kinetochores. *Nat Cell Biol*, 8 (1), 78-83.

Prencipe, M., Fitzpatrick, P., Gorman, S., Mosetto, M., Klinger, R., Furlong, F., . . . O'Sullivan, J. (2009) Cellular senescence induced by aberrant MAD2 levels impacts on paclitaxel responsiveness in vitro. *Brit J Cancer*, 101 (11), 1900-1908.

Puzio-Kuter, A.M. (2011) The role of p53 in metabolic regulation. *Genes Cancer*, 2 (4), 385-391.

Quintyne, N.J., Reing, J.E., Hoffelder, D.R., Gollin, S.M. & Saunders, W.S. (2005) Spindle multipolarity is prevented by centrosomal clustering. *Science*, 307 (5706), 127-129.

Raj, L., Ide, T., Gurkar, A.U., Foley, M., Schenone, M., . . . Lee, S.W. (2011) Selective killing of cancer cells by a small molecule targeting the stress response to ROS. *Nature*. 475(7355): 231-4.

Rajagopalan, H., Nowak, M.A., Vogelstein, B. & Lengauer, C. (2003) The significance of unstable chromosomes in colorectal cancer. *Nat Rev Cancer*, 3 (9), 695-701.

Rebacz, B., Larsen, T.O., Clausen, M.H., Ronnest, M.H., Loffler, H., Ho, A.D. & Kramer, A. (2007) Identification of griseofulvin as an inhibitor of centrosomal clustering in a phenotype-based screen. *Cancer Res*, 67 (13), 6342-6350.

Ren, J.-G., Seth, P., Everett, P., Clish, C.B. & Sukhatme, V.P. (2010) Induction of erythroid differentiation in human erythroleukemia cells by depletion of malic enzyme 2. *PloS one*, 5 (9), e12520.

Reuter, S., Gupta, S.C., Chaturvedi, M.M. & Aggarwal, B.B. (2010) Oxidative stress, inflammation, and cancer: how are they linked? *Free Radical Biol Med*, 49 (11), 1603-1616.

Rieder, C.L. & Maiato, H. (2004) Stuck in division or passing through: what happens when cells cannot satisfy the spindle assembly checkpoint. *Dev Cell*, 7 (5), 637-651.

Roschke, A.V. & Kirsch, I.R. (2005) Perspectives: Targeting Cancer Cells by Exploiting Karyotypic Complexity and Chromosomal Instability. *Cell Cycle*, 4 (5), 679-682.

Roschke, A.V., Lababidi, S., Tonon, G., Gehlhaus, K.S., Bussey, K., Weinstein, J.N. & Kirsch, I.R. (2005) Karyotypic "state"•as a potential determinant for anticancer drug discovery. *Proc Natl Acad Sci U S A*, 102 (8), 2964-2969.

Rowinsky, E.K. (1997) The development and clinical utility of the taxane class of antimicrotubule chemotherapy agents. *Annu Rev Med*, 48, 353-374.

Sajesh, B.V., Bailey, M., Lichtensztejn, Z., Hieter, P. & McManus, K.J. (2013) Synthetic Lethal Targeting of Superoxide Dismutase 1 Selectively Kills RAD54B-Deficient Colorectal Cancer Cells. *Genetics*, 195 (3), 757-767.

Salmela, A.-L. & Kallio, M.J. (2013) Mitosis as an anti-cancer drug target. *Chromosoma*, 122 (5), 431-449.

Schmidt, M. & Bastians, H. (2007) Mitotic drug targets and the development of novel anti-mitotic anticancer drugs. *Drug Resist Updat*, 10 (4-5), 162-181.

Schvartzman, J.-M., Sotillo, R. & Benezra, R. (2010) Mitotic chromosomal instability and cancer: mouse modelling of the human disease. *Nat Rev Cancer*, 10 (2), 102-115.

Shaukat, Z., Wong, H.W., Nicolson, S., Saint, R.B. & Gregory, S.L. (2012) A screen for selective killing of cells with chromosomal instability induced by a spindle checkpoint defect. *PloS one*, 7 (10), e47447.

Sheffer, M., Bacolod, M.D., Zuk, O., Giardina, S.F., Pincas, H., Barany, F., . . . Domany, E. (2009) Association of survival and disease progression with chromosomal

instability: a genomic exploration of colorectal cancer. *Proc Natl Acad Sci U S A*, 106 (17), 7131-7136.

Sheltzer, J.M., Blank, H.M., Pfau, S.J., Tange, Y., George, B.M., Humpton, T.J., . . . Amon, A. (2011) Aneuploidy drives genomic instability in yeast. *Science*, 333 (6045), 1026-1030.

Shiras, A., Chettiar, S.T., Shepal, V., Rajendran, G., Prasad, G.R. & Shastry, P. (2007) Spontaneous transformation of human adult nontumorigenic stem cells to cancer stem cells is driven by genomic instability in a human model of glioblastoma. *Stem cells*, 25 (6), 1478-1489.

Silkworth, W.T., Nardi, I.K., Paul, R., Mogilner, A. & Cimini, D. (2012) Timing of centrosome separation is important for accurate chromosome segregation. *Mol Biol Cell*, 23 (3), 401-411.

Smart, D.K., Ortiz, K.L., Mattson, D., Bradbury, C.M., Bisht, K.S., Sieck, L.K., . . . Gius, D. (2004) Thioredoxin reductase as a potential molecular target for anticancer agents that induce oxidative stress. *Cancer Res*, 64 (18), 6716-6724.

Solomon, D.A., Kim, T., Diaz-Martinez, L.A., Fair, J., Elkahloun, A.G., Harris, B.T., . . . Ladanyi, M. (2011) Mutational inactivation of STAG2 causes aneuploidy in human cancer. *Science*, 333 (6045), 1039-1043.

Sotgia, F., Martinez-Outschoorn, U.E. & Lisanti, M.P. (2013) Cancer metabolism: new validated targets for drug discovery. *Oncotarget*, 4 (8), 1309.

Sotillo, R., Hernando, E., Diaz-Rodriguez, E., Teruya-Feldstein, J., CordÃ³n-Cardo, C., Lowe, S.W. & Benezra, R. (2007) Mad2 overexpression promotes aneuploidy and tumorigenesis in mice. *Cancer cell*, 11 (1), 9-23.

Sotillo, R., Schvartzman, J.-M., Socci, N.D. & Benezra, R. (2010) Mad2-induced chromosome instability leads to lung tumour relapse after oncogene withdrawal. *Nature*, 464 (7287), 436-440.

Stanton, R.C. (2012) Glucose-6-phosphate dehydrogenase, NADPH, and cell survival. *IUBMB life*, 64 (5), 362-369.

Stewenius, Y., Jin, Y., Ora, I., de Kraker, J., Bras, J., Frigyesi, A., . . . Gisselsson, D. (2007) Defective chromosome segregation and telomere dysfunction in aggressive Wilms' tumors. *Clin Cancer Res*, 13 (22), 6593-6602.

Storz, P. (2011) Forkhead homeobox type O transcription factors in the responses to oxidative stress. *Antioxid Redox Signaling*, 14 (4), 593-605.

Strom, L. & Sjogren, C. (2005) Extra Views DNA Damage-Induced Cohesion. *Cell Cycle*, 4 (4), 536-539.

Sturm, I., Bosanquet, A., Hermann, S., Guner, D., Dorken, B. & Daniel, P. (2003) Mutation of p53 and consecutive selective drug resistance in B-CLL occurs as a consequence of prior DNA-damaging chemotherapy. *Cell Death Differ*, 10 (4), 477-484.

Sudakin, V. & Yen, T.J. (2007) Targeting mitosis for anti-cancer therapy. *BioDrugs*, 21, 225-233.

Suzuki, K., Kokuryo, T., Senga, T., Yokoyama, Y., Nagino, M. & Hamaguchi, M. (2010) Novel combination treatment for colorectal cancer using Nek2 siRNA and cisplatin. *Cancer Sci*, 101 (5), 1163-1169.

Swanton, C.,Nicke, B.,Schuett, M.,Eklund, A.C.,Ng, C.,Li, Q., . . . Downward, J. (2009) Chromosomal instability determines taxane response. *Proc Natl Acad Sci U S A*, 106 (21), 8671-8676.

Tanaka, K., Nishioka, J., Kato, K., Nakamura, A., Mouri, T., Miki, C., . . . Nobori, T. (2001) Mitotic checkpoint protein hsMAD2 as a marker predicting liver metastasis of human gastric cancers. *Cancer Sci*, 92 (9), 952-958.

Tang, Y.-C., Williams, B.R., Siegel, J.J. & Amon, A. (2011) Identification of aneuploidy-selective antiproliferation compounds. *Cell*, 144 (4), 499-512.

Tennant, D.A., Durán, R.V. & Gottlieb, E. (2010) Targeting metabolic transformation for cancer therapy. *Nat Rev Cancer*, 10 (4), 267-277.

Thibodeau, S.N., Bren, G. & Schaid, D. (1993) Microsatellite instability in cancer of the proximal colon. *Science*, 260, 816–819.

Thompson, S.L., Bakhoum, S.F. & Compton, D.A. (2010) Mechanisms of Chromosomal Instability. *Curr Biol*, 20 (6), R285-R295.

Thompson, S.L. & Compton, D.A. (2008) Examining the link between chromosomal instability and aneuploidy in human cells. *J Cell Biol*, 180 (4), 665-672.

Thompson, S.L. & Compton, D.A. (2011) Chromosomes and cancer cells. *Chromosome Research*, 19 (3), 433-444.

Torres, E.M., Sokolsky, T., Tucker, C.M., Chan, L.Y., Boselli, M., Dunham, M.J. & Amon, A. (2007) Effects of aneuploidy on cellular physiology and cell division in haploid yeast. *Science*, 317 (5840), 916-924.

Tsuboi, K., Yokozawa, T., Sakura, T., Watanabe, T., Fujisawa, S., Yamauchi, T., . . . Tobinai, K. (2011) A Phase I study to assess the safety, pharmacokinetics and efficacy of barasertib (AZD1152), an Aurora B kinase inhibitor, in Japanese patients with advanced acute myeloid leukemia. *Leukemia Res*, 35 (10), 1384-1389.

Umemori, M., Habara, O., Iwata, T., Maeda, K., Nishinoue, K., Okabe, A., . . . Ueda, R. (2009) RNAi-mediated knockdown showing impaired cell survival in Drosophila wing imaginal disc. *Gene Regul Syst Biol*, 3, 11.

Vander Heiden, M.G., Cantley, L.C. & Thompson, C.B. (2009) Understanding the Warburg effect: the metabolic requirements of cell proliferation. *Science*, 324 (5930), 1029-1033.

Varetti, G. & Musacchio, A. (2008) The spindle assembly checkpoint. *Curr Biol*, 18 (14), R591-R595.

Vazquez, A., Bond, E.E., Levine, A.J. & Bond, G.L. (2008) The genetics of the p53 pathway, apoptosis and cancer therapy. *Nat Rev Drug Discov*, 7 (12), 979-987.

Ventura, J.-J., Hubner, A., Zhang, C., Flavell, R.A., Shokat, K.M. & Davis, R.J. (2006) Chemical genetic analysis of the time course of signal transduction by JNK. *Mol Cell*, 21 (5), 701-710.

Wagner, E.F. & Nebreda, Á.R. (2009) Signal integration by JNK and p38 MAPK pathways in cancer development. *Nat Rev Cancer*, 9 (8), 537-549.

Wallqvist, A., Huang, R., Covell, D.G., Roschke, A.V., Gelhaus, K.S. & Kirsch, I.R. (2005) Drugs aimed at targeting characteristic karyotypic phenotypes of cancer cells. *Mol Cancer Ther*, 4 (10), 1559-1568.

Walther, A., Houlston, R. & Tomlinson, I. (2008) Association between chromosomal instability and prognosis in colorectal cancer: a meta-analysis. *Gut*, 57 (7), 941-950.

Wang, J., Yuan, W., Chen, Z., Wu, S., Chen, J., Ge, J., . . . Chen, Z. (2012) Overexpression of G6PD is associated with poor clinical outcome in gastric cancer. *Tumor Biol*, 33 (1), 95-101.

Wang, X., Jin, D.-Y., Ng, R.W., Feng, H., Wong, Y.C., Cheung, A.L. & Tsao, S.W. (2002) Significance of MAD2 expression to mitotic checkpoint control in ovarian cancer cells. *Cancer Res*, 62 (6), 1662-1668.

Wang, X., Zhou, Y., Qiao, W., Tominaga, Y., Ouchi, M., Ouchi, T. & Deng, C. (2006) Overexpression of aurora kinase A in mouse mammary epithelium induces genetic instability preceding mammary tumor formation. *Oncogene*, 25 (54), 7148-7158.

Warburg, O. (1925) The metabolism of carcinoma cells. *J Cancer Res*, 9 (1), 148-163.

Warburg, O. (1956) On the origin of cancer cells. *Science*, 123 (3191), 309-314.

Warburg, O., Wind, F. & Negelein, E. (1927) The metabolism of tumors in the body. *J Gen Physiol*, 8 (6), 519-530.

Wassmann, K. & Benezra, R. (2001) Mitotic checkpoints: from yeast to cancer. *Curr Opin Genet Dev*, 11 (1), 83-90.

Weaver, B.A. & Cleveland, D.W. (2006) Does aneuploidy cause cancer? *Curr Opin Cell Biol*, 18 (6), 658-667.

Weaver, B.A. & Cleveland, D.W. (2007) Aneuploidy: instigator and inhibitor of tumorigenesis. *Cancer Res*, 67 (21), 10103-10105.

Weaver, B.A., Silk, A.D., Montagna, C., Verdier-Pinard, P. & Cleveland, D.W. (2007) Aneuploidy acts both oncogenically and as a tumor suppressor. *Cancer cell*, 11 (1), 25-36.

Weston, C.R. & Davis, R.J. (2007) The JNK signal transduction pathway. *Curr Opin Cell Biol*, 19 (2), 142-149.

Williams, B.R., Prabhu, V.R., Hunter, K.E., Glazier, C.M., Whittaker, C.A., Housman, D.E. & Amon, A. (2008) Aneuploidy affects proliferation and spontaneous immortalization in mammalian cells. *Science*, 322 (5902), 703-709.

Wirth, K.G., Wutz, G., Kudo, N.R., Desdouets, C., Zetterberg, A., Taghybeeglu, S., . . . Firnberg, N. (2006) Separase: a universal trigger for sister chromatid disjunction but not chromosome cycle progression. *J Cell Biol*, 172 (6), 847-860.

Wong, H.W., Shaukat, Z., Wang, J., Saint, R. & Gregory, S.L. (2014) JNK signaling is needed to tolerate chromosomal instability. *Cell Cycle*, 13 (4), 0-9.

Wood, L.D.,Parsons, D.W.,Jones, S.,Lin, J.,Sjoblom, T.,Leary, R.J., . . . Vogelstein, B. (2007) The genomic landscapes of human breast and colorectal cancers. *Science*, 318 (5853), 1108-1113.

Xu, H., Tomaszewski, J.M. & McKay, M.J. (2011) Can corruption of chromosome cohesion create a conduit to cancer? *Nat Rev Cancer*, 11 (3), 199-210.

Yang, Z., Lončarek, J., Khodjakov, A. & Rieder, C.L. (2008) Extra centrosomes and/or chromosomes prolong mitosis in human cells. *Nat Cell Biol*, 10 (6), 748-751.

Yim, K.-L. (2012) Microsatellite instability in metastatic colorectal cancer: a review of pathology, response to chemotherapy and clinical outcome. *Med Oncol*, 29 (3), 1796-1801.

Yu, R., Lu, W., Chen, J., McCabe, C.J. & Melmed, S. (2003) Overexpressed pituitary tumor-transforming gene causes aneuploidy in live human cells. *Endocrinology*, 144 (11), 4991-4998.

Yun, J., Rago, C., Cheong, I., Pagliarini, R., Angenendt, P., Rajagopalan, H., . . . Zhou, S. (2009) Glucose deprivation contributes to the development of KRAS pathway mutations in tumor cells. *Science*, 325 (5947), 1555-1559.

Yuneva, M., Zamboni, N., Oefner, P., Sachidanandam, R. & Lazebnik, Y. (2007) Deficiency in glutamine but not glucose induces MYC-dependent apoptosis in human cells. *J Cell Biol*, 178 (1), 93-105.

Yunis, J.J. (1983) The chromosomal basis of human neoplasia. *Science*, 221 (4607), 227-236.

Zhang, C., Zhang, Z., Zhu, Y. & Qin, S. (2014) Glucose-6-phosphate Dehydrogenase: a Biomarker and Potential Therapeutic Target for Cancer. *Anticancer Agents Med Chem,* 14(2): 280-9.

Zhang, J., Neisa, R. & Mao, Y. (2009) Oncogenic Adenomatous polyposis coli mutants impair the mitotic checkpoint through direct interaction with Mad2. *Mole Biol Cell*, 20 (9), 2381-2388.

Zhang, N., Ge, G., Meyer, R., Sethi, S., Basu, D., Pradhan, S., . . . El-Naggar, A.K. (2008) Overexpression of Separase induces aneuploidy and mammary tumorigenesis. *Proc Natl Acad Sci U S A*, 105 (35), 13033-13038.

Zhou, J. & Giannakakou, P. (2005) Targeting microtubules for cancer chemotherapy. *Curr Med Chem Anticancer Agents*, 5 (1), 65-71.